Urban geometry and environmental performance in real urban forms

Christodouli Chatzipoulka

Thesis submitted for the Degree of Philosophy in Architecture from the Kent School of Architecture, University of Kent

30 September 2017

The current research has been funded by a GTA scholarship (2012-2015), granted by the University of Kent.

Acknowledgements

First and foremost, I would like to express my sincere gratitude to my supervisor Prof. Marialena Nikolopoulou for the full and continuous support of my Ph.D. research, for her trust, motivation, and guidance. Beyond her immense knowledge and irreplaceable assistance, I would like to acknowledge her great generosity as teacher and human.

I am grateful to my second supervisor, Dr. Richard Watkins, for the valuable feedback, and all the members of the Centre for Architecture and Sustainable Environment (CASE) at the Kent School of Architecture (KSA), for the collaboration and interesting conversations.

I am definitely indebted to Prof. Raphaël Compagnon from the Haute école d'ingénierie et d'architecture de Fribourg, Switzerland, for providing the PPF software and teaching me to use it, as well as for the fruitful collaboration and his scientific contribution to this thesis.

A very special thanks to Fredrik Lindberg from the University of Gothenburg for his help in using the SOLWEIG model, and the constructive feedback during the ICUC9 conference. I would also like to thank Prof. Paul Richens for our insightful meeting over the urban geometry analysis and variables, and Prof. Andreas Matzarakis for his generous help and valuable comments.

I would like to thank all the members of staff, academic and non-academic, at the KSA for providing a warm and stimulating environment for my research, and allowing me to complete my thesis in optimal conditions. I am particularly grateful to the technical team of the School, especially to Brian Wood, Neil Evans and Chris Jones, for the IT support as well as their patience and responsiveness to the increased requirements of my project. I am also thankful to all my fellow doctoral students, Michael Adaji, Bahar Badiee, Alison Charles, Giacomo Chiarani, Tim Fox-Godden, Victoria Gana, Michael Hall, Soha Hirbod, Jamie Jacobs, Gi Min Lee, Imogen Lesser, Giovanna Piga, James Shaw, Khaled Sedki, Leonidas Tsichritzis and Carolina Vasilikou, for their positive feedback, encouragement, and friendship.

I am thankful to all the friends I met in Canterbury for making these four and a half years memorable, and especially my flatmates, Rachelle Ellena, Barbara Franchi, Marco Liguori and Luca Di Gregorio. I am particularly grateful to my friends, Giota, Fotini, Dora, Marietta, Vasiliki and Lefki, for our frequent chats on Skype and for giving me the positive energy that sometimes I thought was lost.

Also, this journey would never have started, if it was not for Dr. Michael Fedeski, the supervisor of my Master thesis at the Welsh School of Architecture, in Cardiff, to convince me to pursue a Ph.D. degree.

And last but not the least, I want to thank my family, my parents Panagiotis and Lemonia and my two siblings Lazaros and Vaia, for supporting and encouraging me throughout my studies and life in general. It would not be an exaggeration to say that without their love I would never be able to accomplish my goals.

Abstract

Solar radiation is energy, a natural and inexhaustible source of heat and light, and as such a major factor to be considered for enhancing urban environmental sustainability. Solar availability on buildings determines to a large degree their active and passive solar potential; whereas, the insolation of open spaces affects their microclimate and in turn, their use and liveability. Solar objectives are thus multiple and may also be conflicting in time and space, especially in temperate climates, where thermal comfort needs vary in seasons.

The subject of the thesis is the relationship between urban geometry and environmental performance of urban forms, explored at the neighbourhood scale and in real urban areas. Specifically, the research investigates statistically casual relationships of urban geometry with environmental phenomena related, directly or indirectly, to the availability of solar radiation. Full consideration is given to the varying solar geometry as a major parameter affecting the interaction between urban geometry and solar radiation, lending it a temporal and geographical -related to latitude- character. The research subject is explored through three distinct studies, which share the same methodology investigating particular topics under the same thematic umbrella. The first and the third study, in the order of these being presented, investigate phenomena occurring in open spaces, namely insolation and thermal diversity; whereas, the second study examines solar availability in open spaces and on building façades.

In the methodology, urban geometry is distinguished into built density, which is associated negatively with solar availability but positively with sustainability at the city-scale, and urban layout. The former expresses total built volume in a site, and the latter is represented by a set of quantified geometric parameters which characterise the way in which the built volume is allocated and distributed within the site. This distinction aims to provide evidence for the significance of urban layout in modifying the solar urban environment as well as addressing conflicting solar design objectives. The performance of the urban forms is examined through a series of performance indicators, namely sky view factor, insolation, solar irradiance and thermal diversity values. Both urban geometry variables and performance indicators are calculated on average in each urban form. The great size of the sample analysed allows their relationships to be investigated in statistical means.

The research belongs to the new era of urban environmental studies which make use of digital 3D models of cities to study spatially expressed phenomena in the built environment. It is based entirely on the analysis of existing urban forms, of 500x500m area, found in two European cities, London and Paris. London constitutes the main case study city, whereas Paris is examined for comparison purposes. The two cities are located at similar geographical latitudes and within the same climatic context, but their urban fabrics exemplify very different geometries. The geometric and environmental analysis of the urban forms as well as the elaboration and processing of the output data are performed using computer-based tools and methods, such as MATLAB software and image processing techniques applied in urban digital elevation models (DEMs) and, SOLWEIG and the RADIANCE-based software, PPF, for SVF and solar simulations.

The research findings contribute to the field of urban environmental studies and design at multiple levels, presenting a significant theoretical, practical, and methodological value. First, they produce a critical insight about the factors affecting the relationship of urban geometry and sun-related phenomena

occurring in the urban environment and lending it a dynamic character. In addition, they provide solid evidence about the enormous potential of urban geometry for promoting multiple -and sometimes conflicting- solar and urban design objectives, informing the relevant on-going discourse. Third, having as case studies real forms in London and Paris, a part of the findings is interpreted into urban design guidelines for enhancing the environmental performance of new and existing areas in the two cities. Last, as the research employs new methods and techniques to explore diverse topics, some of which are relatively new in the literature, it constitutes an important, methodological precedent for future research works.

Contents

List of Figures

List of Figures

List of Figures

List of Tables

Chapter One

Introduction

Chapter One identifies the subject matter of the research within the scope of urban environmental design, and justifies the purposefulness and timelessness of exploring it using real urban forms. The aim of the research reflects points emerged by the consideration of the parameters affecting solar radiation availability in the built environment and the multiplicity of environmental objectives related to it.

1.1 Background

With more than the half of the world population living today in cities (Population Reference Bureau, 2015), urban environmental sustainability has become the frame of reference for all researchers, practitioners and policy makers engaged with the field of urban design and planning. High densities of people signify correspondingly high densities of buildings and activities which render cities focal areas of high levels of energy consumption. For the same reason, cities have nowadays an important role to play in the attainment of national and global aims for reduction of energy use and greenhouse gas emissions, since any improvement in their energy efficiency would have a tremendous impact on the overall demands. At the same time, the intensification of urban built environment leads to serious problems, such as atmospheric pollution, increased air temperatures, noise and reduced green areas, deteriorating the environmental conditions within which people live and work. Urban environmental conditions do not only affect human's health and comfort, but also have energy implications, direct or indirect (Mavrogianni et al., 2011; Santamouris et al., 2001). For instance, increased ambient air temperatures induce extra energy use for the cooling of buildings, while a polluted urban environment encourages the use of private cars and the air-conditioning for buildings' ventilation.

Urban form, as the built structure of a city, is a dynamic in time and space parameter, the geometric characteristics of which determine to a large degree its energy performance and environmental potential (Hawkes et al., 1987; Williams et al., 2000). At city level, urban form is primarily associated with transport-related energy consumption, with compact cities to be regarded generally as more efficient ones (Mees, 2009; Newman and Kenworthy, 2000). Furthermore, the size and morphology of a city affects its interaction with the local climate and thus, the occurrence and intensity of urban climatological phenomena, such as Urban Heat Island (Oke, 1987; Santamouris, 2015; Tzavali et al., 2015). On the other

hand, at the intra-urban scale, where urban form is distinguished in buildings and open spaces, its geometry affects buildings' energy consumption and environmental quality of immediate open spaces. Specifically, the geometric characteristics of open spaces are crucial for relative solar and illuminance availability and wind flow, at the pedestrian level as well as on building façades, dispersion of pollutants (Di Sabatino et al., 2013; Britter and Hanna, 2003; Buonanno et al., 2011) and traffic noise levels (Echevarria Sanchez et al., 2016; Guedes, et al., 2011; Heutschi, 1995). The form of buildings affects heating/cooling demands as well as the potential for implementing environmental passive strategies to offset energy use (Ratti et al., 2003; Steadman et al. 2009; Steemers, 2003).

In this context, it is apparent that the systematic and comprehensive analysis of the urban form constitutes the base to study and understand the environmental phenomena occurring in cities, and respond accordingly to environmental challenges. Such an analysis depends first on the acquisition of raw data, namely 3D urban geometry information, which in the past was a labour- and capital-intensive process involving field surveys and manual digitising (Peeters and Etzion, 2012). At the next stage, appropriate analysis tools are required to process this information and obtain numerical attributes to describe or classify urban forms. Similarly, for environmental analysis purposes, powerful simulation and monitoring programmes are needed to study relevant phenomena and associate them with urban forms' geometric properties. Given the complexity and diversity of urban geometry, as well as the complexity of environmental phenomena within which it interacts, the scope of urban scale studies remained for a long time limited, lacking in means and robustness.

In the last two decades, major technological advances were made in remote sensing and geographical information systems (GIS), which signified the beginning of a new era for the analysis of the urban form and any kind of spatially expressed urban phenomena (Huang et al., 2007; Patino and Duque, 2013). Particularly, the Light Detection and Ranging (LIDAR) technology is considered a ground-breaking advent for surveying and mapping surface topography in a fast, less costly but reliable way (Yu et al., 2009). The availability of high-resolution remote sensing data enables the automated recognition of urban structure information, including land cover and land use, buildings' geometry and vegetation, and thus its digital modelling. Processing this information, metric attributes can be extracted which allow the quantification of urban characteristics and their association with studied urban phenomena (Banzhaf and Netzband, 2012). Such urban metrics have been used in a wide range of studies, including land-use/land-cover mapping and urban sprawl (e.g. Hermosilla et al., 2012a; 2012b; Inostroza, 2013; Malinverni, 2011; Peeters and Etzion, 2012), environmental monitoring (e.g. Edussuriya et al., 2011; Lindberg and

Grimmond, 2011b; Ryu et al., 2017; Yu et al., 2009); energy efficiency and potential assessment (e.g. Geiß et al., 2011; Rylatt et al., 2003a; 2003b; Tooke et al., 2014a; 2014b), and social-economic analysis (e.g. Menis, 2006; Taubenböck et al., 2009; Tompalski and Woyk, 2012). Furthermore, along with an increasing availability of 3D digital models of cities, the efficiency of computer systems has been gradually increased contributing to the flourish of urban analysis studies (Yoshida and Omae, 2005).

The present research makes use of these advances to investigate causal relationships between urban geometry and environmental performance of real urban forms, at the neighbourhood scale. Special emphasis is put on solar access and availability in open spaces and on building façades, with implications for urban microclimate and buildings' solar -passive and active- potential, respectively. The major case study is London, a city of great diversity in urban geometries, which allows a series of wider -more universal- issues affecting the studied relationships to be explored. Moreover, Paris is used comparatively, as a case study city of a very different urban planning tradition, but still of similar geographical latitude and temperate climate.

The following three sections contribute to the understanding of the scope and aim of the research outlining its main features as these emerged by the conceptual consideration of the topic and the examination of the existing literature. Section 1.1.1 discusses the significance of modifying solar availability in the urban environment for promoting more environmentally sustainable cities, and the key role of urban geometry in achieving multiple solar objectives. Section 1.1.2 defines what the term "urban geometry" is referred to, and presents different approaches and methods for analysing and describing it. Section 1.1.3 focuses on past studies examining the relationship between urban geometry and solar performance of urban forms, categorised them -by how they deal with the complexity and diversity of urban geometry- in those based on urban street canyons, generic urban models and urban typologies. Having identified relevant gaps in the literature and justified the purposefulness of using real urban forms for their exploration, the overall aim of the research is presented in Section 1.3. Lastly, Section 1.4 provides a summary of tools and methods used in the research, and Section 1.5 outlines the structure and the content of the thesis.

1.1.1 Solar design and objectives: the role of geometry

Solar radiation is energy, a natural source of heat and light, necessary for every living organisms on earth, and as such, a major factor to be considered for promoting urban environmental sustainability. Solar availability affects living conditions in indoor and outdoor spaces, and thus people's comfort and wellbeing. As indoor living spaces are meant to provide comfortable environments for activities they

accommodate, unless conditions meet occupants' needs and expectations, adjustments are made to fulfil them. Regarding thermal and visual comfort, related to solar availability, providing desirable levels of heating or cooling, and lighting in a space entails the use of energy in the form of heat energy and/or electricity. The energy demands for space heating/cooling and lighting together account for the largest part of buildings' overall energy consumption, with building use and climate context defining the contribution of each. Indicatively, in Europe, energy use only for space heating comprises approximately 70 per cent of energy consumption in residential buildings (WBCSD, 2009). On the other hand, as estimated for the UK context, energy demands in office buildings are mostly related to artificial lighting (Steemers, 2003). In warmer climates, such as that of Athens, annual building energy consumption is dominated by cooling space demands and the use of air-conditioners over the summer period (Santamouris et al., 2001) and, therefore, solar radiation on building fabrics is unwelcome as it causes extra heat gain.

The costs of energy use are not only economic, but mostly environmental since the combustion of fossil fuels, involved in the production of energy worldwide, results in respective carbon emissions and depletion of non-renewable natural resources. It becomes thus evident that energy efficiency is not only a matter of quantity, how much energy is consumed, but also a matter of quality, what type of energy is used. Solar energy is one of the renewable energy resources with the greatest potential; the International Energy Agency (2014) estimates that by 2050, solar energy could contribute to 27 per cent of the global electricity production. Unlike other renewable energy systems, solar photovoltaics and solar thermal collectors can be widely applied in built environments, even in densely built-up urban areas, namely on the building fabric. A major advantage of using building roofs and walls for photovoltaics implementation is the production of electricity at the point of use which will be a requirement for all new buildings in Europe after 2020 (EPBD, 2010).

Unlike indoor thermal comfort that is initially modified by the building fabric, outdoor thermal comfort relies exclusively on ambient microclimatic conditions. In this regard, the significance of solar radiation for achieving thermally desirable environments is even greater. Mean radiant temperature, calculated as the sum of all radiation fluxes to which the human body is exposed, is one of the four environmental factors governing thermal comfort. The other three are wind speed, air temperature and humidity. Unlike air temperature and humidity, mean radiant temperature and wind speed present significant spatial variations outdoors, which in turn define the variations of thermal conditions. Outdoors people do not have the option of controlling their environment by using energy-induced technologies; however, they do

not cease to pursue to feel comfortable (Walton et al., 2007). Research has shown that the use of outdoor spaces -in terms of type of activities and number of participants- is related to the thermal conditions occurring in them (Chen and Ng, 2012; Martinelli et al., 2015; Nikolopoulou and Lykoudis, 2007; Project RUROS, 2004).

In unfavourable conditions, either intense heat or cold, the three types of outdoor activities, as defined by Gehl (1971), may be affected to a different degree. *Necessary* activities, namely in which those involved are to a greater or lesser degree required to participate, such as going to school or to work, or shopping, take place with approximately the same frequency; though people adjust their clothing and behaviour, and opt for the shortest and/or more protected route. In contrast, *optional activities*, namely activities which take place if there is a wish to do so and if place make it possible, like taking a walk, and *social activities*, which differ from optional ones in that they entail some social interaction, like children playing, are limited significantly. Considering that optional and social activities are those enhancing humans' wellbeing and contributing to the social and economic life of a neighbourhood or a city, it becomes apparent that outdoor thermal conditions require to be given a full consideration when modifying the solar availability in the urban environment.

Solar availability in built environments is modified -compared to unobstructed sites- by the presence of buildings which obstruct solar rays and overshadow open spaces and other buildings' façades and roofs. In this way, the geometric characteristics of an urban form, including buildings' size, shape and spacing, determine the solar exposure of its surfaces. Consequently, all the environmental objectives mentioned above regarding the use of solar radiation in the urban environment should be pursued by the manipulation of the urban geometry during the urban design process. Some of these objectives may be mutually achieved facilitating urban design decisions; however, as some of them vary with climate, serious conflicts may be created.

Ensuring adequate levels of illuminance on building façades and maximising solar potential of the building fabric for the implementation of active solar strategies are two constant objectives independent to location and time. On the other hand, the need for maximising or minimising solar gains -referring to indoor spaces- and insolation or shading of open spaces varies with thermal comfort needs in each season/climate. For instance, Martins et al. (2014) examining the solar potential of different urban typologies in a Brazilian city point out the challenge for tropical cities to harness solar energy as renewable resource for electricity production and prevent undesirable solar gains in buildings. Similarly, Jakubiec and Reinhart (2013) testing a new development in Boston (USA) in terms of energy use and daylighting

highlight the need for a compromise between access to daylight and control of solar gains when considering geometric parameters, such as the building height to width street ratio.

Beyond the multiplicity of the objectives, in temperate climates, such as London, Paris, and the greatest part of Europe, urban designers also have to deal with different seasonal thermal needs. Van Esch et al. (2011) studied different urban canyon configurations for the Dutch climate searching for that which would be beneficial both for indoor and outdoor solar conditions, i.e. providing maximum solar irradiation in colder seasons and shading in warmer seasons. Apart from the conflicting seasonal objectives, they point out the difficulty in promoting simultaneous indoor and outdoor requirements, namely the configuration which performs better in terms of façade solar exposure may be disadvantageous for street insolation, and vice versa. Examining urban canyon design for a hot arid climate, Ali-Toudert and Mayer (2006) mention that even though providing shading outdoors is essential for mitigating heat stress experienced by pedestrians, ensuring some solar gains indoors during the winter should also be considered as a design criterion.

Additionally, considering that urban geometry is primarily characterised by the quantity of building volume that it contains, solar design and widely environmental objectives have to be fulfilled while accomplishing specific built density values. Density values are usually predetermined by urban planning policies and strongly associated with density of population and activities. At the city scale, density is associated positively with sustainability in four main ways: reduced energy and CO_2 emissions related to transportation; protection of rural areas; cost and efficiency of infrastructure systems; and the promotion of quality of urban life, including social interactions and ready access to services and facilities (Jabareen, 2006). With built density negatively associated with solar availability, it appears that solar potential in the urban environment might be compromised by the urge for increased densities.

Taking into account the significance of solar design objectives for achieving more energy efficient and environmental friendly cities in the future, the understanding of causal relationships between geometry and solar performance of urban forms becomes imperative. Identifying and quantifying the effect of urban geometry parameters on urban solar availability would allow a more sophisticated and responsive urban design. Like Oke (1988, pp. 108) notes focusing on urban canyon geometries, "*by concentrating on quantified relations, it appears that it may be possible to find a range of canyon geometries that are compatible with the apparently conflicting design objectives*". As presented more analytically in Section 1.1.3, the topic has been explored by several studies. Some examine the extent to which increasing built density and solar availability are mutually exclusive goals. Others investigate the effects of specific urban

geometry parameters, such as urban form randomness and buildings' compactness, sometimes equalising them methodologically with that of density. Most studies focus on the impact of urban geometry on buildings' solar performance and/or energy demands; whereas, its effect on the insolation of open spaces has not received the attention but of few researchers.

A crucial factor which requires to be studied when examining the relationship between urban geometry and solar availability is solar geometry, namely the geometric relationship between the Earth and the Sun. As the Earth rotates and orbits around the sun, the position of the sun to a given point on the Earth changes in time, hourly and seasonally, by geographical latitude. The position of the sun in relation to a location, as defined by two angles [°] (i.e. solar azimuth and solar altitude), determines shaded and sunlit surfaces of a physical object as well as the geometry of its casting shadow, i.e. shadow pattern. To summarise, the solar exposure of an urban form is the result of its geometry and the relative position of it to the Sun, with the latter depending on time and the geographical latitude of the location.

Acknowledging the significance of the latitude parameter for the relationship between urban geometry and solar access in the urban environment, several studies have included it as a varying factor in their parametric analysis. For instance, Arnfield (1990), adopting Oke's (1988) suggestion for possible urban canyon geometries compatible with conflicting design objectives, performs a parametric study in which the effect of height-to-width ratio, orientation and latitude is examined on irradiance levels on canyon floor and walls. Based on the performance of the geometries tested, the paper provides some guidelines for tropical, mid-latitude and high-latitude cities, all assuming clear sky conditions. Oliveira Panão et al. (2008) suggest a method for recognising urban forms with optimum building energy efficiency, namely maximising the absorption of solar radiation in winter and minimising it in summer, for different latitudes, within the range of 35-50°. The parametric analysis is based on different urban typologies varying geometric parameters, such as building dimensions and spacing, and grid azimuth. One of the findings is that high latitudes are restrictive regarding optimal solutions, with the pavilion typology being the best option for 50° latitude and terraces for 45° latitude. Using a similar logic, Vermeulen et al. (2015) examine the potential for maximising solar irradiation of buildings by varying buildings' dimensions (pavilions) and their distribution in a grid area, for latitudes of 40°, 50° and 60°. Among others, the results show that the capacity for improvement is more important at northern latitude; whereas, considering the relative improvement of the solar potential and energy implications, the optimisation of urban layout is found to be more suitable at 50° latitude.

By considering different latitudes in their analysis, the above studies acknowledge the influence of the sun path on the causal relation between urban geometry and solar exposure of urban forms. However, the sensitivity of their quantitative relationship to varying solar altitudes has not been examined yet. This research deems that the understanding of the solar altitude effect is critical for establishing a conceptual framework for a more sophisticated and informed solar design.

1.1.2 Urban geometry

The research adopts the term "urban geometry" to refer to the geometry of urban forms, namely building volumes and open spaces contained in an urban form, and their spatial relationship, relative configuration within it. It is noted that "urban morphology" is also used in the literature referring to the geometrical characteristics of built environments (e.g. Adolphe, 2001; Ng et al., 2011; Yoshida and Omae, 2005). The online edition of English Oxford dictionary defines geometry as "*the branch of mathematics concerned with the properties and relations of points, lines, surfaces, solids, and higher dimensional analogues*", and morphology as the study of the forms of things, in particular, "*the branch of biology that deals with the form of living organisms, and with relationships between their structures*". This suggests that "morphology" has a wider, more dynamic meaning to "geometry" involving not only geometric but also temporal and biophysical attributes of forms. In any case, the use of urban geometry in this research underlines its quantitative approach as opposed to quantitative and qualitative methods employed by the distinct discipline, urban morphology, to study "*the spatial structure, character of urban forms as well as the process of their development"* (Schirmer and Axhausen, 2016, pp.101).

Furthermore, the above definition of urban geometry indicates that the urban form is perceived in its simplest and most fundamental representation, namely as a composition of built and non-built spaces (Marshall, 2009). The latter corresponds to the aggregation of void in between built volumes as these are configurated and aggregated spatially within the urban site, neglecting any discrimination in use or ownership regime, i.e. street or squares, public or private. The analysis of the built environment in blocks, plots and buildings, represents a historic-geographical morphological approach (Oliveira and Monteiro, 2015) and aims to recognise and characterise urban typologies (e.g. Gil et al., 2012; Ghosh and Vale, 2009; Wheeler, 2015). Similarly, in environmental studies, such distinctions are meaningful when the purpose is to assess the performance of specific typologies, particularly in relation to buildings' energy performance (e.g. Arboit et al., 2008; 2010; Braulio-Gonzalo et al., 2016). Nonetheless, the layout of continuous open spaces between buildings is essential for defining urban forms, especially for environmental analysis purposes (Hamaina et al., 2012; Hermosilla et al., 2014).

Urban geometry varies significantly from city to city as well as within city resulting in an enormous diversity of built environments around the world. The great number of parameters involved in the production of the 3D urban space creates complex geometries which can be hardly reproduced in mathematics unless they are from the beginning strictly planned, i.e. produced by a repetitive pattern. In any case, the study of urban geometry requires this to be analysed and described in a meaningful -to the purpose of the study- way.

The analysis of urban forms' geometry is based to a great extent on traditional mathematics which are employed to measure properties of the space, such as distance, perimeter, area and volume -as opposed to new mathematical theories which describe structural relationships among spatial elements- (March and Steadman, 1971). Building volumes are physical objects of defined size and shape and thus, their geometry can be accurately represented by a series of metrics, the so-called building metrics. On the other hand, the geometry of open spaces -as this is defined by the configuration of buildings in a site- is much more complex to be expressed in metrical forms. The shortage of effective open space metrics for characterising urban forms is highlighted by Hermosilla et al. (2014) and linked to the fact that the analysis of urban forms centres on the built part. In this context, the most widely used urban form metrics are those quantifying the built form. Berghauser-Pont and Haupt (2010), exploring the connection between density, urban form and performance, suggest four such metrics for expressing associated concepts: *intensity* (FSI: Floor Space Index), *compactness* (GSI: Ground Space Index), *pressure on non-built space* (OSR: Open Space Ratio) and *building height* (L: Layers). Yoshida and Omae (2005) propose six parameters based on urban blocks for the quantitive comparison of cities: (i) surface area per projected area, (ii) volume per projected area, (iii) building to land ratio, (iv) mean height of buildings, (v) surface area of buildings per unit volume of buildings, and (vi) mean volume of buildings.

Beyond basic metrics, such as the aforementioned ones, there are quantified urban form parameters which have been introduced in the urban analysis by applying special mathematical and spatial theories. For instance, fractal geometry provides an alternative to Euclidean geometry as it allows the comparison of irregular urban forms based on measures of complexity (Thomas et al., 2008). The theory of fractals has been used in urban spatial analysis since 1990s (Batty and Kim, 1992; Batty and Longley, 1994; Frankhauser, 1994) for the description of the structure of linear networks, e.g. street networks (e.g. Strano et al., 2013), surfaces, i.e. built footprints (e.g. Thomas and Frankhauser, 2013), or boundaries of an urban form (e.g. Huang et al., 2007). Respectively, several fractal indices have been developed expressing relevant properties, such as *centrality, nuclearity, accessibility, diversity, continuity* and *porosity*, all of

which concern 2D geometries. Fractal analysis can be performed at all spatial scales; however, in most studies, it aims at the comparison of cities considered individually and studied as a unit (Batty, 2008; Thomas et al., 2008). Different types of complexity -as measured by fractal indices- are associated positively with environmental, social and economic sustainability of cities (Salat et al., 2010; Salat and Bourdic, 2011).

Another way for analysing urban space is space syntax, a technique developed at University College London, to support the understanding of the `social logic of space' (Hillier, 1996; Hillier and Hanson, 1984). Space syntax analysis is applied mostly on open public spaces, i.e. streets, and the concept behind it is that human perception of space and thus, spatial behaviour, i.e. pedestrian movement, may be affected by physical properties of the built environment. Specifically, topological relationships between spatial elements in an urban area are represented using distinctive elements of space syntax, which are translated into an axial map (the set of longest lines of view through open space). From the axial map graph, several measures, under a “meta-measure” of accessibility, can be extracted to quantify the spatial relationships in the urban area, such as *global* and *local integration*, and *connectivity* (Oliveira and Monteiro, 2015). With the scope of space syntax to have extended beyond pedestrian movement, such measures have been also used to address urban environmental issues (Space Syntax website). Nonetheless, the effectiveness of axial maps to represent the open space and 3D urban environment has been questioned (Ratti, 2004; 2005), especially in associating them with environmental phenomena for which open space metrics are crucial (Hamaina et al., 2012).

The quantification of urban forms’ geometric attributes aims to describe them, i.e. reducing the complexity of an urban geometry to a defined number of variables, and/or to classify them into suitable generalisations, i.e. limiting the diversity of urban geometries found in a city or a wider geographical region. Apparently, the classification of urban forms into general typologies prerequires their description based on a set of variables. For instance, Gil et al. (2012) propose a method for classifying urban forms based on twenty-five quantified attributes, including density (e.g. ground space index), dimension (e.g. perimeter of blocks), shape (e.g. proportion of blocks), land use (e.g. private and public space area) and network (e.g. global and local accessibility). The method is based on GIS analysis for retrieving attributes’ values and k-means cluster analysis for their statistical elaboration. A similar method has been employed by Schirmer and Axhausen (2016) for a multiscale classification of urban typologies, as well as in a study that examines the solar potential in different urban typologies (Martins et al., 2014).

Indeed, the study of urban geometry prerequires an appropriate handling of its complexity and diversity. The use of geometric measures is thus necessary for its analysis and association with studied phenomena. A review of relevant studies is presented in the next section highlighting the geometric parameters considered in the analysis, as well as the context, i.e. generic, idealised or real, that those are varying.

1.1.3 Urban geometry in solar environmental analysis

In this section, a review on studies examining the impact of urban geometry on the solar, environmental performance of urban forms is presented. The main purpose is to examine how the complex and diverse urban geometry is represented in different methodological approaches, which is related to geometric variables used to describe and associate it quantitatively with the studied phenomena. Furthermore, relevant findings are selectively discussed as to exemplify the scope of the studies as well as the amplitude of the urban geometry effect.

Prior to this, it is worth highlighting that most of the studies explore the effect of urban geometry on building energy consumption, namely heating, cooling and lighting energy demands, or building solar potential. This reflects the fact that, since the energy crisis in the early 1970s, the goal for reduction of energy use has dominated the overall environmental research agenda (Falkner, 2014). Considering that buildings concentrate a large proportion of energy demands, globally and within cities (UN-Habitat, 2008), the research community was urged to seek for strategic solutions to improve their energy efficiency. As major factors affecting buildings' energy consumption, Baker and Steemers (2000) identify climate, urban context (or geometry), building design, systems efficiency and occupant behaviour. They suggest that design, systems and behaviour together could account for variations in energy demands by a factor of 10 (2.5, 2, and 2, respectively). Following on their work, Ratti et al. (2005) consider that urban geometry may be the missing factor, 2.5 in explaining twenty-fold variations observed. In a similar study by Salat (2009) for Paris, the effect of urban geometry was quantified to a factor of 1.8.

Based on the literature research, three major categories of studies are identified depending on whether they consider urban street canyons, generic urban models, or idealized urban typologies for examining the effect of urban geometry.

Urban street canyon

Starting from the far-reaching work of Oke (1987; 1988) which has established it in the field of urban climatology, the urban street canyon has been proved an efficient way in representing the two crucial parameters for solar access, density and orientation. The complexity of urban geometry is limited to the

two dimensions of the street canyon in a cross section, expressed as a ratio, i.e. the ratio of building height to street width (H/W). In this way, the H/W ratio indicates the level of built obstruction, related to built density; whereas, the orientation of a street canyon is considered as that of its longest axis.

Urban street canyon has been mostly used as spatial unit in studies investigating microclimatic conditions in open spaces with direct implications for outdoor thermal comfort. In the case that these involve on-site measurements in actual streets, along with the H/W ratio, the sky view factor (SVF) is also used as an indicator of urban canyon geometry. As concerns the impact of the urban canyon configuration on solar availability, this is examined in terms of shading fractions (e.g. Bourbia and Awbi, 2004b), or more usually, mean radiant temperature values considered in the calculation of thermal comfort indices (e.g. Ali-Toudert and Mayer, 2007a; 2007b; Emmanuel et al., 2007; Johansson, 2006). The significance of promoting outdoor comfort in regions characterised by harsh climatic conditions justifies that most of the studies have been carried out in hot-arid (e.g. Ali-Toudert and Mayer, 2006; Bourbia and Awbi, 2004a; 2004b; Johansson, 2006; Pearlmutter et al., 1999; 2007) or hot-humid climates (e.g. Emmanuel et al., 2007; Johansson and Emmanuel, 2006). Compared to cold climates, open spaces in hot climates have a major social and cultural role to play acting as an extension of indoor spaces hosting daily activities and social events. As traditional urban forms in hot arid regions present noticeably higher H/W ratio than the contemporary ones, the findings usually suggest that the traditional urban environment provides more comfortable outdoor thermal conditions (Bourbia and Awbi, 2004a; 2004b; Johansson, 2006). In contrast, in hot-humid climates, where the enhancement of air movement is crucial for mitigating heat stress (Givoni, 1998), the benefits of increasing H/W ratio to provide shading are offset by lower wind speeds and higher values of humidity (Kakon et al., 2009).

The urban canyon geometry has been also used in some studies examining the effect of geometry and orientation on buildings' solar and energy performance. Strømann-Andersen and Sattrup (2011) investigate energy consumption for offices and residential buildings in Copenhagen, testing six canyons, with aspect ratio from 3 to 5, for north-south and east-west orientations (Fig. 1.1). Using dynamic thermal and daylight simulations, the impact of the aspect ratio was found in the range of up to +30% for offices, and +19% for housing, compared to unobstructed sites. Aspect ratio and orientation of urban canyons were also two parameters considered by van Esch et al. (2012) to investigate solar access and potential for passive solar heating strategies. Four street widths, representing common aspect ratios in Dutch cities, and north-south and east-west street orientations were studied with respect to global radiation yield on canyon surfaces and direct solar radiation on building envelopes. Regarding global radiation, the influence

of street width was pronounced: increasing the street width by 5m yielded an increase by 19%, for both canyon orientations and in different seasons. Unlike global radiation, solar exposure of building envelopes was found to be affected both by street width and orientation.

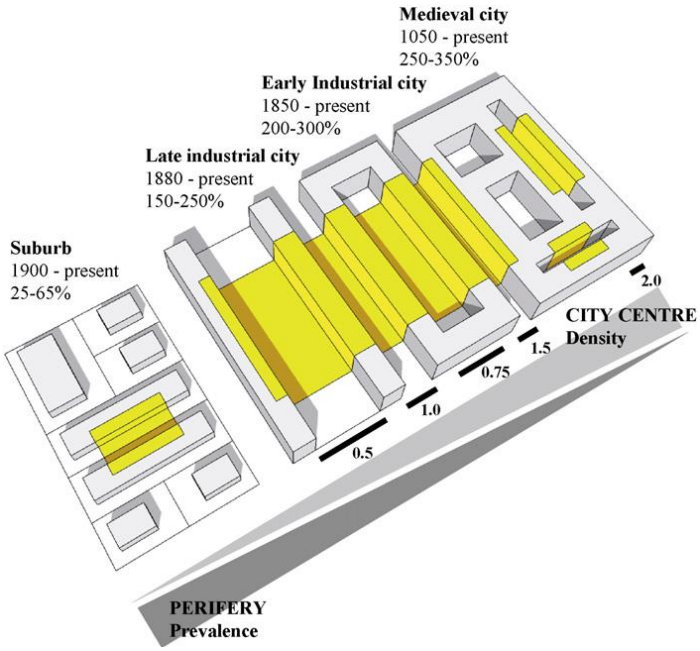

Figure 1.1: Representative aspect ratios in Copenhagen, considered in the study of Strømann-Andersen and Sattrup (2011).

In conclusion, the great advantage of using urban canyon geometry for studying the occurrence of environmental quantities, such as solar availability and mean radiant temperature, is at the same time its major disadvantage. The simplicity of the model allows for complex phenomena to be examined and the results to be extrapolated based on two single parameters, H/W ratio and orientation. On the other hand, the reduction of the urban geometry to only two parameters does not allow the effect of diverse urban layouts to be considered.

Generic models

The common characteristic of the studies grouped and presented in this section is that all perform parametric analysis based on generic urban models, (i.e. models composed of rectangular building volumes on a grid layout). Furthermore, they acknowledge the negative effect of density on solar availability, and explore ways to mitigate or offset it by modifying the urban layout. For doing so, they either examine the effect of different ways to increase density or, for a given density, different building configurations.

Steemers (2003) identifies three ways in which an urban form can change to increase density: (i) by increasing building depth, (ii) by increasing building height or reducing spacing, namely changing the height-to-width ratio, and (iii) by increasing 'compactness' (referring to different typologies). Otherwise, putting it more generally, the built volume can increase in two ways either horizontally, by increasing site coverage, or vertically, by increasing building height. Kristl and Krainer (2001) investigated the combined influence of building dimensioning (i.e. height and width) and orientation on density layout, using the iso-shadow method, for Ljubljana location. In the parametric analysis, the spacing between buildings was restricted by the iso-shadow contour of 80% of yearly solar radiation on the site, defined as minimum satisfactory value for the insolation of the opposite buildings (Fig. 1.2). It was found that by increasing building width, layout density increases substantially, namely the extra building volume produced by increasing site coverage compensates for the extra site area required; the opposite occurs when increasing building height. In relation to the orientation of the buildings, the results indicated that north-south orientation (referred to the orientation of the long facades of the buildings) is the most efficient in terms of land use.

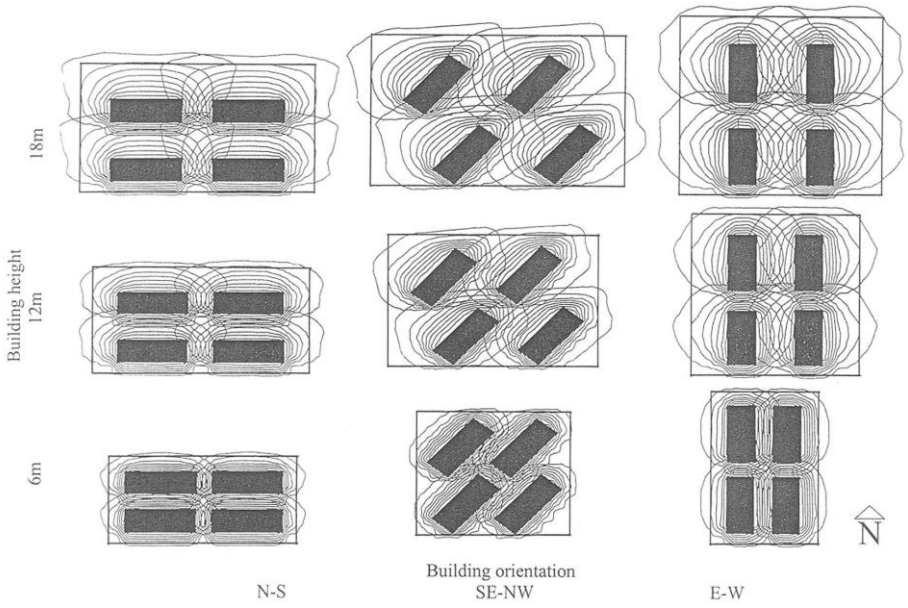

Figure 1.2: Iso-shadows (ensuring 80% of yearly solar radiation on the site) for 24m building width and varying building height and orientation, from the study of Kristl and Krainer (2001).

Building aspect ratio (width-to-depth), site coverage and orientation were three design parameters considered in the parametric analysis of Li et al. (2015) examining photovoltaic and solar thermal potential on building envelopes, per building floor area. Three density scenarios were tested, low, medium and

high, varying number of building floors from 11, to 18 and 26, respectively. Solar simulations were performed using weather data for Beijing (China). The results showed that, increasing building aspect and site coverage, solar potential tends to increase, although the effect of mutual shading becomes more severe. Compared to unobstructed buildings, photovoltaic and solar thermal potential may be reduced up to 50% and 26%, respectively, in high-density scenarios due to the overshadowing effect. A similar study was conducted by Lu and Du (2013) for another Chinese city, Harbin, instigating daylight and sunlight availability in high built densities. Three urban layouts were considered; the first and second layouts were composed of square and rectangular in plan buildings, respectively, and the third one was a combination of the two previous (Fig. 1.3). The assessment was based on vertical daylight factor and sunlight hours occurring on façades, with the best performance being achieved by the layout of square buildings, and the worst one by the rectangular buildings.

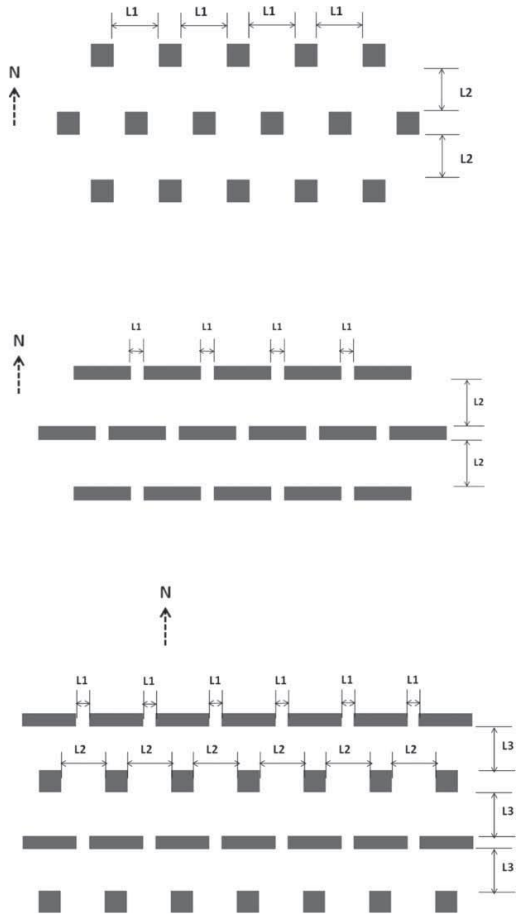

Figure 1.3: Three layouts, i.e. from to top to bottom: square, rectangular and combination of two, tested in the parametric analysis of Lu and Du (2013).

Cheng et al. (2006a; 2006b) explored whether the urban design intention for densification and sustainability are exclusive or not, examining daylight access and potential for solar systems. The study consists of two parts. In the first part, sky view factor at the ground, daylight factor/availability and solar potentials on building envelopes were computed for urban blocks in Sao Paolo, Brazil. According to the results, sky view factor, daylight factor and solar potential on roofs have a strong correlation with plot ratio and building height; whereas, solar potential on buildings facades was found to correlate better with site coverage. The authors suggest that the former environmental quantities are more dependent on vertical obstruction angles, namely light coming from the top; whereas, the latter ones are more influenced by horizontal obstruction angles and light coming from sides.

In the second part, simulations were performed for eighteen generic models which were produced varying horizontal and vertical layout (uniform and random), plot ratio and site coverage (Fig. 1.4). The results indicated that horizontal and vertical randomness is beneficial, especially in models of high plot ratio. Comparing high-density random and low-density uniform models, it was found that it is feasible the usable floor area to be increased and, at the same time, ground openness and daylight availability on building facades to be maintained, or even increase. On the other hand, the results concerning solar potential on building envelopes were different. Models of high site coverage and uniform layout were found to perform better due to increased roof area, which, in a uniform vertical layout, is totally unobstructed and exposed to the sun. In models of low site coverage, the solar potential is mostly related to the solar exposure of building facades, which increases with vertical randomness, while is almost unaffected by horizontal one.

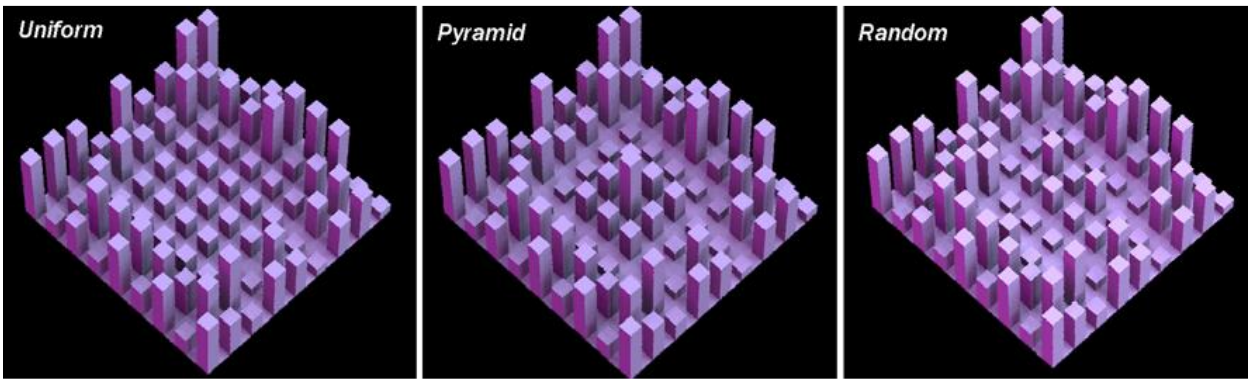

Figure 1.4: Generic models testing uniform, pyramid and random skylines, respectively, in Cheng et al. (2006a).

To summarise, the above studies demonstrate that it is feasible to offset the negative effect of density on daylight and solar availability by regulating either the way in which the density of an urban form is being

increased, or its horizontal and vertical layout. Furthermore, the influence of urban geometry parameters, such as site coverage and building height, and vertical and horizontal randomness, may differ depending on the solar performance criterion they are assessed for. Regarding the use of generic models, it allows for the impact of specific geometric parameters to be isolated and examined. Additionally, the findings may be directly applicable in cities, such as developing Asian cities, where new urban developments are of large scale and the most typical urban typology is that of free-standing buildings, i.e. pavilions (Ng and Wong, 2004; 2005). However, in other parts of the world and especially in historic cities, the typologies of built form are diverse and more complex. For this reason, the findings based on generic models are less relevant and rather theoretical to be applied.

Urban typologies

The studies of the third category investigate the impact of urban geometry comparing the environmental performance of urban typologies. At the scale of urban blocks, built forms may share some relatively homogenous geometric characteristics which allow their classification into distinct typologies. The consideration of urban typologies in environmental studies addresses the diversity of urban geometries found in different cities, as well as their complexity since the repetitive pattern is relatively regulated, "idealized" to be representative of a wider range of actual urban forms. As presented below, the simplification in defining geometrically urban typologies, or otherwise, how realistic the built forms are, varies depending on the methodology applied.

The analysis of built form types in environmental studies was launched by Martin and March (1972) and the research team of the Centre for Land Use and Built Form, at Cambridge University, in the late 1960s. They selected simplified urban typologies based on archetypal built forms to compared them in terms of built potential (total floor area of the built form to the site area) and daylight availability. Initial results focused on two typologies, courtyards and pavilions, with the former to be representative of traditional built forms and the latter reflecting the more contemporary tower buildings. Since then, their research work has inspired several scholars, and their archetypal built forms have been adopted and tested by numerous studies (e.g. Gupta, 1984; Steadman, 2014; Steemers et al., 1997).

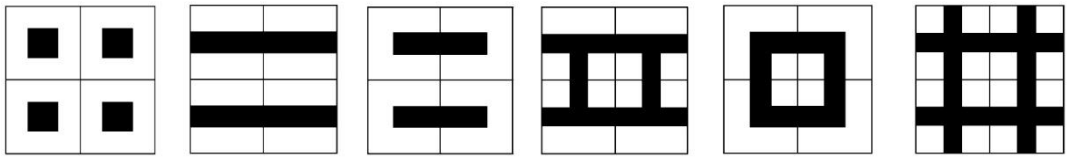

Figure 1.5: Generic built forms based on Martin and March (1972) and examined by Ratti et al. (2003). From left to right: pavilions, terraces, slabs, terraces-courts, pavilion-courts and courts.

For instance, Ratti et al. (2003) revisited the work of Martin and March assessing six generic typologies in terms of daylight availability, using SVF as indicator performance (Fig. 1.5). According to the results, the initial finding that the courtyard typology performs better than the pavilion was not clearly approved. In fact, the favourably lower height of the courtyards was compensated by their higher obstruction of façades from lateral sides. Comparing the performance of all six typologies, it was found that, when both the built volume and passive to non-passive ratio are constant in a given site, the daylight distribution is hardly affected by the built form. The analysis was repeated for an array of urban courtyard dwellings, and two realistic pavilion types which were evaluated considering hot-arid climatic conditions, in terms of surface-to-volume ratio, shadow densities, daylight accessibility and openness to the sky. This more realistic and environmentally holistic approach indicated that the courtyard type performs better as it responses to the complexities of the particular climate.

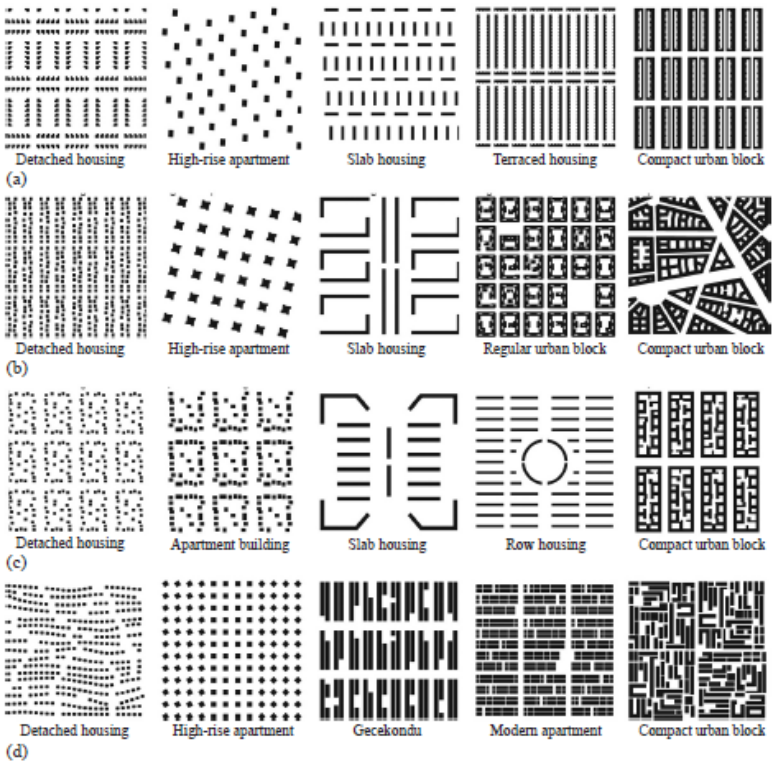

Figure 1.6: grounds of 'idealised' typologies identified for London (a), Paris (b), Berlin (c); and Istanbul (d), and studied by LSE cities (2014).

The research conducted by the LSE Cities (2014), at the London School of Economics and Political Science, was also based on urban typologies, such as high-rise apartments, slab and terraced housing, and examined heat energy consumption in residential buildings. However, the spatial configurations studied were derived from the geometrical analysis of specific cities. The research focused on the four largest European cities, namely London, Paris, Berlin and Istanbul, from which the five most dominant building configurations were identified. From in total 100 real urban geometry samples analysed, 20 "idealized'" urban typologies were created, five for each city, through a *purification* process (Fig. 1.6). The typologies were assessed in terms of annual heat energy demand per square meter of floor area, assuming the climatic conditions of Paris. Beyond the effect of different typologies, the influence of four geometrical parameters was investigated, i.e. built density, surface-to-volume ratio, building height and site coverage. Testing the correlation of each of those parameters with heat energy demands, the r coefficients obtained were -0.77, 0.80, -0.88 and -0.40, respectively. In general, more compact typologies and of higher buildings were found to have the largest heat-energy efficiency and detached housing the lowest.

The study of Zhang et al. (2012) explores the relationship between density, built form typology and sky view factor, as an environmental indicator related to daylight availability and insolation levels. The 'Normalisalisation + Replication" method was employed for generating seven urban typologies based on real residential urban blocks, three from European cities (Paris, Barcelona and Amsterdam) and four from the city of Singapore (Fig. 1.7). These were evaluated in two ways, based on façade and ground area with SVF value within an identified as preferred range and, then the same façade and ground area divided by total floor area. Since all the three European typologies were of lower density, using the first performance indicator, they performed much better compared to those of Singapore; however, weighting their performance by total floor area, the results were the opposite. Furthermore, the sensitivity of the performance of the seven typologies to variations of density was examined increasing the building height, revealing that the Barcelona and Paris typologies are the most sensitive. The Amsterdam typology was found to have the potential for achieving high densities maintaining relatively adequate sky exposure.

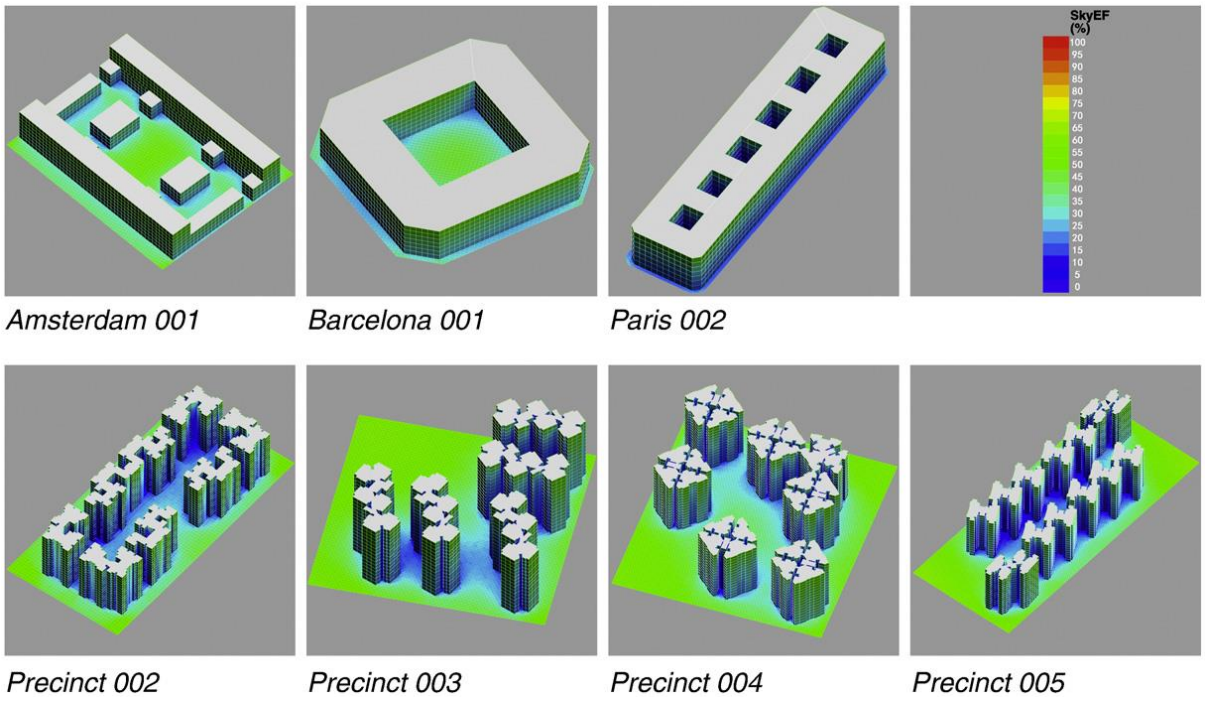

Figure 1.7: Seven urban typologies compared by Zhang et al. (2012) in terms of daylight availability and insolation level.

Finally, Ratti et al. (2005) compared the energy performance of different urban typologies found in Europe; instead of theoretical or idealized typologies, they employed sections of existing cities from Berlin, London and Toulouse. The three urban forms were first characterised in terms of surface-to-volume ratio and passive to non-passive zone ratio. Among the three typologies Toulouse featured the

highest surface-to-volume and passive to non-passive ratio, and the lowest ones belonged to Berlin. The two urban geometry parameters were considered in the calculation of building energy consumption (heating/cooling, ventilation and lighting) performed in the LT model for London's climatic conditions. With Toulouse achieving the best energy performance and Berlin the worst one, the overall finding of the study is summarized in that the building energy consumption increases as the passive to non-passive ratio decreases.

To conclude, urban typologies considered in environmental studies may be generic, such as the archetypal urban patterns identified by Martin and March (1972), or may be more realistic specified for individual cities. In general terms, the research findings agree with those of studies using parametric analysis and simple rectangular building forms on that the urban layout does affect the environmental performance of urban forms. However, most of the studies focus on comparing urban typologies which are defined descriptively, for instance, pavilions versus courtyards or Barcelona block versus Singapore block. The measurable parameters considered are limited in number and their effect is identified comparing the relative performance of different typologies, rather than through statistical analysis. The exception among the reviewed studies is that of the LSE Cities (2014) where the sample of 20 urban typologies allowed the statistical exploration of causal relations; nonetheless, the urban parameters considered were only four and the most basic.

From urban canyons to generic models, and to idealised urban typologies, urban geometry is rationalised as to be associated with resulting environmental phenomena. The present research is based on a very big sample of real urban forms to explore statistically the impact of quantitative geometric parameters on sun-related environmental phenomena, namely insolation, solar availability and spatial thermal diversity. It is acknowledged that this is feasible because, unlike building energy consumption or urban microclimate, the solar exposure of an urban form is highly predictable and determined by two factors, the geometry of the urban form and its position in relation to the sun.

1.2 Research aim and questions

The research explores causal relationships between urban geometry and environmental performance at the neighbourhood scale. More precisely, it examines through a thorough statistical analysis the nature and strength of relationships between urban geometry parameters and performance indicators related to solar radiation availability in the built environment. The aspects of urban environmental performance studied are insolation and spatial thermal diversity in open spaces and, solar availability on building façades and ground. With respect to open spaces, the performance indicators considered are associated with urban microclimate and thus, outdoor thermal comfort. Solar irradiation of façades affects the solar passive and active potential of buildings, with both comfort and energy implications.

Solar radiation is strictly directional and as such, its interaction with the built form is highly predictable. Consequently, the solar exposure of urban surfaces, whether they are sunlit or shaded at a given time, is determined by solely two factors, the geometry of the urban form and its position in relation to the sun. The geometry of an urban form is characterised by its built density, which quantifies the built volume in the site, and urban layout, which refers to how the built volume is allocated spatially, horizontally and vertically, within the site. The position of the sun changes continuously in time, and with location's geographical latitude.

Acknowledging the above, the research investigates in depth the interrelation of urban geometry and solar geometry in defining the solar access and, by extension, solar availability in the urban fabric, and forming the happening of associated environmental phenomena. Its aim is to provide solid evidence for the significance of built density and urban layout in urban environmental design, and the potential for promoting multiple, solar and urban design objectives through their deliberate manipulation. This is linked to the hypothesis that the three elements of the study, urban geometry, solar geometry and resulting sun-related phenomena, are bound in a dynamic relationship of spatial, temporal and geographical characteristics. Temporal and geographical -in terms of latitude- aspects of the relationship are induced by solar geometry; the spatial characteristics of it refer to urban layout, and the way in which this is interrelated to density resulting in diverse urban geometries. Following on that, the scope of the research can be specified into the following research questions:

- To what extent does built density decide environmental phenomena related to the availability of solar radiation and which is the role of urban layout?

Considering that urban geometry has two aspects, the quantitative, i.e. built density, and the qualitative one, i.e. urban layout, the research objective is to gain a better insight into the role of each in defining solar availability and related environmental phenomena. This is pursued following two approaches. First, acknowledging the causal relation between density and solar access, the research explores this causality, i.e. strength of their statistical relationship, in London and Paris, two cities of similar latitudes but very different in terms of urban geometry. Second, controlling the effect of density, it examines whether and, how urban layout affects the availability of solar radiation.

- Whether, and how does the varying solar geometry affect the relationship between urban geometry and sun-related phenomena?

The second question reflects the hypothesis of the research regarding the dynamic relationship of urban geometry with the studied phenomena due to the varying solar geometry. Since the position of the sun in the sky at a location is decided by time and geographical latitude, the effect of them is examined thoroughly and mutually. The effect of time is considered instantaneously -referring to specific sun angles- and on average over different periods -referring to sun paths-. To investigate the sensitivity of the findings to the latitude, a part of the research is repeated testing the same group of urban forms for different locations, Athens and Helsinki.

- Are there environmentally preferable density values?

The research methodology is based on the conceptual distinction of urban geometry into built density, which is negatively associated with solar availability, and urban layout. This is urged by the opposite environmental connotations of built density at difference spatial scales, which suggests a compromise between the two objectives, namely urban densification and environmental quality. The topic is examined considering two environmental objectives relevant to temperate climates, i.e. enhancement of the seasonal solar performance of urban forms and maximisation of thermal diversity in their open spaces.

The three questions are addressed by the research as a whole and link conceptually and narratively the three individual studies comprising it. Each of the three studies constitutes an independent piece of work with its own specific objectives, discussed in the beginning of the respective chapters; however, they all act complementarily in providing a more comprehensive answer to the overriding questions.

To summarise, the research aims to broaden our knowledge and understanding on the dynamic relationship of urban geometry with solar availability, and other environmental phenomena related to it. This is considered to contribute substantially to the ongoing research and discourse on urban geometry considerations in the environmental design, showing the potential for promoting multiple and many times conflicting, urban and solar design objectives. Additionally, all the three studies are based on the analysis of real urban forms found in two European cities, London and Paris, which adds to the research outcomes a practical value. In other words, pursuing its major objective which concerns the understanding of the studied relationships, the research also targets to produce some useful information for urban designers and architects working in the case study cities, especially the main one, i.e. London. According to the topics explored, the research outcomes are meant to be interpreted into a set of guidelines for addressing various environmental design issues, such as diverse seasonal thermal needs indoors and outdoors, solar energy generation on façades, and outdoor thermal diversity.

1.3 Outline of tools and methods used

The present research is based exclusively on the use of computer for the generation/extraction of data, as well as their elaboration and analysis. Various computer tools and methods have been employed at the different methodological stages and in the three studies of the research, for the analysis of the urban forms and the statistical exploration of the results. The studied urban forms are sections from existing urban areas and their 3D geometry was retrieved from shapefiles processed in a GIS package (ArcMap 10.3). The geometric analysis of the urban forms has performed in MATLAB applying image processing techniques on urban forms' digital elevation models (DEMs). Solar radiation simulations have performed using SOLWEIG model and PPF software, while wind maps used for the generation of thermal diversity maps have been produced also in MATLAB. MATLAB has been used extensively in the research for performing different tasks, including -apart for the aforementioned- elaboration of the simulation results and extraction of performance indicators' values, and performing statistical tests. Furthermore, an important part of the statistical analysis has been performed in the SPSS statistical package. The above outline the major tools and methods employed in the research and indicate their great diversity; detailed information regarding them is provided in Chapter Two.

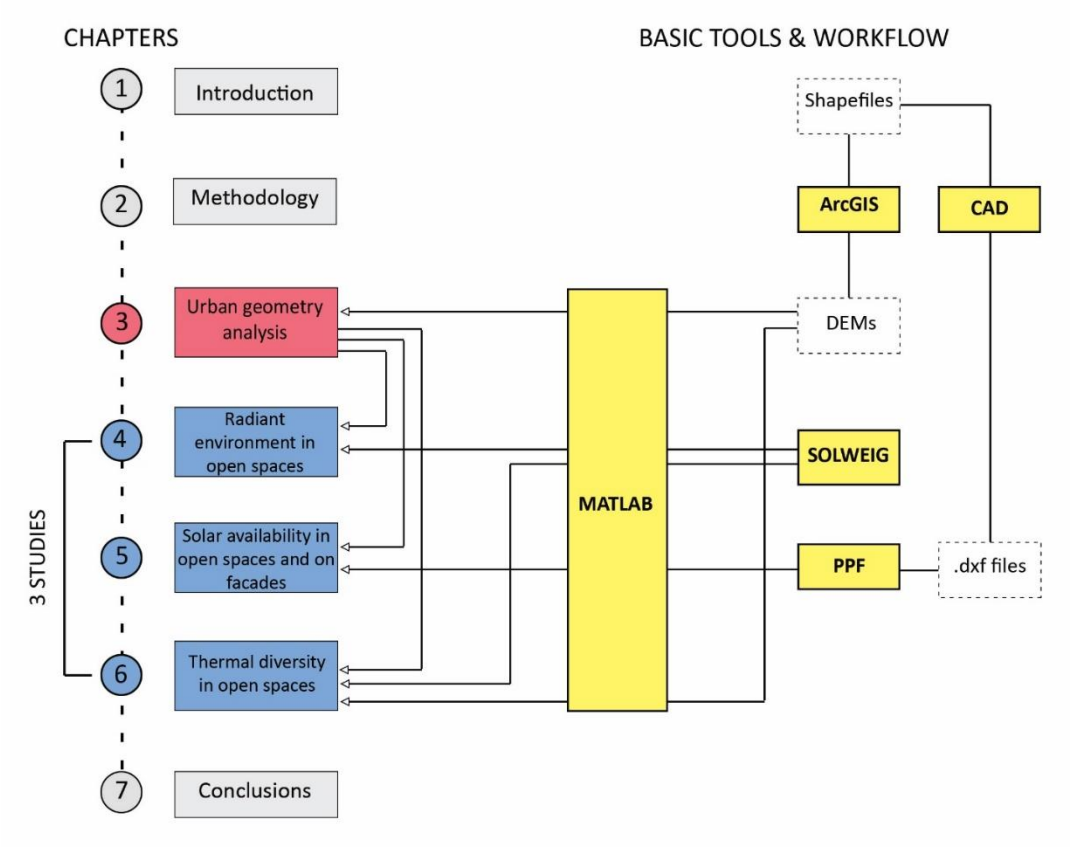

Figure 1.8: Structure of thesis and basic computer tools used in the analysis.

1.4 Structure and content of the thesis

The thesis is organised and presented in seven chapters. Chapters One, Two and Three have a preparatory and supporting role for the comprehension of the three distinct studies of the research which are presenting in Chapters Four, Five and Six; lastly, Chapter Seven outlines the overall conclusions (Fig. 1.8). Having completed the first, introductory chapter which presents the overall topic and aim of the research, the content of the following chapters and their role in the thesis are described below.

Chapter Two presents the overall methodological approach followed, and applied in all the studies. Furthermore, it introduces the main case study city, namely London, and the second one, Paris, which is considered in two -out of three studies- for comparative analysis. The criteria for the selection of the urban forms to be studied are also presented. Finally, the methods and tools employed for the geometric and environmental analysis of the urban forms, as well as the statistical analysis of the results are discussed. The purpose of Chapter Two is to describe the common features of the three studies, in terms

of methodology and methods used, and outline their major differences which are associated to the topics they focus on and relevant objectives.

Chapter Three focuses on the urban geometry analysis and consists of three parts. First, urban geometric measures employed in urban environmental studies are reviewed with respect to the geometric property they refer to, as well as the environmental phenomena they are related to. The second part presents the urban geometry variables selected to be computed for all urban forms and considered for the comparison of London's and Paris' urban geometries. Next, the results of the geometrical analysis of the two cities are presented and discussed extensively. The special purpose of Chapter Three is to introduce urban geometric measures included in the analysis, and identify particularities of urban geometries of the two case study cities as them to be taken into account later in the interpretation of the results.

Chapter Four, Five and Six present the first, second and third study, respectively, and are characterised by the same internal structure. This features an introduction including a targeted literature review, the objectives of the study, a methodology section (outlining the main methodological features and methods employed for the environmental analysis), the results of the study, a discussion section and finally, the conclusions. It is noted that Chapter Five -examining solar availability in open spaces and on building façades- constitutes a hyper-chapter since apart from the main part it includes three more, consecutive sub-studies.

Chapter Four presents the first out of three studies, which explores the radiant environment in open spaces. Specifically, it investigates the relationship between urban geometry and average insolation of open spaces. An earlier study on urban forms of London revealed a strong relationship between density and average mean radiant temperature under cloudy sky conditions, and on sunny daytime hours for increased solar altitudes. Since increased solar altitudes usually coincides with higher intensity of solar radiation and in order for the effect of the former to be isolated, the focus is shifted to the relationship between geometry and insolation of open spaces. Furthermore, considering that the findings may be influenced by the wide range of density values found in London, Paris is also analysed and examined comparatively.

Chapter Five presents the second study which deals with solar availability in open spaces and on building façades. This uses urban forms of London to investigate the relationship of mean SVF and solar irradiances with ten urban geometry variables. Solar radiation simulations have been performed for three time periods, the entire year, a winter month and a summer month, so as to explore whether the studied

relationships are influenced by solar altitudes, as well as to examine the seasonal performance of urban forms. Beyond the main study, three sub-studies have been conducted looking at: (i) the effect of orientation, (ii) the effect of location (i.e. latitude and sky conditions) and (iii) the relationship of SVF and solar availability.

Chapter Six presents the last study which focuses again on open spaces exploring the occurrence of spatial thermal diversity within them. Like the first study, the analysis is carried out comparatively for urban forms of London and Paris. The concept of spatial thermal diversity is first introduced, and next the method employed for mapping and quantifying it is presented. Using a formula which was developed for this purpose, thermal diversity values are computed based on average and instantaneous thermal diversity maps. Next, the relationship between thermal diversity and degree of built obstruction, expressed by density and site coverage, is examined.

Finally, Chapter Seven is the concluding chapter which concentrates the major contributions of the thesis to knowledge and the subject area of urban environmental design. Specifically, the chapter is divided into three parts. In the first part, the most significant findings are provided aggregately in relation to the research aim and questions, as those defined in Section 1.2. Next, their applications in and implications for urban environmental research and practice are discussed highlighting the dual character of the contribution of the thesis. Lastly, suggestions about possible directions for future research are made underlining particularly the need for the major findings to be tested further.

1.5 Conclusions

This chapter introduces the subject and aim of the research under which the three studies are linked to each other, and sets the scene for the rest of the chapters which present the different parts of the current thesis. Prior to the formulation of the research aim and questions, it was considered necessary to provide a broad overview on the subject considering its two main components, namely urban geometry and solar availability, and how these are related in a real context. The significance of the solar radiation for promoting urban environmental sustainability was discussed, as well as the key role of urban geometry and solar geometry in deciding the solar exposure of urban surfaces. Special emphasis was put on multiple, and many times, conflicting solar design objectives to be pursued by the modification of urban geometry in the urban design process. Furthermore, different ways in which past studies have dealt with the complexity and diversity of urban geometry investigating relevant topics were reviewed, highlighting their differences to the current methodological approach. Overall, it became evident that the relationship

between urban geometry and solar availability needs to be explored systematically and in depth, incorporating the newly available resources which enable the study of real urban forms. This is anticipated to contribute to a more informed and responsive urban environmental design as concerns the attainment of solar-related targets. Finally, major methods and tools employed in the research were briefly outlined indicating its wide scope; these are analytically presented and discussed in Chapter Two along with the methodological approach and stages followed.

Chapter Two

Methodology and methods used

Chapter Two presents the methodology of the research, as well as the methods and tools used for the investigation of relationships between urban geometry and sun-related phenomena. More specifically, it presents the three methodological stages which are common in all three studies, and outlines their major differences in terms of case studies, simulation tools and performance indicators used. These are related to the topic which each study focuses on and the respective research objectives. Furthermore, the method employed for the geometric analysis of the urban forms is discussed, while urban geometry variables considered in the research are presented analytically in the following chapter.

2.1 Introduction

The thesis is an articulated research which consists of three distinct studies. All of them lie under the same thematic umbrella examining relationships between urban geometry and aspects of environmental performance in the urban environment, mostly related to solar radiation availability and solar access. The first and third study, in the order of these being presented, investigate phenomena occurring in open spaces, namely outdoor radiant environment and thermal diversity; whereas, the second study examines simultaneously solar availability in open spaces and on building façades. The methodology approach is common and related to the fact that the impact of urban geometry on the above phenomena is investigated statistically using real urban forms, at the neighbourhood scale. On the other hand, the studies present differences in case studies used, and geometric and environmental parameters considered in the analysis which are defined by the topic that they focus on and their research objectives.

This chapter describes the overall process followed in the research. The first part outlines the methodological stages characterising the three studies, as well as their major differences which are explained further later. The second part presents the major case study, London, and Paris which has been analysed comparatively in two -out of three- studies. The research is based on urban forms selected from each city and their urban digital elevation models (DEMs); so, the next section provides detailed information regarding the processes followed for the generation of the DEMs of the two cities, and the selection of urban forms to be analysed. Furthermore, the two solar simulation tools employed for the

environmental analysis of the urban forms, SOLWEIG and PPF, are presented, as well as performance indicators considered in each study. The last section mentions in brief statistical tests and software employed for the exploration of the relationships between urban geometry variables and performance indicators.

2.2 Methodological stages and approach

The methodological stages of the research are three, as follows:

(i) the analysis of the geometry of the urban forms, computing a set of geometric variables;

(ii) their environmental analysis, computing selected performance indicators;

(iii) the statistical elaboration of the results of the two previous stages in order for their potential correlations to be examined.

In turn, the methodological approach is defined by some principles. First, since the research focuses on entire urban areas, rather specific points within them, all data, namely urban geometry variables and performance indicators, concern average values and are obtained by computer-based methods. Furthermore, unlike other studies which apply a top-down methodological approach limiting the complexity of urban geometry to representative urban typologies found in cities, this research examines the studied relationships in real urban forms. Therefore, their statistical exploration is based on the great magnitude of the sample used and, consequently, the acquisition of a tremendous size of raw data. Finally, because the research aim is to investigate the impact of urban geometry, other parameters that may significantly affect the occurrence of the studied phenomena in real conditions, such as building materials, are isolated and not considered.

In this context, only two studies have been found in the literature which can be regarded as close precedents of this research. The first one is the work of Lindberg and Grimmond (2011a) which employs a similar methodology to investigate the influence of building morphology and nature of vegetation on shadow patterns and mean radiant temperatures in 19 sites in London. The other one is the study by Mohajeri et al. (2016) which focuses on the relationship between six density indicators, such as site coverage and plot ratio, and buildings' solar potential in 16 neighbourhoods of the city of Geneva, Switzerland.

All the above form the core of the methodology applied in the three studies. On the other hand, there are parameters which differ as adjusted accordingly to the specific objectives of each study. These parameters are outlined in the following:

(i) Cities used as case studies and number of urban forms. The two studies focusing on the environmental performance of open spaces are based on 132 urban forms in total, 72 in London and 60 in Paris. The second study examining solar availability both on the ground level and building façades is based on 24 -out of 72- urban forms of London.

(ii) Urban geometry variables included in the statistical analysis.

(iii) Environmental indicators examined and thus, simulation tools employed for their computation.

Table 2.1 presents an overview of the above parameters in each study. The following sections provide information about the case studies, as well as the methods and tools used in the different stages of the analysis. The geometric analysis of the studied urban forms is presented in Chapter Three and urban geometry variables considered are given analytically in Section 3.3.2. For facilitating the reading of the thesis, more specific aspects of the methodology and their connection with the objectives are discussed in the beginning of the chapters presenting each study, i.e. Chapters Four, Five and Six.

Table 2.1: Main methodological features in each of three studies.

	Studies	**Simulations**	**Cities**	**No. of urban forms**	**Urban geometry variables**	**Environmental performance indicators**
1	Radiant environment	ground	London Paris	72 60	• all 18 variables • average SVF	• average SVF • average insolation • average mean radiant temperature
2	Solar availability	ground & facades	London	24	• 10 variables • average SVF	• average irradiances • average SVF
3	Thermal diversity	ground	London Paris	72 60	• density • coverage	• thermal diversity values

2.3 Case studies

London is the major case study of the present research with urban forms used in all three studies. As the capital and most populous city of the United Kingdom, and the second largest city (referring to Greater London's urban area) in the European Union, London has drawn the attention of numerous researchers dealing with the environmental impacts of urbanisation and energy performance of built environment. Numerous studies have reported on London's urban climate and urban heat island characteristics (Bohnenstengel et al., 2001; Drew et al., 2013; Giridharan and Kolokotroni, 2009; Grawe et al., 2013; Watkins et al., 2002) and their energy- and comfort-related implications (Day et al., 2009; Kolokotroni et al., 2006; 2012; Mavrogianni et al., 2011; Watkins et al., 2007). Studies have also investigated energy demands in London's domestic and non-domestic buildings (Choudhary, 2012; Ghoudhary and Tian, 2014; Ratti et al., 2005; Rode et al., 2014; Steadman et al., 2014), or solar and other renewable energy potential (Ahmed, 2016; Coles et al., 2016; Sarralde et al., 2015; Simms et al., 2008). Whereas, other studies have been focused on the variation of microclimatic conditions and their relationship with urban characteristics, such as geometry, ground surface and vegetation, in specific sites (Lindberg et al., 2016; Shahrestani et al., 2015), or across the city (Lindberg and Grimmond, 2010; 2011a). It is thus apparent that London offers plenty of research data which offer ground for comparison. More importantly, it presents a significant diversity, in terms of geometry, which was considered vital for the purposes of the research.

Additionally, for the two studies examining relationships between urban geometry and environmental phenomena in outdoor spaces, a second city has been selected to be comparatively analysed, Paris. London (51°30'26'N, 0°7'39'W) and Paris (48°51'24'N, 2°21'03'E) are located in close proximity, and thus, are of similar geographical latitudes and within a similar climatic context. Monthly weather data for the locations are provided for comparison in Appendix A. On the other hand, they present major differences in their urban geometry, which are tightly interwoven with their history and tradition in urban planning in the last centuries. Paris exemplifies the planned European cities with its tight urban fabric and prominent wide and straight boulevards, and a high degree of order, compactness and uniformity (Benevolo, 1993; Evenson, 1979). On the other hand, London is considered a general exemption, "*the most resistant* [city] *to a general plan*" (Benevolo, 1993, pp. 204). Its urban area has been rather developed by an order of magnetism around its centre, i.e. Central London, and its overall urban fabric presents a high degree of incoherence and heterogeneity (Hall, 1989). The comparative analysis of urban

forms in the two cities provides a deeper insight on the causal relationships between geometry and resulting radiant and thermal environment in open spaces.

For London's analysis, 72 urban forms were selected from three representative areas: in central, west and north London, which are of high, medium and low built density, and of 2 x 6km, 1.5 x 6.5km and 2.5 x 6km surface area, respectively (Fig. 2.1). Paris is represented by 60 urban forms from its entire urban area enclosed by the city's current peripheral road (Fig. 2.2). All urban forms are of 500 x 500m size which corresponds to the so-called neighbourhood scale. Similar spatial scales have been used by previous studies on relevant topics, either focusing on buildings (Martins et al., 2014; Ratti et al., 2005; 2006; Rode et al., 2014), or open spaces (Lau et al., 2015; Lindberg and Grimmond, 2011a; Thorson et al., 2011).

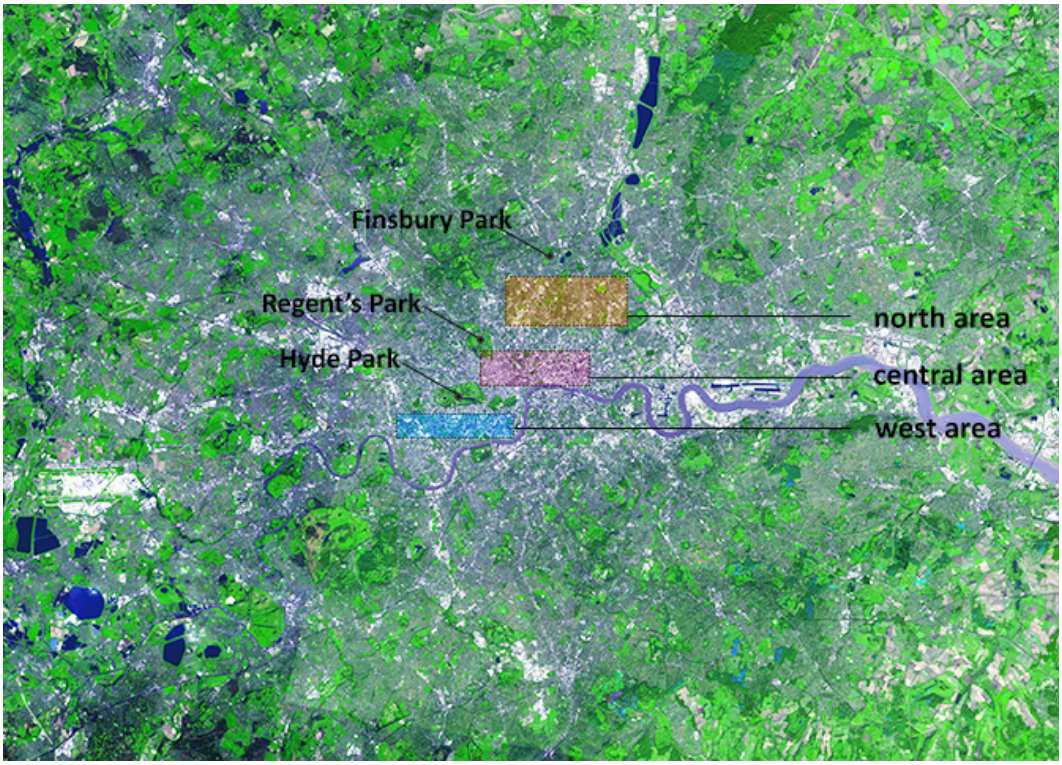

Figure 2.1: Satellite image of Greater London Urban Area with coloured rectangular shapes spotting the three areas analysed.

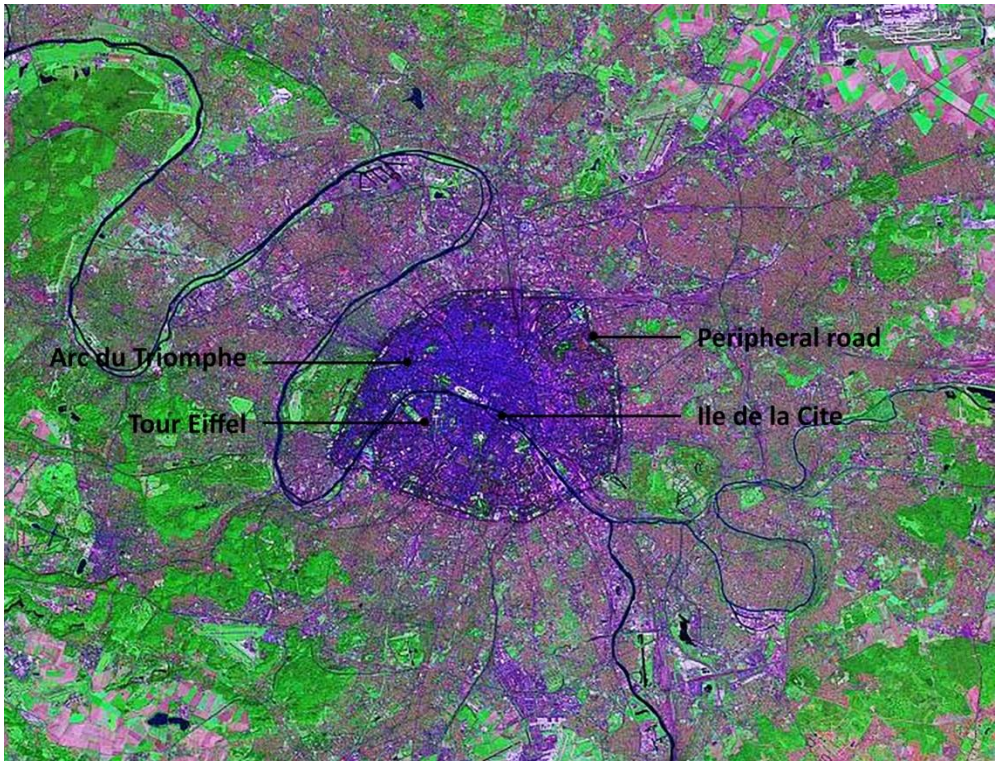

Figure 2.2: Satellite image of Paris' urban area, in dark purple colour the area enclosed by the city's peripheral road and included in the shapefile obtained.

It is worth highlighting that the idea behind the processing of urban DEMs is essentially to perform environmental analysis, replacing demanding in time and computer effort simulation programmes (Ratti and Richens, 2004). For this purpose, a series of urban geometry parameters, such as surface-to-volume ratio, height-to-width ratio and directionality, are computed and used as environmental indicators for assessing urban forms' performance. In the context of the current research, urban geometry parameters derived from the analysis of urban forms' DEMs are not used as environmental indicators, rather their relationship with the environmental performance of urban forms is explored through an extensive statistical analysis.

Employing the particular technique for the analysis of urban geometry presents some advantages, as well as limitations, compared to the other method used for this purpose, which is based on vectorial models. The main difference between the two methods is that, in the latter, buildings volumes are recognized as objects, i.e. shapes of specific perimeter, area, etc.; therefore, the calculation of buildings' metrics are straightforward and precise. On the other hand, processing urban DEMs, measurements of buildings' metrics involve counting of pixels (measurements on the horizontal plane) and pixels' values (considering

vertical dimension), and their accuracy is affected by the resolution of DEMs, i.e. the higher the resolution and the more accurate the measurement (Fig. 2.3). For instance, the built area is obtained by counting the pixels with value higher than 0 and multiplying it with pixels' scale. Similarly, the total built volume is calculated by summing the pixel values and multiplying by the scale. The measurement of building perimeter (used also in the calculation of façade area) is more complicated and requires first the detection of edge pixels (Fig. 2.3c). The algorithm used is based on that of Ratti (2001) which is described in Ratti and Richens (2004).

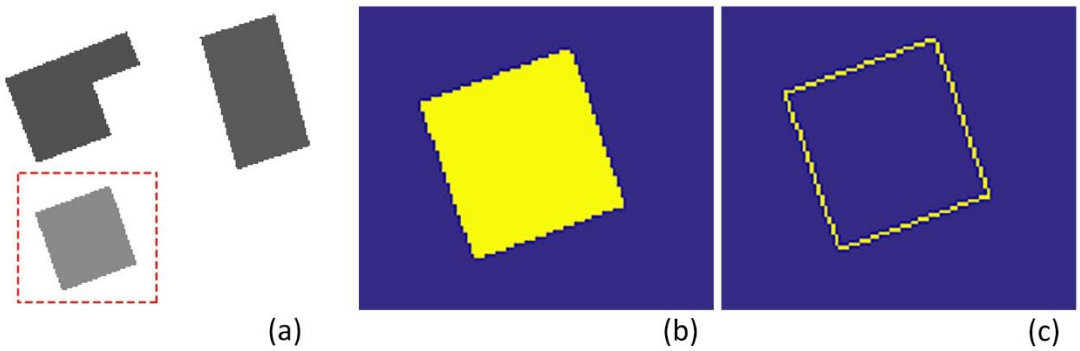

Figure 2.3: Some building as appear in DEM (a), pixels defining its footprint area (b), and perimeter(c), highlighted in yellow.

Nevertheless, processing DEMs offers a considerable freedom and flexibility in computing more sophisticated metrics, especially regarding open space, such as *directionality* and *mean outdoor distance* used in this research and defined in Section 3.3.2. This great advantage of using DEMs for the analysis of urban geometry stems from the fact that in the particular method built and non-built spaces are treated in equal terms, namely as pixels; whereas, in vectorial models, the built volumes are well-defined objects but the open space is treated as a complimentary area (Hermosilla et al., 2014).

2.3.1 Generation of DEMs

The DEMs used were generated based on the 3D information of buildings' geometry, downloaded from online database in shapefile format (.shp). The shapefile of London was obtained from the Centre for Environmental Data Archive; while this of Paris was obtained from Service de la Topographie et de la Documentation Foncière. Their conversion into DEMs was done in the ESRI ArcGIS ArcMap 10.3 software, a Geographical Information System package. It is noted that the shapefile of London was too large to be processed, even for the 16G RAM of the machine used. For this reason, three smaller areas within it were selected and isolated from the original shapefile. Since at that stage, there was no detailed information

regarding the urban geometry of different areas of London, the three areas were selected as representative of different built densities.

Furthermore, the shapefiles of the two cities have been generated by different technological methods which entails important differences in the precision of the information that these contain. The shapefile of London was generated using remotely sensed data (data collected by a sensor that is not in direct contact with the area being mapped, e.g. a satellite) which had as a result large features, such as canopies of big trees, to appear as built constructions. This problem was overcome by comparing the shapefiles of the selected areas with images provided by Google Maps and deleting the objects that did not represent buildings. On the other hand, the shapefile of Paris was generated by digitalising the ground map of the city and inserting manually building height information in number of floors. Therefore, Paris' shapefile was more precise regarding building footprints but, the building height information had to be interpreted from number of floors to actual height in meters. This was done by multiplying the number of floors by 3 [m] reflecting typical floor height, and then adding 1.5 [m] to account for raised ground levels.

Next, the shapefiles of the three areas of London and Paris were converted into DEMs of 0.5m spatial resolution, namely each pixel in DEMs represent an 0.5 x 0.5m area. The resolution of DEM affects the calculation of urban geometry parameters, and especially those related to buildings' perimeters; on the other hand, the higher the resolution is the greater the computational effort needed for their analysis. The spatial resolution applied is considered high compared to those used by previous studies. For instance, the urban geometry analysis performed by Ratti et al. (2005; 2006) was based on DEMs of 1.56m pixels, whereas the DEM used by Thorson et al. (2011) had a resolution of 1m pixel.

Moreover, the DEMs produced are 2.5DEMs, namely they represent building footprints and heights, but not the geometry of roofs which are considered horizontal planes. Hence, the analysis of urban geometry concerns the geometry of main building volumes and their relative configuration within the site. In practice, the roofs may affect solar availability in urban environments, e.g. if they are pitched and of significant height, by casting shadows on other buildings and the ground. However, since the research aim is not to evaluate the actual performance of the studied urban forms, but to draw conclusions on the mechanisms governing the relationship between urban geometry and environmental performance, this was not regarded as a restriction; on the contrary, it was desirable. Finally, the elevation of the ground is constantly equal to zero, meaning that potential inclinations of the ground surface in different urban areas were not considered. This was necessary as the impact of slopes on solar availability might interfere with that of urban geometry which is the focus of the research.

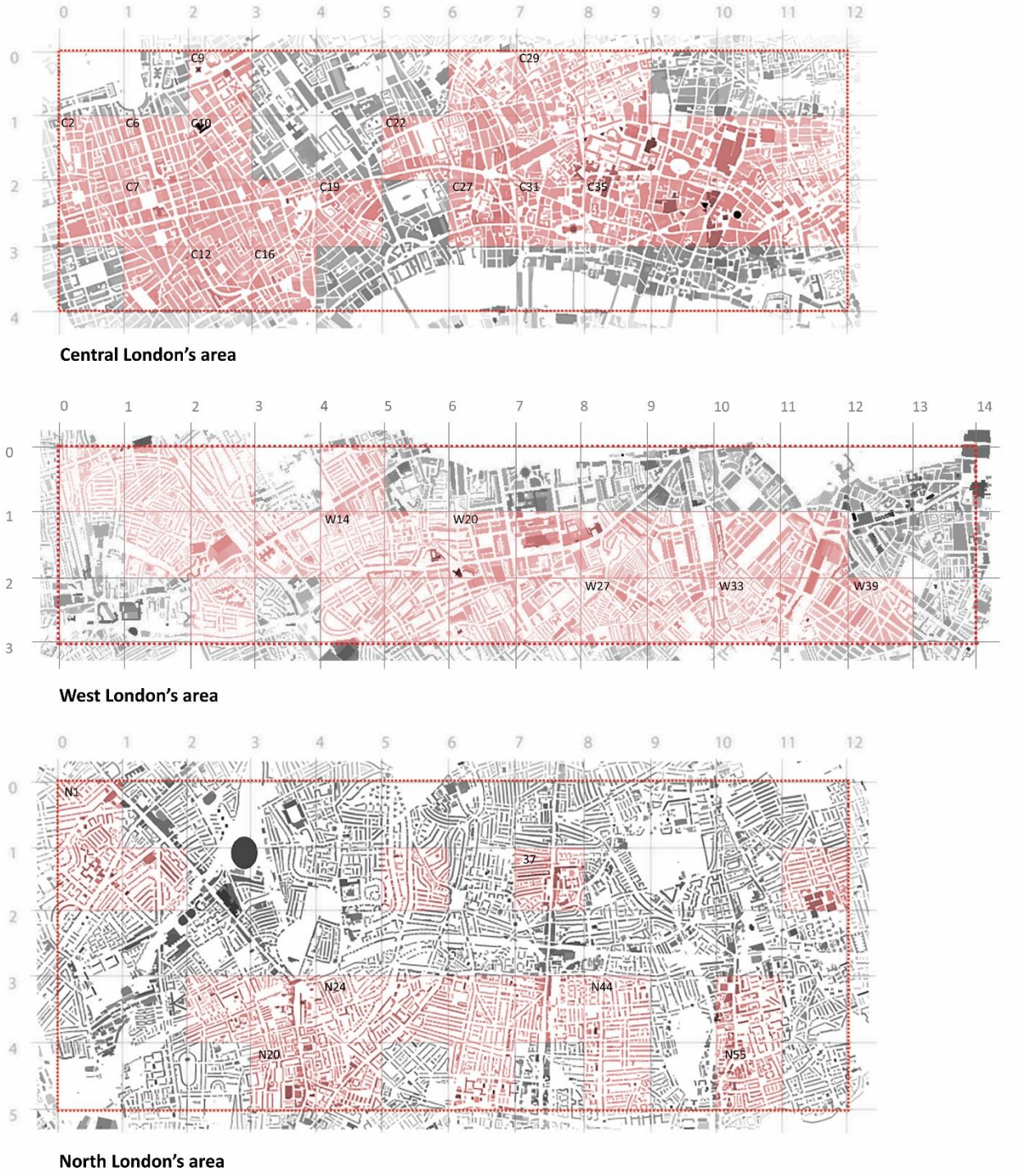

Figure 2.4: DEMs of three areas in London, divided into cells of 500 x 500m; 72 urban forms selected to be included in the analysis (28 in central, 25 in west and 19 in north London) highlighted in red; 24 urban forms included in the second study identified by their naming.

2.3.2 Selection of urban forms

Once the DEMs of the three areas of London and Paris were produced, they were inserted in Mathworks MATLAB software and divided into cells of 500 x 500m surface area. For the selection of the urban forms to be studied, all cells were first analysed computing a series of urban geometry variables, which are presented analytically in Section 3.3.2. The selection criteria were the following: (i) continuity of urban fabric, (ii) acquisition of a wide range of built density values, and (iii) inclusion of different urban geometries, referring to urban layout.

In this way, many of the initial cells were removed from the analysis as inappropriate because they presented some sort of discontinuity in their urban fabric, i.e. part of them fell into large urban voids, such as parks, railways, rivers (Thames in London and Seine in Paris) or canals. Additionally, in the case of Paris, the cells including monuments, such as Eiffel Tower and Palais de Tokyo, were also rejected because their height -as that was calculated from the number of floors in the shapefile- was strikingly lower than the actual one. The second criterion applied was the two samples to cover wide range of density values. So, the remaining cells were ranked by built density values, identifying their range in London and Paris. When the density of a cell was unique, this was automatically included in the sample. When many cells presented the same density, the condition for their selection was the inclusion of different layouts. This was accomplished first by observation and then, by comparing the values of urban geometry variables computed for them.

The above process was first completed for London, in which the range of density values was found to be significantly large, i.e. 3 to 33 m^3/m^2. The highest densities are identified in the City of London (central London), and the lowest ones in the district of Islington (north London). The final number of cells (hereafter referred to as *urban forms*) selected was 72, including 28 in central London, 25 in west London and 19 in north London (Fig. 2.4). In Paris, density values present a relative homogeneity with their range to be limited, i.e. 5 to 11 m^3/m^2. For this reason, another criterion was applied which was the final sample to include squares across the urban area of Paris. In this way, the sample of 60 urban forms selected may be regarded as representative of urban geometries found across the city (Fig. 2.5). Its size is smaller but still comparable to the number of squares selected from the three areas of London; considering the range of densities that it covers, it becomes apparent that in Paris' sample, different density values are represented on average by a larger number of urban forms.

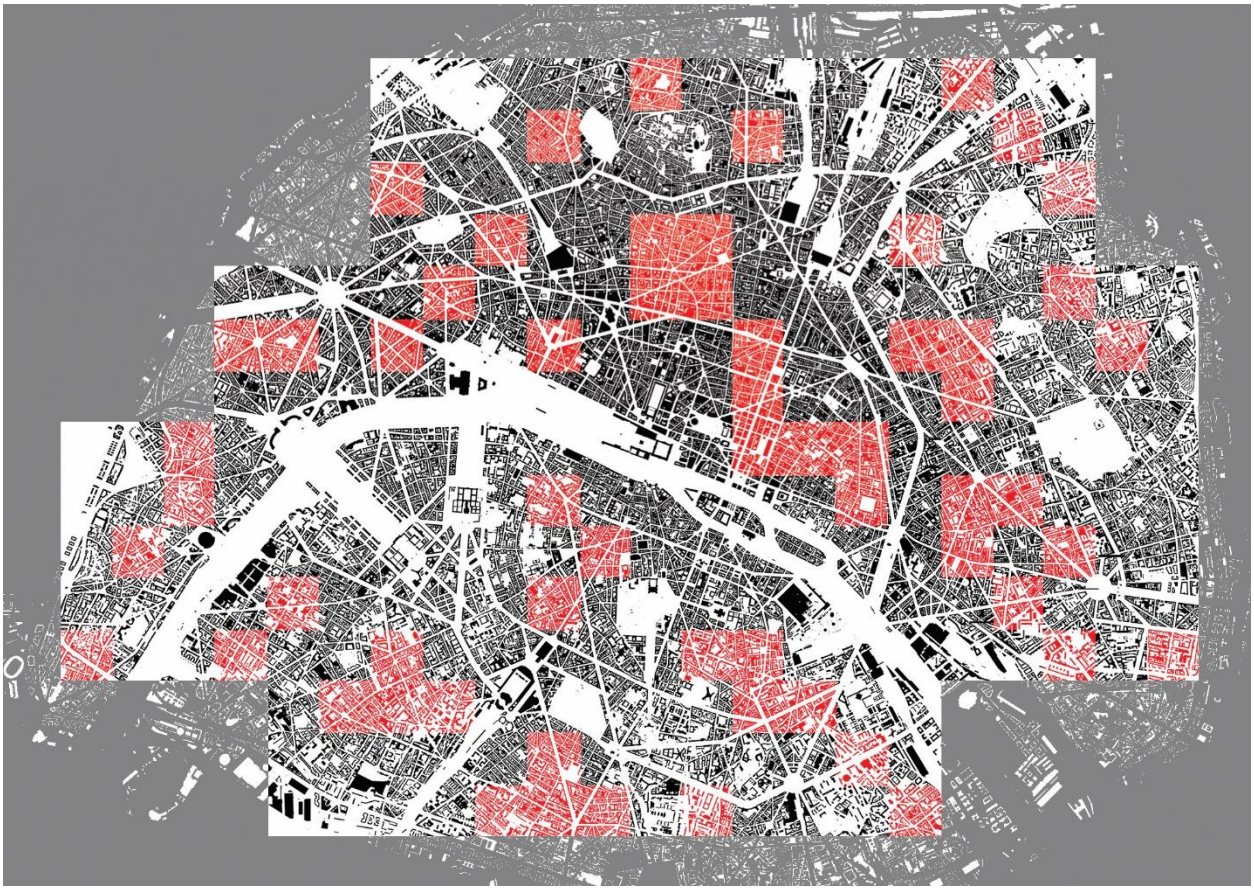

Figure 2.5: Shapefile of Paris: analysed area on white background, and 60 selected urban forms (of 500x500m area each) highlighted in red.

The sample of 132 urban forms in total, 72 for London and 60 for Paris, was used in the first and third study, which focus mostly on the relationship of density parameter with the environmental performance of open spaces. Since the scope of the second study broadens as to examine solar availability both in open spaces and on building façades, it was considered necessary the analysis to focus entirely on the major case study, i.e. London, and include a smaller number of urban forms. In addition, a key objective of this study is to examine comparatively the impact of urban density and urban layout -as two distinct parameters of urban geometry. For this reason, ensuring diverse but also continuous density values in the new sample was deemed crucial for the selection of urban forms.

Examining the density values in the 72 urban forms of London, it was ascertained that those of density higher than 22 m^3/m^2 were only three, all in the City of London -of approximately 28, 29 and 33 m^3/m^2-. As their inclusion would induce a significant discontinuity in the sample, the particular urban forms were removed, and the studied range of densities was limited to between 3 - 22 m^3/m^2. Next, the criterion applied was the continuity of density values to be achieved by pairs of similar density but as much as

possible different layouts. As before, the diversity of urban layouts was evaluated first by observation, and then comparing the values of geometric variables.

Through this process, 24 urban forms were selected to be include in the second study, including 6 in north, 5 in west and 13 in central London, covering densities between 3-6, 5-11 and 10 -22 m^3/m^2, respectively. The DEMs of 24 urban forms are presented in Appendix B, and their positions within three London's areas are seen in Figure 2.4. The naming used for distinguishing them is formed by a letter, denoting the area they belong to (i.e. C for central, W for west, and N for north) and a number, which derives from the numbering of the cells in the maps of the three areas (by columns, starting from the top left cell).

2.4 Environmental simulations

2.4.1 Overview on urban solar simulation tools

Modelling solar radiation availability in urban settlements dates back to simple computer models developed in the 1980s to assist with site layout planning. In particular, the "solar envelope" introduced by Knowles (1981) was based on the imperative that a new building should not overshadow their surroundings during critical periods of solar access. Similar models, which regulate the buildable volume within a given site derived from the sun's relative motion, have been developed incorporating new tools for its calculation and representation (Capeluto and Shaviv, 2001; Capeluto et al., 2006; Morello and Ratti, 2009). To support solar access decision-making in new developments was also the purpose of computer programmes, such as TOWNSCOPE II, developed in the context of the POLIS project (Teller and Azar, 2001). As pointed out by Littlefair (1998), the major limitations of the then available computer programmes concern mostly the treatment of diffuse radiation, and reflected radiation from the ground and obstruction.

From 2000 onwards, significant advances were made to urban solar radiation modelling which increase the accuracy of simulations as well as the efficiency of the models. Means of accounting the effects of nearby obstructions, i.e. shading by, and inter-reflection from other buildings and surfaces, and considering realistic, anisotropic sky lighting were the two major areas of improvement (Mardaljevic and Rylatt, 2003; Robinson and Stone, 2005). Equally important, models were optimised to become more scalable and thus, more efficient in computational time and resources, as well special emphasis was put on the visualisation of simulation data (Compagnon, 2004; Mardaljevic and Rylatt, 2003). These advances have fostered the use of solar radiation modelling for evaluating the feasibility of solar active strategies (i.e. solar thermal collectors and photovoltaic cells) and potential offset in energy demands for

heating/cooling or lighting (i.e. passive design) at urban scale. Many of the relevant simulation tools make use of the backwards ray-tracing programme RADIANCE (Ward Larson and Shakespeare, 1998), including CBDM (Mardaljevic, 2010), DIVA (Jakubiec and Reinhart, 2011), and PPF (Compagnon, 2004). Whereas, SUNtool (Robinson et al., 2007) and its successor CitySim (Robinson et al., 2009) simulate holistic urban fluxes employing a Simplified Radiosity Algorithm (Robinson and Stone, 2005) for predicting radiant energy flux on building surfaces.

On the other hand, the wide application of urban solar modelling relies on the availability of 3D geometry information, the modelling of complex urban geometries and the reliable import and export of them in different programmes involved in the process (Horvat and Dubois, 2012). Given the increasing use of remote sensing technologies for obtaining high-resolution data that allow the creation of digital urban models, the above issues are addressed by the implementation of solar radiation models in Geographical Information Systems (GIS). Most of these tools, such as the well-known ArcGIS Solar Analyst (Fu and Rich, 2000) and GRASS r.sun (Šúri and Hofierka, 2004), have been developed for evaluating the photovoltaic potential of roofs. The accuracy of their solar radiation modelling varies, and improvement is required regarding the establishment of an adequate characterisation of radiation components, the consideration of changing atmospheric conditions and the effect of shadows (Martins et al., 2015). Nonetheless, there is a vast, ongoing research for the optimisation of methods and the incorporation of various technologies, such as LIDAR and image processing (e.g. Carneiro et al., 2009; Jakubiec and Reinhart, 2013). More recent models are able to simulate solar availability both on roofs and façades (Hofierka and Zlocha, 2012; Lindberg et al., 2015; Redweik et al., 2013).

Beyond tools which simulate solar radiation availability on buildings, there is another category of computer programmes which involve solar radiation modelling on the ground level to assess microclimatic variations in open spaces. Such programmes are the SOLWEIG model (Lindberg et al., 2008), RayMan (Matzarakis et al., 2007; 2010) and ENVI-met model (Bruse and Fleer, 1998), in an increasing order of complexity and number of parameters considered in the modelling. SOLWEIG simulates spatial variations of 3D radiant fluxes, based on which it calculates variations of mean radiant temperature in open spaces. RayMan calculates mean radiant temperature, but also considers other environmental inputs for calculating thermal comfort indices, such as Physiological Equivalent Temperature – PET (Höppe, 1999). Finally, the ENVI-met model uses a holistic approach in which all aspects of microclimate are simulated, including air flow, and linked in a complex model.

The above outline in brief the major applications of urban solar modelling nowadays, and some of the computer programmes employed. A detailed review on available computational solar models, along with their advantages and limitations, is presented in Freitas et al. (2015).

2.4.2 Radiation simulations

In the context of this research, two simulation tools have been used, the SOLWEIG model and PPF software; both can accurately simulate solar quantities over large urban areas. SOLWEIG simulations were performed for analysing the outdoor radiant environment in the 72 urban forms of London and 60 urban forms of Paris. The data derived from the simulations were used to calculate the environmental indicators in the first and third study (Chapters Four and Six, respectively). It was selected among alternative programmes for two basic reasons. The first one is related to the purposes of the research and the fact that the studies examine radiant environment and solar availability in open spaces, without any intention to evaluate overall microclimatic conditions or outdoor thermal comfort. Since SOLWEIG performs solar modelling in an efficient and straightforward way, there was no need for more complex tools, such as RayMan and Envi-Met mentioned before. The second reason is that SOLWEIG uses urban DEMs as 3D geometry input, and MATLAB as compiler, which facilitates the processing of output files (all done in MATLAB). The model has been evaluated by several studies and in different locations (Lindberg and Grimmond, 2011b; Lindberg et al. 2008; Chen et al., 2014), and used for assessing mean radiant temperature variations as well as, their relationship with other urban parameters (e.g. Lau et al., 2015; Lindberg and Grimmond, 2011a; Lindberg et al., 2014; 2016; Thorsson et al., 2011).

PPF has been employed for simulating solar availability in 24 urban forms of London selected for the second study (Chapter Five). It is a powerful solar modelling tool and, at the same time, flexible to modifications for meeting specific requirements of different research projects. For instance, for the purposes of this research, PPF was adjusted to simulate solar irradiance both on ground and façades, which constituted a sufficient criterion for its suitability. It has been developed by Compagnon (2000) in the context of the PREcis project (2000), and tested performing irradiance and illuminance simulations for urban areas in various European cities. Afterwards, it has been employed by several studies, such as this of Cheng et al. (2006a; 2006b) which investigated the diverse influences of built density on daylight access and solar system potential, examining existing areas and generic models. Furthermore, Montavon et al. (2004) demonstrated its usefulness for estimating solar energy and passive potential on building fabrics, comparing building layouts across three Swiss cities.

More information about the two programmes and simulations performed are given in the following sections.

2.4.2.1 SOLWEIG software

The SOlar LongWave Environmental Irradiance Geometry (SOLWEIG) model simulates spatial variations of 3D radiation fluxes (incoming to / outgoing from the ground, direct and reflected) and mean radiant temperature (MRT) in complex urban settings (Lindberg et al., 2008). SOLWEIG is a 2D model, namely simulations concern exclusively horizontal surfaces, ground and roofs. Ground simulations are performed for a notional plane at 1.1m height above the ground. The model requires the following inputs for running: a 3D geometry in DEM format, a 24-hour weather file (including temperature, humidity, global, direct and diffuse solar radiation information) and geographical information of location (i.e. latitude, longitude and elevation) (Fig. 2.6).

The simulation of radiation fluxes involves the calculation of spatial variations of sky view factor and shadow patterns which are both based on the *shadow casting algorithm* developed by Ratti and Richens (1999). Briefly, the algorithm is applied in DEMs and casts shadows on horizontal planes, i.e. ground and roofs, for a given sun position which is defined by two input values, solar altitude and solar azimuth. After the application of the algorithm, each pixel in the DEM is assigned either 0 or 1, denoting sunlit and shaded conditions, respectively. The SVF is calculated by repeated application of the algorithm for 1000 random sun positions and averaging of pixels' values. A detailed description of the technique is given in Ratti (2001). It is noted that simulations of spatial variation of SVF and shadow patterns can be performed independently to MRT ones, based on urban geometry, and urban geometry and time/location, respectively.

All the simulation results are generated in matrices of the same size as the DEM used, and provided in tables (.asc) and images (.tiff). Simulated quantities are thus computed for every pixel in DEMs and, the matrices represent the same spatial resolution, i.e. 0.5m. Figure 2.7 demonstrates the DEM of an urban form and three sorts of maps produced in SOLWEIG: (i) SVF maps, (ii) shadow patterns, and (iii) MRT maps. As seen, the original area of the urban forms was extended by 100m in all directions to consider the effect of the surrounding buildings.

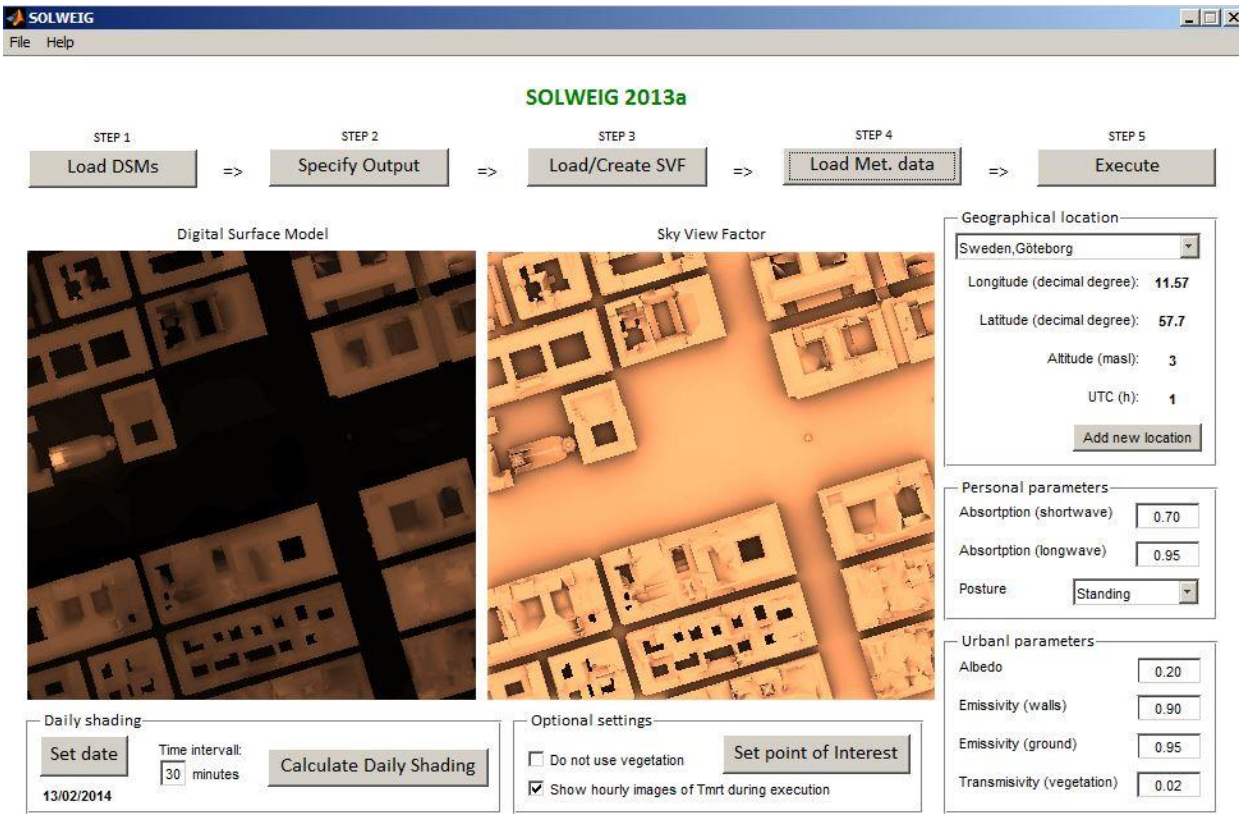

Figure 2.6: Interface of SOLWEIG 2013a showing all input parameters (personal and urban parameters seen at the right are set to the default values).

The research used the SOLWEIG 2013a version which was available when this commenced. In the latest versions, it is possible to use any time resolutions in the weather file -considered in MRT simulations- which was restricted to 1 hour in the version used. Mean radiant temperature analysis was conducted for 72 urban forms of London, and hourly MRT simulations were run for 8 days (21 June, 26 July, 23 April, 20 March, 19 October, 23 November, 19 January and 29 December). Hourly weather data were obtained from London's weather file, representative of a typical year, based on data collected from Islington weather station in North London (ECOTECT Weather File Library). The weather file provides representative weeks for each season, from which, 26 July and 29 December were selected as representative days of the summer and winter period, respectively. Regarding the rest of them, sunny and cloudy days have been considered, evenly distributed in the year, in order for the effect of sky conditions and solar altitudes to be examined. It is noted that urban and personal parameters considered in the calculation of MRT are set to default values, as appeared in Figure 2.6.

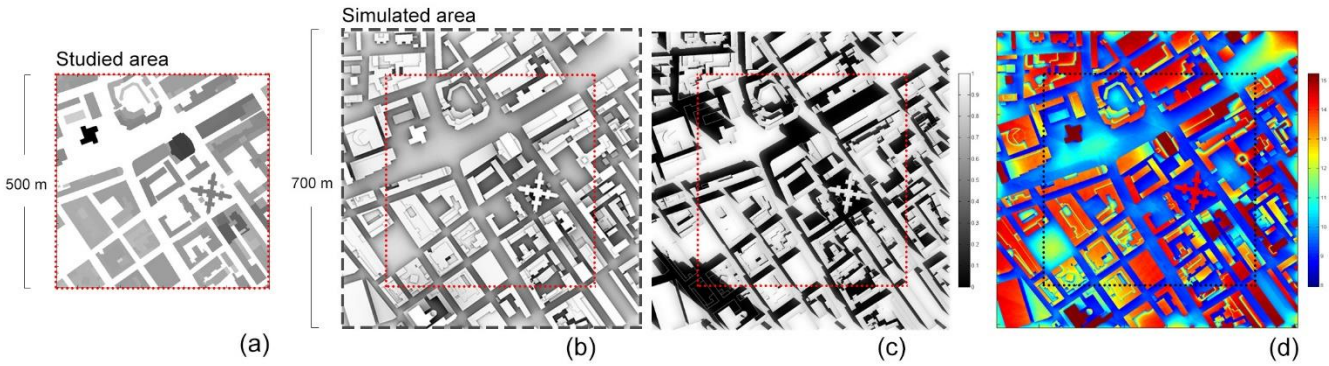

Figure 2.7: Urban form C9 in central London (see Figure 2.4): a) DEM, b) SVF map, c) shadow pattern at 9am on 23 April and d) MRT map at 9am on 23 April (cloudy hour).

SVF maps and shadow patterns were produced for all 132 urban forms, 72 in London and 60 in Paris. Shadow patterns were generated for three representative days, 21 June (summer solstice), 21 March (equinox) and 21 December (winter solstice), from sunrise until sunset, at 10-min intervals, as suggested for complex environments by previous studies (Lindberg and Grimmond, 2011b; Yu et al., 2009). In this way, and based on locations' latitude, the shadow patterns produced on 21 June, 21 March and 21 December were 99, 73 and 47 for London's urban forms, and 97, 73 and 49, for Paris' ones, respectively.

2.4.2.2 PPF software

For the assessment of urban solar availability in 24 urban forms of London, irradiance and SVF simulations were performed in PPF software. Direct (*Id*), diffused from the sky (*Is*) and reflected by buildings (*Ib*) irradiances [W/m^2] are computed separately; while global (*Ig*) irradiance is calculated as the sum of them, as described below:

$$Ig = Id + Is + Ib$$

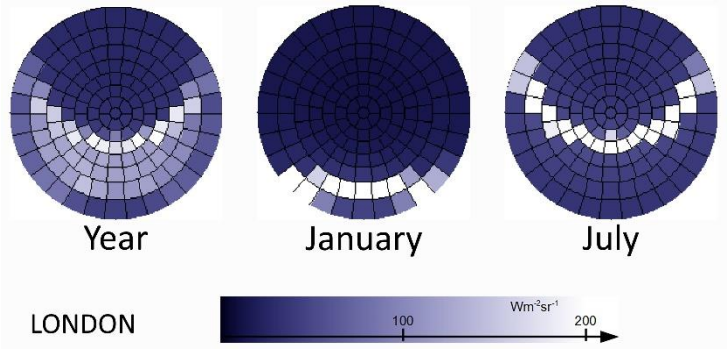

Figure 2.8: Stereographic views of the sky vault representing sky models generated for the year, January and July, and used in PPF simulations.

As mentioned in Section 2.4.2.2, PPF is based on the RADIANCE ray-tracing programme, and uses sky models which represent average radiance distributions on the sky vault for a given time period (Compagnon, 2004). Specifically, for the irradiation simulations, climatic data of London (hourly direct and diffuse horizontal irradiance values) were obtained from METEONORM software (Remund et al., 2015) and processed statistically in order to build up three sky models: aggregating weather data of the entire year, January and July (Fig. 2.8). Only daytime hours were considered, i.e. hours between sunrise and sunset on a day, which are 4317 for the year, 249 for January and 489 for July.

The 3D digital models of the urban forms were re-produced in a CAD software including the surrounding buildings, and inserted in PPF in .dxf format (Fig. 2.9). As previously for SOLWEIG simulations, surrounding buildings to the studied areas were included in the models for their effect to be considered. SVF and irradiance values were computed at each node of a grid of 2-meter spatial resolution, adjusted onto the buildings' surfaces of the models, and on a horizontal plane at 1.1m above the ground -as done by default in SOLWEIG simulations- corresponding to the average level of the center of gravity of a standing person in Central Europe (Matzarakis et al., 1999). Prior to the study, a sensitivity analysis was performed using two urban forms, one in central and another in north London, and testing two grids, of 1m and 2m. The results showed that increasing the scale of the grid affects maximum and minimum values but its effect on average SVF and irradiance values was negligible, independently of time period. Indicatively, the relative difference in average SVF computed for the two grids was approximately at 10^{-5} level, and in average irradiances at 10^{-4} level.

Finally, there are two input parameters that affect the reflected irradiance values and should be fully considered in the interpretation of the results. First, the albedo value is set to 0.2 for all surfaces in the models (default value). Second, the number of bounds of solar rays is set to 1, instead of 2 which is the default value. The reduction of the number of bounds was regarded necessary due to the size of the urban forms and the enormous number of simulations run in PPF (more than 210) as them to be complete in reasonable time. However, it is acknowledged that it undermines the significance of the reflected component in the overall solar availability and its effect is excepted to be more evident in urban forms of higher density.

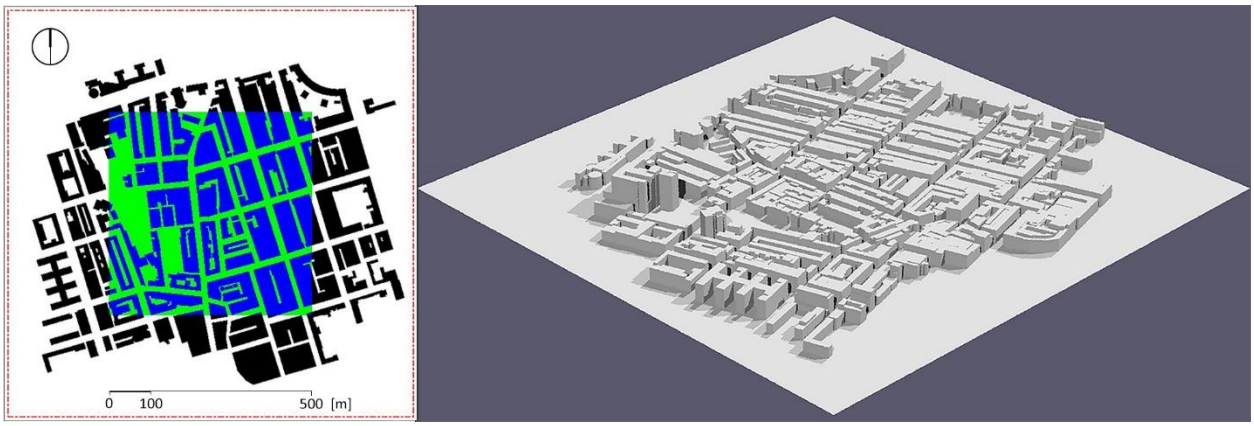

Figure 2.9: Left, ground map of a 3D model as seen in PPF: in colour the simulated area (i.e. building volumes in blue, ground in green), in black the surrounding building volumes. Right, perspective view of the same model.

2.4.2.3 Performance indicators computed

For the statistical exploration of the relationship between urban geometry and environmental performance of urban forms, the research considers as performance indicators the average values of the environmental quantities simulated in SOLWEIG and PPF. The processing of the output data and computation of average values were all done in MATLAB. For this purpose, special scripts were written for the automatisation of the process, i.e. computing all urban forms' mean values at once and storing them in tables.

From SOLWEIG simulations, the performance indicators obtained and used in the first study are the three following:

- Average SVF (mSVF), [-]
- Average insolation (mSOL), [-]
- Average mean radiant temperature (mMRT), [°C]

All of them refer to the open space of the urban forms, and are obtained from the processing of SVF maps, shadow patterns, and MRT maps, respectively. Specifically, the values of the pixels identified as un-built space were extracted and next averaged. mSVF expresses the average openness of the open space to the sky; as SVF for a given point, mSVF ranges from 0 to 1, with 1 denoting a completely unobstructed open space. In shadow patterns for a given time, the pixel value can be either 0 (shaded pixel) or 1 (sunlit pixel) and, thus, the mSOL value also ranges between 0 and 1, with 1 denoting an entirely sunlit open space. Hence, mSOL measures sunlit open space over total open space expressing average solar exposure at a given time. It is noted that, apart from instantaneous shadow patterns, daytime average ones were also

produced for the studied days, i.e. 21 June, 21 March and 21 December, and respective mSOL values were computed and used in the analysis. Finally, MRT expresses (in °C units) the sum of radiation fluxes to which a human body is exposed and is one of the four environmental factors governing thermal comfort. Respectively, mMRT expresses the above quantity on average over the open space.

From PPF simulations, the performance indicators computed, and used in the second study, are the following:

- Average SVF (mSVF), [-]
- Average **g**lobal irradiance (mI_g), [W/m^2]
- Average **d**irect irradiance (mI_d), [W/m^2]
- Average diffused -from the **s**ky- irradiance (mI_s), [W/m^2]
- Average reflected -from **b**uildings- irradiance (mI_b), [W/m^2]

In this case, all five indicators are computed separately for ground and building façades of 24 urban forms. Unlike SOLWEIG, where each simulated value corresponds to a surface of constant area (i.e. 0.5x0.5m), in PPF models there are patches of the grid of different surface area (occurring at the edges of different surfaces). For this reason, for the computation of mean SVF and irradiances, the simulated values were averaged after weighted by surface area.

Ground and façades mSVF expresses the openness of the open space and building façades, respectively, to the sky. The values of ground mSVF (horizontal surface) range from 0 to1, while those of façades mSVF (vertical surfaces) from 0 to 0.5, with 0.5 denoting a totally unobstructed façade. It is noted that SVF is widely used in the literature as indicator of solar availability (Robinson, 2006), both on façades and ground. Mean irradiance expresses the radiant flux (power) received by a surface per area unit and on average over the given time period. As mean global irradiance expresses the sum of all radiant fluxes, i.e. direct from the sun, diffused from the sky and reflected by the buildings, it is also referred to hereafter as total irradiance and used as indicator of overall solar availability.

Finally, the performance indicator used in the third study is thermal diversity, referring to the open space of studied urban forms. The values are calculated based on thermal diversity maps, which in turn are generated using shadow patterns -simulated already in SOLWEIG- and wind maps -produced in MATLAB-. Since the presentation of the method used for the generation of thermal diversity maps presupposes the introduction of the concept of thermal diversity, all the details are provided in the respective chapter (i.e. Chapter Six).

Figure 2.10 demonstrates the tools involved in the computation of performance indicators used in each of the three studies.

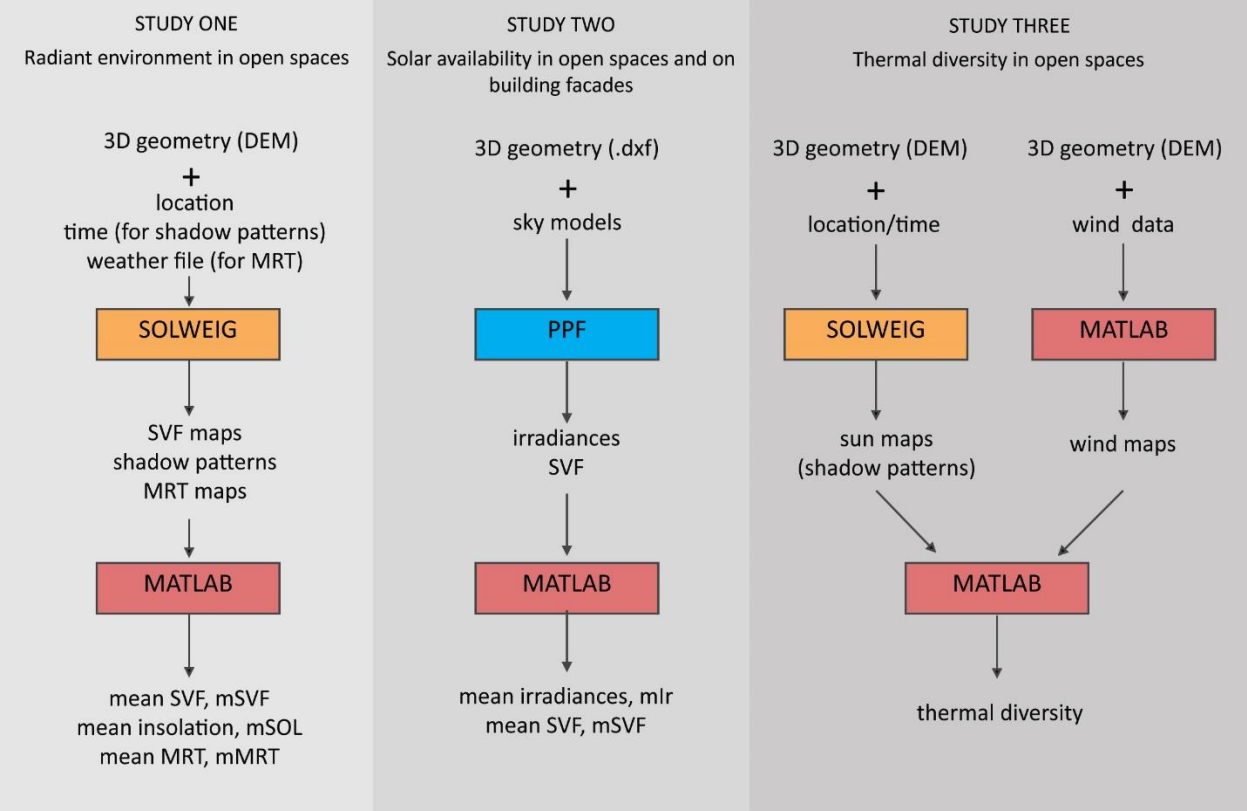

Figure 2.10: Process followed for the computation of environmental performance indicators considered in each of three studies.

2.4.3 Limitations of simulation tools and outcomes

Simulation models are meant to imitate a situation or process happening in real life, but could never reproduce it perfectly as they unavoidably entail some sort of uncertainty due to simplifications and/or approximations made in modelling. The same stands for the simulation tools used in the context of this research, and should be always acknowledged as a limitation when referring to/interpreting their outcomes.

As discussed previously, the scope and scale of the research necessitate the employment of computer-based solar simulations for the generation of environmental data to be used in the statistical analysis, i.e. performance indicators (see Section 2.2). Carrying out actual measurements was not an option for practical and mostly, methodological reasons. A major one is that the research examines the role of urban geometry in defining solar availability at the neighbourhood scale which requires other parameters

affecting it in a real context, such as building materials, vegetation, urban equipment, etc., to be isolated and neglected in the analysis. This is possible using a simulation computer programme but not when carrying out solar radiation measurements in situ. On the other hand, neglecting such important parameters means that the simulation results do not represent the potential solar availability in the urban forms studied, but reflect the relative impact of their geometry on it. In other words, the rather theoretical approach followed limits the usefulness of the simulations for assessing the urban forms' actual performance. At the same time, as the major research findings derive from the comparative analysis of the urban forms rather their evaluation in terms of absolute values of performance, their sensitivity to the solar modelling limitations is also limited.

Unlike the simulation of other environmental factors, such as wind and temperature, the attitude of which in space is complex or even chaotic, solar radiation modelling is relatively straightforward thanks to the directionality of solar rays. In this regard, its limitations stem to a great degree from the -necessary- representations of the sky/solar geometry in the modelling. SOLWEIG and PPF simulations, as presented in Sections 2.4.2.1 and 2.4.2.2 respectively, are based on very different concepts of sky/sun representation associated to their analysis purposes. In PPF which is intended for solar and daylight simulations, sky conditions, i.e. average radiance distributions, are represented in sky models. It is noted that sky models are generated by aggregating actual climatic data for a given period; hence, cloudiness, atmospheric conditions, etc. are all considered. As seen in Figure 2.8, these constitute stereographic projections of the sky vault divided into 145 patches. Similarly, the built geometry is represented by a mesh of evenly distributed points created in front of vertical surfaces and above horizontal ones. Simply put, the centres of the patches are the radiation sources (i.e. direct and diffuse radiance) and the points of the mesh are the receivers. Apparently, the representation of the sky geometry and urban surfaces by points constitutes a limitation of PPF simulations but, as mentioned above, this is an issue that all solar simulation programmes need to address in a way. In fact, the way in which PPF and all RADIANCE-based programmes address it is established as efficient and accurate, and is well documented (Ward Larson and Shakespeare, 1998).

SOLWEIG is intended for simulating instantaneous 3D radiation fluxes and mean radiant temperature variations at the pedestrian level. The model has been validated against measurements and other simulation tools' results, and the embedded formulas can be found analytically in Lindberg et al. (2008). Nonetheless, in this research, SOLWEIG has been employed mainly for obtaining SVF values, and shadow patterns for specific moments in time, the computation of which involves purely geometric expressions -

rather physics- treated by the algorithm of Ratti and Richens (1999). The algorithm is very efficient in generating shadow patterns for specific solar angles with the outcomes being sensitive only to the resolution of the DEMs. In SVF calculations, the sky vault area is represented by finite number of sky points, i.e. 1000, randomly distributed on it; therefore, the SVF value obtained expresses the percentage of 1000 points from which a point (pixel in the DEM) can been seen. Respectively, in PPF, the SVF value expresses the percentage of 145 fixed sky patches from the centre of which a point (node of the grid mesh) can been seen. Both approaches calculate by approximation the SVF and thus, entail some limitations to be admitted.

2.5 Statistical analysis

Statistical analysis is first conducted to explore the variance and interdependence of urban geometry variables in the urban forms of London and Paris (presented analytically in Section 3.4). In the three studies, statistical analysis concerns the relationship of urban geometry variables and environmental performance indicators. Pearson Correlation, partial correlation -with control for independent variables-, Curve Estimation, Regression and Principal Component Analysis are among the tests employed throughout the research. These tests were performed using either MATLAB Statistics Toolbox or SPSS statistical package; whereas, for the visualisation of Regression analysis results, trendlines and coefficient of determinations, R^2, in scatter plots were determined in Microsoft Excel programme. More details about statistical tests performed are provided in the corresponding chapters, prior to the presentation of the results.

2.6 Conclusions

In this chapter, major aspects of the research methodology including methods and tools used for the analysis of urban forms were outlined. The three studies comprising the research are based on different case study cities and number of urban forms, with the first and the third study to examine comparatively 72 urban forms in London and 60 urban forms in Paris, and the second study to focus on 24 -out of 72- urban forms of London. Furthermore, the first and third study investigate environmental phenomena in open spaces, solar access and thermal diversity, respectively, using for solar simulations the SOLWEIG model. On the other hand, the second study employs PPF software for simulating solar availability in open spaces and on building façades, in different time periods.

Beyond the differences, which are summarised in Table 2.1, the studies follow the same methodological logic characterised by three methodological stages, the geometric and environmental analysis of urban

forms, and the statistical analysis of the relationships between selected urban geometry variables and performance indicators. Unlike the environmental and statistical analysis which are performed separately for each study, the geometric analysis of all urban forms considered in the research was performed all at once. Specifically, a set of urban geometry parameters was computed in MATLAB processing the DEMs of the urban forms. The obtained values are used to compare the urban geometries found in London and Paris, and constitute a source from which geometric variables are selected to be examined in each study, depending on its focus. The above are discussed analytically in Chapter Three, which commences with a literature review on urban geometry parameters used in urban environmental studies.

Chapter Three

Urban geometry variables and analysis

Chapter Three presents the geometric analysis of the studied urban forms, namely the first of the three methodological stages, and is organised in three parts. In the first part, urban geometry measures being employed in urban environmental studies are reviewed with respect to the geometric parameter they refer to, grouping together those with overlapping or similar meaning. The second part presents the geometric variables selected to be considered in the analysis. The last part presents comparatively the results of the geometric analysis of the urban forms of London and Paris, revealing considerable differences between the two cities.

3.1 Introduction

Each urban form features a unique geometry, which is decided by the shape of building volumes, and their relative spatial configuration within the site. The enormous number of parameters involved in the production of the 3D built environment results in complex geometries which vary significantly from city to city, as well as within a city. In turn, their interaction with the local climate creates a great disparity between different indoor and outdoor climates. The study of relationships of urban geometry with resulting environmental phenomena occurring within the built environment requires the reduction of its complexity to a finite number of parameters. The effective representation of urban geometry's characteristics, especially those being related to the respective phenomenon, is deemed crucial for the potential associations to be meaningful.

The analysis of the geometry of the studied urban forms constitutes the first of the three stages of the research methodology. Unlike the environmental analysis, which is performed separately in the three studies depending on the environmental phenomenon and case studies they focus on, the geometric analysis was performed once for all 132 urban forms of London and Paris. This involved the computation of eighteen urban geometric measures in MATLAB using special algorithms written for this purpose. These geometric measures -referred to as urban geometry variables- are used for the comparison of urban geometries of the two case study cities, exemplifying the capability of such measures to describe the

variations of urban geometry. Next, each of the studies focuses on selected urban geometry variables as their relationship with the studied phenomena to be explored statistically.

The chapter commences with a review on geometric measures used in urban environmental studies. The purpose of the review is to classify them according to the urban geometry parameter they refer to, as well as to discuss the aspects of urban environmental performance they are related to in the literature. This will contribute to a better understanding of the issues entailed in the geometric analysis of urban forms for environmental purposes and facilitates the introduction of the selected urban geometry variables which are presented next. The last part of the chapter compares the results of the analysis of the urban forms of London and Paris, highlighting their significant differences.

3.2 Review on urban geometry measures in environmental studies

Urban geometric measures are presented in groups depending on the geometric parameter they refer to, namely density, randomness, compactness and complexity, and building dimensioning. In addition, the aspects of urban environmental performance which have been found to affect, either solar radiation availability, wind environment, or buildings' energy performance, are discussed. Solar availability and wind field refer to the ground level, with implications for urban microclimate and outdoor thermal comfort, and the building fabric, with implications for buildings' environmental potential. Their occurrence and variations in the urban environment are highly related to geometric characteristics of the open space. On the other hand, buildings' energy performance is also affected by the form of the buildings themselves; for instance, compactness and plan depth are related to heat losses through the building fabric and efficacy of passive design strategies potentially employed, respectively.

Built and un-built space, i.e. buildings and open spaces, constitute a strong dipole characterizing the urban environment. Unlike building volumes which are well-defined objects, open spaces are either conceived as 2D surfaces outlined by building footprints' perimeters, or as 3D spaces contained in between buildings. This is reflected to the analysis of urban geometry which, based on traditional mathematics, is usually limited to measuring geometrical properties of the built form, so-called building metrics, involving dimensions, perimeter, area, volume, and combinations of them. It is noted that these properties are highly interrelated to each other. For instance, assuming a building of rectangular shape, its footprint perimeter multiplied by its height gives façades' area, and its footprint area multiplied by its height represents its volume. The same also applies when referring to an urban form, namely to all building volumes over a given site area, either cumulatively or on average.

The urban geometric measures reviewed below are categorized in "basic" and "indicators". What distinguishes them is that the latter have been proposed and used in the context of urban climatology and urban environmental studies for evaluating the environmental performance of urban forms. In other words, they intend to express aspects of the geometry which are associated in a specific way with urban microclimate and buildings' energy performance, and thus are used as performance indicators. In contrast, basic measures include essential measurements of urban geometry which may still be associated with urban forms' environmental performance, but their meaning is more universal, i.e. they are equally used in urban morphology studies. Lastly, sky view factor is presented separately as a third category, as it is a special geometric measure which can be considered both as a geometric and environmental indicator.

3.2.1 Basic urban geometry parameters

3.2.1.1 Density indices

Built density

How densely an urban environment is built-up affects directly solar availability as well as the airflow in the urban canopy. The absolute measure of built density is this expressing total built volume within a site over site area [m^3/m^2]. Since building volumes are that obstruct solar radiation and airflow, built density is commonly used as a measure of how obstructed a built environment is. Adolphe (2001) suggests the same measurement, naming it *absolute rugosity*, to assess the global effect of an urban form on the slowing down of the mean wind speed. This expresses mean height (H_m) of urban canopy given by the product of the height of the buildings by the area they occupy, divided by the total site area [m^3/m^2]:

$$H_m = \frac{\sum_{built} A_i * h_i}{\sum_{built} A_i + \sum_{non-built} A_J}, [m]$$

Where, A_i is the footprint of the building i, h_i the height of the building i and A_j the area of non-built element.

In researches of which the findings refer directly to thermal and daylight conditions inside buildings and, building energy performance, built density is commonly given by *floor area ratio* (FAR) (also referred to as *plot ratio* or *floor space index*) that indicates the usable floor area per unit site area [m^2/m^2] (e.g. Lee et al., 2016; Zhang et al., 2012). Building volume and total usable floor area are linked using as rule of thumb that a floor in a conventional building, such as an office or residential building, is about 3m high, i.e. building volume divided by 3 gives usable floor area, and vice versa.

Site coverage

Site coverage (also, referred to as *ground coverage*, *(soil) occupation factor* or *plan area density/ratio*) is defined as the ratio of the total area occupied by buildings over the total site area [/]. It expresses the horizontality of an urban form as it quantifies the built form on the ground level, and thus, in a negative way, the open space. Site coverage is among the most widely used variables and its impact on urban microclimatic conditions as well as buildings' environmental performance is examined by numerous studies (e.g. Rode et al., 2014; Sarralde et al., 2015). Indicatively, site coverage was found to be decisive for *horizontal obstruction angles* in the built environment, and consequently for daylight and solar quantities both on ground and building façades (Cheng et al., 2006b). Furthermore, the percentage of building footprint area over site area is regarded a crucial factor regarding the wind field in the urban canopy, especially at the pedestrian level affecting outdoor thermal comfort conditions (Ng et al., 2011; Yuan and Ng, 2012). Finally, site coverage may also be measured over the plots' area (Arboit et al., 2008; 2010; Martins et al., 2014), which as concerns the effect of coverage may lead to misleading findings (Salat and Nowacki, 2010).

Mean building height

Mean building height expresses the average height of buildings in an area and is measured in meters [m] and, less commonly, in number of stories (e.g. Zhang et al., 2012). More precisely, two ways are identified for calculating it in meters, either by simply averaging the height of buildings in an area (sum of all buildings' height divided by number of buildings), or by averaging the height of buildings weighted by their footprint area. In the study of Martins et al. (2014), these two measurements represent distinct variables of urban geometry, *building height* and *verticality*, respectively. In either way, mean building height expresses the vertical distribution of the built form in an urban area and affects both its aerodynamic properties, especially vertical wind profile in the urban canopy, and solar and daylight availability. Like site coverage is associated with horizontal obstruction angles affecting radiation coming from the sides, building height is related to vertical obstruction angles affecting radiation coming from the top (Cheng et al., 2006a). Examining energy demands for representative European urban typologies, mean building height was found to be the strongest variable -among plot ratio, site coverage and surface-to-volume ratio- and correlates with them negatively (Rode et al., 2014).

At this point, it is important to underline that site coverage and mean building height are two major urban geometric measures. They are strongly related to built density, as this is equal to the product of their values, or stated otherwise, for a given density the two variables are inversely proportional. Thus, considering building height constant, the variations of site coverage means respective variations in density

values, and the inverse. This is the reason that in several studies, the two variables and especially site coverage are considered as expressing density parameter (e.g. Mohajeri et al., 2016; Nault et al., 2015). However, studying real urban forms -as opposed to generic models or models representing idealized typologies- their methodological equation with built density may involve risks since the findings may be influenced by their interrelation. Furthermore, it is noted that site coverage, independently to urban forms studied, i.e. of homogeneous or non-homogeneous layout, expresses an absolute measurement, namely the built-up area. In contrast, mean building height is a statistical expression which -in urban forms of varying building height- does not represent an actual measurement. Apparently, the same applies to all geometric metrics expressing a measurement on average.

Mean distance between buildings

Mean distance between buildings [m] expresses on average the distance between buildings in an area. It quantifies an aspect of the open space and is therefore negatively related to site coverage. However, urban forms of higher site coverage do not necessarily feature lower mean distance between buildings, especially in those of non-repetitive layout, where the horizontal distribution of building volumes is uneven. This metric has been considered in studies investigating solar energy and thermal potential in representative urban configurations (Martins et al., 2014; Sarralde et. al, 2015), as well as urban natural ventilation potential (Ng and Wong, 2004; 2005).

Height-to-width ratio

The height-to-width ratio (H/W, referred to also as aspect ratio) is the ratio of building height to street width, i.e. distance between buildings. This is commonly used by studies which select street canyon geometry as spatial unit to examine the impact of density. Expressing two-dimensionally the relationship between built and non-built space, aspect ratio enables the examination of various environmental phenomena occurring in the urban canopy. For instance, H/W and orientation of urban canyons have been the variables in studies on urban microclimate (e.g. Ali-Toudert and Mayer, 2006; 2007a; 2007b; Bourbia and Awbi, 2004a; 2004b; Johansson, 2006; Johansson and Emmanuel, 2006) and solar availability on building facades (e.g. Strømann-Andersen and Sattrup, 2011; van Esch et al., 2012). Moreover, there have been several studies that examine wind flow regime in street canyons as a function of their height-to-width ratio, for different wind directions and speeds (Chan et al., 2001; 2003; Oke, 1988). Finally, H/W has been also used as a performance indicator in research works investigating the environmental performance of real urban forms and typologies in which it is averaged, either over the entire urban area or by direction (Burian et al., 2005; Martins et al., 2014; PREcis, 2000).

3.2.1.2 Randomness of urban layout

Vertical randomness

More than the average building height, it is *the differences in heights of neighboring buildings* which affects the ventilation conditions in the urban environment (Givoni, 1998, pp. 285). Buildings that rise appreciably above the roof of the surrounding buildings can greatly modify the urban wind field, increasing the vertically induced airflow. This means higher wind speeds both on buildings' facades and at the pedestrian level, with implications for natural ventilation potential and outdoor thermal comfort (Ng and Wong, 2004; 2005). Furthermore, a random skyline, compared to a uniform one, was found to be beneficial also for the average daylight availability on building façades as well as their solar potential (Cheng et al., 2006a; 2006b; Ng and Wong, 2004). The above findings have been derived from parametric studies in which different skylines are distinguished descriptively, i.e. *uniform* when all buildings are of the same height, *random* when the building heights are randomly different, and *pyramid* or *stratum* when the buildings in the middle of the model are higher than their surroundings. In a more recent study, the impact of vertical randomness on roofs' solar potential has been examined by considering standard deviation of building height (Sarralde et. al, 2015), which is a common measurement of the particular geometric property.

Horizontal randomness

Like vertical randomness, the effect of horizontal randomness on microclimatic conditions and buildings' environmental performance has been examined based on parametric analysis and different scenarios of building layout. *Uniform*, *staggered*, and *random* layout scenarios refer to the horizontal alignment of buildings comprising an urban form, with *uniform* describing a perfect alignment to both axes of the horizontal plane, *staggered* an alignment to one of the two axes, and *random* a random configuration. Unlike vertical randomness though, horizontal randomness is considered to have opposite results on wind and, solar and daylight availability, especially at the ground level. The alignment of building volumes -combined to adequate distances between them- increases the air permeability of urban forms and, enhances the potential for urban natural ventilation (Ng et al., 2011; Yuan and Ng, 2012). On the other hand, horizontally random layouts were found to be beneficial for solar and daylight potential, especially in increased densities (Cheng et al., 2006b). It is noted that, so far, there has not been proposed by relevant studies any measure expressing the horizontal randomness of the urban form.

3.2.1.3 Compactness and complexity indices

Compactness and complexity are two geometry properties which at the city scale are positively associated with urban -environmental- sustainability, however, having distinct meanings and underpinning different

concepts. A compact urban form is an urban form featuring high spatial concentrations of population, activities and built form (Jenks et al., 1996). In other words, compactness when referring to the city level is a matter of density. On the other hand, complexity is a less intuitively perceived parameter of geometry which applies to modern mathematics and the theory of fractals. Putting it in a simple way, a complex urban fabric is this featuring complex patterns of relationships of its structural elements, i.e. network of streets/building volumes (Marshall, 2009); namely, complexity is a matter of order. Compactness combined with mixing of land use presents important environmental benefits associated to reduced transport-related energy demands and the economic feasibility of combined heat and power (CHP) systems and district heating (DH) energy provision (Owens, 1987; Steemers, 2003). The relationship between complexity and urban environmental sustainability has drawn considerably less research attention; it is considered positive since high complexity means increased diversity -as concerns the built form and thus, uses and activities- and connectivity -as concerns street networks- (Salat et al., 2010).

At the intermediate urban scale, the semantic content of the words alters significantly and tend to be similar, but not identical. Compactness retrieves its literal meaning, as a numerical quantity representing the degree to which a shape, i.e. built form, is compact; while the term complexity usually refers to how undulating a surface is which influences the sum of its total area. Apparently, when examining an individual building, the more undulating its fabric, the less compact its shape is. However, considering an entire urban form, its total surface area, i.e. including roofs, façades and ground, is not affected only by how compact the building volumes are, but also by the total built volume and the number of building volumes in which the latter is distributed.

Compactness

Compactness of a built form is typically measured as functions of its surface area and volume, and is considered a positive attribute for buildings' energy efficiency implying reduced heat exchange with the ambient environment (heat losses and gains). In most studies, compactness is measured by the ratio of total buildings' surface area to their volume [m^2/m^3], the so-called *surface-to-volume ratio* (also referred to as *form factor*) (e.g. Arboit et al., 2008; Nault et al., 2015). Instead of that -or along of that-, several studies propose *form factor* (also referred to as *compacity*) as indicator of compactness (Adolphe, 2001; Bourdic et al., 2012). Form factor is a non-dimensional form indicator and calculated as follows:

$$FF = \sum_{buildings} \frac{S}{V^{2/3}}, [-]$$

Where, S is external surface area of building, and V building volume. It is pointed out that both surface-to-volume and form factor measure compactness negatively as the greater the surface area of the built form over its volume, the higher their values would be. In contrast, the inverse ratio, namely building volume to surface area, is related to compactness positively, in meters, and expresses the average depth of the building from the envelope. It has been used in the context of the Project ZED (1997) and is strongly associated with buildings' passive potential. Alternatively, average building depth can be calculated by the floor plan area to perimeter length ratio, based on a typical floor plan. A more sophisticated measurement is this referred to as *convolution index*, which is defined as follows (Leung, 2009, cited in Hii et al., 2011):

$$C = \frac{P_f - P_c}{P_c}, [/]$$

Where, P_f is perimeter of building footprint and P_c perimeter of the smallest convex shape of the building footprint.

Except for studies examining buildings' energy performance, the compactness parameter has been also considered in studies focusing on open spaces. Sharmin et al. (2015), investigating the relationship between urban form and outdoor microclimatic variations, used three indicators of compactness: two versions of surface-to-volume ratio, one considering only buildings' surface area and another including also plot's surface area, and form factor. Among the three, a better correlation was observed by including open ground surfaces along with building surfaces. However, overall, the compactness parameter was found to be a better indicator for air temperature and humidity variations, rather than for globe and mean radiant temperature; thus, it was argued that it may be better suited to energy performance and indoor comfort studies.

Complexity

Unlike compactness which expresses on average a property of building volumes in an urban area, *complexity* is usually referred to in the literature as a property of the entire urban form and associated to its overall radiant and aerodynamic performance. Similar terms used are these of *irregularity* and *roughness,* all implying an increased urban surface which interacts with solar radiation and wind. For instance, research findings have shown that the more complex the urban forms, the more the solar radiation they absorb, i.e. the lower their albedo (Aida, 1982; Steemers et al., 1998). Defining complexity as urban surfaces' total area, this is affected by various parameters, such as built density and number of building volumes in a positive way, and compactness of building volumes in a negative way.

3.2.1.4 Building dimensions

Building width and depth (also found as length and width, width and thickness) refer to the horizontal dimensions of the longest and shortest of sides of orthogonal in plan buildings. These measurements as well as their ratio have been considered mostly in parametric studies using generic models, and examined along with the effect of orientation (e.g. Kristl and Krainer, 2001; Li et al., 2015; Lu and Du, 2013). Nevertheless, they are of limited relevance to complex urban geometries where neither buildings' footprints are of orthogonal shape, even more of the same shape, nor they feature a strict orientation.

3.2.2 Urban geometry measures as performance indicators

Some urban geometry measures are used as environmental performance indicators; they can be classified in two categories, numeric and graphic indicators. The numeric indicators are expressed by single numbers, while the graphic, expressing geometric measures as a function of azimuth or height, are meaningful when they are plotted in graphs.

3.2.2.1 Numeric indicators

Passive potentials

The concept of the passive to non-passive ratio was first perceived in the context of the development of the LT model (Baker and Steemers, 1996) and means to quantify the potentially passively served space of a building, in terms of daylight and ventilation. It is based on a rule of thumb assuming that the perimeter zone of buildings lying within 6m distance from the façades (i.e. twice the ceiling height assuming typical ceiling height 3m) can be lit and ventilated using windows on the external walls -classified as 'passive'-, whereas the space beyond this distance cannot -classified as 'non-passive'-. In this way, the higher the value of the ratio, the higher the potential for passive strategies.

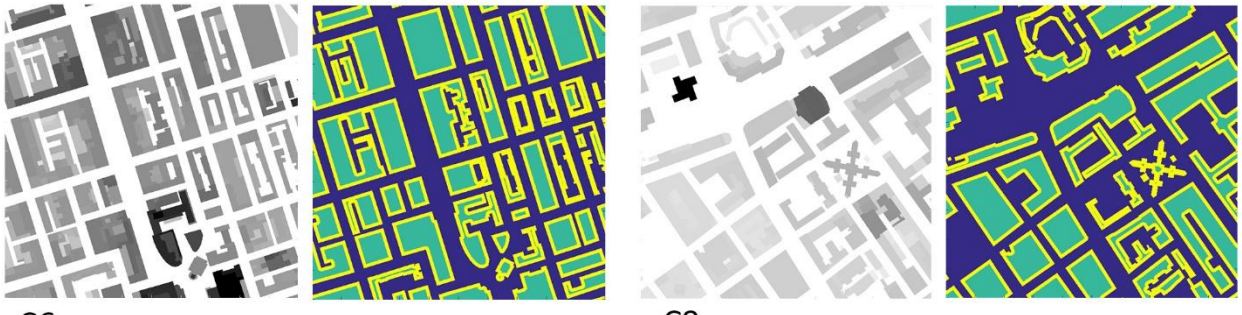

Figure 3.1: DEMs of two urban forms in central London's area and aside, passive zones (highlighted in yellow) and non-passive zones (highlighted in green) of their buildings corresponding to the ground level, computed in MATLAB using the algorithm of Ratti (2001).

Apparently, the passive-to-non passive ratio is negatively related to the compactness of the build form; the more compact the build form is, the smaller the ratio will be. Therefore, when assessing heat energy demands of buildings, compactness is considered a positive attribute; while, examining buildings' passive potential, it is regarded negative. It is argued that since the heat exchange through the building fabric can be modified by insulating it, the maximization of the passive potential is of higher significance in the urban design (Project ZED, 1997). Nevertheless, the optimum degree of compactness, meaning this that ensures an optimum balance between heat losses/gains and passive potential, depends on the climate with which the built form interacts (Ratti et al., 2005).

Figure 3.2: Orientation of passive zones -show in different colours- based on buildings' ground floor in central area of London studied, computed in MATLAB using the algorithm of Ratti (2001).

Passive and non-passive zones, along with other parameters needed by the LT method to calculate energy consumption in buildings, can be derived by image processing of urban DEMs (Fig. 3.1). Regarding solar passive potential, an important information to be also considered is the orientation of the passive zones which can be also computed using the same technique (Fig. 3.2).

Mean contiguity factor

Mean contiguity factor is a measure of buildings' adjacency and used as indicator of the heat transmissions between adjacent buildings with implications for building energy consumption (Adolphe, 2001; 2009). It expresses the ratio of the vertical envelope area adjacent to other buildings to the total vertical area of the building envelope, weighted by floor area, and is calculated as follows:

$$C_t = \frac{\sum_{buildings} \frac{A_{adj} * A_{floor}}{A_{vert}}}{\sum_{buildings} A_{floor}} \text{, [/]}$$

Where A_{adj} represents the area of the building's adjacent vertical surfaces, A_{floor} the floor area of the building and A_{vert} the area of the building's exposed vertical surfaces. It is pointed out that continuity

factor is of relevance only when in the analysis adjacent buildings are recognized as separate shapes/volumes. In contrast, in image processing and DEMs adjacent buildings are treated as one building volume.

Open space ratio

Open space ratio, or otherwise *spaciousness* is one of the measures examined in Spacematrix method -a space analysis tool- and defined as the ratio of non-built ground area to total floor area (Berghauser Pont and Haupt, 2010). In this way, it expresses how spacious the urban space is or, reversely, the 'pressure' on the open space yield by the built mass. From another perspective, it associates the size of the open space, which determine to a large degree solar and daylight availability in urban canyons, with the indoor space to be served. In a study examining the relationship between seven geometric variables (floor area ratio, site coverage, open space ratio, area-to-perimeter ratio, compactness, convolution index and building height) and the "annual total solar radiation per unit floor area", open space ratio was the only parameter that showed an indicative correlation trend (Hii et al., 2011).

Porosity

Porosity measures how penetrable an urban area is for the airflow, and is defined as the ratio of open space's volume to built volume in the urban canopy layer (UCL) for a given area. So, for evaluating the parameter, it is first necessary to define the volume of the UCL. Gal and Unger (2009) mention two ways to compute urban porosity depending on whether the height of the UCL is considered constant or not. Provided that the area is characterised by a relative small variation in building heights, the height of the UCL may be considered constant. In this case, porosity ($P_{constant}$) is given by the following formula:

$$P_{constant} = \frac{A_T * h_{constant} - V_{built}}{A_T * h_{constant}}, [/]$$

Where, A_T is the total site area, $h_{constant}$ the height of the UCL and V_{built} the total built volume on the given site. The second way to compute porosity is based on varying UCL heights by spatial units. In each spatial unit, the height of the UCL is determined as this of the highest building within the respective area, and the overall porosity is calculated by the following formula:

$$P_{variable} = \frac{\sum_i A_i * h_i - V_i}{\sum_i A_i * h_i}, [/]$$

Where, A_i is the area of the spatial unit i, h_i the height of the UCL for the spatial unit i, and V_i the total built volume in the spatial unit. Another approach for calculating the porosity of an urban form is based on the distinction of non-built spaces into open ended elements and cavities, taking into account only the former.

In this way, porosity describes the fraction of the non-built space within an urban form where the air -as fluid medium- may flow freely (Adolphe, 2001; 2009).

3.2.2.2 Graph indicators

Frontal area density

Frontal area density expresses the resistance that the wind encounters by building facades. Along with mean building height and site coverage, it is used in formulas for the estimation of the aerodynamic properties of urban areas (drag and turbulence production) (Grimmond and Oke, 1999). A simple way to define it is as the sum of the area of the vertical building surfaces divided by the area of the site [m_2/m_2] (Edussuriya et al., 2011). However, frontal area density is typically defined as a function of wind direction, θ, specifying the resistance mounted by building facades for different wind directions, and given by the following formula:

$$\lambda_{F(\theta)} = \frac{\sum_i \cos \varphi_i * A_i}{A_T}, [/]$$

Where, A_i, is the front area of the building i that faces the wind direction of θ; ϕ_i is the angle of incidence between the wind direction of θ and the perpendicular to the front surface of the building i; A_T the total site area.

Sinuosity

Sinuosity is a parameter which is related to the horizontal dispersion of the airflow and expresses the horizontal wind permeability of an urban fabric as a function of the wind direction (Adolphe, 2001). For a given azimuth, it is measured by weighting the elementary sinuosity factor of each linear segment by its length, taking into account only the useful - for horizontal wind dispersion - non-built space, namely the open-ended streets. It can be plotted against azimuth on a polar diagram and calculated by the following:

$$S_\theta = \frac{\sum_{seg.roads} L_i * cos^2(\theta_i)}{\sum_{seg.roads} L_i}, [/]$$

Where, L_i is the length of the street linear segment i and θ_i the angle between the given azimuth of flow and the azimuth of the street linear segment i.

Directionality

Wind and solar radiation are climatic factors of strong directional nature, and as such, interact with the direction of open spaces. The *directionality* parameter, first introduced in the context of the Project ZED (1997), expresses the difference in the permeability of an urban texture in the horizontal plane; where permeability is defined as mean square deviation of the height profile (built and non-built elements) for

any given direction. Results can be plotted on a polar diagram, the so-called *variance plot*, demonstrating how permeability varies with azimuth (Fig. 3.3). For instance, in isotropic urban forms, the amplitude of the averaged height profile will vary slightly, while in urban forms with strong directional elements, such as of a grid-iron street layout, the polar diagram will show a greater amplitude of variations.

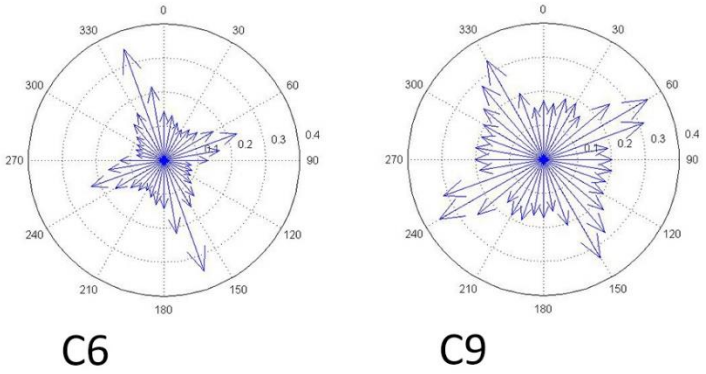

Figure 3.3: Variance plots for two urban forms appeared in Figure 3.1, C6 and C9, showing variation of their permeability by azimuth. (Computed using Ratti's (2001) algorithm.)

Occlusivity

Occlusivity expresses the openness of an urban form to the sky and is measured as total perimeter or section plan area of buildings as a function of height above the ground. It can be expressed graphically in Cartesian axes, where the x axis denotes the height and the y axis the total perimeter or floor area of buildings at different heights (Fig. 3.4). The slope of the curve characterises the occlusivity of the urban form, i.e. the steeper the slope, the higher the occlusivity. Furthermore, if it refers to floor area, the area under the curve is equal to the total built volume. Increased inclusivity indicates greater exposure to sky diffused radiation during the day and loss of longwave radiation during the night. Moreover, increased occlusivity is associated to enhanced vertical airfow in the urban canopy which, in turn, enhances the dispersion of pollutants by interaction with the free-following wind (Edusssuriya et al., 2011; Project ZED, 1997).

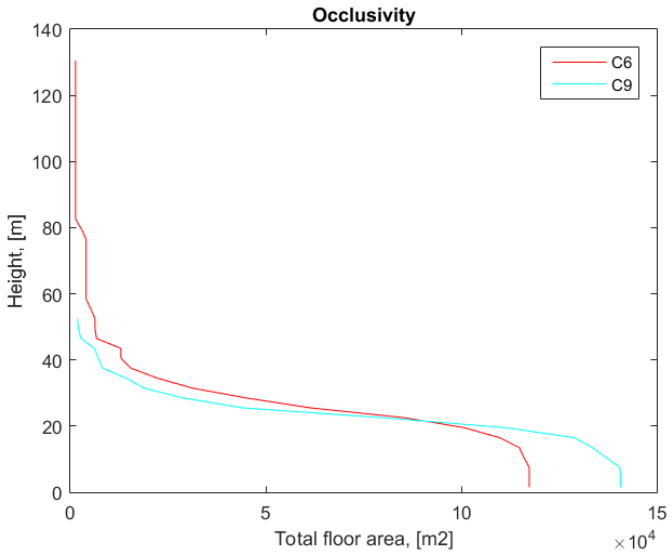

Figure 3.4: Occlusivity computed for two urban forms appeared in Figure 3.1, C6 and C9, denoting their openness to the sky vault.

Façade orientation

The orientation of building façades, along with their degree of obstruction, determines their insolation and thus, their potential for solar passive and active strategies. Orientation rose is a graph which aggregates the total façade surface area in an urban form per orientation referring to azimuth sectors. Considering the sun path, it indicates façade area and orientation potentially exposed to the highest irradiation and illuminance levels. For the obstruction of façades to be considered, façade surface area can be weighted by SVF values, as in orientation roses computed in PPF software (Fig. 3.5).

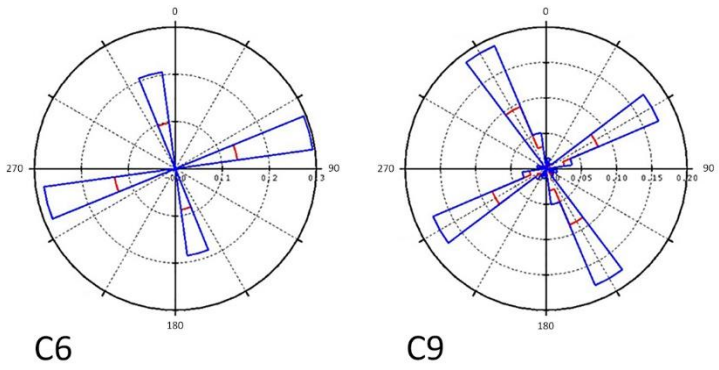

Figure 3.5: Orientation roses computed in PPF for two urban forms appeared in Figure 3.1, C6 and C9, denoting façade surface area (blue line) and façade surface area weighted by SVF (red line) by orientation, i.e. 30 azimuth sectors.

3.2.3 Sky view factor

Sky view factor constitutes a special category as it is being used in the literature equally as an urban geometry indicator and performance indicator, and as such it is treated in this research. Specifically, in the first and the second studies, the relationship of SVF with urban geometry variables is first examined and next, its relationship with solar indicators considered, namely mean insolation of open spaces and mean solar irradiances, respectively.

Introduced initially by urban climatology studies, sky view factor (SVF) is a measure of the degree to which the sky is obscured by surrounding buildings for a given point, thus denoting its openness to the sky. It has been also defined as the ratio of the radiation received by a planar surface to the radiation emitted by the entire hemispheric radiative environment (Watson and Johnson, 1987). Expressing a ratio, SVF is a dimensionless measure the value of which ranges from 0 to 1, representing a totally obstructed and unobstructed point, respectively (Oke, 1988). There is a wide range of methods to determine this parameter, including the analysis of fish-eye photos (Steyn, 1980). Furthermore, in the last decades, methods to derive continuous images of SVF have been developed, using raster urban models, i.e. DEMs, (Lindberg and Grimmond, 2010; Ratti and Richens, 1999) or vector models (Gal et al., 2009), allowing SVF to be calculated over extensive urban areas.

SVF is determined by the surrounding urban geometry and is often used as a built density index expressing it in a negative way, i.e. higher SVF denotes a less obstructed open space and hence, lower levels of built density. Various studies have included it as an urban geometry parameter investigating its relationship with spatial variations of urban air and surface temperatures (e.g. Eliasson, 1996; Giridharan et al., 2007; Yamashita et al., 1986), and outdoor thermal comfort (e.g. He et al., 2015; Krüger et al., 2011; 2016; Sharmin et al., 2015). (Relevant findings are referred to in Section 4.1). On the other hand, since the SVF value for a given point determines its capability to exchange radiation with the sky vault, the correlation with relevant phenomena is so strong that it has been used in urban climate models (e.g. Oke, 1981; Unger, 2006), and as performance indicator in urban design studies (Cheng et al., 2006a; 2006b; Project PREcis, 2000; Ratti et al., 2003; Zhang et al., 2012).

3.3 Selection of urban geometry variables

3.3.1 Selection criteria

A set of 18 urban geometry variables were selected for the first stage of the analysis, namely the geometrical analysis of 72 urban forms in London and 60 urban forms in Paris. This includes some of the urban geometric measures found in the literature, as well as some others, developed within the context of the current research. The criteria for the selection stems from the methodology and can be outlined in the following:

(i) The urban geometry variables ought to be numeric and expressed by a single number, as to allow the statistical exploration of their relationship with performance indicators.

(ii) They need to refer to essential properties of urban geometry, not to constitute environmental performance indicators. This criterion is related to that the aim of the research is to investigate relationships between urban geometry and environmental performance of urban forms, rather to assess environmentally the studied urban forms.

(iii) They need to treat the built form as built volumes, not as containers of living space; hence, measures which involve buildings' floor area are excluded. The reason behind this is that performance indicators computed on urban surfaces are not meant to be associated with potential implications for the indoor environment.

(iv) Overall, the set of variables needs to capture as much as possible the variations of urban geometry.

3.3.2 Selected variables and their computation

The research makes a distinction between built density quantifying the built form over an area, and all other urban geometry variables describing how the given built volume is shaped and configured within the area, (referred to hereafter as *urban layout descriptors*). This is deemed necessary for the exploration of the subject matter, the relationship of urban geometry and environmental performance, and emerges from the admittance of two facts.

First, the quantity of a built form, either being a building or this of an entire city, denotes the quantity of internal spaces contained, and in this way, is related to population and human activities which are what urban settlements are all about. Therefore, density values, along with land uses, to be implemented in an urban area are usually defined at urban planning level and conform to certain economic and development policies. On the other hand, regulations regarding the layout of open spaces and buildings, as well as the

form of buildings are usually of more local character and thus more flexible. Second, the negative effect of increasing densities on solar and daylight availability is a given; thus, the methodological isolation of the density parameter allows for the counterbalancing effect of other parameters of urban geometry to be investigated.

With respect to urban geometry variables considered in the analysis, they include eighteen measures, i.e. *built density* and seventeen *urban layout descriptors*. Prior to their presentation, it is important to remind that employing urban DEMs and image processing techniques for computing geometric measures entails a specific way of processing 3D geometry information, which affects how the variable is defined and what its value expresses (see Section 2.3.1). In particular, the built form is analysed into built volumes (i.e. adjacent buildings count as one volume); consequently, when referring to a building metric, this is measured based on built volumes in an urban form.

The list of the urban geometry variables computed for the analysis of urban forms in London and Paris is as follows:

Built density –referred to also simply as *density* – is defined as total built volume within the site over site area, [m^3/m^2].

Site coverage (SCo) is defined as total built area over site area, [%].

Mean building height (MeH) expresses mean height of built form, i.e. mean building height weighted by footprint area, [m].

Standard deviation of building height (StH) expresses standard deviation of height of the built form, i.e. standard deviation of building height weighted by footprint area, [m].

Standard deviation of site height (StS) expresses standard deviation of height of the entire urban form, including built forms and open spaces, weighted by footprint area [m].

Maximum building height (MaH), is equal to the height of the tallest building in the area, [m].

Mean outdoor distance (MeD) expresses mean distance between built volumes, [m]. Its calculation is based on the `bwdist` function in MATLAB, performed for the binary image of urban forms' ground maps, which computes for non-built pixels -of 0 value- their Euclidean distance from the nearest built one -of 1 value- (Fig. 3.6).

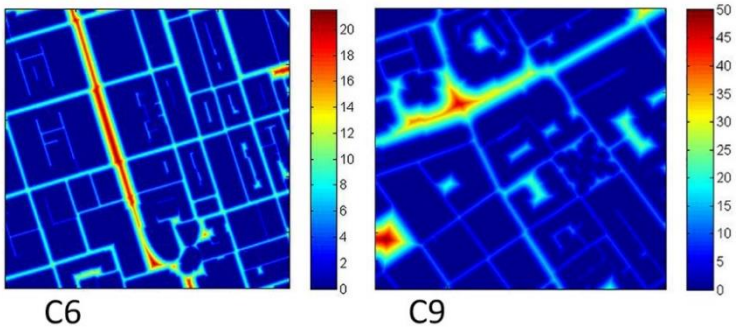

Figure 3.6: Maps obtained performing the `bwdist` *function for the ground maps of two urban forms appeared in Figure 3.1, C6 and C9, based on which the variables, mean outdoor distance, standard deviation of outdoor distance and maximum outdoor distance, were calculated.*

Standard deviation of outdoor distance (StD) is based on the same function as the mean outdoor distance variable -above- and expresses standard deviation of distance between built volumes, [m].

Max outdoor distance (MaD) is also based on the same function as the mean outdoor distance variable -above- and expresses maximum distance between built volumes, [m].

Compactness (Com) is defined as total building surface to building volume ratio, [m^2/m^3].

Complexity (Cex) is defined as total façade surface area over site area, [m^2/m^2]. Total façade area is obtained by summing façade areas computed at 3m height intervals -from the ground level to the maximum building height-. This means that setbacks of built volumes above the ground are considered.

Facades-to-street ratio (FaS) is defined as façade surface area to un-built area ratio, [m^2/m^2]. Unlike *complexity*, in the measurement of this variable, façade area is calculated based on the perimeter of building footprints on the ground level and the respective pixels' values, which means that only façades adjacent to open spaces are considered.

Number of building volumes (NoB) is the total number of built volumes in an urban form, including those which are not entirely within it but trimmed by the boundaries of the DEM. The calculation of the variable is based on `bwconncomp` function, performed for the ground maps of urban forms, which identifies continuous areas of 1s pixel values -built areas- surrounding by 0s pixel values -unbuilt area- (Fig. 3.7a).

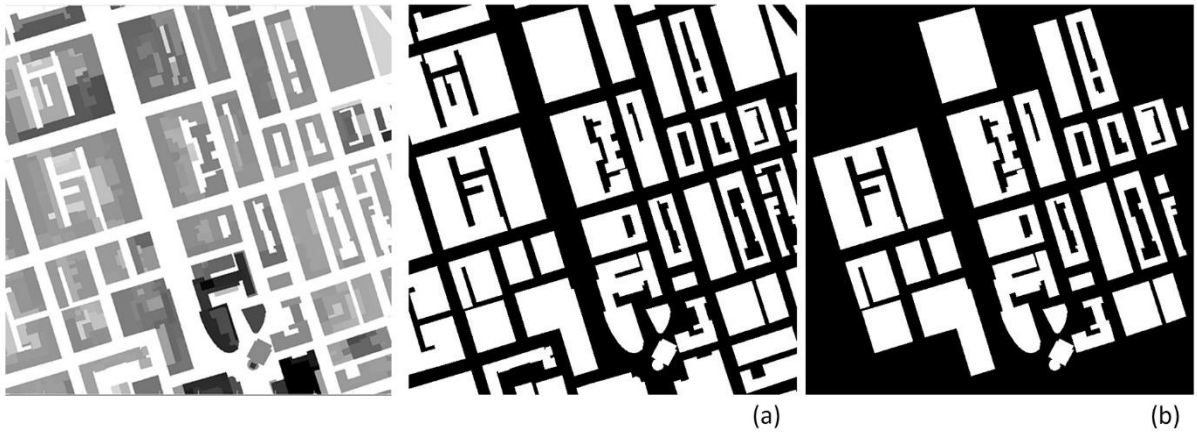

Figure 3.7: Left: the DEM of an urban form in central London (i.e. C6). Aside: binary image of its ground map where continuous built areas -appeared in white- count as individual built volumes in the calculation of number of building volumes (a); built volumes left after removing those trimmed by the edges of the DEM and considered in the calculation of mean building footprint, standard deviation of building footprint, mean building volume and standard deviation of building volume (b).

Mean building footprint (MeF) expresses mean footprint area of built volumes which lie entirely in a site area, [m^2]. For its calculation, a special script was written which removes those found on the edges and, next averages the surface area for the rest (Fig. 3.7b). Similar scripts were used for the following three variables.

Standard deviation of building footprint (StF) expresses standard deviation of footprint area considering built volumes that lie entirely within the boundaries of the urban form, [m^2].

Mean building volume (MeV) expresses mean volume considering built volumes that lie entirely within the boundaries of the urban form, [m^3].

Standard deviation of building volume (StV) expresses standard deviation of volume considering built volumes that lie entirely within the boundaries of the urban form, [m^3].

Directionality (Dir) is defined as the standard deviation of ground's permeability in 36 directions weighted by site coverage. The variable is conceived in the context of the research, but initially inspired by the *variance plot* of Ratti et al. (2006) which is a polar diagram showing the variance of the average urban profile in different directions. The computation of permeability is based on the same algorithm (Ratti, 2001) but instead of DEMs, the ground maps of the urban forms are used, and the values are weighted by their built area. The script used for the computation of *directionality* is given in Appendix C.

The names and abbreviations of the selected urban geometry variables are concentrated and presented in Table 3.1. In relation to the geometric measures reviewed in Section 3.2, some new are introduced, either adopted by urban morphology studies or conceived in the context of the present research. *Mean building volume* has been used in the study of Yoshida and Omae (2005) for the morphological analysis of urban blocks. In the same study, total building surface per projected area is proposed as a crucial morphological measure; instead the present research considers total building façade area over site area, referred to as *complexity*, focusing on the effect of façades' undulations. A similar measure is this expressed by *façades-to-street ratio* which combines façade surface area with open space surface area.

Standard deviation of outdoor distance and *maximum outdoor distance* are considered along with *mean outdoor distance* as basic measurements of the open space. The three metrics have been used before in the study of Hermosilla et al. (2014) for the characterization of urban typologies. Four variables refer to building height and thus the vertical expression of the built form, *mean building height*, *standard deviation of building height*, *standard deviation of site height* and *maximum building height*, with the latter being used as descriptive feature of urban areas in several studies (e.g. Hermosilla et al., 2012b; 2014). *Standard deviation of building height* and *standard deviation of site height* express the vertical randomness of the built form and entire urban form, respectively. In absence of a measure quantifying the horizontal randomness of urban layouts, the research considers several variables which are identified to be indirectly related to this. These are *standard deviation of outdoor distance* and *standard deviation of building footprint,* both associated positively with horizontal randomness*,* and *directionality,* associated negatively as the more directional an urban layout is, the less random it tends to be. Finally, *number of building volumes* has been also used for the classifications of urban areas (Hermosilla et al., 2014); dividing *built density* and *site coverage* by the number of building volumes existing within an area gives mean building volume and footprint, respectively. However, in the current research, *mean building footprint* and *mean building volume* as well as, *standard deviation of building footprint* and *standard deviation of building volume* refer to built volumes lying entirely within the boundaries of the urban form, while *number of building volumes* refers to all built volumes including them extending beyond the boundaries.

It becomes thus apparent that some urban geometry variables selected initially to be computed for all the urban forms are strongly related to each other, as their calculation involves similar measurements. Furthermore, variables such as *maximum building height* and *maximum outdoor distance* are regarded useful in characterising urban areas, but they refer to local expression of the geometry of an urban form, rather the entire urban form. In any case, the above variables were selected for the comparative analysis

of London and Paris, the results of which are presented in the following section. The geometric analysis of the urban forms of the two cities highlights their major differences and, moreover, examines to what extent geometric measures such as those employed can capture the variations of urban geometry in real urban forms.

Table 3.1: 18 urban geometry variables considered in the analysis, built density and 17 urban layout descriptors.

Urban geometry variables		
Name	**Unit**	**Abbreviation**
Built density	m^3/m^2	
***Layout descriptors*:**		
Site coverage	%	SCo
Mean building height	m	MeH
Standard deviation of building height	m	StH
Standard deviation of site building	m	StS
Maximum building height	m	MaH
Mean outdoor distance	m	MeD
Standard deviation of outdoor distance	m	StD
Max outdoor distance	m	MaD
Compactness	m^2/m^3	Com
Complexity	m^2/m^2	Cex
Facades-to-street ratio	m^2/m^2	FaS
Number of building volumes	-	NoB
Mean building footprint	m^2	MeF
Standard deviation of building footprint	m^2	StF
Mean building volume	m^3	MeV
Standard deviation of building volume	m^3	StV
Directionality	-	Dir

3.4. Analysis of urban forms in London and Paris

3.4.1 Descriptive statistics

Urban geometry variables, namely density and seventeen urban layout descriptors, were computed for 72 urban forms of London and 60 urban forms of Paris, and the results are examined comparatively. Figure 3.8 summarises visually the descriptive statistics by variable, for the two cities. The same information is provided analytically in tables in Appendix D (Tables D.1 and D.2, for London and Paris, respectively).

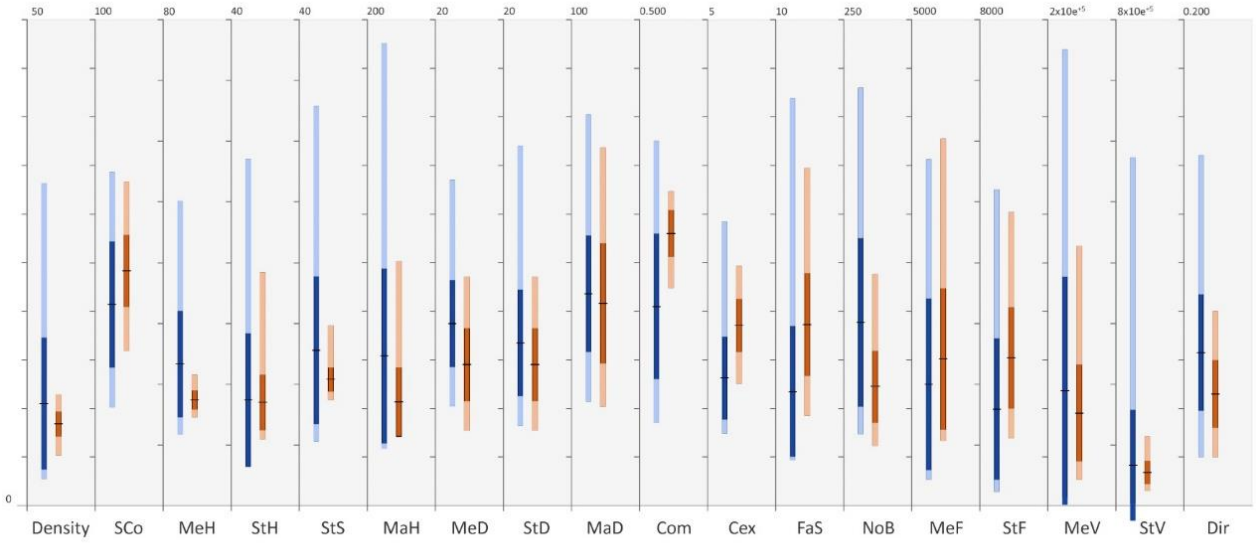

Figure 3.8: Graphical visualisation of descriptive statistics for 18 urban geometry variables computed for London's (blue bars) and Paris' (orange bars) urban forms: range of values (light colour), mean values, standard deviation of values (dark colour). (Enlarged as Figure D.1 in Appendix D.)

A first observation is that the ranges and standard deviations of values of all the variables are greater for London compared to Paris, and in some cases the difference is significantly big. This reflects the fact that urban geometries across the city of Paris present a relative homogeneity and uniformity. In contrast, in London, the urban geometry variables differ considerably among urban forms. Furthermore, it is observed that, in both cities -and especially in London- the mean values of the variables tend to be lower than the middle value of the respective ranges, due to some extremely high maximum values.

Regarding density, the range for London is about 5 times greater than for Paris, with the former being between 2.8 and 33.1 and the latter between 5.2 and 11.4 [m^3/m^2]; however, their mean values are relatively close, 10.5 and 8.4, respectively. This is attributed to that areas of higher density in London are concentrated spatially between Westminster and the City of London, and represent a small number of

urban forms in the sample. With respect to *mean building height* (MeH), the difference is even greater, with the values ranging from 11.8 to 50.1m among London's urban forms, and only 14.6 to 21.5m in those of Paris. Unlike *density* and *mean building height* though, the ranges of site coverage (SCo) values in the two cities are relatively close and, interestingly, the mean value in Paris is higher, i.e. 48.3% to 41.4%. Summarising the above, it is apparent that the great variation of density in London are accompanied by equally important variations in the horizontality and verticality of the built form. In contrast, in Paris, the urban forms differ significantly in terms of horizontality, but the verticality parameter is found to be rather constant. Combining this with the limited range of densities implies that the interrelation of density, site coverage, mean building height is governed by different patterns than in London.

Examining the rest of the variables, some interesting points are worth to be mentioned. First, unlike *mean building height* (MeH), *standard deviation of building height* (StH) varies significantly in Paris with the average values for the two cities being very close. Second, *mean outdoor distance* (MeD) and *standard deviation of outdoor distance* (StD) are found to be on average greater in London, with higher mean outdoor distances to be directly related with lower site coverages. Thus, Paris's urban forms present on average less open space, narrower streets, of relatively constant width. Third, Paris' built forms feature a lower degree of compactness, i.e. higher Com values. Increased façade surface in Paris is also reflected to higher mean values of *complexity* (Cex) and *façades-to-street ratio* (FaS). Fourth, with respect to *mean building footprint* (MeF) and *standard deviation of building footprint* (StF), the two samples feature similar ranges of values, but on average their values are higher in Paris. In contrast, *mean building volume* (MeV) and *standard deviation of building volume* (StV) vary significantly more in London which is explained by some extremely high values in London's sample. Specifically, in central London, some significantly large building volumes coexist near very small ones (Fig. 3.9), which constitutes another indication of the heterogeneousness of the urban geometry in London.

Overall, it can be argued that urban geometry variables which refer to the characteristics of horizontal urban layout, such as *site coverage*, *mean outdoor distance*, and *mean building footprint*, are found to vary equally in the two cities. On the other hand, there is an important number of variables, most of them related to height and volume metrics, for which the sample of London presents extremely high maximum values, stretching upwards the respective range.

Figure 3.9: Example of urban form in central London with very large and very small building volumes, justifying extremely high standard deviation of building volume values.

3.4.2 Correlation of urban geometry variables

The interrelation of the urban geometry variables in London's and Paris' samples was next examined, performing Pearson Correlation (two-tailed) analysis. In general, it was expected that some variables would present strong correlations considering that the geometric parameters that they express are related in the urban planning process, and/or their calculations involve the same metrics. Nonetheless, the way in and the degree to which this occurs in the two cities differ significantly, providing a better insight about their geometries.

3.4.2.1 London's results

The results of the correlation test for the urban forms of London, presented analytically in Appendix D (Table D.3), demonstrate a significant correlation -at 0.001 level- among most of the variables. With respect to density, this is found to correlate extremely well with most of the urban layout descriptors, except for those referring to outdoor distance parameters, and especially, standard deviation and maximum outdoor distance. Interpreting the signs of the correlation coefficient (r) values, increasing built density in London coincides with less open spaces and consequently, smaller distance between buildings, taller buildings on average and in absolute values, less uniform skylines, greater total façade surface area but more compact built forms. Also, urban forms of higher density tend to have smaller number of building volumes, of larger footprint area and volume, as well as greater diversity in building footprints and volumes, and last, lower degrees of directionality.

Furthermore, the r values for density and six -out of seventeen- urban layout descriptors are above 0.9 denoting a very strong linearity. These variables are -in decreasing order of significance- *mean building height* (r=0.960), *façades-to-street ratio* (0.959), *standard deviation of site height* (r=0.949), *complexity* (r=0.944), *mean building volume* (r=0.925) and *site coverage* (r=0.901). Regarding mean building height and site coverage, their strong correlation with density indicates that the density of urban forms in London increases mutually in vertical and horizontal means. This symmetrical development of the built form in London is reasonable but not the only way of intensification of the built environment, and should be regarded as a special characteristic of London. As shown in the graphs, the relationship of density and mean building height is almost perfectly linear (Fig. 3.10a); whereas, this of density and site coverage is better described by a logarithmic curve (Fig. 3.10b). The latter is fully justified considering that site coverage is a ratio with maximum possible value, i.e. 100%, which never occurs since some open space is always necessary to serve the function of streets. On the other hand, building height has no maximum value, and theoretically can increase to infinity, increasing simultaneously built density.

With respect to the rest of urban layout descriptors correlating extremely well with density in London's sample, *complexity* is one of them which -by definition- are affected positively by the increase of the size of the built form. However, the relationship is not a straightforward one since there are other influential parameters, such as compactness and number of building volumes. It is thus considered that the very strong correlation in the case of London is also caused by the great range of density values. The fact that *façades-to-street ratio* presents a slightly higher r value is attributed to the fact that its measurement involves façade surface area and open space area, with both being related to density in a specific way. Similarly, *standard deviation of site height* correlates better with density compared to *standard deviation of building height* because its measurement involves the open space not only the built form. Lastly, the strong positive relationship between density and mean building volume is expected and, in this case, empowered by that urban forms of higher density tend to contain less building volumes. However, as applies for all the variables, the significance of the relationship may be stretched by the considerable range of density values.

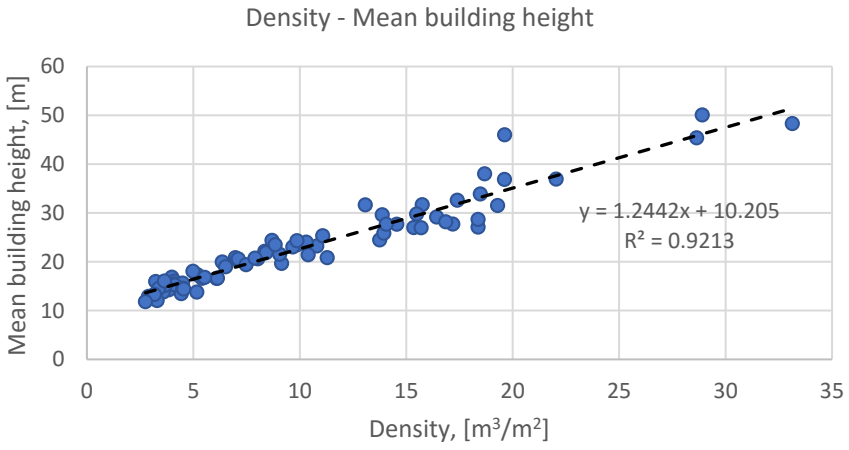

(a)

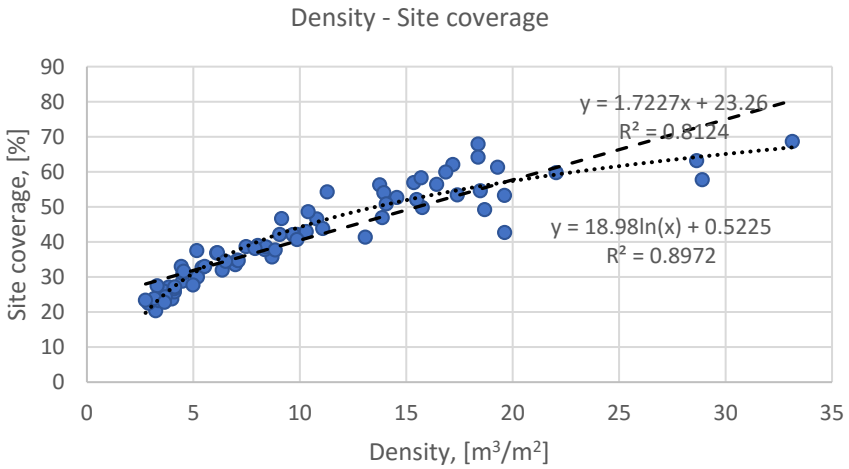

(b)

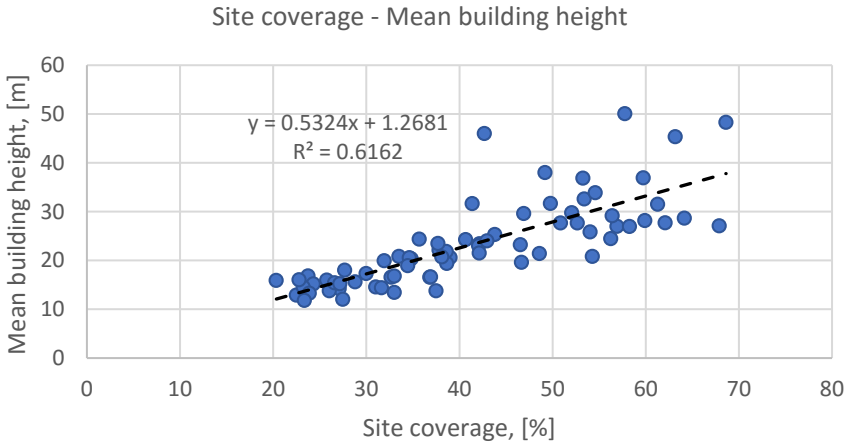

(c)

Figure 3.10: Scatter plots and trendlines showing the relationship between density and mean building height (a), density and site coverage (b), and site coverage and mean building height (c) in 72 urban forms of London.

Considering the correlations between urban layout descriptors, it is observed that all those correlating significantly ($p<0.001$) with density correlate also to each other at the same level of significance. On the other hand, *standard deviation of outdoor distance* and *maximum outdoor distance* differentiate from the rest presenting significant correlation only with *mean outdoor distance* and *directionality*. Interestingly, the only variable, including density, which presents significant correlation with all the others is directionality.

The above implies the decisive role that the density parameter plays in the sample of London, causing a strong interrelation among most of the urban geometry variables. To verify this, partial correlation test was performed with control for the density variable; the results are provided in Appendix D (Table D.4). Comparing them with those in Table D.3, the difference is noticeable and lies in smaller number of significant correlations as well as reduced amplitude of significance. Two characteristic examples are *max building height* (MaH) and *directionality* (Dir) which, controlling the impact of density, correlate significantly with much fewer urban layout descriptors. Nevertheless, there are also identified variables, such as StD and MaD, for which the control of density causes more correlations.

It is worth highlighting that, the sign of some relationships has switched from positive to negative, and the inverse. This concerns the relationships between urban layout descriptors quantifying built area and open space, i.e. SCo and MeD, and those referring to building and site height, i.e. MeH, StH, StS and MaH. As discussed before, SCo and MeH are positively related in London since the horizontality and verticality of built forms tend to increase simultaneously when density increases. However, controlling density, meaning for a given density value, the relationship becomes negative, as higher site coverage means lower building height, and inversely. Partial correlation analysis with control for density is widely used in this research to test the relationship between urban layout descriptors and performance indicators; so, the competitive relationship of the two parameters is appeared also in the results of the studies and discussed further.

3.4.2.2 Paris' results

With respect to Paris' urban forms, the interrelation of the urban geometry variables is considerably reduced, both in terms of occurrence and amplitude (see Appendix D, Table D.5). Examining number of significant correlations as well as absolute r values, the variables which present the highest and lowest interrelations is *site coverage* and *mean building height*, respectively. The former correlates with all the variables but *compactness*, and the latter does so only with *built density*, *site coverage*, *standard deviation of building* and *standard deviation of site height*, and *compactness.* Interestingly, the relationships of *mean building height* with *site coverage* and *mean outdoor distance* are negative. This constitutes a major difference between the two cities, indicating that, in Paris, urban forms with less open space tend to have lower building heights, and is discussed further below examining the interrelation of the particular variables with density.

As in London, density correlates with most urban layout descriptors. Specifically, in Paris, density presents significant correlations with all descriptors except for *standard deviation of site height* and *directionality*. However, the r values obtained are noticeably lower, with strongest correlations being for *façades-to-street ratio* (r=0.840), *site coverage* (r=0.826), and *complexity* (r=0.795). Moreover, there are two interesting points to be discussed. First, the relationship between density and coverage is strong and positive, but the relationship between density and mean building height is almost null. Second, whereas, in London density correlates positively with *standard deviation of building height* and *maximum building height*, in Paris the respective relationships are found negative.

Starting from the first point, and plotting mean building height against density values, it appears that the relationship is slightly positive but extremely weak (Fig. 3.11a). The respective graph for site coverage, it shows that the relationship is clearly positive and almost equally well described by logarithmic and linear curves (Fig. 3.11b). (The logarithmic curve achieves a higher R^2 underlining the argument developed before). It becomes thus apparent that in Paris the built form increases quantitatively in the horizontal direction, rather than the vertical one which remains -at least on average- relatively constant. Furthermore, the negative relationship of the variables, as shown in Figure 3.11c, indicates a rather counteracting effect of their combination on resulting density, keeping the density range limited.

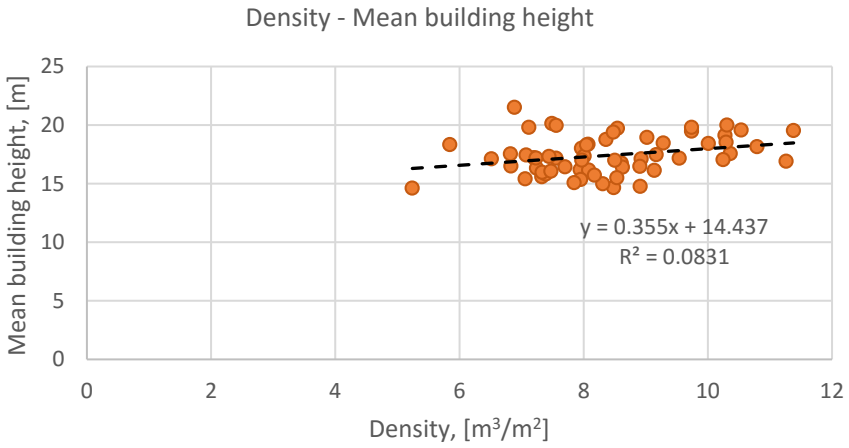

(a)

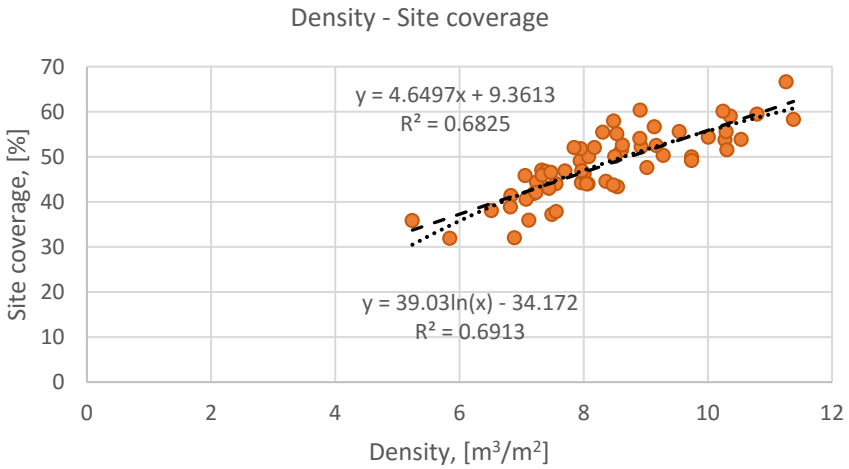

(b)

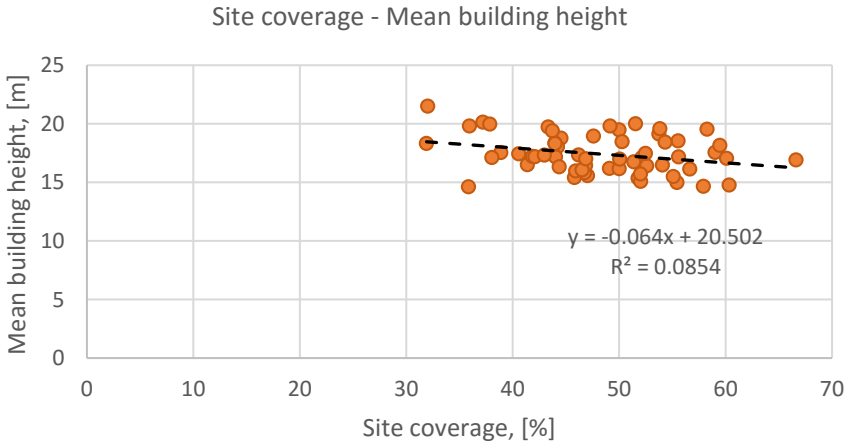

(c)

Figure 3.11: Scatter plots and trendlines showing the relationship between density and mean building height (a), density and site coverage (b), and site coverage and mean building height in 60 urban forms of Paris.

Regarding the negative correlation of density with *standard deviation of building height* and *maximum building height*, the plots in Figures 3.12a and 3.12b are very informative. It is observed that higher StH and MaH values are found in urban forms of relatively lower densities. More precisely, for higher densities, i.e. above $9m^3/m^2$, the values of the two variables are close to the lowest extreme of the range, presenting small variations; while, in lower densities, the points tend to spread upwards recording higher values. To allow the association of this finding with actual urban geometries, the three urban forms of highest maximum building height (P9, P10, and P59) and those of highest densities (P6, P17 and P18) are identified in Figures 3.12b and 3.12c, and their DEMs are presented in Figure 3.13. Comparing them, it becomes apparent that their differences are not limited to maximum values and uniformity of building heights, but are more radical. The urban forms P6, P17, and P18 are representative of urban geometries found in the wider historic centre of Paris, with its geometric characteristics being so consistent that can classify as a distinct urban typology. Their main features are urban blocks of closed shape, i.e. with contiguous elevations on the street side, and of constant height, which are bounded by a rigid street network.

On the other hand, tracing the urban forms of highest maximum building height on the map of Paris, it is ascertained that these are geographically defined, with most of them lying on the outskirts of the city, the so-called *banlieue*. These areas, built in the post-war years in response to housing shortage and to rid those of slums, are characterised by a mix of typologies, i.e. tower blocks and slab housing. This explains why the respective urban forms feature high maximum building heights, and less uniform skylines, and deviate so much from the homogeneous and “compact” urban geometries found in central areas of Paris. Furthermore, their built density is found to be rather moderate as any increase in average building height is outbalanced by low site coverage values.

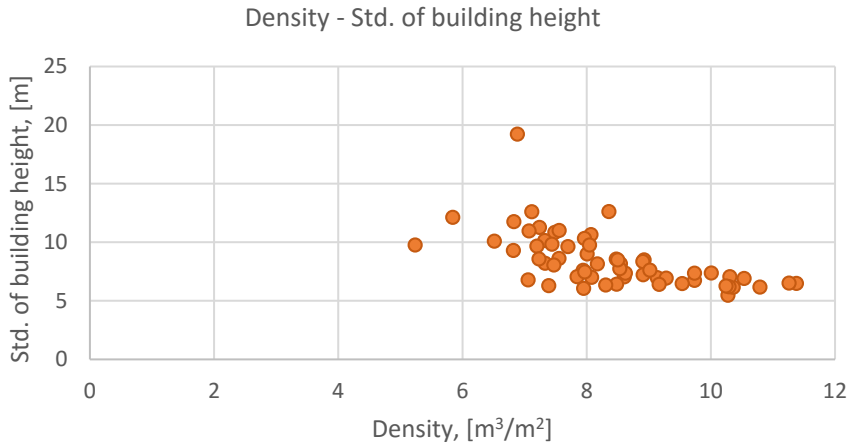

(a)

(b)

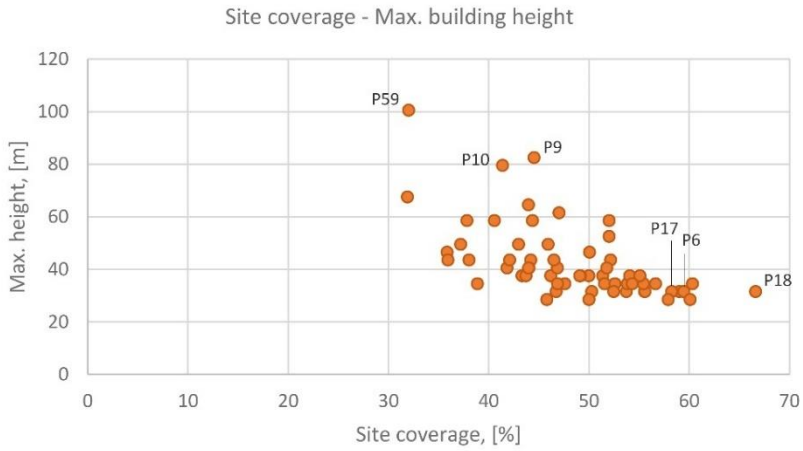

(c)

Figure 3.12: Scatter plots and trendlines showing the relationship between density and standard deviation of building height (a), density and maximum building height (b), and site coverage and max. building height (c) in 60 urban forms of Paris.

Figure 3.13: DEMs of three urban forms with highest buildings (a), and with highest density (b) in Paris' sample.

3.4.3 Principal component analysis

Having ascertained strong correlations between urban geometry variables, the next step was to perform Principal Component Analysis (PCA) examining simultaneously the variability within and co-variation across the variables, i.e. variance and correlation. Table 3.2 juxtaposes the tables of total variance explained by extracting an increasing number of factors, i.e. components, for London and Paris. It is observed that the same number of factors can explained a greater percentage of the variance of the data in London, compared to Paris, which is reasonable considering the stronger and wider correlations across the variables in London's sample. Indicatively, just one extracted factor can explain about 63% and 45% of the variance of the urban geometry data in London and Paris, respectively.

Examining the results based on the extraction of three components allows them to be plotted in 3D space and potential clusters of variables to be appeared. Initially, the test was performed without rotating factors; the factor loadings (correlation between specific variable and specific factor) and communalities (influence of each variable from all three factors) are given separately for London and Paris in Appendix D

(Table D.6 - D.7). As seen in Figure 3.14a, in the case of London, the structure of the loading matrix is rather clear. A big cluster is created by variables found to correlate strongly with density (i.e. SCo, MeH, StH, StS, MaxH, Cex, FaS, MeF, StF, MeV and StV) mostly affected by Component 1. Another cluster is this of the variables associated with outdoor distance (i.e MeD, StD and MaD) which correlate better with Component 2; while compactness and number of building volumes are paired together and mostly influenced by Component 3. Interestingly, the directionality variable stands alone, in between outdoor distance variables, and the pair of Com and NoB. By rotating the factors -which is used in PCA analysis for the better interpretation of the extracted factors- the positions of the variables in relation to three axes do not change much and the same clusters retain (Fig. 3.14b).

Table 3.2. Principal Component Analysis for 18 urban geometry variables: tables showing total variance explained by extracting an increasing number of factors, i.e. components, in London's (left) and Paris' (right) sample.

LONDON **Total Variance Explained**

Component	Initial Eigenvalues Total	% of Variance	Cumulative %
1	11.331	62.949	62.949
2	3.040	16.888	79.837
3	1.297	7.204	87.041
4	0.782	4.346	91.387
5	0.503	2.796	94.183
6	0.325	1.805	95.987
7	0.252	1.401	97.388
8	0.183	1.017	98.405
9	0.082	0.454	98.859
10	0.066	0.368	99.227
11	0.054	0.299	99.526
12	0.030	0.167	99.693
13	0.020	0.111	99.804
14	0.016	0.090	99.894
15	0.012	0.064	99.958
16	0.005	0.028	99.986
17	0.002	0.011	99.997
18	0.001	0.003	100.000

Extraction Method: Principal Component Analysis.

PARIS **Total Variance Explained**

Component	Initial Eigenvalues Total	% of Variance	Cumulative %
1	8.110	45.057	45.057
2	3.799	21.105	66.162
3	1.833	10.183	76.345
4	1.148	6.379	82.723
5	0.826	4.588	87.311
6	0.631	3.504	90.815
7	0.486	2.701	93.516
8	0.423	2.352	95.868
9	0.220	1.222	97.089
10	0.200	1.112	98.201
11	0.118	0.656	98.858
12	0.098	0.545	99.402
13	0.059	0.326	99.728
14	0.035	0.194	99.923
15	0.010	0.054	99.977
16	0.002	0.013	99.989
17	0.001	0.008	99.997
18	0.001	0.003	100.000

Extraction Method: Principal Component Analysis.

Examining the same plots for Paris, in that obtained without rotation, the variables are found to be spread all over the space and the structure of the loading matrix is not clear (Fig. 3.15a). Testing all types of rotation, Promax rotation was found to be the most successful, producing the simplest structure (Fig.

3.15b). According to this, there are three main clusters, one of variables strongly associated with density (i.e. SCo, Cex, and FaS), another one of variables referring to outdoor distance (i.e. MeD, StD and MaD), and last one created *number of building volumes* (NoB), *maximum building height* (MaH) and *standard deviation of building height* (StH); whereas, the rest of the variables rest in the intermediate space.

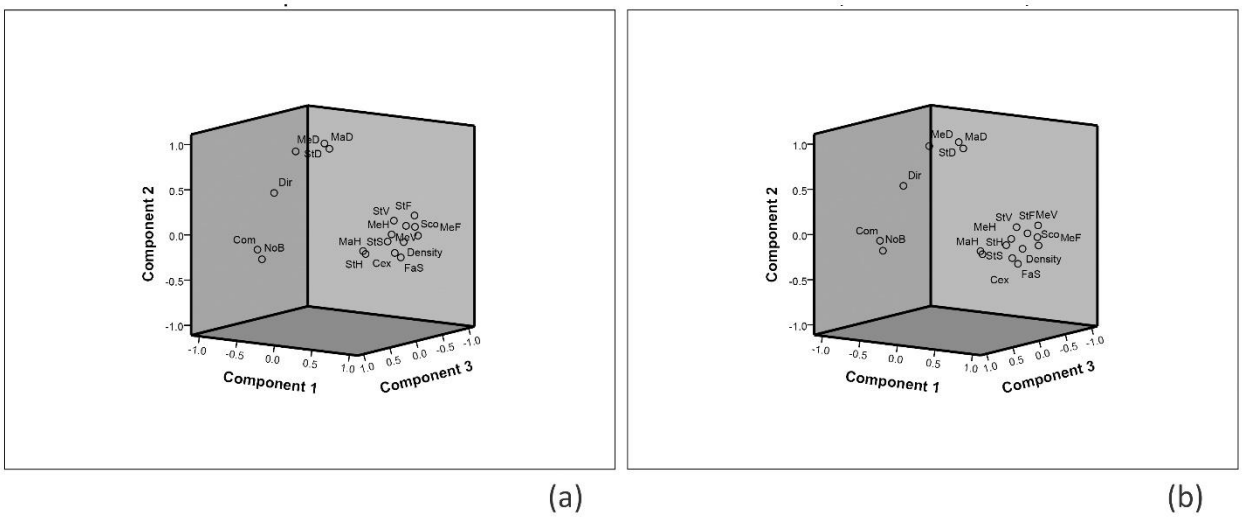

Figure 3.14: Principal Component Analysis for 18 urban geometry variables in London's sample: plot of variables in 3D space when number of components is set to three, without rotation (a) and with rotation (b).

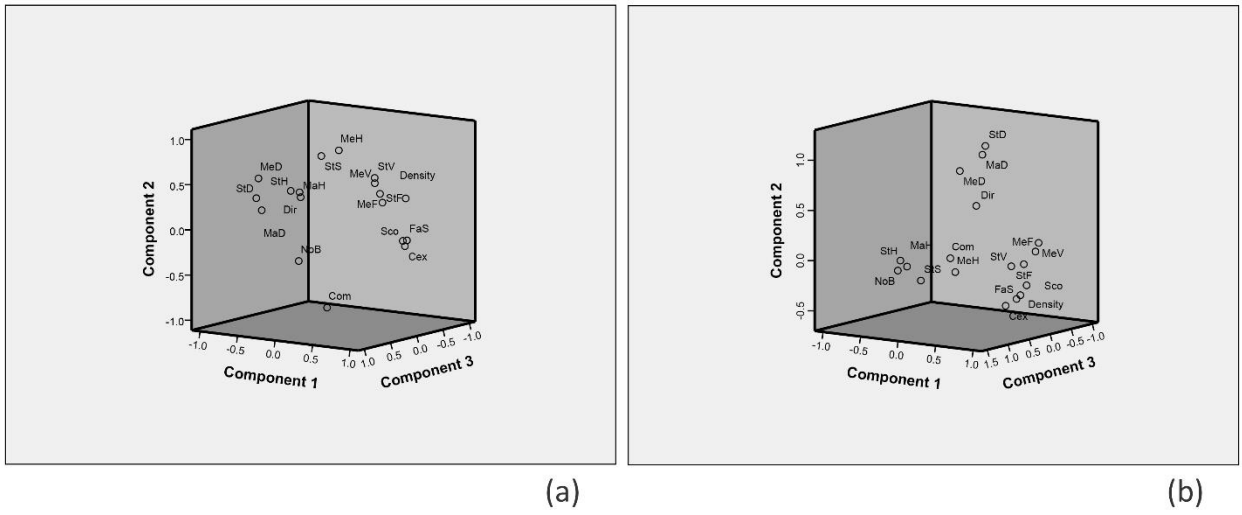

Figure 3.15: Principal Component Analysis for 18 urban geometry variables in Paris's sample: plot of variables in 3D space when number of components is set to three, without rotation (a) and with Promax rotation (b).

It is noted that in the next chapter, where the relationship of urban geometry with mean SVF values is examined, the PCA factors extracted and used for London and Paris are three and five, respectively. The reason for this is that the factors should explain similar percentages of the variance of the urban geometry variables in the two cities. As seen in Table 3.2, three factors for London and five for Paris explain about 87% of the variance which is considered an adequate percentage for replacing the initial variables.

3.5 Conclusions

Chapter Three along with the first two chapters of the thesis provide the background information required for the understanding of the three studies of the research which follow. After a comprehensive review on urban geometric metrics, which are identified in the literature to be associated with aspects of urban environmental performance, the eighteen urban geometry variables selected to be included in the analysis were presented. They include some of the reviewed metrics, some adopted by urban morphology studies and others conceived in the context of this research. The criteria for their selection -discussed in Section 3.3.1- reflects two purposes. The first one concerns the comparative analysis of the geometry of urban forms in two case study cities, London and Paris. The second one is that the urban geometry variables selected are used as a source from which each study derives independent variables, the impact of which on studied performance indicators is next explored statistically.

The geometric analysis of the urban forms in London and Paris reveals considerable differences between the two cities and, at the same time, tests the capability of urban geometry metrics to capture such differences. A major outcome is the dominant role of the density variable which is distinguished from the rest of geometric measures, referred to as urban layout descriptors. Density correlates significantly with most urban layout descriptors. Some correlations are expected as the amount of built volume existing in an urban area is related to other metrics, such as façade surface area. Façade surface area is considered in the calculation of *complexity* and *façades-to-street ratio*. In other cases, it is related to the fact that density equals to the product of site coverage and mean building height. Finally, there are correlations of density, such as with standard deviation of building height and outdoor distance, as well as maximum height and outdoor distance, which are not causal and thus may or may not occur depending on the city.

Comparing London to Paris, a significant difference is the range of density values which are considerably wider in the sample of the former. This justifies to some degree why density correlates stronger with urban layout descriptors and thus the variance of urban geometry in London's urban forms can be explained by fewer factors in Principal Component Analysis. Another important difference is that in

London, urban forms of higher density tend to have higher site coverage and mean building height values, which denotes that the density in London increases both vertically and horizontally. In contrast, in Paris, density presents significant positive correlation only with site coverage. As revealed, higher densities coincide with higher site coverages found in "compact" urban geometries of the historic centre where the building height is relatively low and constant. In lower densities, mean building height varies considerably with higher values to be found on the outskirts of the city of Paris, the so-called *banlieues.* What is important though is that, unlike the range of density and mean building height values, that of site coverage is similar in the two cities. The above are highlighted as to be taken into account especially in the first and the third studies which examine relationships between urban geometry and environmental phenomena comparatively in London and Paris.

With respect to the collinearity of urban geometry variables, it is a wider issue which has been pointed out in many studies exploring statistically relationships between urban geometry and environmental performance of urban forms (Martins et al., 2014; Mohajeri et al., 2016; Nault et al., 2015). As discussed before, this is to a great degree inevitable as most of them refer to basic geometric measurements which are by definition interrelated, and also denotes that there are particular mechanisms governing the production of the urban space in each city. Thus, as shown in studies examining the effect of various urban factors, such as vegetation and albedo, the problem of collinearity is not limited to geometric variables but concerns in general urban variables (Giridharan, 2007; Yang and Chen, 2016).

The present research faces the collinearity of the independent variables in different ways in the three studies, as each of them focuses on different urban geometry variables. The first study focuses on sky view factor (SVF), which is first examined as a dependent variable and next, as an independent one. Specifically, in the first part, the relationship of SVF with eighteen urban geometry variables is investigated through a series of statistical tests, including partial correlation tests as well as linear regression for factors obtained by the PCA analysis. Next, the effect of SVF on mean insolation of the open spaces of urban forms in London and Paris is examined.

The second study examines the effect of density and urban layout on solar availability in urban forms of London. Urban geometry is represented by *built density* and nine urban layout descriptors, respectively. The urban layout descriptors were selected from seventeen presented in Section 3.3.2. *Site coverage* and *mean building height* were automatically included as major urban design and planning parameters. Descriptors which were found to be less dependent on density, i.e. *directionality*, *compactness*, *number of building volumes* and *mean outdoor distance* (see Fig. 3.15) were also selected; whereas, from those

strongly related to density, *standard deviation of building height*, *standard deviation of building footprint* and *complexity* were preferred. Overall, the selection aimed for the urban layout descriptors to cover as many parameters of urban geometry as possible, and for those to be interpretable into design guidelines. *Directionality* which is a less tangible measure is selected to be considered along with *standard deviation of building footprint* to account for the horizontal randomness parameter. The effect of urban layout descriptors on solar availability indicators is investigated performing partial correlation analysis, which as discussed in Section 5.3.1, is proven an effective way to control the collinearity effect.

The last study examines the impact of the level of built obstruction on the occurrence of spatial thermal diversity in the open spaces of urban forms in London and Paris, considering two independent variables. These are density, expressing 3D obstruction, and site coverage, expressing 2D obstruction. The consideration of site coverage was considered necessary as the range of density values in Paris is very limited affecting the relevant findings.

Chapter Four

Radiant environment in open spaces

Chapter Four presents a study on the relationship between urban geometry and solar exposure of open spaces. An early study on the variations of average hourly mean radiant temperature (MRT) in the 72 urban forms of London is presented first, and sets the scene for the topics to be next explored. Among others, this showed that, under clear sky conditions, the relationship between urban geometry and MRT varies in the day because of varying solar altitude angles. To isolate the effect of solar radiation intensity, an extensive investigation was conducted shifting the focus on the relationship between urban geometry and average instantaneous and daytime shadow fractions, namely mean insolation of open spaces. Special emphasis is put on mean ground sky view factor (SVF) which is used as an integrated urban geometry variable. Beyond London's urban forms which constitutes the main case study, 60 urban forms of Paris are also examined, in order for the sensitivity of the findings to different urban geometries to be tested.

4.1 Introduction

Open spaces play a key role in urban environmental design as they constitute the interface between architectural and urban scales interacting with buildings and the urban canopy. Outdoor thermal conditions are the result of the modification of the urban climate by urban geometry, (referred to as *urban structure*), *urban cover*, *urban fabric* and *urban metabolism* (Oke, 2006), and affect both outdoor and indoor microclimates, with implications for thermal sensation and buildings' energy performance (Santamouris, 2001). Among the four modifiers of the urban climate, urban geometry has been characterized as the most relevant to the climatic variations at the micro-scale, corresponding to the intermediate urban scale, i.e. streets and blocks (Oke, 1987; 2006). At this scale, the occurrence of microclimatic variations is highly associated to the radiant environment as solar radiation availability in the daytime and long-wave radiation emitted by the urban surfaces at night are very sensitive to the variations of urban geometry.

The radiant environment close to the ground is highly related to thermal conditions experienced by pedestrians and users of open spaces, such as streets and squares. The sum of all radiation fluxes to which the human body is exposed is one of the four environmental factors governing thermal comfort, and

expressed by mean radiant temperature (MRT). In turn, solar irradiation of outdoor spaces depends on their openness to the sky vault (diffuse solar and sky component) which results from the geometry of the urban form, and their exposure to the sun (direct solar component) which is decided by the urban geometry and orientation of it in relation to the sun's position. Additionally, the solar exposure of open spaces affects their surface temperature, which is not only considered in the calculation of MRT but may also influence local air temperatures (He et al, 2015). Insolation levels and resulting MRT have an increased weighting in outdoor thermal sensation and, particularly, MRT is regarded as a more accurate indicator for its evaluation than using air temperature (Peng et al., 2011).

The vast majority of researches on outdoor thermal environment, either measurement- or modelling based, have adopted the urban street canyon as the basic structural unit to focus on (e.g. Ali-Toudert and Mayer, 2007a; 2007b; Andreou & Axarli, 2012; Bourbia and Awbi, 2004a; 2004b; Johansson, 2006; Pearlmutter et al., 1999). Urban street canyon geometry, characterised by a height-to-width ratio and orientation -as this defined by its longest axis- allows the effect of the two crucial parameters for solar access, urban geometry and orientation, to be studied (Arnfield, 1990). For instance, H/W and street orientation have been considered as design parameters in several studies assessing shading levels in hot climates (e.g. Ali-Toudert and Mayer, 2006; 2007b; Bourbia and Awbi, 2004b; Emmanuel et al., 2007).

In researches on real street canyons, where their length is finite and the building height usually varies, along with or instead of H/W, sky view factor is being used as an indicator of urban geometry (e.g. Bourbia and Boucheriba, 2010; Krüger et al., 2011; 2016; Sharmin et al., 2015; Wang and Akbari, 2014). Sky view factor (SVF) is a measure of the openness of a point to the sky which controls two major environmental processes: loss of longwave radiation to the sky responsible for the cooling down of the urban surfaces at night, and sky diffuse radiation received by them during the day, associated also to illuminance levels. Its association with the above environmental phenomena is so strong that, in several studies, it has been proposed as an environmental performance indicator (Cheng et al., 2006a; 2006b; Project PREcis, 2000; Ratti et al., 2003; Zhang et al., 2012).

The effect of SVF has been extensively studied on daytime and nocturnal air temperatures, in different climatic context, associated with the intensity of Urban Heat Island phenomenon and outdoor thermal comfort (e.g. Cheung et al., 2016; Eliasson, 1996; Giridharan et al., 2007, He et al, 2015; Krüger et al., 2011; Przybylak et al., 2017; Yamashita et al., 1986). The relevant findings have not been clear regarding the existence and strength of the correlation, especially regarding daytime air temperatures. On other hand, the relationship of SVF with surface temperature and MRT have been found to be statistically

stronger (Bourbia and Boucheriba, 2010; Krüger et al., 2011; Wang and Akbari, 2014). It is reasonable a negative relationship to occur at night, since the more open to the "cold" sky a surface is the higher its heat losses. Interestingly thought, SVF has been also positively associated to insolation levels of open spaces, and thus higher surface and mean radiant temperature during sunny hours (Bourbia and Boucheriba, 2010; Krüger et al., 2011; Lin et al., 2010; Pearlmutter et al., 1999; Wang and Akbari, 2014). Apparently, the more open to the sky a point is, the more likely to be seen by the sun; however, at a given time, assuming two points of the same SVF, the one may be in shade and the other sunlit. The limitation of the SVF parameter to accurately predict solar access at given points in open spaces has been highlighted by researchers (e.g. Krüger et al., 2011).

4.2 Objectives

The present study examines the relationships between urban geometry, solar access and mean radiant temperature at the pedestrian level. It consists of two main parts. The first part presents the findings regarding the impact of urban geometry on average hourly MRT in the open spaces of 72 London's urban forms. The second part focuses on the relationship between mean ground SVF and mean insolation of open spaces including in the analysis 60 urban forms from Paris. The number of urban forms examined made feasible the statistical exploration of the relationships in question, which combined with the spatial scale at which the topic is being investigated, constitute two major features of the research. In this regard, the work of Lindberg and Grimmond (2011a) can be considered an important precedent as they employ a similar methodology to investigate the influence of building morphology and vegetation on shadow patterns and mean radiant temperatures in London.

Unlike most of past research works which have examined similar topics focusing on isolated street canyons or specific points in open spaces, this one is based on average values of SVF, insolation and MRT across entire real urban forms. Correspondingly, the research aim of this study is not to evaluate the performance of different urban geometries, but to examine whether and to what extent the average radiant environment in open spaces can be estimated by urban geometry parameters. In this context, SVF acquires an increased weighting, acting simultaneously as urban geometry variable and performance indicator, i.e. bridging the two components of the studied relationship.

Considering that MRT expresses the sum of shortwave radiation -strongly related to solar exposure- and longwave radiation -strongly related to openness to the sky, i.e. SVF-, the objectives to be pursued are reduced to the following two:

(i) to investigate whether mean ground SVF can be estimated using simple urban geometry variables, as those considered in the analysis;

(ii) to examine whether and to what extend mean ground SVF can be used as indicator for estimating average insolation of open spaces.

It is worth highlighting that the orientation of open spaces in relation to the sun's position is not considered and thus, its impact on their solar exposure remains a missing factor in the equation. However, assuming the theoretical schema saying that solar access is solely the result of the combination of urban geometry and orientation, the orientation effect may be identifiable in the results in an indirect way. For instance, if urban geometry variables can predict the insolation levels in open spaces, this would mean that the orientation effect is limited. However, the opposite is not necessarily true, since a weak relationship between urban geometry variables and solar access may also stem from their imperfection to express the urban geometry, and specifically the urban layout. Considering mean ground SVF as the result of a given geometry, integrating build density and some urban layout information into a single measurement, allows this study to adjust the above schema as seen in Figure 4.1.

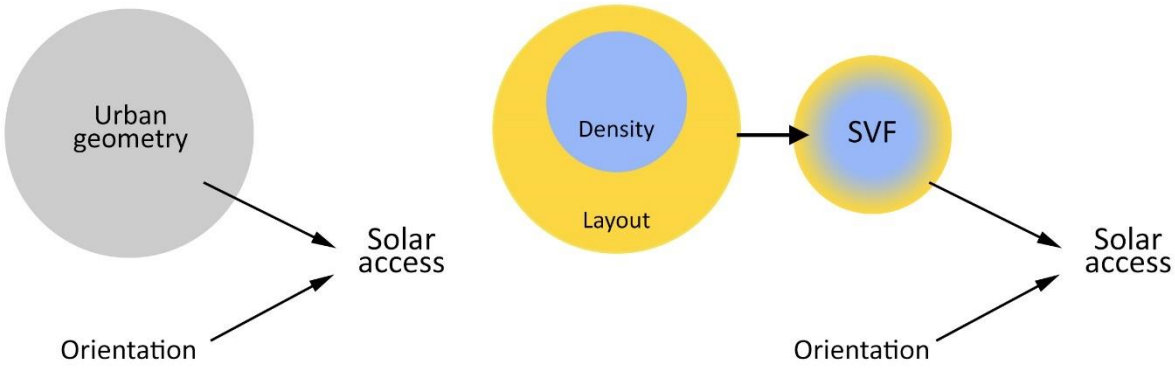

Figure 4.1: Theoretical schema depicting the methodological approach.

4.3 Methodology

The study is based on the statistical investigation of the relationships between urban geometry variables and environmental quantities associated to urban radiant environment. Regarding the urban geometry variables considered, these are built density and 17 urban layout descriptors presented analytically in Section 3.3.2. Outdoor radiant environment is expressed by average mean radiant temperature (mMRT), average ground sky view factor (mSVF) and shadow fractions, i.e. mean insolation (mSOL) of open spaces

(see Section 2.4.2.3). The respective simulations were performed in SOLWEIG, and next the extraction and averaging of the pixels' values belonging to open spaces was done in MATLAB.

For mean radiant temperature analysis, hourly MRT simulations were run for 8 days of a typical year in London. Mean insolation values were computed based on shadow patterns produced for three representative days, i.e. 21 June (summer solstice), 21 March (equinox) and 21 December (winter solstice), from sunrise until sunset, at 10-min intervals. Beyond instantaneous mSOL, i.e. computed for a given time on each day, daytime average mSOL values were also computed and examined. More information about SOLWEIG simulations are given in Section 2.4.2.1. Finally, the statistical analysis was performed in MATLAB and SPSS statistical package.

4.4. Results

4.4.1 Mean radiant temperature in the open spaces of London

The mean radiant temperature analysis was conducted for the 72 urban forms of London, and this had an explorative character regarding the impact of urban geometry on hourly average MRT (mMRT). MRT simulations have been performed for 8 days, including sunny and cloudy ones, evenly distributed in the year, for the effects of sky conditions and solar altitude to be investigated. The presentation of the results focuses on three days, i.e. 19 January (cloudy day), 26 July (summer sunny day) and 29 December (winter sunny day) which summarise the overall findings. The weather files used in SOLWEIG, are given in Appendix E.

Prior to the discussion of the results, it is important to remind that MRT simulations performed in SOLWEIG are steady-state and consider only urban geometry, provided as a DEM, meteorological parameters, provided in an hourly weather file, and geographical information of the location (see Section 2.4.2.1). Given that the urban forms are compared using the same weather files and location, the variations of mMRT are driven solely by their different urban geometries. This has greatly facilitated the purposes of this study which focuses on the impact of urban geometry; however, it entails that the simulation results may be of limited validity regarding actual MRT values since the latter are also influenced by other parameters, such as vegetation, building and pavement materials. Furthermore, the results provided are indicative of hourly mMRT differences among the studied urban forms under different weather conditions. However, it is acknowledged that averaging MRT values over an area blurs any spatial variations of it which may be significant, especially under sunny sky conditions. It is thus clarified that the comparison of the urban forms' performance is meant to identify the impact of urban

geometry on average radiant environment; while any reference to the implications of the results for outdoor thermal conditions should be considering the above.

4.4.1.1 Mean radiant temperature simulation results

Hourly mMRT in the 72 urban forms of London were found to be strongly affected by urban geometry, and, especially, the density-related part of it. As shown in Section 3.4.2.1, a great part of the variance of the urban geometry variables in London are explained by built density, since the latter is correlated significantly with most of urban layout descriptors. The density parameter is actually so dominant that the distinction between 'geometry' and 'density' when referring to their influence is difficult to be drawn. In this way, the different range of density values in three studied areas, i.e. central, west and north, made feasible the illustration of the significance of urban geometry for their average radiant environment, under different sky conditions.

The analysis of the mMRT results revealed that their hourly variations are described by two different patterns, depending on the availability or not of direct solar radiation. In absence of direct radiation, i.e. at night-time and under fully overcast conditions, the outdoor spaces of central London's urban forms are warmer than those of west and north London, due to greater longwave radiation emitted and reflected by building volumes. For the same reason, west London's urban forms are also warmer than those of north London. In other words, when the radiant environment in open spaces is governed by long-wave radiation, then this is strongly related to urban forms' density.

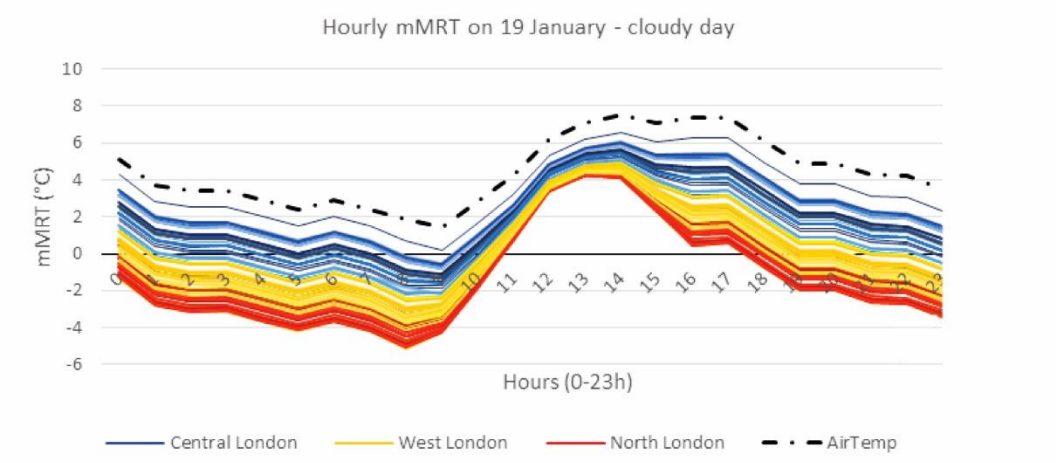

Figure 4.2: Hourly mMRT values in outdoor space of 72 squares on 19 January, a winter cloudy day.

At night, mMRT is always lower to air temperature, and the difference between minimum and maximum mMRT (ΔmMRT) among the urban forms is constantly about 5 to 6 °C. On the other hand, on cloudy

daytime hours, the difference is reduced, due to the diffuse solar radiation which is in greater supply in areas of lower density. Furthermore, whether mMRT exceeds or not the air temperature depends on the intensity of diffuse radiation. For instance, Figure 4.2 presents hourly mMRT in the 72 urban forms of London on 19 January, a cloudy winter day. As seen, the lines representing the urban forms are parallel over the night hours, denoting that their mMRT is exclusively defined by their geometry, the effect of which is constant in time. From sunrise and until midday, the lines start to converge upwards, with ΔmMRT to be minimised at noon (1.9 ^{o}C). On the specific day, the levels of diffuse irradiance were very limited, ranging between 2 and 60 W/m^2, and thus the mMRT values remain lower than air temperature all over the day.

Testing the relationship of hourly mMRT at night with density, this was found to be constant and better described by a logarithm curve, with the linear trend achieving an equally high R^2 (Fig. 4.3). The relationship of hourly daytime mMRT and density is also very strong and negative, but its strength varies slightly in time influenced by the presence of diffuse radiation. At times that the diffuse radiation intensity is low, the relationship remains logarithmic; when diffuse radiation availability is relatively increased, i.e. at 12.00, at 13.00 and 14.00 (of 60, 61 and 54 W/m^2, respectively), it is better described as linear (Fig. 4.4).

Under sunny conditions, the variation of mean radiant temperature is highly related to whether a point is sunlit or in shade; so, not surprisingly, average daytime MRT values are found to be higher in north London due to the larger insolation of their open spaces, and lower in central London, where solar access is seriously restricted. Furthermore, the maximum difference between warmest and coolest urban forms (ΔmMRT) is in general much greater than in absence of direct radiation. Figure 4.5 demonstrates hourly mMRT on 26 July, a representative summer sunny day. As seen, from sunrise to sunset, mMRT in all urban forms is higher than the air temperature with their difference to increase towards midday. Simultaneously, ΔmMRT increases in the same way, with the lines to converge at sunrise and sunset, and diverge towards noon. Indicatively, on 26 July, at 6.00 in the morning (global, direct normal and diffuse radiation: 124, 508 and 38 W/m^2) the air temperature is 12.9 °C and the highest and lowest mMRT are 19.3 and 11.5 °C, i.e. ΔmMRT 7.8 °C. At 10.00 on the same day, (global, direct normal and diffuse radiation: 621, 608 and 186 W/m^2) the air temperature rises to 17.6 °C, and maximum and minimum mMRT appears to be 44 and 25.7 °C, respectively, i.e. ΔmMRT 18.3 °C. Moreover, the highest hourly mMRT recorded is 48 °C in an urban form in north London at 13.00 (global, direct normal and diffuse radiation: 729, 550 and 265 W/m^2), about 28°C higher than the air temperature which at that time is 20.2 °C.

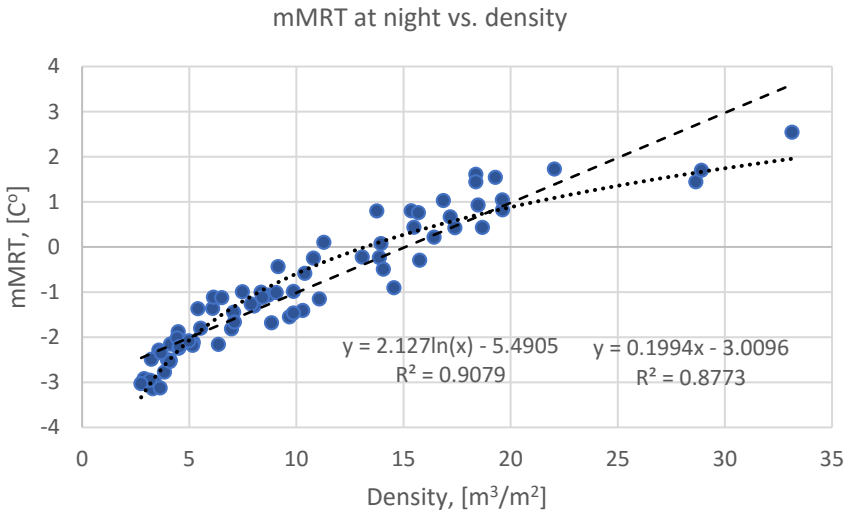

Figure 4.3: Average mean radiant temperature (mMRT) values in 72 urban forms in London on 19 January at 3 a.m., plotted against density.

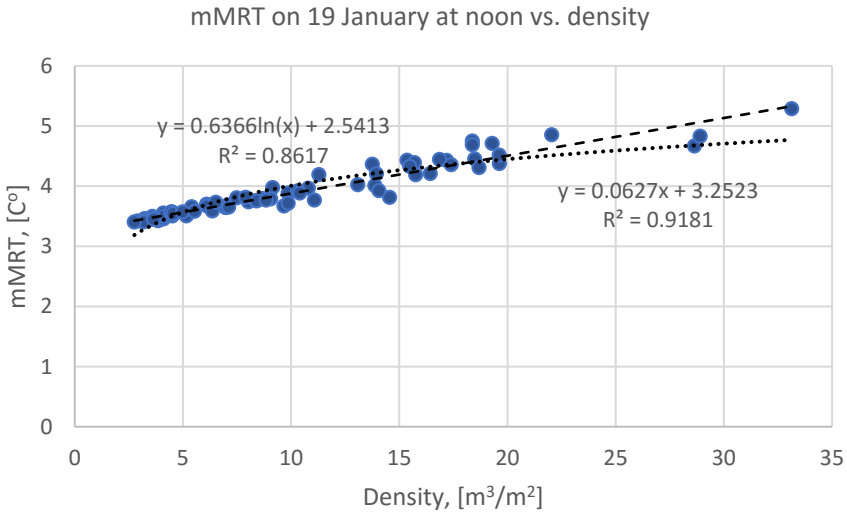

Figure 4.4: Average mean radiant temperature (mMRT) values in 72 urban forms in London on 19 January (cloudy day) at noon, plotted against density.

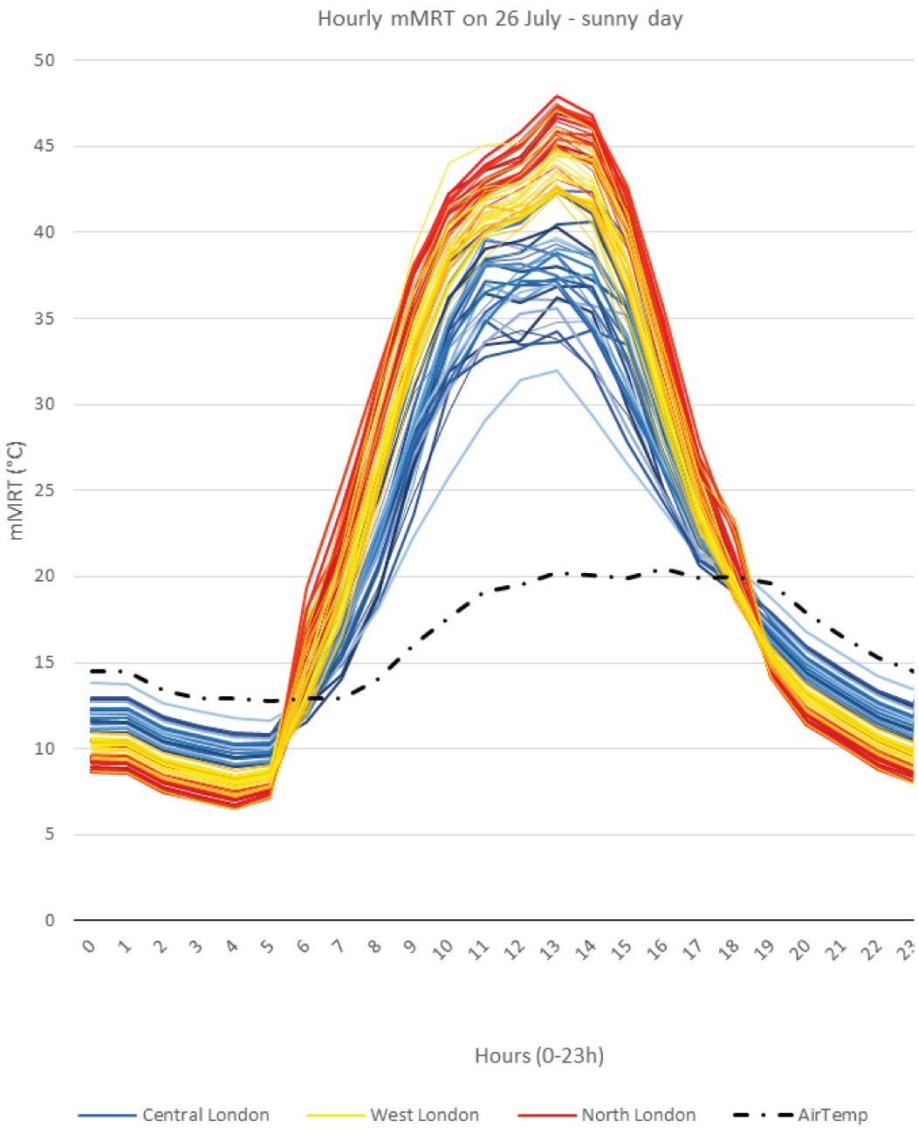

Figure 4.5: Hourly average mean radiant temperatures (mMRT) in the open spaces of London's urban forms on 26 July, representative of a summer sunny day.

Observing the lines in Figure 4.5, it is seen that these are distinguished by colour, with the red ones representing urban forms of north London to be higher and the blue ones representing urban forms of central London to be constantly lower in the daytime. Consequently, the effect of their density on their mMRT is evident and clear: urban forms of lower density tend to experience higher mMRT, and the reverse. This is confirmed by the regression analysis which shows that the relationship is very strong (R^2>0.8) for most of the hours, especially those close to noon (Fig. 4.6). As on the cloudy day, in the morning and evening hours, the relationship is better described by a logarithmic curve, while towards to midday it becomes linear.

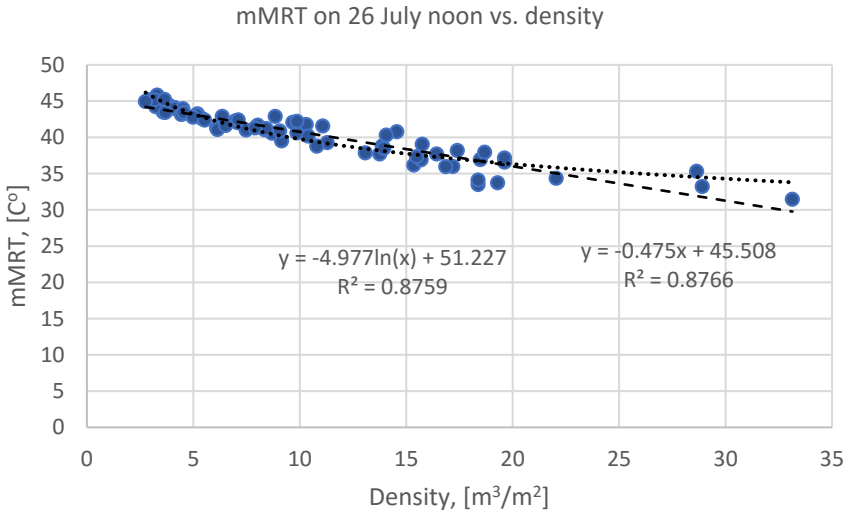

Figure 4.6: Average mean radiant temperature (mMRT) values in 72 urban forms of London on 26 July (sunny summer day) at noon, plotted against density.

Examining a winter sunny day, the effect of the density parameter is found to be less decisive for their mMRT. As shown in Figure 4.7, which illustrates hourly mMRT on 29 December, the order of the lines is not defined by colour, i.e. area of London, at least not as clearly as in Figure 4.5, but it is rather complicated. This may be attributed to the combination of two factors: lower solar altitude angles and lower levels of solar radiation, compared to those on 26 July. In particular, lower solar altitudes amplify the orientation effect on the insolation of open spaces and thus their mMRT. On 29 December, the sun's altitude does not exceed 15.5°; so, the sun is so low in the sky that most of the open spaces are overshadowed by the surroundings buildings and any solar access in them is limited to solar radiation coming from the sides. Under these circumstances, when an open space of an urban form is aligned to the sun's azimuth and is sunlit, this is reflected on its mMRT which increases significantly in relation to others' values. Moreover, due to lower intensity of solar radiation as well as the excessive overshadowing, the variations of mMRT values in different urban forms are rather limited which makes the orientation effect even more noticeable. Indicatively, maximum ΔmMRT on that day is 8.7 °C, at noon (global, direct normal and diffuse radiation: 204, 67 and 532 W/m^2).

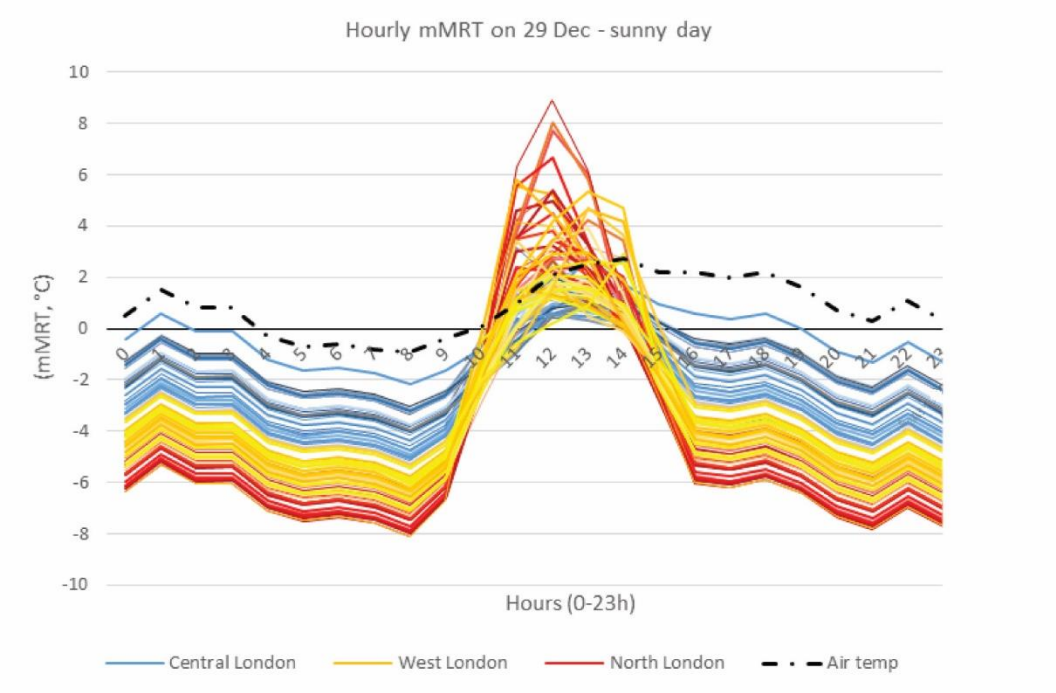

Figure 4.7: Hourly average mean radiant temperatures (mMRT) in the open spaces of London's urban forms on 29 December, representative of a winter sunny day.

Examining the lines of different colours in Figure 4.7, it appears that the orientation effect -in absolute values- is more profound in urban forms of north and west London, with red and yellow lines presenting peak values between 11.00 and 14.00. This is better demonstrated in Figure 4.8, where mMRT values at noon are plotted against urban forms' density. As seen, the largest discrepancies from the trendlines are found in urban forms of low and medium densities. The R^2 values obtained from regression tests also indicate that the relationship between density and hourly mMRT is much weaker than it was on 26 July.

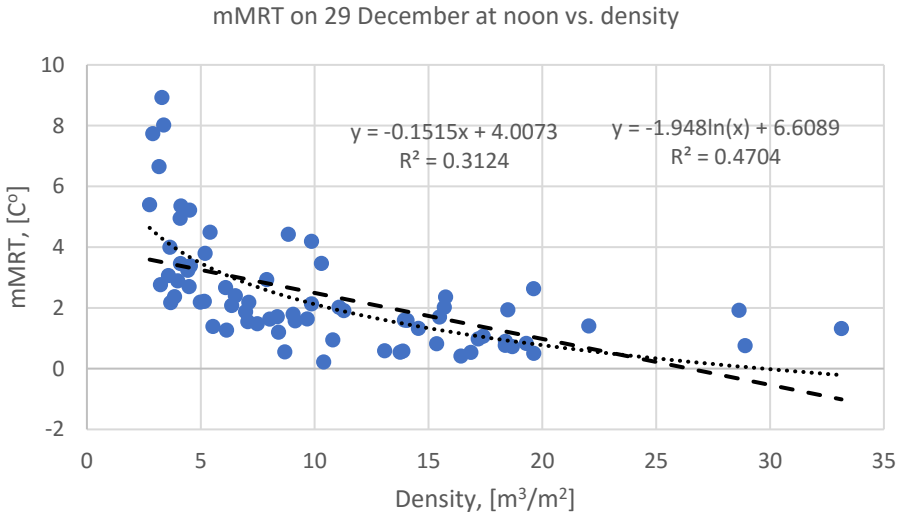

Figure 4.8: Average mean radiant temperature (mMRT) values in 72 urban forms of London on 29 December (winter sunny day) at noon, plotted against density.

To summarise, when MRT is exclusively determined by urban geometry, namely in absence of direct radiation, the lines in the graphs present constantly the same order. Under these sky conditions, the relationship of density and mMRT is significantly strong. The fact that, in presence of direct radiation, the vertical order of the urban forms changes in time -i.e. an urban form may present higher mMRT at a time and lower at another, compared to other urban forms- implies the influence of a parameter which changes in time. This parameter is considered to be the orientation of urban forms' open spaces in relation to the varying sun's position. The change in the order of the lines is observed both in Figures 4.5 and 4.7; in the former, it concerns mostly urban forms of central and west London, and in the latter, urban forms of north and west London. However, on a summer sunny day, the effect of orientation is less noticeable, and it is assumed that the reason is related to higher solar altitudes combined with higher solar radiation intensity. The relationship between density and mMRT during sunny hours is found to get stronger as the sun's altitude increases. Given that the range of density values is large, its increasing impact results in a greater range of mMRT values which, amplified by higher solar irradiance, offsets the effect of the orientation.

4.4.1.2 Relationship of mSVF and hourly mMRT

Having examined the variations of hourly mMRT in the urban forms of London on different days, their relationship with mSVF was next tested performing linear regression tests. The results confirmed the existence of two patterns of relationships depending on sky conditions, as discussed in the previous section. In this way, at night and during cloudy daytime hours, mSVF and hourly mMRT present an

extremely strong, almost perfectly linear relationship (R^2> 0.980). During sunny hours, the strength of the correlation is found to increase with increasing solar altitude angle, as found before for density but the R^2 achieved are generally higher. Figure 4.9 demonstrates R^2 values obtained testing mSVF and hourly mMRT on 6 sunny days considered in the analysis. As seen, a similar pattern is revealed for all the days. Precisely, at night all R^2 values are on a straight line close to 1, and in the daytime they create an inverse U-shaped curve. It is observed that on 20 March, 26 July and 21 June which represent the half year, i.e. from 21 March to 21 September (two equinox days), the correlation is constantly very strong (R^2> 0.9) from early morning hours until late afternoon.

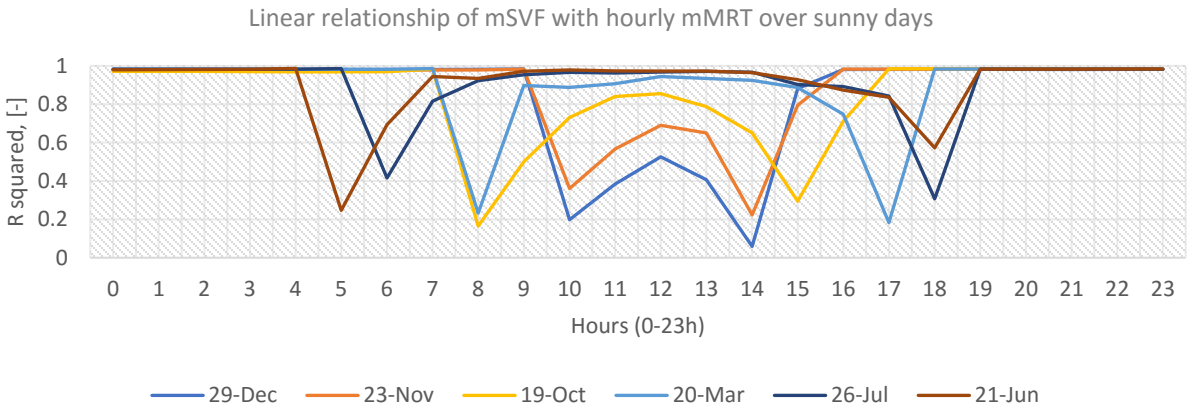

Figure 4.9: Variations of R^2 values obtained testing the relationship of mSVF with hourly mMRT values with on the sunny days studied.

In conclusion, mean ground SVF is found to be an excellent indicator of average mean radiant temperature in open spaces, not only in absence of direct radiation as expected, but also during most of sunny hours in the year. Considering that mMRT under sunny conditions is strongly affected by the availability of direct solar radiation, it means that mSVF also indicates the solar exposure of open spaces. Moreover, the higher the solar altitude is, the higher the degree of confidence. However, it is acknowledged that the strength of the relationship may be influenced by the intensity of solar radiation -which is usually higher for higher solar altitudes- as well as the wide range of density values in London's case. For this reason, the next part of the study focuses solely on shadow fractions, increasing the case study cities to two, London and Paris.

4.4.2 Urban geometry, SVF and solar access in open spaces in London and Paris

This part of the study is based on a sample of in total 132 urban forms, 72 from London and 60 from Paris. The analysis of Paris' urban forms intends to test the findings obtained from London's analysis and, thus, gain a wider understanding about the studied relationships. The two cities are located at similar geographical latitudes which makes them comparable in terms of sun paths on specific days. On the other hand, they present major differences in urban geometries that they feature, which enables the exploration of the special role of urban layout. Their comparative examination aims to answer two questions, which are the followings: (i) whether and to what extend urban geometry variables can predict average SVF (mSVF), and (ii) to what extend mSVF can predict mean insolation (mSOL) of open spaces. These questions are dealt with separately in the following sections.

4.4.2.1 Relationship of urban geometry variables and SVF

mSVF is determined by the urban geometry and expresses, in a reverse way, how obstructed the open spaces are from the surrounding buildings. Therefore, it is affected by the density parameter; however, their relationship is not straightforward as urban forms of the same density but of different layout may present diverse mSVF. In this section, the correlations between mSVF and density, and mSVF and 17 urban layout descriptors are examined separately for the urban forms of London and Paris.

Examining density and mSVF, the statistical analysis reveals a strong negative correlation for both cities, with the correlation coefficient for London ($r=-0.940$, $p<0.001$) to be considerably higher than for Paris ($r=-0.787$, $p<0.001$). The curve estimation test shows that the relationship for both cities is better described by a logarithm model rather than a linear one; however, the R^2 values are fairly close (Fig. 4.10). In general, the variations of density can explain a greater part of the variations of mSVF in London compared to Paris where the range of density values was found to be significantly limited.

The relationship of mSVF and 17 urban layout descriptors was next tested performing a series of statistical tests. Pearson Correlation results (two-tailed) are presented in Table 4.1 (Column A). The correlation coefficient (r) values obtained demonstrate that mSVF correlates significantly with most of independent variables, both for the urban forms of London and Paris. For London, the strongest variable is *site coverage* (SCo) with r being -0.950 (Fig. 4.11a); whereas, for Paris, it is *complexity* (Cex) with r value -0.936 (Fig. 4.11b). It is noticeable that, in Paris, the correlation between Cex and mSVF is significantly higher than that achieved by density (see Figure 4.10b).

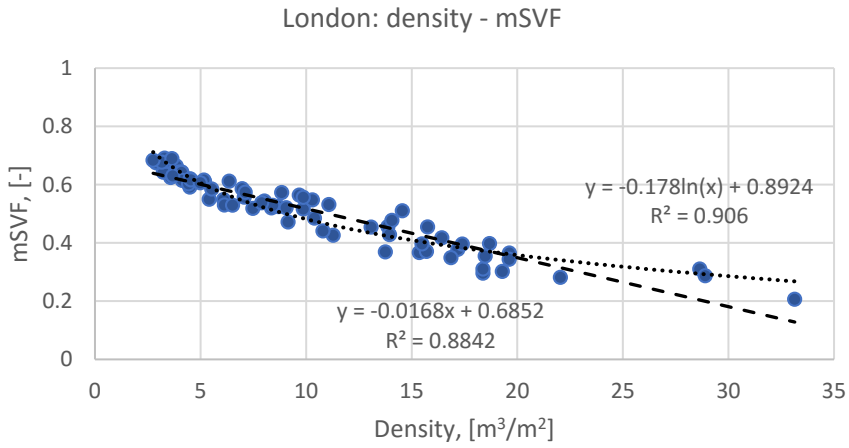

(a)

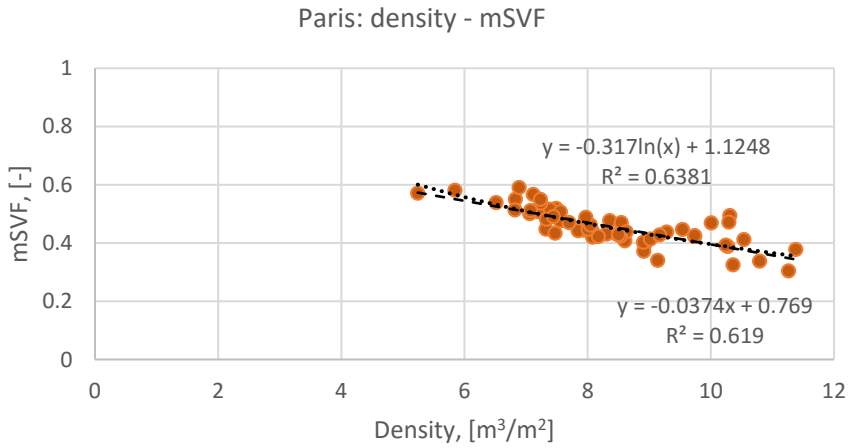

(b)

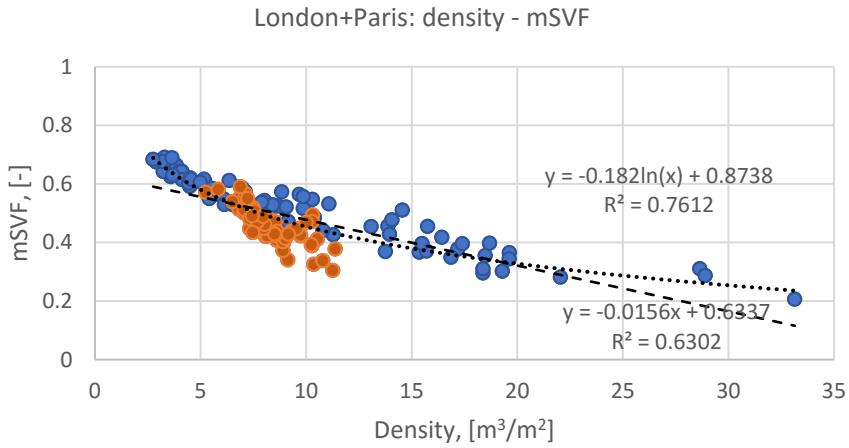

(c)

Figure 4.10: Mean ground SVF values plotted against density values, for urban forms of London (a), Paris (b), and London and Paris combined (c).

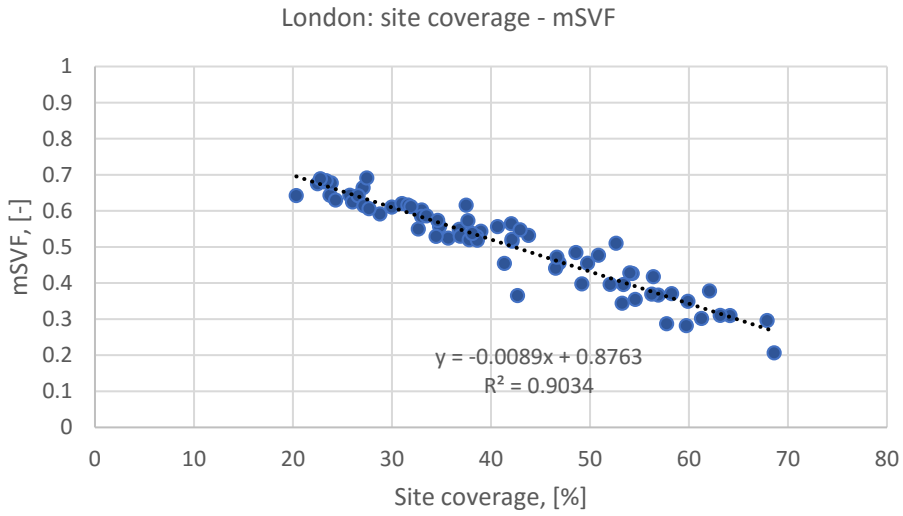

(a)

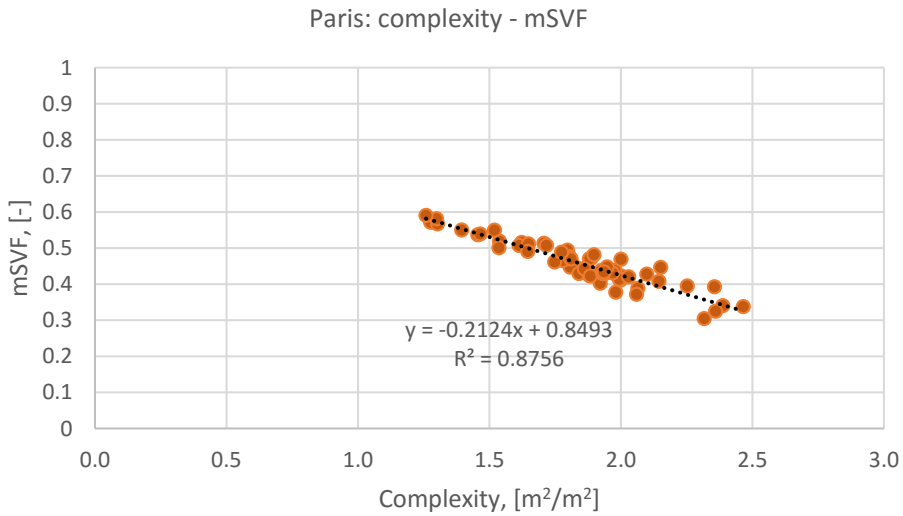

(b)

Figure 4.11: Correlation of mSVF with strongest urban geometry variables, site coverage for London (a) and complexity for Paris (b).

Nonetheless, the results are apparently affected by the intercorrelation of the variables. This explains why the MeH, StH, StS, and MaH variables were found to correlate negatively with mSVF in London, but positively with mSVF in Paris. Especially, in the case of London, it is the strong correlation of most of urban layout descriptors with density that causes the noticeably high r values. This is confirmed by the fact that performing partial correlation with control for density the r values of most of the descriptors, such as Cex, FaS and NOB, reduce drastically. On the other hand, in Paris, the effect of controlling density is less significant with the correlations for *compactness* (Com), *complexity* (Cex) and *façades-to-street ratio* (FaS)

remaining significant strong (r>0.8). Moreover, controlling the density effect, the significance of *mean outdoor distance* is remarkably increased (r=0.893, p<0.01) with this becoming the most influential variable for Paris, while the strongest variable for London remains site coverage (r=-0.698, p<0.01). Site coverage and mean outdoor distance are two variables measuring, in different ways, the open space; thus, it can be argued that mSVF is primarily affected by the quantitative characteristics of the open space. This may also explain why the effect of mean building height on mSVF is found to be positive; since, for a given density, higher mean building heights means increased open spaces.

Performing Stepwise Linear Regression analysis, considering all urban geometry variables, the linear models of three variables obtained include two common variables for London and Paris, complexity and mean outdoor distance, and the R^2 achieved are particularly high. Specifically, in London, mSVF is predicted as a function of *site coverage*, *complexity* and *mean outdoor distance* (mSVF= 0.847 -0.005*SCo - 0.135*Cex + 0.006*MeD) with R^2 being 0.984. Whereas, in Paris, mSVF is given as a function of *complexity*, *mean outdoor distance* and *mean building volume* (mSVF= 0.591 - 0.120*Cex + 0.19*MeD - 5.473e-7*MeV) with R^2 being 0.956.

Table 4.1. Pearson Correlation and partial correlation results for mSVF and urban geometry variables.

A.	**B. Correlation**				**C. Part.Corr. Ctrl_Density**			
	London		**Paris**		**London**		**Paris**	
	r	p	r	p	r	p	r	p
Density	-0.940	0.000	-0.787	0.000				
Sco	-0.950	0.000	-0.871	0.000	-0.698	0.000	-0.634	0.000
MeH	-0.869	0.000	0.137	0.298	0.347	0.003	0.615	0.000
StH	-0.684	0.000	0.669	0.000	0.358	0.002	0.385	0.003
StS	-0.858	0.000	0.393	0.002	0.331	0.005	0.522	0.000
MaH	-0.663	0.000	0.530	0.000	0.117	0.330	0.238	0.069
MeD	0.458	0.000	0.869	0.000	0.526	0.000	0.893	0.000
StD	0.173	0.145	0.678	0.000	0.317	0.007	0.641	0.000
MaD	0.159	0.182	0.532	0.000	0.205	0.087	0.387	0.002
Com	0.856	0.000	-0.190	0.145	0.301	0.011	-0.842	0.000
Cex	-0.940	0.000	-0.936	0.000	-0.468	0.000	-0.829	0.000
FaS	-0.943	0.000	-0.929	0.000	-0.425	0.000	-0.800	0.000
NOB	0.777	0.000	0.413	0.001	0.291	0.014	-0.216	0.100
MeF	-0.835	0.000	-0.546	0.000	-0.621	0.000	0.157	0.237
StF	-0.757	0.000	-0.537	0.000	-0.070	0.564	-0.172	0.194
MeV	-0.842	0.000	-0.491	0.000	0.217	0.069	0.197	0.135
StV	-0.584	0.000	-0.373	0.003	0.372	0.001	0.067	0.612
Dir	0.705	0.000	0.409	0.001	0.454	0.000	0.434	0.001

** Significant at 0.01 level
*Significant at 0.05 level

Acknowledging the strong collinearity of the urban geometry variables, and in order to examine to what extent their total variance can explain the variations of mSVF, regression analysis was performed considering as independent variables, the factors derived from the Principal Component Analysis (PCA) test. These are three for London and five for Paris, explaining 87% of the variance of the urban geometry variables in the two cities (see Section 3.4.3). The R^2 values obtained are significantly high, 0.971 for London's urban forms and 0.962 for those of Paris. Overall, it can be argued that even though the correlation between density and mSVF differs in strength between the two cities, being significantly lower for Paris, urban geometry variables can explain to a large degree mSVF variations in both.

Finally, the sensitivity of the results to the spatial scale of the study was examined repeating targeted tests for London having reduced the scale of its urban forms to half. In this way, the initial 72 cells were divided into 4, producing 288 new urban forms of 250 x 250m size. Next, urban geometry variables and mSVF values were computed for them, and their relationship was tested statistically following the same process as before. The results showed a small decrease in the strength of the correlation between density and mSVF, from r= -0.940 to r= -0.892. Figure 4.12 demonstrates the linear and logarithm curves describing their relationship, with the latter achieving higher R^2. Moreover, partial correlation test with control for density reveals that the most influential urban layout descriptors remain the same, even though their order in terms of significance alters: MeD (r=0.661), SCo (r=-0.659), and Cex (r=-0.517).

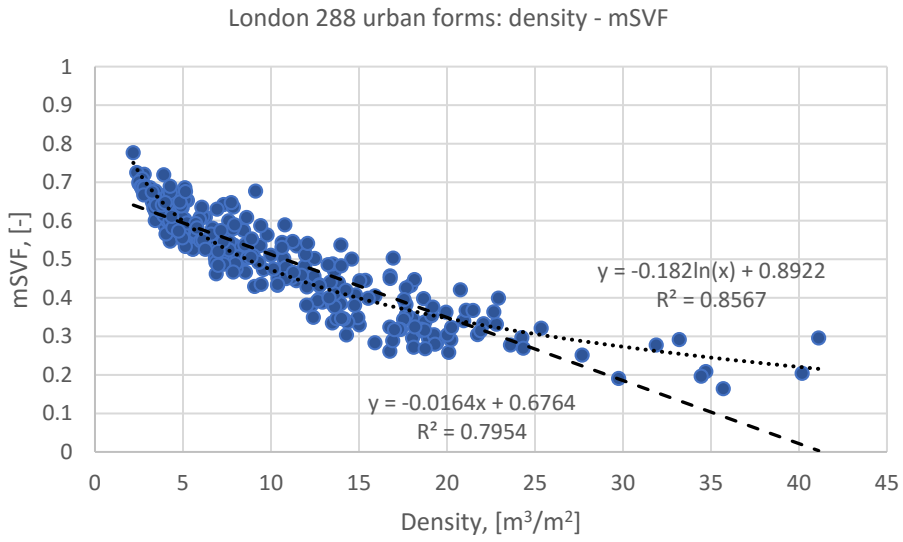

Figure 4.12: Mean SVF values plotted against density values, for 288 urban forms of London derived from the division of the initial ones.

4.4.2.2 Relationship between mSVF and mean insolation of open spaces

Focusing on mean insolation of open spaces allows to explore further the findings regarding the effect of varying solar altitudes in the day, as well as seasonally, isolating the solar intensity parameter. mSOL values were computed for three days, i.e. 21 June, 21 March, and 21 December, based on shadow patterns produced at 10-min intervals. mSOL expressing mean insolation of open spaces at a given time are referred to as *instantaneous mSOL*, while mSOL expressing mean insolation over the day as *daytime mSOL*. Their correlation with mSVF of open spaces was examined statistically performing regression analysis, first for London's urban forms and next for those of Paris.

London

First, the relationship of mSVF and daytime mSOL for London's urban forms was tested performing Linear Regression analysis. The R^2 values obtained for 21 June, 21 March, and 21 December were 0.976, 0.976 and 0.719, respectively. The relationship is thus equally strong and almost perfectly linear on the summer solstice and equinox days, and less strong but still significant on the winter solstice. Figure 4.13 demonstrates the linear models obtained for the three days when intercept is set to zero. As seen, the relationship gets stronger as the effect of mSVF on daytime mSOL -i.e. slope- increases.

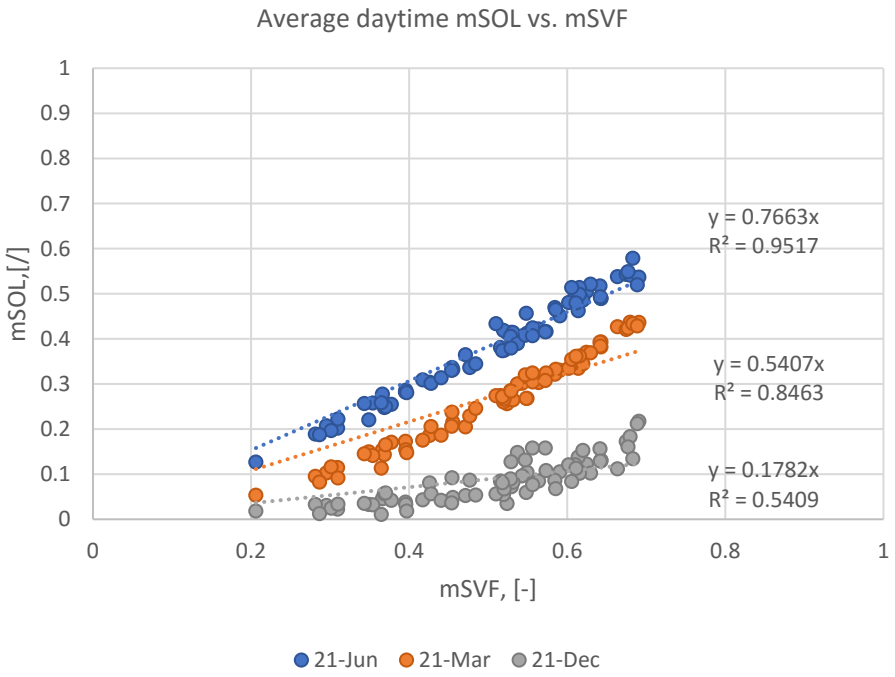

Figure 4.13: Average daytime mSOL values for 72 urban forms of London on 21 June, 21 March and 21 December, plotted against their ground mSVF, and linear models when intercept is set to zero.

Next, instantaneous mSOL values on each day were plotted against urban forms' mSVF. It was found that their relationship was best described by either linear or logarithmic curves depending on time. Furthermore, the strength of the relationship, in both cases, was found to vary in the day, in a specific way: R^2 values are at their lowest at the sunrise and sunset time and increase closer to midday. Figures 4.14, 4.15 and 4.16 demonstrate mSOL values at indicative times -from sunrise to midday- plotted against mSVF, on 21 June, 21 March and 21 December, respectively. Observing the three plots, it becomes apparent from the slope of the trendlines that the effect of mSVF on instantaneous mSOL increases towards midday; while the R^2 values show that their relationship also gets stronger. However, the influence of the solar altitude is not straightforward, as there are identified casess which do not follow the general rule. For instance, on 21 June, the highest R^2 appears at 10 a.m. rather at noon, and on 21 March, the strength of the relationship is found to be higher at 10 a.m. compared to 11 a.m. Nonetheless, in both cases, the respective R^2 are very close and significantly high. This may be interpreted as that the sensitivity of the mSVF-mSOL relationship to solar altitude reduces once the relationship gets strong enough, i.e. for high enough solar altitudes.

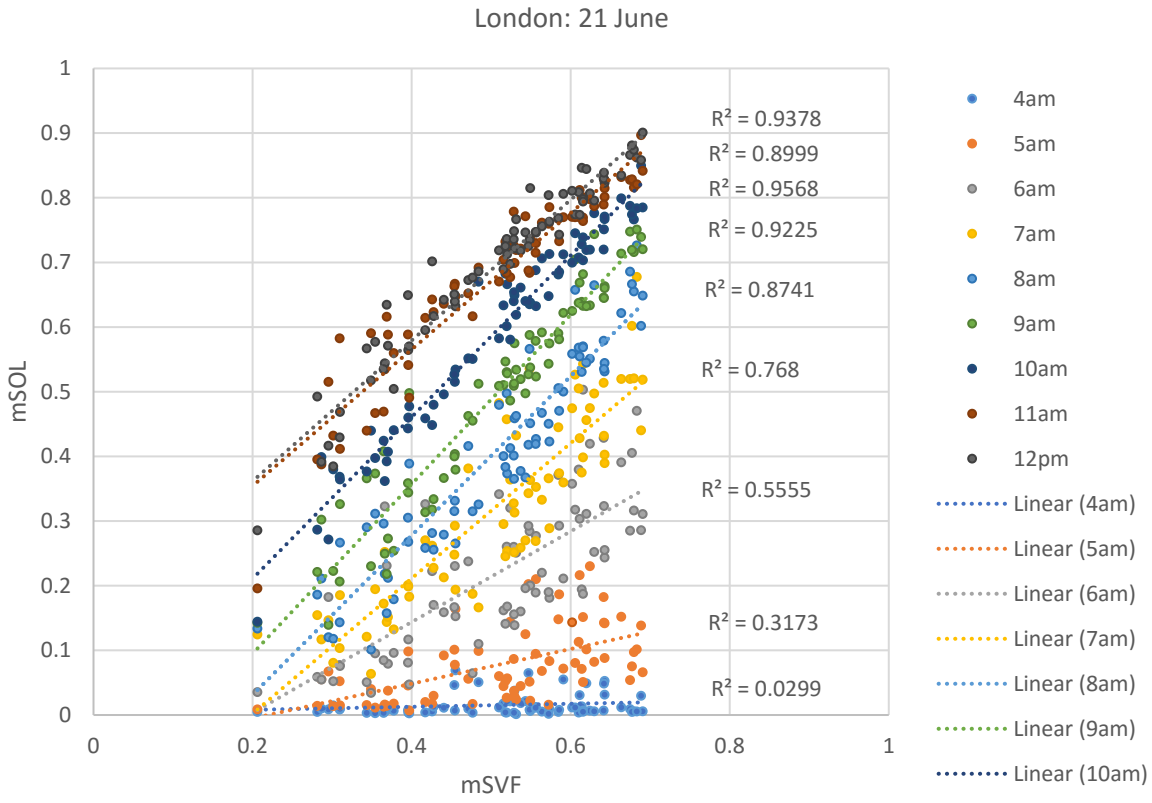

Figure 4.14: Mean insolation (mSOL) values plotted against mean SVF (mSVF) values for representative hours, from sunrise to midday, on 21 June; and R^2 derived by linear regression.

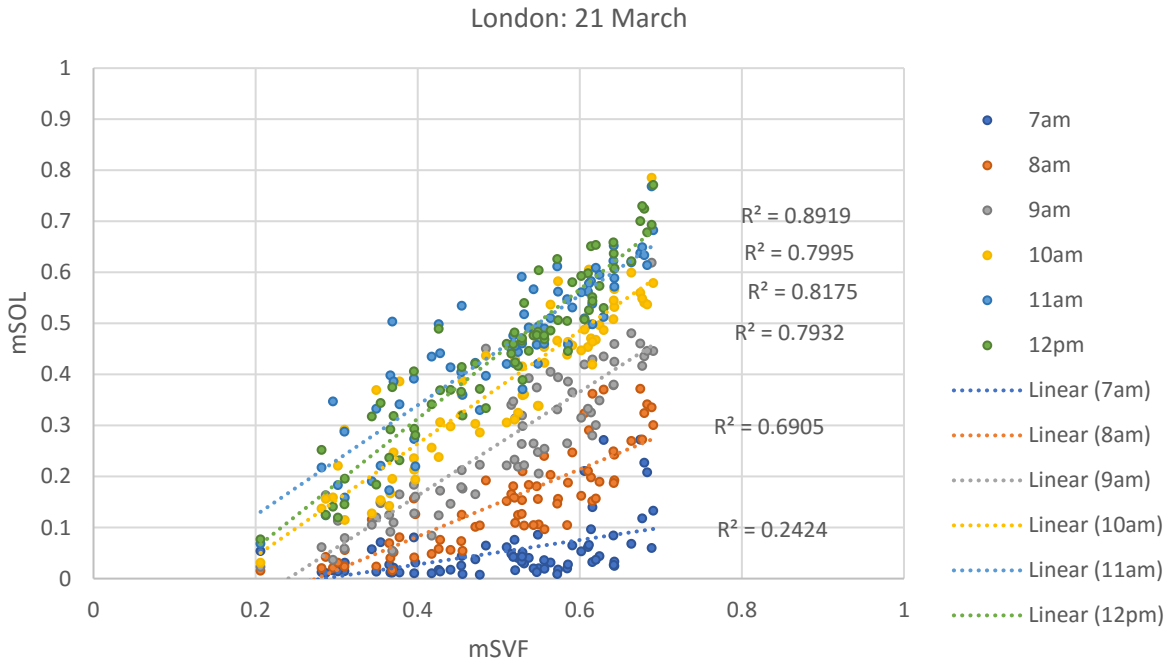

Figure 4.15: Mean insolation (mSOL) values plotted against mean SVF (mSVF) values for representative hours, from sunrise to midday, on 21 March; and R^2 derived by linear regression.

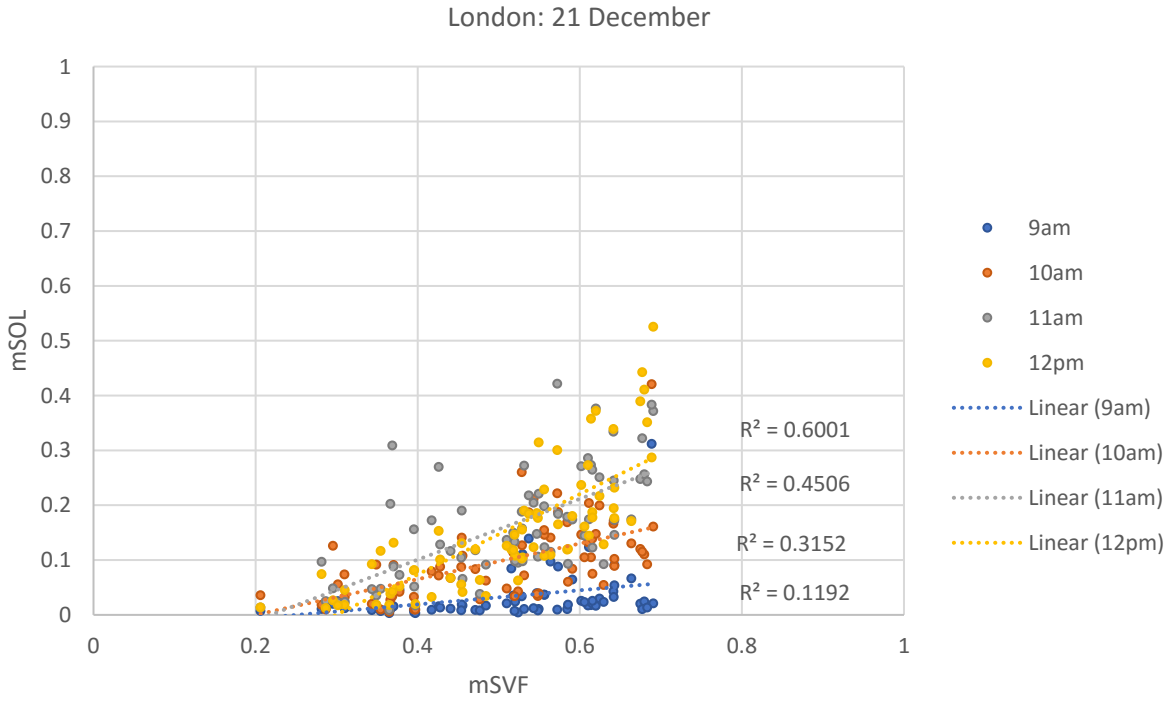

Figure 4.16: Mean insolation (mSOL) values plotted against mean SVF (mSVF) values for representative hours, from sunrise to midday, on 21 December; and R2 derived by linear regression.

The next step was to plot all R^2 values obtained from linear regression tests on each day against time. As shown in Figures 4.17, 4.18, and 4.19, the plotted points form similar in shape curves, resembling projections of sun paths. The curves feature an inverse U shape, quite symmetrical to the vertical notional axis passing from the middle of the day. The rate of change of R^2 is increased the hours after sunrise and before sunset, and gradually reduces getting closer to midday. Moreover, moving from the winter solstice to the summer solstice, the relationship between mSVF and instantaneous mSOL becomes stronger and for longer time over the day. Indicatively, on 21 June, R^2 is above 0.8 between 7.00 a.m. and 7.00 p.m.; while the respective time for 21 March is identified between 9.00 a.m. and 15.00 p.m. On 21 December, maximum R^2 values are presented between 11.30 a.m. and 12.30 p.m. with these being close to 0.6.

For the sake of comparison, the relationship of instantaneous mSOL values with density was also examined, and the respective R^2 values were plotted on the same graphs (i.e. Fig. 4.17, 4.18 and 4.19). It is observed that mSVF achieves higher R^2 values than density, for most of the hours on different days. Hence, although mSVF and density are strongly related to each other, the former performs better as indicator of the insolation of open spaces. This is reasonable considering that density is a crucial parameter of urban geometry, but nonetheless a single measure; whereas, mSVF is an integrated measure of the geometry capturing more information of it.

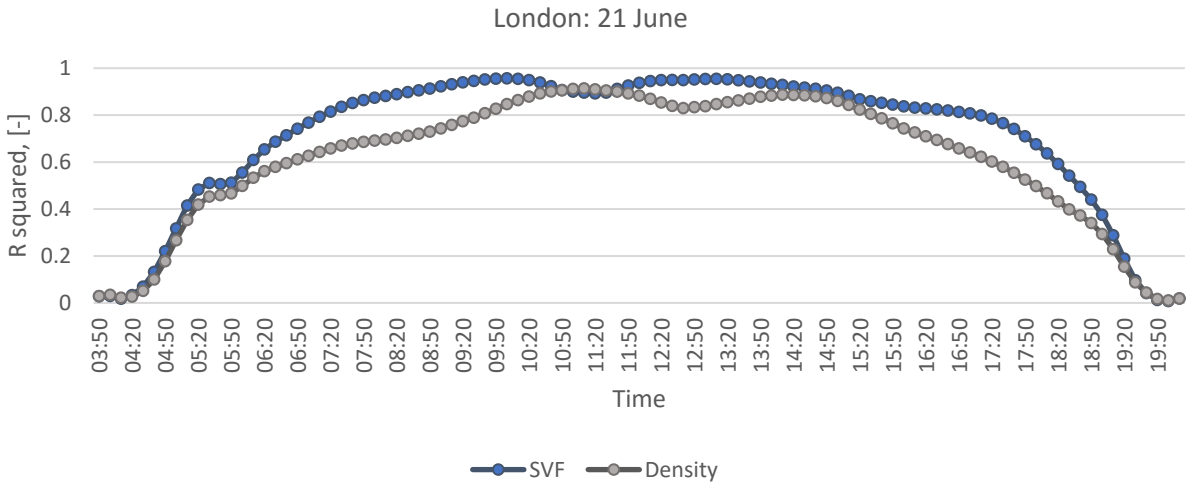

Figure 4.17: Variations of R^2 describing the strength of the linear relationship between mSVF and mSOL, and density and mSOL, on 21 June, for London's urban forms.

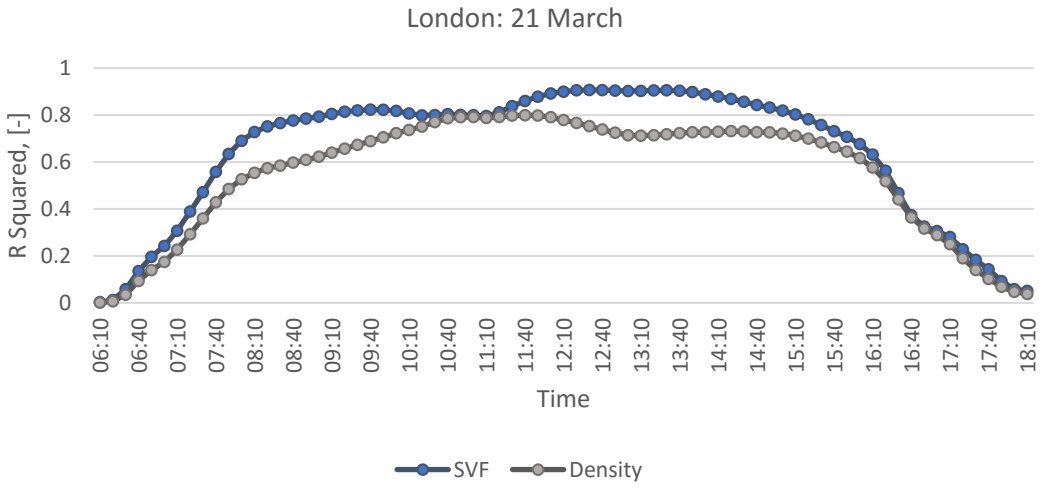

Figure 4.18: Variations of R^2 describing the strength of the linear relationship between mSVF and mSOL, and density and mSOL, on 21 March, for London's urban forms.

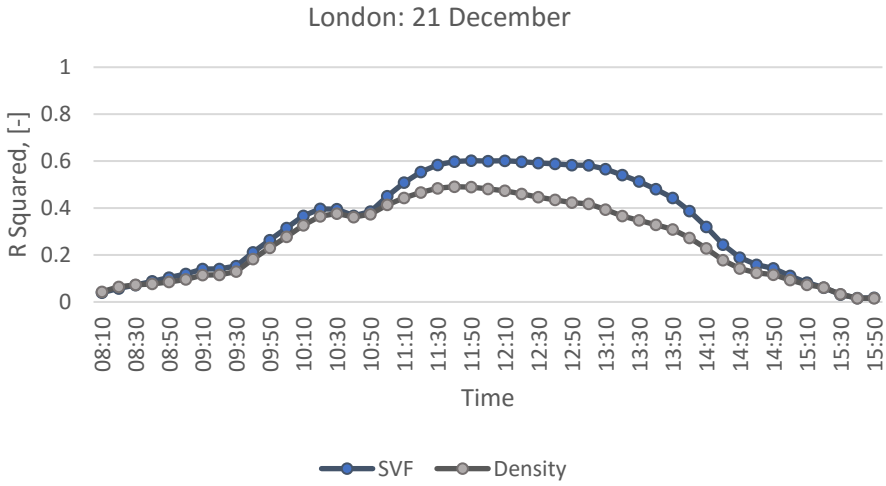

Figure 4.19: Variations of R^2 describing the strength of the linear relationship between mSVF and mSOL, and density and mSOL, on 21 December, for London's urban forms.

Lastly, since the variations of the strength of the relationship of mSVF and instantaneous mSOL in time is attributed to the sun's altitude, and to investigate this further, all R^2 values obtained for all three days were combined and plotted against solar altitude angle occurring at the given time. Precise solar altitude angles were obtained using online NOAA Solar Position Calculator. As seen in Figure 4.20, the effect of solar altitude on the relationship of mSVF with mSOL is quite clear, as the points of different days outline a relatively smooth and well-defined curve, i.e. they present similar R^2 for any given altitude. Furthermore, the rate of increase of R^2 as a function of sun's altitude is not constant, but reduces from lower to higher

altitude angles. By observation, and by approximation, two critical angles can be identified with respect to the rate of increase of R^2, based on the given points. Up to 20°, the rate is high and on average 0.035, i.e. for an increase of altitude angle by one degree, the R^2 increases by 0.035. At 20°, the impact of solar altitude begins to reduce significantly and, for angles larger than 50°, the value of R^2 tends to stabilise above 0.9 denoting an almost perfectly linear relationship. However, based on the quadratic curve achieving the best fit for the relationship, this presents maximum R^2, 0.957, for solar altitude angle equal to 47°, after which R^2 starts to reduce. Either based on the given points or the estimation curve, for solar altitude angles above 30°, the linear relationship between mSVF and mSOL is characterised by R^2 higher than 0.8 indicating a significantly high correlation. Drawing the line of 30°, on London's annual sun path, it is apparent that mSVF can explain instantaneous average insolation of open spaces for a great part of the daytime hours in a year (Fig. 4.21).

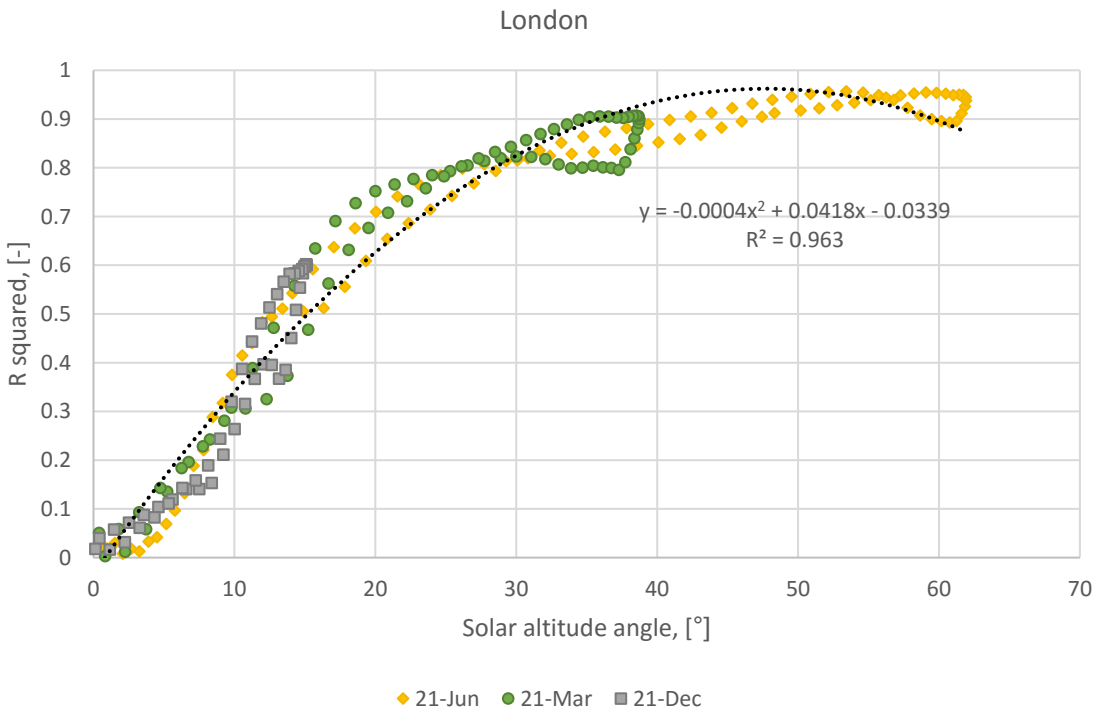

Figure 4.20: All R^2 for the linear relationship of mSVF and mSOL obtained for three days, plotted against solar altitude angle, for London's urban forms.

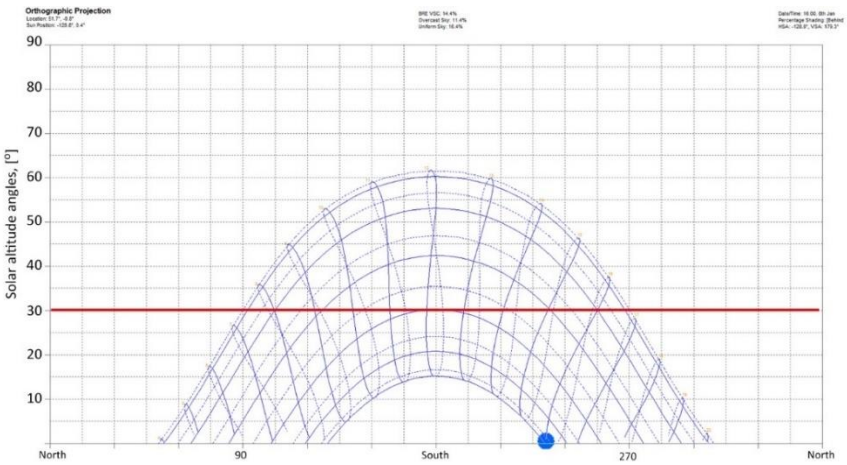

Figure 4.21: Sun's altitude angle of 30^{o} is highlighted by red line on London's sun path (orthographic) projection; for all sun's positions above it, the relationship between mSVF and mSOL is significantly strong, i.e. R^2>0.8.

Paris

After London, the relationship between mSVF and mSOL was tested statistically for the urban forms of Paris. The results agree on the general finding that the effect of mSVF on average insolation of open spaces increases with increasing solar altitude angle, and so does the strength of their relationship. However, the relationships in question are less consistent, and the R^2 values -on average and regarding the maximum ones- are reduced compared to those found for London's sample.

Regarding mSVF and daytime average insolation in open spaces, their relationship was found to be almost perfectly linear on 21 June and 21 March, and slightly stronger on the equinox day, with R^2 being 0.932 and 0.964, respectively. On 21 December, the correlation is considerably weaker, 0.552, and much lower than for London. Moreover, and despite any differences in the coefficients of determination, the lineal models produced setting intercept to zero, as shown in Figure 4.22, agree to a large degree with those of London (see Figure 4.13). Comparing the factors defining the slopes of the lines, i.e. the effect of mSVF on daytime mSOL on each day, their difference is at 10^{-2} level.

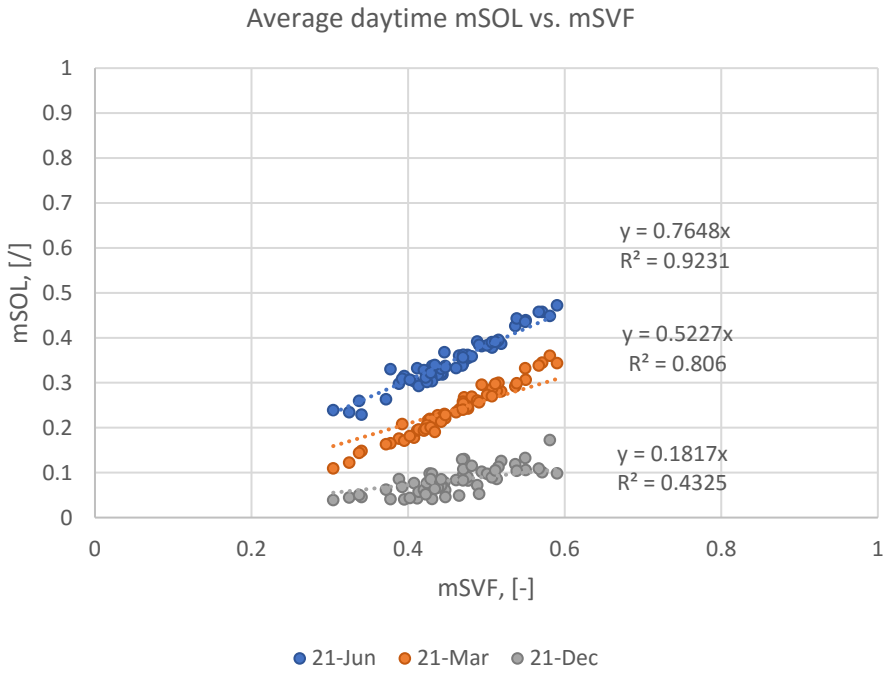

Figure 4.22: Average daytime mSOL values for 60 urban forms of Paris on 21 June, 21 March and 21 December, plotted against their ground mSVF, and linear models when intercept is equal to zero.

Moving on instantaneous mean insolations in Paris, their relationship with mSVF is stronger than with density. In Paris, their R^2 difference is more significant compared to London, which is attributed to the limited range of density values. More importantly though, plotting the R^2 values for the mSVF-mSOL relationship against time -for each day- the shape produced was less smooth, and presented a lower degree of symmetry compared to those for London (e.g. Fig. 4.24). This is also appeared in Figure 4.23 where R^2 values obtained from all three days are combined and plotted against solar altitude angle occurring at the respective time. As seen, the points outline a curve of similar shape as before for London (see Figure 4.20), but this is less well-defined since the points are scattered over a greater area. This means that, for a given solar altitude, the discrepancy of R^2 values is much larger.

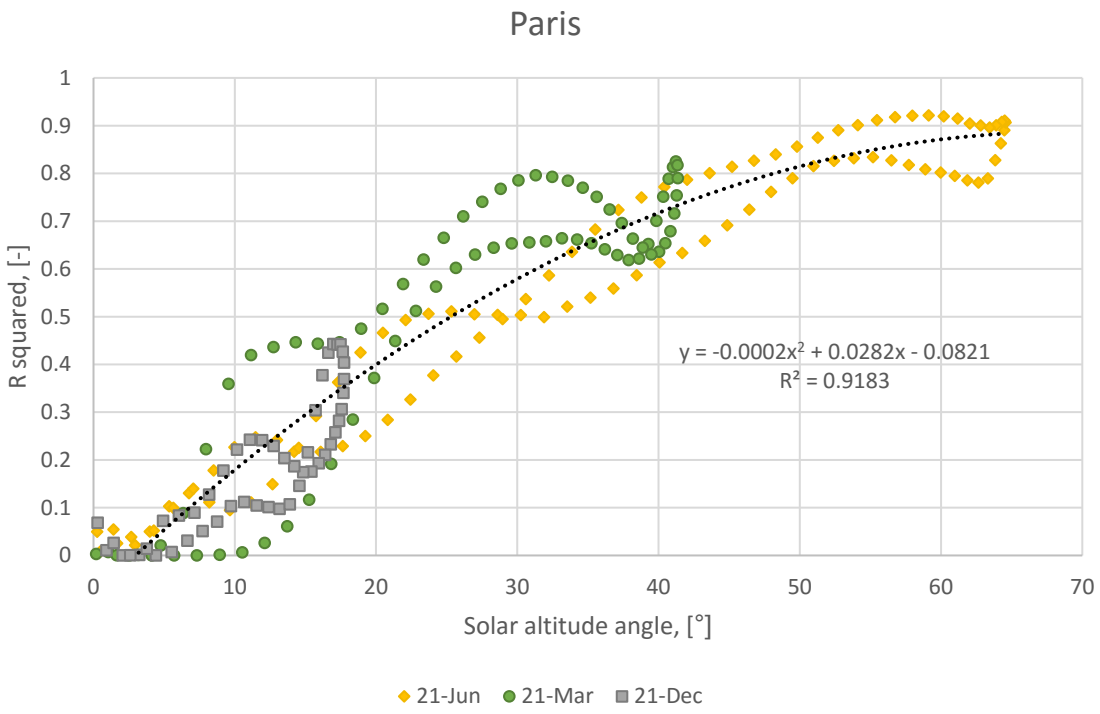

Figure 4.23: All R^2 for the linear relationship of mSVF and mSOL obtained for three days, plotted against solar altitude angle, for Paris' urban forms.

To explore the reason for which the relationship between mSVF and instantaneous mSOL presents discrepancies in Paris, a targeted analysis was carried out focusing on 21 March and mSOL at 30-min intervals. Linear regression tests were performed considering as independent variables the PCA factors explaining 87% of the variance of urban geometry variables in the two samples, which are three for London, and five for Paris (see Section 3.4.3). For the sake of comparison, the R^2 values are plotted on the same graphs with those obtained testing as predictors mSVF and density, and presented in Figure 4.22. In the case of London, the PCA factors perform slightly better -as predictors of mSOL- in the early morning hours but regarding the rest of day the same as mSVF (Fig. 4.24a). Regarding Paris, the combination of the PCA factors performs sometimes better and others worse than mSVF (Fig. 4.24b). Moreover, it seems that the smoothness and symmetry of the curve outlined are slightly enhanced; however, it is still less smooth and less symmetrical compared to London, as well as the R^2 values achieved are lower. Considering the above, it can be argued that it is not mSVF less capable to predict mean insolation of open spaces in Paris, but in general the urban geometry variables. This may imply that, the missing factor, i.e. the orientation effect, is more significant on the insolation of open spaces in Paris.

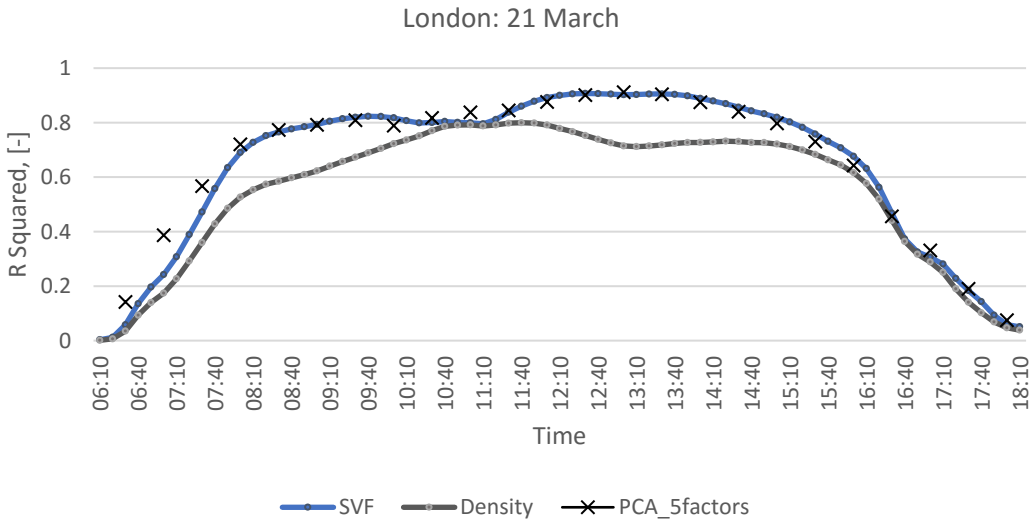

(a)

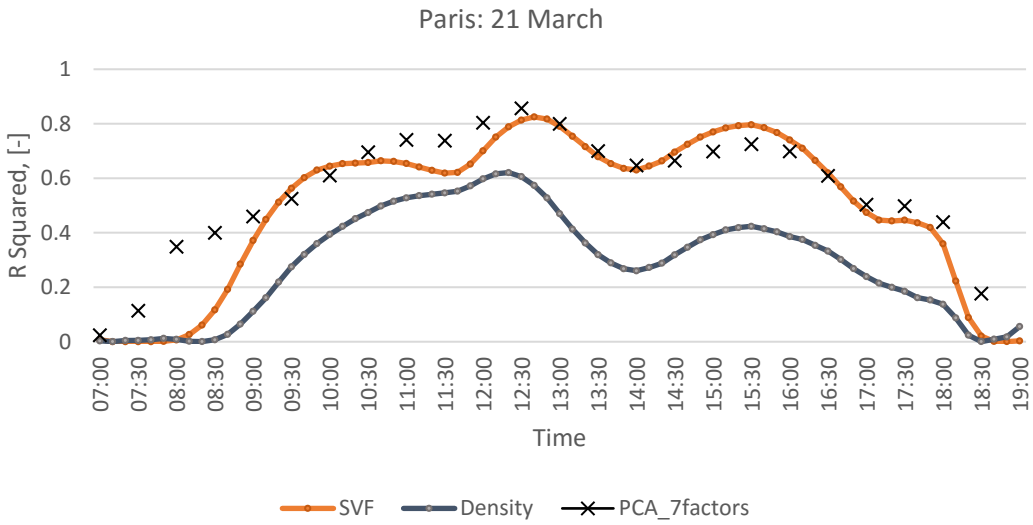

(b)

Figure 4.24: Variations of R^2 describing the strength of the linear relationship between mSVF and 5 PCA factors, - compared to mSVF and mSOL, density and mSOL- on 21 March, for London (a) and Paris (b).

4.5 Discussion

The study of Lindberg and Grimmond (2011a) investigating 19 sites on a north-south LiDAR transect across the city of London ascertained a strong relationship between morphological parameters considered (i.e. site coverage and mean building height), mean ground SVF, daytime average shadow fractions and daytime average MRT. The present study builds on their findings conducting a more extensive and in depth investigation on the relationships in question. Furthermore, the consideration of a second city,

Paris, allows the relationships to be tested for different urban geometries, contributing to the discussion and overall conclusions in two ways. First, the analysis of Paris confirms the major findings emerged from London's case, giving to them some extra validity. Second, it reveals some numerical discrepancies which, if examined along with results of the geometrical analysis of the cities, increase the understanding of the subject matter.

Regarding mean ground SVF in London, its correlation with density and all urban layout descriptors associated with it, such as *site coverage* (SCo), *complexity* (Cex) and *façades-to-street* (FaS), is significantly strong. The negative relationship of site coverage and mean building height with mean ground SVF for London was found before to be characterised by R^2, 0.830.and 0.860, respectively (Lindberg and Grimmond, 2011a). For the sake of comparison, the same test was repeated in the context of this study and the respective R^2 were found to be relatively close to the above, but higher for site coverage, 0.903, and lower for mean building height, 0.756. In contrast, for Paris, the correlation is statistically significant for coverage (R^2=0.758), but not for building height (R^2=0.019). In Paris, the relationship of mSVF with major geometry variables, such as density and mean building height, is affected by the limited ranges of their values. It is noticeable thought that even though the range of density values in London is 5 times greater than in Paris (i.e. 30.4 over 6.1), the range of SVF values is only 1.7 times greater (i.e. 0.485 over 0.286). This is related to that the relationship of the two is found to be logarithmic (Fig. 4.10), but also supports the argument that SVF contains more information than built density.

Regarding the logarithmic relationship of density and mean ground SVF, it shows that the impact of density on mSVF is not constant but reduces gradually with increasing density. This is reasonable, and justified by the fact that zero mean ground SVF is a theoretical value which cannot occur, given that it refers to the open space of an urban form. Plotting density and mSVF values computed for the two cities on the same graph (see Figure 4.10c), it appears that Paris' urban forms of high density tend to present lower mSVF, compared to those of London of same density. This is because in Paris higher densities are achieved mainly by increasing site coverage, namely reducing the open space. As found in Section 4.4.2.1 and argued by previous studies (Cheng et al., 2006a; 2006b), ground mSVF is primarily affected by the quantitive characteristics of open spaces. Nonetheless, combining the data of the two cities, the relationship remains statistically significant (R^2=0.761) and hence, the logarithmic model provided might be useful for a quick estimation of mSVF based on the density value of an urban area (Fig. 4.10c).

On the other hand, the relationship between mSVF and mean insolation (mSOL) values were found to be better fitted either by linear or logarithmic trendlines, at different instances. For lower solar altitudes -

when the correlation was generally weak- the relationships tended to be logarithmic; whereas for higher ones, -when the correlation became stronger- the relationships were better described by linear curves. However, since the R^2 values achieved by both kind of regressions were relatively close, and to ensure consistency, the graphs showing the strength of the relationship as a function of time/solar altitude were produced based on linear regression results.

With respect to the relationship of mSVF with daytime average insolation of open spaces, it was found to be almost perfectly linear on 21 March and 21 June, for both cities. These findings are in agreement with those of Lindberg and Grimmond (2011a) who, testing the same relationship for dates of similar sun's altitudes, i.e. 25 September and 3 June, reported a perfect fit (R^2=0.99), both on an autumn day and summer day. This study also considered a winter day, the analysis of which revealed an important reduction in the correlation of mSVF with daytime average insolation for very low solar altitudes. The fact that the impact of sun altitudes becomes apparent when comparing the results of 21 December and 21 March but not when comparing those of 21 March and 21 June indicates that the relationship is sensitive at the lower range of solar altitudes. In other words, the strength of the relationship increases with increasing sun altitude angle up to a degree. This point is also emerged by the analysis of the relationship between mSVF and instantaneous average insolation, especially for London, on 21 June (Fig. 4.17) and 21 March (Fig. 4.18), which showed that the impact of the sun's altitude is increased the hours after sunrise and before sunset. Additionally, it is worth highlighting that the correlation of mSVF with daytime and instantaneous average mSOL becomes stronger as the effect of mSVF on them does so. Interestingly, the effect of mSVF on daytime average insolation is found to be very similar for the two cities, on all three days considered (see Figure 4.13 for London, and Figure 4.22 for Paris).

Regarding the relationship between mSVF and instantaneous insolation of open spaces, the numeric results -in terms of R^2 values- for London's and Paris's urban forms present important differences with the relationship being stronger and more consistent for London. Considering the schema in Figure 4.1, the reduced correlation of mSVF with open spaces' insolation in Paris might be seen as an increase in the significance of the orientation parameter. The reason for the amplification of the orientation effect in Paris is twofold, and stems from quantitative and qualitative characteristics of its urban geometry. First of all, Paris presents a relative uniformity as concerns built density values across its urban area. Given that density has clearly a negative impact on SVF and solar access, the wider range of density and SVF values in London amplifies the strength of the relationship, blurring the effect of the orientation. On the other hand, instantaneous mSOL in Paris is more dependent on urban layout and, especially, the layout of the

open space in relation to the sun position. In particular, the effect of orientation is found to be extremely profound for compact urban geometries of Paris because of the existence of boulevards, i.e. long and wide straight street axis, which cut across the otherwise dense urban fabric and are not found in London. The coincidence of the azimuth of such a continuous and linear open space with the sun azimuth increases dramatically the average insolation of the urban form, especially for low sun altitudes when most of the open space is in shade (Fig. 4.25). Nevertheless, as mentioned previously, the results of the two cities regarding daytime average insolation are numerically very close on the summer solstice and equinox days and, hence, it can be argued that the orientation has an increased significance when considering solar access at a given time and for lower solar altitudes.

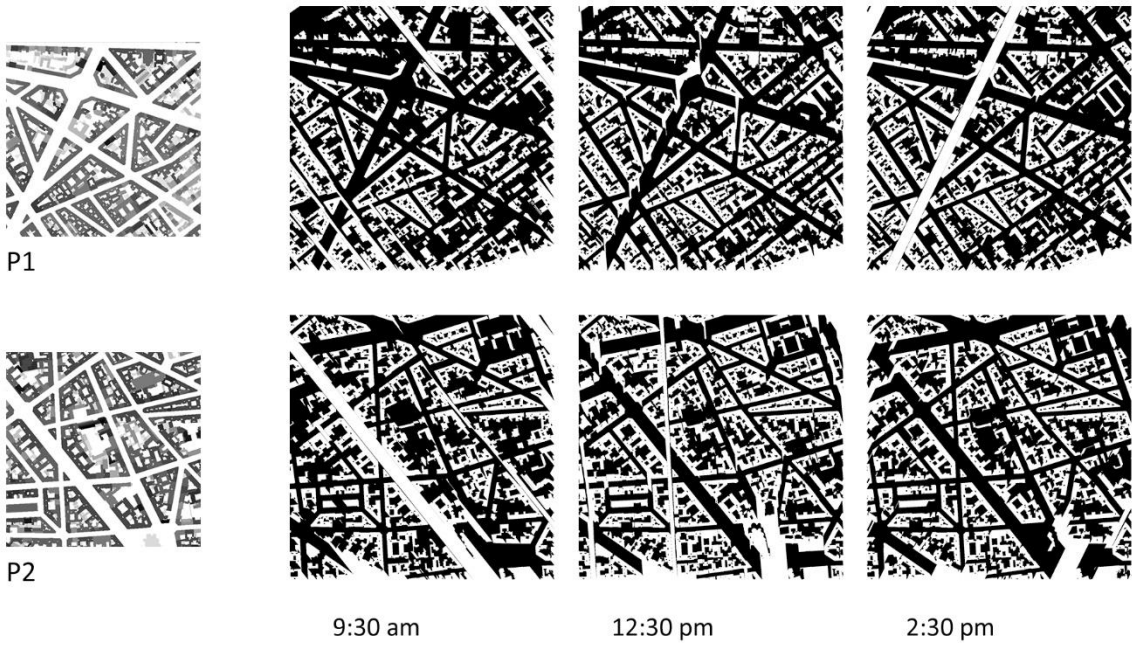

Figure 4.25: Two urban forms in Paris exemplifying the increased effect of orientation due to the presence of boulevards: shadow patterns on 21 December at different times.

The considerably different urban geometries of the two cities highlight the importance of the findings that their analyses confirm, and specifically, the increasing effect of mSVF on solar exposure of open spaces as well as their increasing correlation as sun altitude increases. This finding is deemed reasonable thinking of it as that, when the sun rises higher in the sky vault, the openness of the outdoor space to the sky approaches its exposure to the sun. However, the relationship is not linear meaning that the impact of solar altitude is not constant. According to the quadratic curves in Figures 4.20 and 4.23, the coefficient of determination presents theoretically a maximum value for a solar altitude angle beyond which the

correlation starts to reduce. Given the latitudes of the two cities, the range of solar altitude angles tested is approximately from 0° to 65° which does not allow to examine whether the quadratic models are valid or not. However, assuming the extreme case that an urban form is located at the Equator and the sun altitude happens to be 90°, then, all its open spaces would be sunlit independently to their mSVF. In this case, the relationship between mSVF and mSOL would be null. The example indicates that the strength of the mSVF -mSOL correlation must present a maximum value; however, it does not provide evidence for whether the relationship is quadratic (i.e. symmetric to the maximum value). Furthermore, the sun altitude angle for which the maximum R^2 value is achieved, -referred to as critical angle-, must be unique for each urban form, and related to its mean height-to-width ratio: the higher the ratio, the higher the critical solar altitude angle. It is thus important to underline that the critical angles identified on the graphs (i.e. Fig. 4.20 and Fig. 4.23) refer to the specific samples representing average values for the urban forms studied.

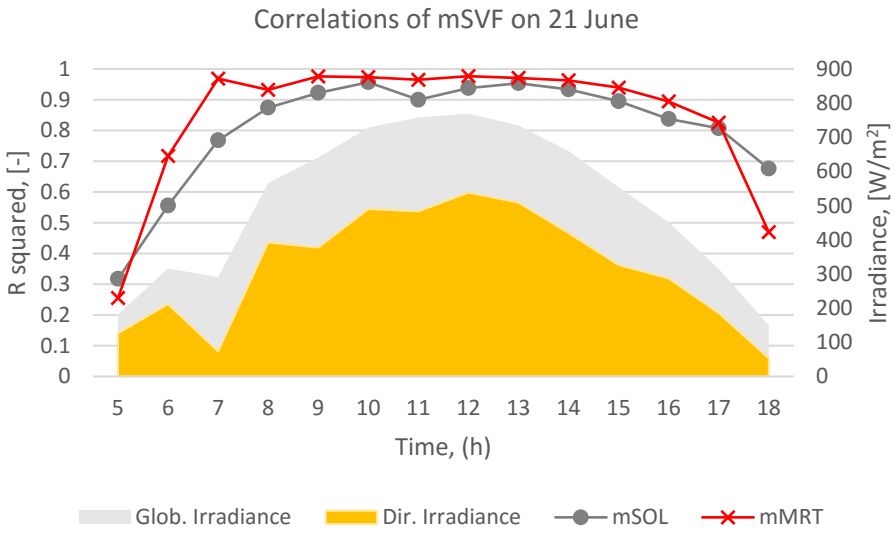

Figure 4.26: Correlation of mSVF with hourly mSOL and mMRT on the summer solstice, along hourly values of global and direct irradiance (only hours with direct irradiance considered).

All the above, derived from the exploration of the relationship between urban geometry and solar access at the pedestrian level, contribute to understanding the urban radiant environment experienced by pedestrians and users of open spaces under sunny conditions. Specifically, the findings explain the reasons behind the variations of average mean radiant temperatures (mMRT) in the urban forms of London on sunny days, presented Section 4.4.1. The initial assumption was that the relationship between urban geometry and mMRT may be also influenced by solar intensity. In an attempt to identify the influence of

solar intensity, the correlation between mSVF and mSOL was tested against the correlation between mSVF and mMRT, on same dates/hours (i.e. same solar altitudes). Among the days considered for MRT and shadow patterns simulations, there were two common, the summer solstice and equinox days, and allowed the comparison. Indicatively, Figure 4.26 compares the coefficients of determination obtained for mSOL and mMRT on 21 June, while the respective graph for 21 March is very similar. It seems that the influence of solar radiation is positive on most of the hours, increasing the correlation; however, this is not proportional to the solar intensity and, overall, is limited.

Finally, it is noted that the spatial scale at which the relationships of urban geometry and average radiant environment were examined (i.e. 500 x 500m) is a crucial parameter which needs to be acknowledged when referring to the research findings. In particular, it is assumed that the statistical significance of them may be affected considering smaller urban areas. However, the fact that a previous study for London presented similar results considering sites of smaller area (i.e. 400 x 400m in Lindberg and Grimmond, 2011a) indicates that an important decrease in the strength of the correlations is more likely to occur at considerably smaller scales. Furthermore, the relationship between urban geometry and mSVF was found to be slightly affected by reducing London's urban forms size area to half (i.e. 250 x 250m), which defines a range of spatial scales at which the relevant findings could be used with some confidence.

4.6 Conclusions

Chapter Four provides a considerable insight about the impact of urban geometry on the urban radiant environment at the neighbourhood scale, associated with outdoor thermal conditions and the urban microclimate. The relationships studied were those between urban geometry variables, average ground SVF, average insolation of open spaces and average mean radiant temperature, and explored statistically. With respect to the questions posed in Section 4.2 the major findings are outlined below:

- *Can mean ground SVF be estimated using simple urban geometry variables?*

  Mean ground SVF was found to correlate significantly strong with urban geometry variables, in both cities. The strongest variable for London is *site coverage* (r=-0.950) and for Paris *complexity* (r=-0.936). Furthermore, for a given density, the most influential variable for mean ground SVF in London remains *site coverage* (r=-0.698), while for Paris this is *mean outdoor distance* (r=0.893). As *site coverage* and *mean outdoor distance* are two variables measuring, in different ways, the open space, it can be argued that mean ground SVF is primarily affected by the quantitative characteristics of the open space. Regarding *built density*, its relationship with mean ground SVF was found to be better

described by logarithmic curves, and much stronger for London (R^2= 0.903) than Paris (R^2=0.638). This significant difference between the two cities is related with the limited range of density values characterizing the sample of Paris. Overall, as revealed by testing Principal Component Analysis factors as independent variables, urban geometry can explain the variations of mean ground SVF equally well in London (R^2= 0.971) and Paris (R^2= 0.962).

- *Can mean ground SVF -and to what extent- be used as indicator for estimating average insolation of open spaces?*

The correlation between mean ground SVF and shadow fractions and thus, the capability of the former to predict average insolation of open spaces was found to vary with solar altitudes. The results showed that the effect of solar altitude is not constant, but is of greater significance for lower altitudes and diminishes for higher ones. In this way, the strength of the correlation increases up to a point beyond which it is relatively constant. The above patterns were revealed by the analysis of both cities; however, the relationships are much stronger and more consistent in London's urban forms. This is attributed to that the variations of insolation of open spaces in Paris are more subject to the differentiation of urban layout and, especially, the layout of the open space in relation to the sun position. Mean ground SVF was found to predict better the insolation of open spaces than built density, proving that it contains more urban geometry information; nonetheless, it cannot express the orientation parameter. Indicatively, for London, the correlation of mean ground SVF with mean insolation of open spaces at a given time is characterised by R^2 higher than 0.8 when solar altitude exceeds 30°; whereas, for Paris, the estimation curve (R^2=0.918) denotes that at solar altitude of 30° the respective R^2 value is approximately 0.6.

Considering the above, it is of great importance that the results regarding daytime average insolation of open spaces in the two cities are numerically close, especially on 21 June and 21 March. On both days, the relationship of mean ground SVF and daytime average insolation was found to be almost perfectly linear, with R^2 being higher than 0.930; whereas, adjusting the linear models by setting intercept to zero, the R^2 obtained are 0.952 and 0.846 for London, and 0.923 and 0.806 for Paris, on 21 June and 21 March, respectively. Combining the numeric models, outdoor daytime average insolation can be estimated as a function of mean ground SVF, with multiplying factors 0.766 (21 June) and 0.532 (21 March). Therefore, it can be argued that mean ground SVF can accurately estimate average daytime insolation of spaces for half of the year, i.e. from spring equinox day to autumn equinox day, for locations of similar latitude to London and Paris.

Overall, the study demonstrates that mean ground SVF is a key parameter when studying the outdoor radiant environment, as it bridges urban geometry information with resulting radiation fluxes occurring in the open space. It defines longwave radiation emitted by open spaces to the sky as well as sky diffuse radiation received by them in the daytime; and, it can predict, to an important degree, their insolation under sunny sky conditions. By extension, mean ground SVF can estimate average mean radiant temperatures under all sky conditions, both in absence and presence of direct solar radiation. The calculation of SVF over entire urban areas is nowadays feasible using suitable simulation tools (Gal et al., 2009; Lindberg and Grimmond, 2010); it prerequires though the availability of 3D models of cities. Alternatively, the estimation of mean SVF by easily calculated urban geometry variables would facilitate its use as performance indicator, for a quick environmental evaluation of urban forms.

Closing Chapter Four, it is important highlighting once again the major finding, that the relationship between urban geometry and solar access and, thus, solar availability, in open spaces varies with solar altitude. Even though this was basically ascertained examining the relationship of mean SVF with shadow fractions, it creates a domino of research questions. In particular, considering that solar altitudes do not only vary in the day but also seasonally, the understanding of the impact of solar altitude might contribute to promoting the seasonal solar performance of urban forms. This constituted the research hypothesis in planning and executing the next study, which examines solar availability in open spaces and on building façades and follows in Chapter Five.

Chapter Five

Solar availability on building façades and ground

Chapter Five examines solar availability in open spaces and on building façades, with implications for outdoor thermal comfort and buildings' solar potential, respectively. The study investigates the relationship of mean SVF and mean irradiances -computed for the entire year, January and July-, with density and nine urban layout descriptors. The major aim is to explore to what extent urban layout can counterbalance the negative effect of density and potentially enhance the seasonal solar performance of urban forms. In addition to the main study, three more have been carried out exploring relevant issues using the same urban forms. Specifically, they revisit from another perspective issues which have been revealed and discussed in Chapter Four; these are: (i) the effect of orientation on solar availability, (ii) the effect of solar altitudes and sky conditions on the relationship between urban geometry and solar availability, and (iii) the effectiveness of mean SVF in predicting solar availability.

5.1 Introduction

Solar radiation is a major factor to be considered for promoting environmental sustainability in urban settlements, as it is strongly associated with their energy efficiency and liveability. Solar availability on building façades and roofs determines to a great extent their passive and active solar potential; while the insolation of outdoor spaces affects their microclimate and, in turn, their use (Littlefair, 2001; 2011). Unlike other environmental factors such as wind and temperature, solar exposure of urban surfaces can be accurately simulated due to the directional nature of solar rays, and their predictable interaction with urban geometry.

Referring to urban geometry, the present study makes a distinction between urban density and urban layout. Urban density refers to the magnitude of total built volume in a given site, while urban layout, to the way in which this built volume is distributed spatially within the site, horizontally and vertically. The negative correlation between built density and, solar and daylight availability has been widely reported (Sanaieian et al., 2014) with implications for buildings' energy performance (e.g. Steemers, 2003; Strømann-Andersen and Sattrup, 2011) and, urban microclimate and outdoor thermal comfort (e.g. Ali-Toudert and Mayer, 2006; Emmanuel et al., 2007).

Nonetheless, increased built density is an objective of urban planning as it is associated positively with urban environmental sustainability, especially at the city scale (Jabareen, 2006). Therefore, for

temperate and cold climates, where enhancing solar availability is crucial, the counterbalance of the negative impact of increasing density is sought through the deliberate manipulation of urban layout (e.g. Kristl and Krainer, 2001; Lu and Du, 2013). For instance, even given the same density, varying the combinations of site coverage and building height alters the level of solar irradiation (Lee et al., 2016), with decreasing site coverage being found beneficial for solar thermal and energy potential on façades and solar availability on the ground (Cheng et al., 2006a; 2006b). Nonetheless, when photovoltaics and solar thermal potential are examined on entire building envelopes, the impact of site coverage is inversed as increasing building footprint area means larger roof area (Li et al., 2015). Another parameter of urban layout that has been found to be influential, especially in urban environments of high density, is vertical and horizontal randomness, the increase of which may lead to higher solar potential on building envelopes, daylight availability on façades as well as openness of the open space to the sky (Cheng et al., 2006b; Ng and Wong, 2004). It is pointed out that, until recently, most of the studies examining relationships between urban geometry variables and solar availability indicators were based upon computer-based parametric investigations on generic models of urban canyons, or simple configurations of rectangular building volumes. It is therefore important that such research findings are tested in real urban forms.

Compared to buildings' solar performance, the study of solar availability in urban environments is considerably more complex, and demanding in terms of computational time and resources. This partially explains why the major researches on this topic have been conducted in the context of collaborative research projects, e.g. Project ZED (1997) and its successor Project PREcis (2000) up to the ongoing IEA SHC Task 51 Solar Energy in Urban Planning. As included in the conclusions of IEA SHC Task 41 Solar Energy and Architecture (Wall et al., 2012, pp. 1258), "[…] *a vast development is needed regarding strategies, methods, tools and case studies on the urban level*." However, as computer technology and capacity advances, studies performing solar radiation simulations at urban scale increase gradually.

Beyond powerful simulation tools required, the investigation of solar performance of existing urban areas relies also on the availability of their 3D geometry information. Thanks to recent advances in LIDAR technology and availability of modern GIS-based 3D models of cities, an increasing number of studies deal now with solar availability in real urban forms (Biljecki et al., 2015). A category of those uses 3D urban models of cities in order to evaluate solar energy and passive potential on building envelopes (e.g. Brito et al., 2012; Redweik et al., 2013). There has also been some research which uses data derived from the morphological analysis of cities to identify representative typologies and next, based on them, examine how to optimize the solar potential by controlling urban morphological variables. For instance, Sarralde et al. (2015) tested the impact of eight such variables on the solar

energy potential analyzing different possible scenarios of urban morphology in Greater London. According to the neighbourhood-scale statistical model employed, the optimum combinations of variables could increase the solar irradiation of roofs and façades by 9% and 45%, respectively, with site coverage and average distance between buildings being the most influential for façades. Similarly, in the study of Martins et al. (2014) for the Brazilian city of Maceió, solar energy potential, daylight availability and potential solar gains were assessed on building envelopes of representative urban configurations, varying morphological parameters' values. Building height to street width ratio, average distance between buildings and albedo were identified as the most relevant factors to the solar irradiation and illuminance levels on building surfaces, with their overall impact to rise up to 75% for south façades.

Unlike aforementioned studies that apply a top-down methodological approach, a recent study by Mohajeri et al. (2016) focused on the relationship between six density indicators, such as site coverage, plot ratio and population, and buildings' solar potential in 16 neighbourhoods of the city of Geneva (Switzerland). The results showed a strong negative linear relationship between annual solar irradiation and, built volume-to-area ratio, site coverage and plot ratio. The difference between high-density and low-density neighbourhoods was in the order of 30% - 40%, depending on the indicator. Furthermore, moving from the centre to the suburbs, the façade PV and solar thermal potential was found to increase from 3% to 20%, and from 49% to 85%, respectively.

5.2 Objectives

The present study combines three distinct objectives, which in turn determine the methodology employed. The first objective is to investigate statistically the relationship between urban geometry and solar availability in real urban areas. The statistical exploration of relationships between urban geometry variables and performance indicators is enabled by the big sample of urban forms analysed.

The second objective is to examine simultaneously the solar availability on building façades and in open spaces, which up to now have received the attention of only few researchers (e.g. van Esch et al., 2012; Zhang et al., 2012). In contrast to solar irradiation of building envelopes that could be interpreted into potential for energy savings and/or energy generation, the consideration of solar availability in open spaces does not present an explicitly quantified motivation such those related to reduced energy consumption, CO_2 emissions and cost. Nonetheless, the microclimatic conditions in open spaces do affect the thermal comfort or discomfort levels experienced by people and, thus, the duration and quality of their outdoor activities (Nikolopoulou and Lykoudis, 2007). Such activities may significantly promote individual and collective well-being of inhabitants contributing to more livable as well as, economically and socially, sustainable cities (Nikolopoulou et al., 2001). In order for solar

availability on building façades and in open spaces to be studied in equal terms, the solar indicators ought to be common and meaningful in both cases. Thus, mean sky view factor and irradiance values were selected to be examined, instead of indicators referring directly to buildings' solar potential and outdoor thermal comfort (e.g. irradiation values above given thresholds and mean radiant temperature, respectively).

Finally, the targets regarding the modification of the solar availability on urban surfaces may vary in time (e.g. seasons), as well as due to different purposes of the solar use (e.g. passive heating, photovoltaics), leading to major conflicts in urban environmental design. In temperate climates, such a conflict results from the seasons' different thermal needs: in general, opting for maximizing thermal gains in winter and minimizing them in summer, both indoors and outdoors (Littlefair et al., 2000). Considering the above as typical case for London's buildings and open spaces, the study aims to investigate the role of urban geometry in the seasonal solar performance of urban forms in the particular city. For this purpose, solar irradiation of façades and ground is considered for three time periods: the entire year, a winter month (January) and a summer month (July). In addition, the consideration of different months accomplishes another purpose, which is to investigate the impact of solar altitude angles on causal relationships between urban geometry and solar availability.

5.3 Methodology

For investigating the relationship of urban geometry and solar availability in open spaces and on building façades in depth and pursuing the aforementioned objectives, the reduction of the number of the studied urban forms was considered necessary. The selection criteria included the acquisition of a continuity of density values and inclusion of as much as possible different urban layouts in the sample, which would allow the comparative analysis of the impact of the two parameters of urban geometry, i.e. density and layout. Most of density values are represented by more than one urban forms, which also decided their final number (see Section 2.4.3). In this way, from the initial 72 urban forms of London, 24 have been selected to be considered in the analysis, 6 urban forms from north, 5 from west and 13 from central London, covering density values between 3-6, 5-11 and 10 -22 m^3/m^2, respectively (Fig. 5.1). The DEMs of 24 urban forms are given in Appendix B, and their positions in three London's areas are shown in Figure 2.4. The naming used for distinguishing them is defined by a letter, which indicates the area they belong to (i.e. C for central, W for west, and N for north) and a

number, which derives from the numbering of the cells in the maps of the three areas (by columns, starting from the top left cell). For instance, C2 is the second cell in central London's map.

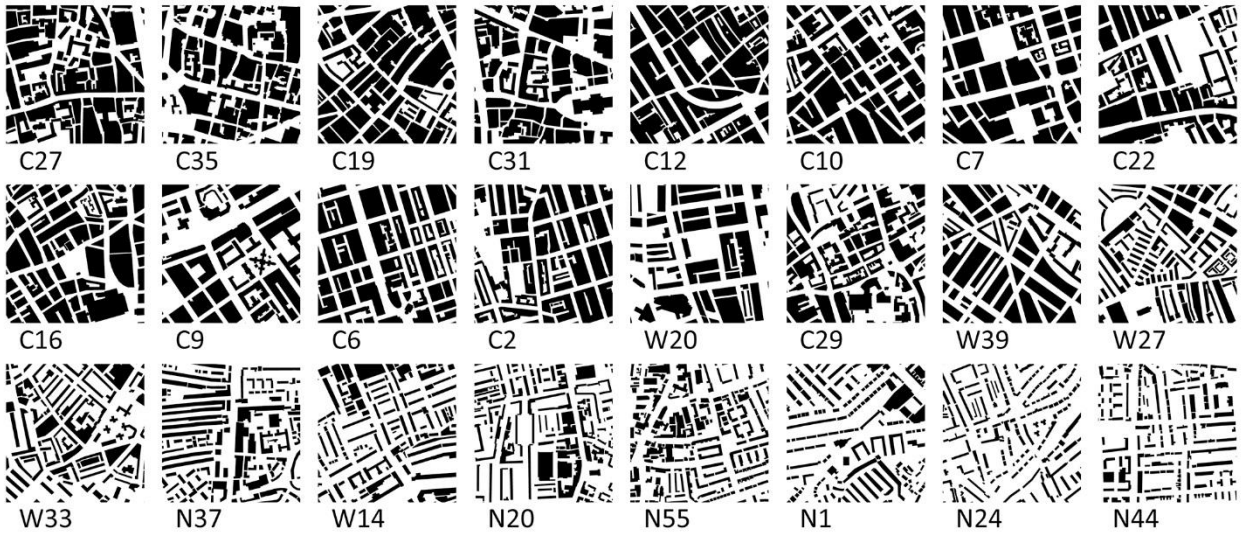

Figure 5.1: Twenty-four urban forms from central (C), west (W) and north (N) London, in decreasing order of density.

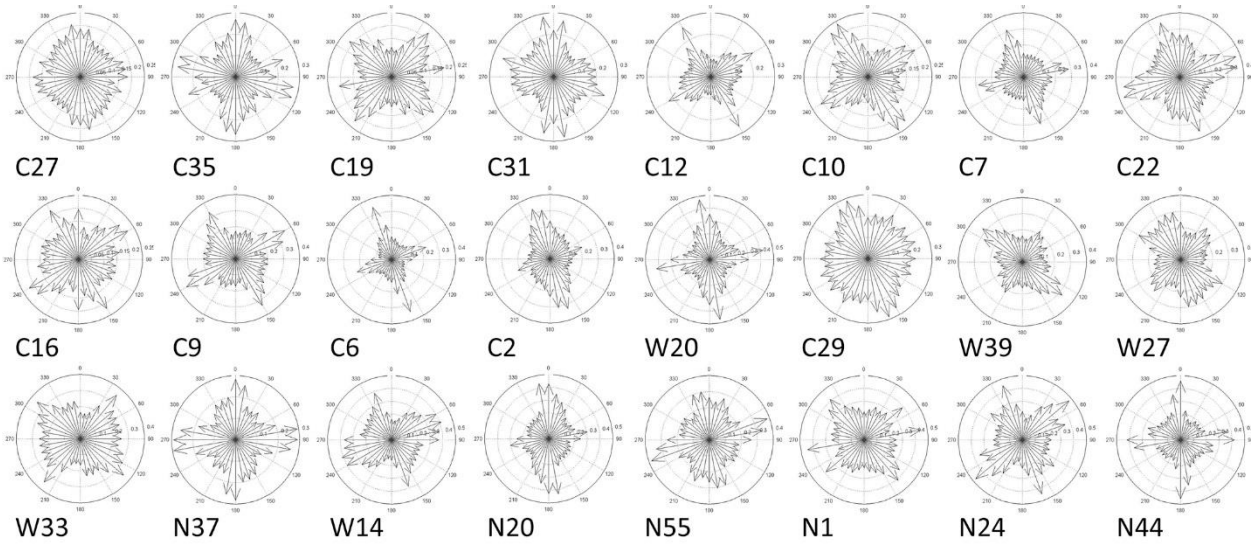

Figure 5.2: Polar diagrams showing the variance of ground's permeability of the 24 urban forms in 36 directions.

5.3.1 Urban geometry variables used

The present study is based on the distinction of urban geometry into density and urban layout, examining to what extent urban layout can counterbalance the negative effect of density on urban solar availability. Since the analysis of London revealed a strong collinearity for most urban geometry variables, it was deemed reasonable them to be reduced to the most basic in describing the variation of urban geometry and relevant to urban design decisions. In this way, beyond density, measured as

total built volume on a given site over site area [m^3/m^2], nine -out of the initial 17- urban layout descriptors presented in Section 3.3.2 were considered in the study which are the following:

Site coverage (SCo) – total buildings' footprint area over site area, [%];

Mean building height (MeH) – building height weighted by footprint area, [m];

Standard deviation of building height (StH), [m];

Standard deviation of building footprint area (StF), [m^2];

Directionality (Dir) – standard deviation of ground's permeability in 36 directions weighted by site coverage, [-] (Fig. 5.2);

Complexity (Cex) – total façades' surface area over site area, [m^2/m^2];

Compactness (Com) – total buildings surface-to-volume ratio, [m^2/m^3];

Number of building volumes (NoB) within the area;

Mean outdoor distance (MeD) – mean distance of outdoor space from the nearest building façade, [m].

For the interpretation of the results into practical information for professionals in the field of urban design, the meaning of the nine urban layout descriptors is briefly discussed below. *Site coverage* and *mean building height* express the horizontality and verticality of an urban form respectively. Since the product of their values is equal to built density, for a given density the two variables are inversely proportional. *Standard deviation of building height* expresses the degree of vertical randomness, i.e. the higher the StH value the less uniform the urban form's skyline. In the absence of a single variable measuring urban horizontal randomness, the study employs two variables which are associated to it, i.e. *standard deviation of building footprint area* and *directionality*. A higher value of StF demonstrates a less even distribution of the built-up area in the site. *Directionality* expresses the horizontal permeability of an urban form -as a porous medium- at the ground level: the more permeable an urban form at the ground level the less random its horizontal layout. *Complexity* expresses how undulating an urban form is, the more undulating the form the higher the Cex; whereas, *compactness* expresses negatively how compact the built form is. *Number of building volumes* expresses into how many building volumes the given built density is divided. Last, *mean outdoor distance* is proportional to mean distance between building volumes, expressing mean street width.

The values of 10 urban geometry variables for 24 urban forms of London are presented analytically in Appendix F. Pearson correlation analysis (two-tailed) was performed to test their interdependence,

and, as expected considering the previous analysis for 72 urban forms, most of urban layout descriptors present a significant correlation with density, which also causes their strong interdependence (Table 5.1). Controlling the effect of density, the most significant correlations appeared are these of site coverage with mean building height, mean building height with mean outdoor distance, and compactness with number of building volumes (Table 5.2).

Table 5.1. Pearson Correlation (two-tailed) results for all urban geometry variables.

	Density	SCo	MeH	StH	StF	Dir	Cex	Com	NoB	MeD
Density		0.931**	0.968**	0.628**	0.898**	-0.663**	0.965**	-0.920**	-0.846**	-0.285
SCo			0.829**	0.546**	0.922**	-0.693**	0.882**	-0.939**	-0.883**	-0.414*
MeH				0.633**	0.824**	-0.581**	0.937**	-0.887**	-0.827**	-0.107
StH					0.484*	-0.307	0.589**	-0.572**	-0.529**	-0.137
StF						-0.563	0.850**	-0.882**	-0.874**	-0.324
Dir							0.706**	0.606**	0.505*	0.575**
Cex								-0.834**	-0.770**	-0.401
Com									0.954**	0.148
NoB										0.053
MeD										

** Correlation is significant at the 0.01 level

* Correlation is significant at the 0.05 level

Table 5.2. Partial correlation results for all urban layout variables with control for the density variable.

	SCo	MeH	StH	StF	Dir	Cex	Com	NoB	MeD
SCo		-0.791**	-0.137	0.535*	-0.277	-0.167	-0.574*	0.493*	-0.426*
MeH			0.133	-0.411	0.324	0.049	0.036	-0.061	0.704**
StH				-0.230	0.188	-0.081	0.019	0.005	0.057
StF					0.099	-0.134	-0.324	-0.486*	-0.160
Dir						-0.336	-0.016	-0.141	0.538*
Cex							0.517*	0.328	-0.497*
Com								0.842**	-0.305
NoB									-0.369
MeD									

** Correlation is significant at the 0.01 level

* Correlation is significant at the 0.05 level

5.3.2 Solar availability analysis

For the assessment of solar availability in open spaces and on building façades of 24 urban forms, mean SVF (mSVF) [-] and mean irradiances [W/m^2] have been selected to be examined, all computed in PPF software (see Section 2.4.2.2). Global, direct, diffused from sky -referred to as *diffused*- and reflected by buildings -referred to as *reflected*- irradiances were computed for three sky models: entire year, January and July, presented in Figure 5.3. Number of daylight hours, mean direct and diffuse

horizontal irradiance by sky model are provided in Table 5.3. It is noted that the sum of direct and diffuse horizontal irradiance denotes maximum irradiance in London, for an unobstructed, horizontal site, for the respective time period.

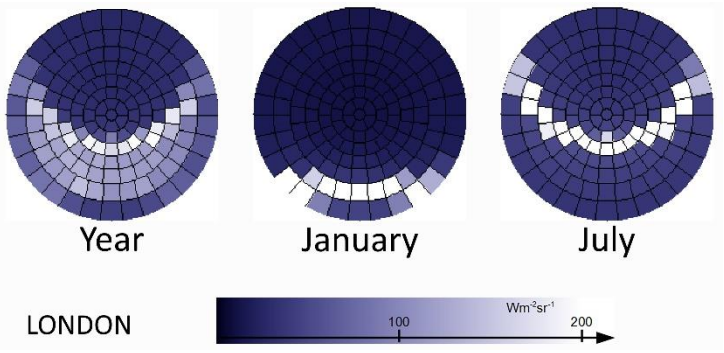

Figure 5.3: Stereographic views of the sky vault representing sky models generated for the year, January and July, and used in PPF simulations.

Table 5.3. Daylight hours, mean direct and diffuse irradiance values for the three sky models for London.

	Year	January	July
London			
daylight hours, [h]	4317	249	489
mean direct horizontal irradiance, [W/m^2]	102	32	157
mean diffuse horizontal irradiance, [W/m2]	120	52	136

5.3.3 Statistical analysis

The relationships of urban geometry variables and mean irradiances were explored performing statistical tests in MATLAB software. Since the relationships are found to be fairly linear, Pearson Correlation and linear regression tests were capable of describing them adequately. Furthermore, partial correlation analysis was employed to examine the effect of urban layout descriptors, controlling the effect of density.

It is noted that in the tables and graphs presented in support of the results of this study, the blue colour is used referring to façades and the green colour to ground, for facilitating their visual distinction.

5.4 Relationship of urban geometry and solar availability

5.4.1 Mean irradiances by time periods

This section presents mean irradiance values on ground and building façades computed for the year, January and July. Figures 5.4 - 5.6 present the results in bar graphs, by time period, allowing the comparison of the 24 urban forms, ordered by decreasing density value. These should be considered in comparison to the actual solar availability, for an unobstructed site, as this is expressed by mean direct and diffuse horizontal irradiances given in Table 5.3. Special emphasis is put on the proportion in which global irradiance consists of direct, diffused and reflected irradiation in different periods. Since global irradiance is calculated as the sum of them, its statistical relationship with urban geometry variables -examined next- is the result of the relationship of each of its components, weighted by the percentage in which they comprise it.

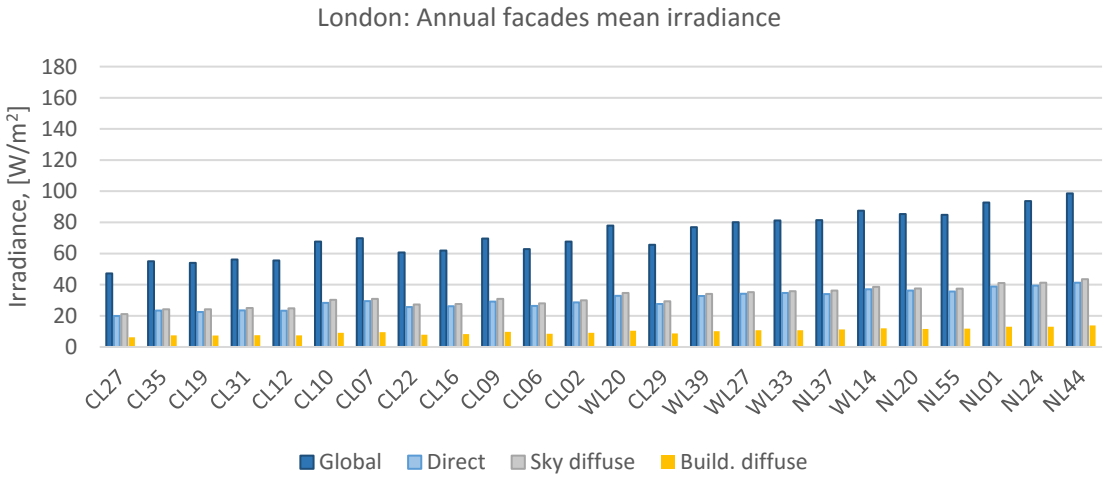

(a)

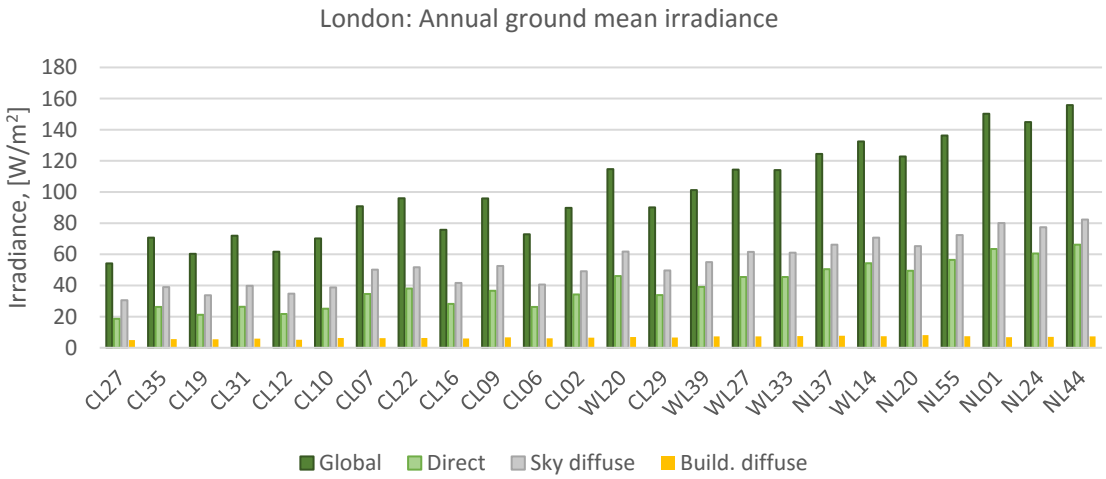

(b)

Figure 5.4: Mean global, direct, diffused and reflected irradiance values by urban forms, obtained for the year's sky model, for façades (a) and ground (b).

Over the year, direct and diffuse horizontal irradiances in London are in a relative balance with the former being 102 and the latter 120, W/m^2. Regarding annual global irradiance on façades, this consists constantly of direct radiation by 42-43%, diffused by 44-45% and reflected by 13-14%, in all urban forms (Fig. 5.4a). Hence, diffused radiation constitutes the greatest part of annual irradiation received by the façades, but with the direct solar component being equally important. With respect to ground, the respective percentages vary considerably more among the urban forms, and are found to be affected by their density. The percentage of direct irradiation varies approximately from 34 to 42% (decreasing with density), diffused from 53 to 56% (increasing with density), and reflected from 5 to 9% (increasing with density) (Fig. 5.4b). It becomes thus apparent that, over the year, the solar availability on the ground level derives by a larger degree from the sky vault, and the more densely built-up an urban form is, the higher the relative difference between diffuse and direct radiation available in open spaces.

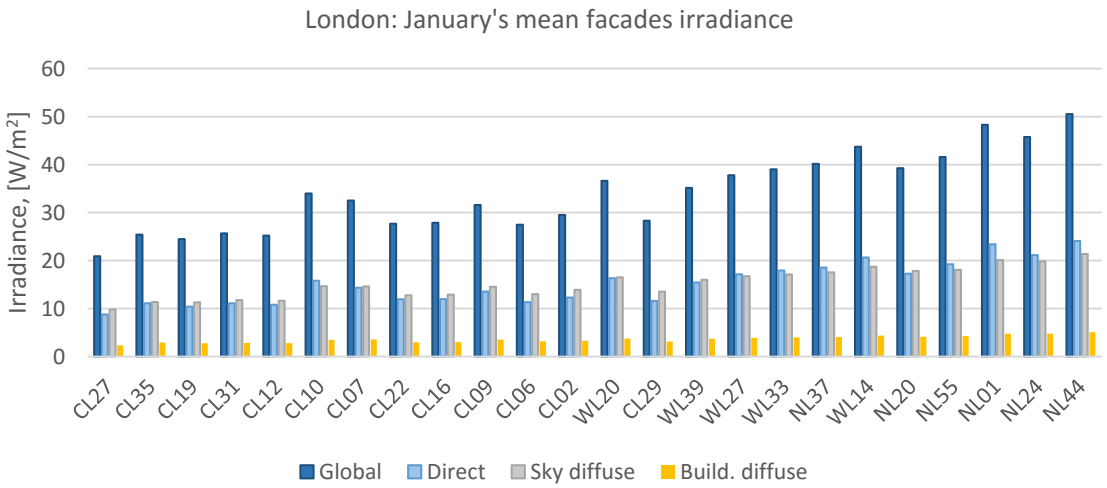

(a)

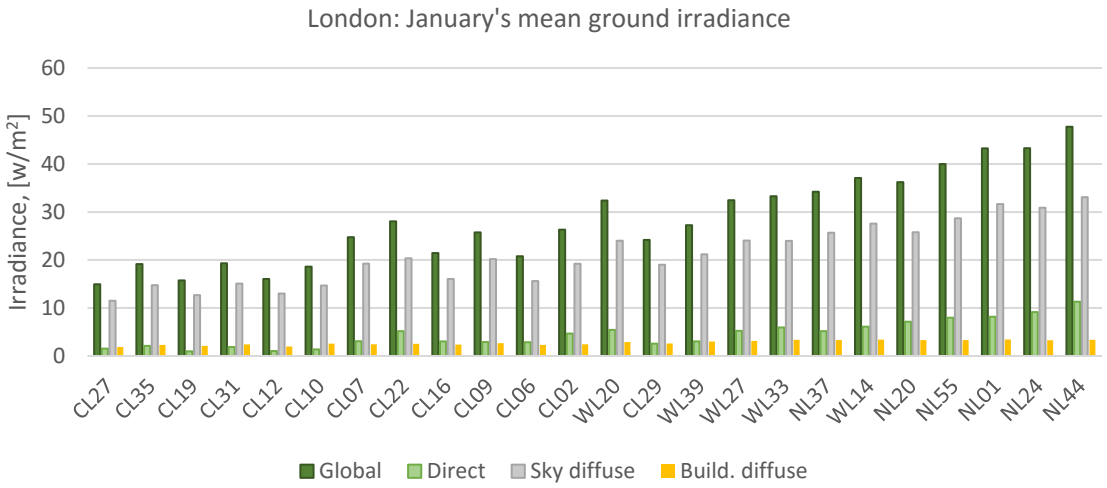

(b)

Figure 5.5: Mean global, direct, diffused and reflected irradiance values by urban forms, obtained for January's sky model, for façades (a) and ground (b).

In January, solar availability is in general limited in London with mean direct and diffuse horizontal irradiance being 32 and 52 W/m^2, respectively. Over this month, mean façades global irradiances comprise direct irradiance by about 41-49%, diffused by 42-48% and reflected 10-12% (Fig. 5.5). Hence, there are urban forms with higher mean direct irradiance compared to diffused one, and the reverse. Nonetheless, the percentages of the two major solar components are fairly close. Unlike façades, the solar availability in open spaces is dominated by sky diffused radiation which comprises 69-81% of global irradiance; whereas, direct radiation represents only 6-24%. As found for the entire year, the higher the density, the lower the percentage of direct irradiance is in the total irradiation available on the ground level. The same effect is observed also for façades but is not as powerful.

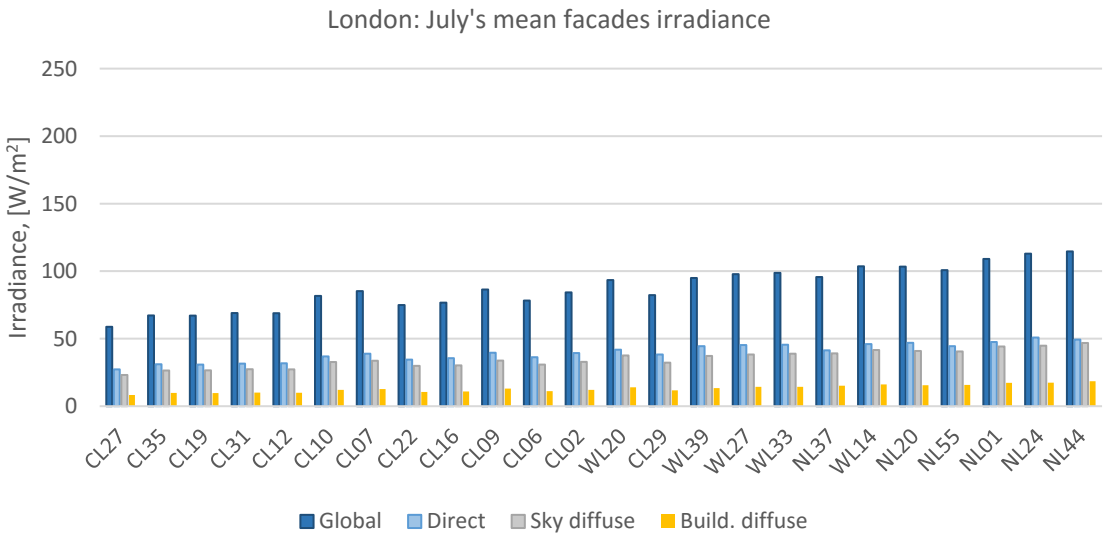

(a)

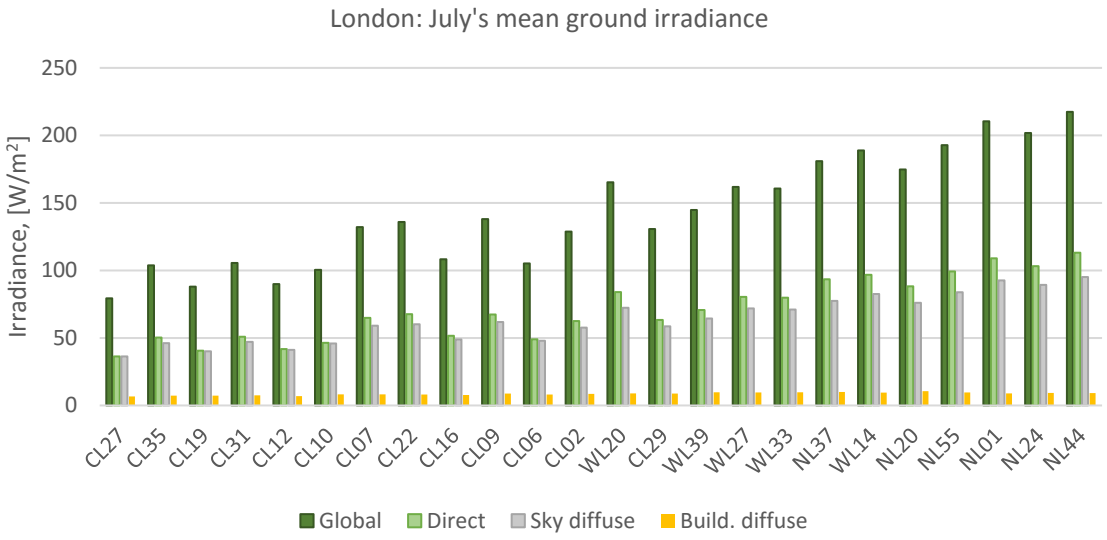

(b)

Figure 5.6: Mean global, direct, diffused and reflected irradiance values by urban forms, obtained for July's sky model, for façades (a) and ground (b).

Finally, July is the only period among the three considered in which mean direct horizontal irradiance in London is higher to the diffuse one, i.e. 157 and 136 W/m^2, respectively. This is reflected on mean direct and diffused irradiances computed on the ground and façades of the urban forms, with the direct solar component to be constantly higher (Fig. 5.6). Mean façade global irradiance consists of direct irradiance by about 43-47% (increasing with density), diffused by 39-41% (decreasing with density) and reflected by 14-16% (decreasing with density). Respectively, mean ground global irradiance consists of direct irradiance by 46-52% (decreasing with density), diffused by 43-46% (increasing with density) and reflected by 4-8% (increasing with density).

Overall, the average façade and ground solar availability in urban forms may present different percentages of direct, diffused and reflected irradiances, in the same time period, as they are affected by urban forms' density. The percentages of direct and sky diffused irradiances for façades are rather close, which indicates that the effect of density is reduced compared to ground. The greatest difference between the two occurs in July, when the direct radiation surpasses in percentage the diffused one, in all urban forms. In contrast, ground's solar availability is dominated by the diffuse component over the year and especially in January; and it is only in July that the two major solar components are found in similar percentages. The above information indicates where solar availability, namely total solar irradiation of building façades and open spaces, comes from in different time periods, and is useful in the consideration of the results presented in the following sections.

5.4.2 Urban geometry and solar indicators

5.4.2.1 Urban geometry and mean SVF

Starting with density, the analysis reveals a significantly strong, negative correlation with ground mSVF (r=-0.950) and façades mSVF (r=-0.958). Figures 5.7 and 5.8 demonstrate that the relationships can be equally well described by linear and logarithmic models; however, as discussed before (see Section 4.5), their logarithmic relationship is more realistic. This becomes evident by testing the extreme scenario of zero density value for which the logarithmic models give SVF values closer to 1 than the linear ones. Furthermore, the correlation between mean ground SVF and façades SVF is still significant but moderate (r=0.622), with both decreasing as density increases (Fig. 5.9). The moderate correlation between ground and façades mSVF values implies that the solar availability on horizontal and vertical urban surfaces may be affected differently by urban layout.

To investigate which urban layout descriptors affect mSVF values the most, partial correlation analysis was performed controlling the density variable. It was found that the strongest variables for ground mSVF were *mean outdoor distance* (MeD, r=0.736), *site coverage* (r=-0.654), *directionality* (r=0.486) and *complexity* (r=-0.478); whilst for façades they were *complexity* (r=-0.622), *standard deviation of building height* (r=0.579) and *directionality* (r=0.479) (Table 5.4).

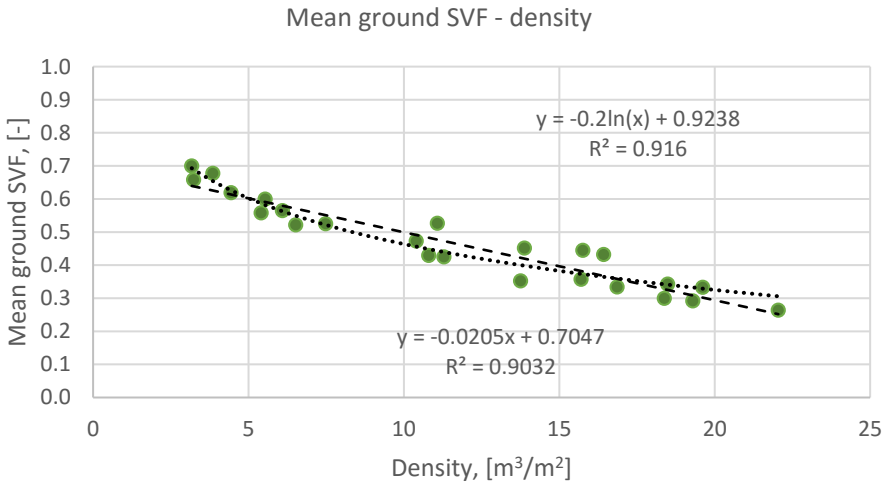

Figure 5.7: Linear and logarithmic regression models describing the relationship of mean ground SVF and density values, for 24 urban forms of London.

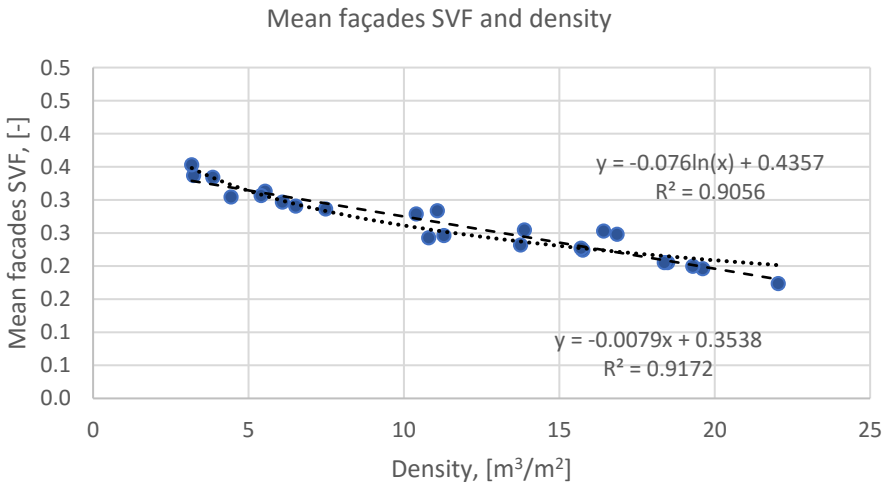

Figure 5.8: Linear and logarithmic regression models describing the relationship of mean façades SVF and density values, for 24 urban forms of London.

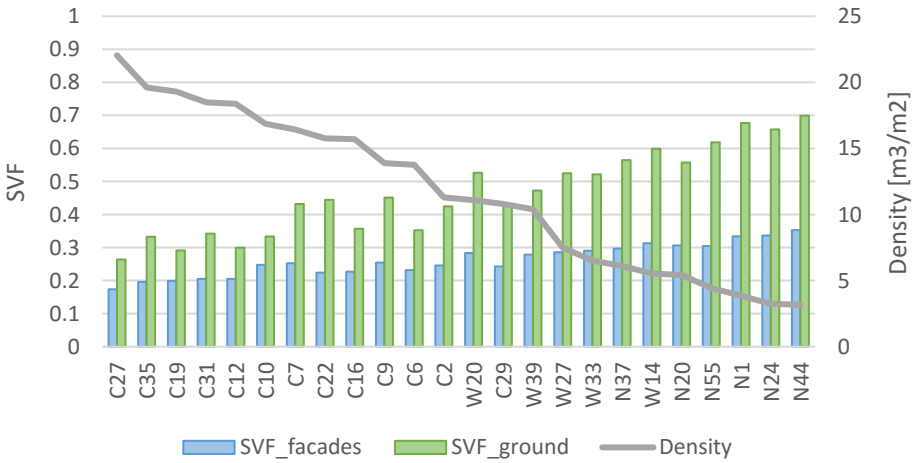

Figure 5.9: Density and mean SVF values, of ground and façades, in 24 urban forms of London.

Table 5.4. Correlation coefficients obtained from partial correlation test, with control for density, for mSVF and 9 urban layout descriptors.

	SCo	MeH	StH	StF	Dir	Cex	Com	NoB	MeD
Ground									
mSVF	**-0.654****	0.519	0.163	-0.404	**0.486***	**-0.478***	0.163	0.263	**0.736****
Façades									
mSVF	-0.257	0.0105	**0.579****	-0.141	**0.479***	**-0.622****	0.039	0.043	0.408

** Correlation is significant at the 0.01 level

* Correlation is significant at the 0.05 level

It is observed that, for a given density, the urban layout descriptors which are the most influential for ground mSVF are related to quantitative characteristics of the open space, namely mean street width (expressed by MeD) and total open space's area (expressed inversely by SCo). However, these two parameters do not present any significant effect on façades mSVF. In contrast, vertical randomness of urban forms (expressed by StH) was found to influence positively façades but not ground mSVF. On the other hand, there are variables which affect both, Cex and Dir, the former negatively and the latter positively. This indicates that the more undulating the building façades are, the greater the sky obstruction for the open spaces and façades, and increasing the directionality of the horizontal layout increases the overall openness of the urban form to the sky.

Additionally, mean building height (MeH) appears to correlate positively with mean ground and façades SVF, and in the case of the former the correlation is statistically significant (r=0.519, p=0.011). This counter-intuitive finding is explained by the inversely proportional relationship of MeH and SCo variables for a given density (see Table 5.2), in combination to the fact that SCo is associated negatively to SVF values: higher MeH means lower SCo which, in turn, is associated with higher mean SVF values. SCo expresses an absolute measurement in an urban form (i.e. percentage of the built-up area), while MeH expresses an averaged one (i.e. mean building height); this makes SCo more accurate in information encapsulated. As shown in Tables 5.6 - 5.9, the relationship of MeH with mean solar irradiances was also found positive and therefore, the relevant results are not further discussed in this study.

5.4.2.2 Urban geometry and *mean irradiances*

5.4.2.2.1 Density and mean irradiance values

Regarding the relationship between urban geometry and solar availability, the correlation between density and mean values of all the components of solar radiation is negative and significantly strong (|r|>0.880) (Table 5.5). This was expected as, in general, the more densely built-up an urban form is the more obstructed its ground and façades are to the sun and sky vault. Furthermore, with less solar

radiation incident on their surfaces, the reflected irradiance also decreases. Nonetheless, observing the correlation coefficient (r) values, some small differences between façades and ground, and among the time periods considered are identified. Density seems to correlate better with mean façades irradiance values than ground ones, with only exception diffused and reflected irradiance in January (and thus global irradiance too). Furthermore, among the three periods, the r values for January are in general lower than those for the year and July, which are similar. Figures 5.10a-c demonstrate the linear regression models describing the relationship between density and, mean global and direct irradiance values for ground and façades, in different time periods.

Table 5.5. Correlation coefficient values from Pearson Correlation test for density and mean irradiance values, for façades and ground, in three time periods.

	Façades				Ground			
	Ig	**Id**	**Ib**	**Is**	**Ig**	**Id**	**Ib**	**Is**
Year	-0.957	-0.958	-0.957	-0.946	-0.949	-0.941	-0.949	-0.895
January	-0.922	-0.895	-0.947	-0.930	-0.944	-0.886	-0.948	-0.944
July	-0.962	-0.954	-0.960	-0.948	-0.948	-0.940	-0.949	-0.884

All significant at 0.001 level

5.4.2.2.2 Seasonal effect of density

The seasonal effect of density on solar availability is examined based on the results of January and July, separately for façades and ground, as to be associated to the resulting potential for indoor and outdoor environment. In January, a representative winter month, the excessive overshadowing due to low solar angles was found to affect primarily the solar irradiation of open spaces. As shown in Figure 5.10b, the façades of the urban forms admit more solar radiation, global and direct, compared to the ground. In contrast, in July, as the sun motion coincides with higher positions in the sky vault, the open spaces are more exposed to the solar radiation, in all urban forms independently to density (Fig. 5.10c). Furthermore, the absolute and relative differences between mean irradiance values on ground and façades increase with decreasing density; the lower the density of an urban form, the greater the heat stress exerted over the ground related to that on building façades.

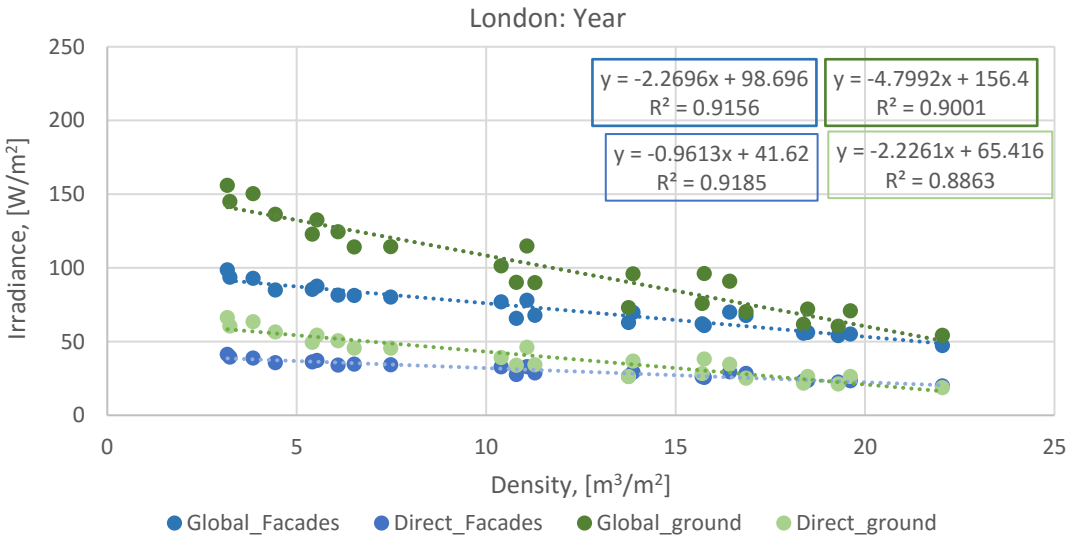

(a)

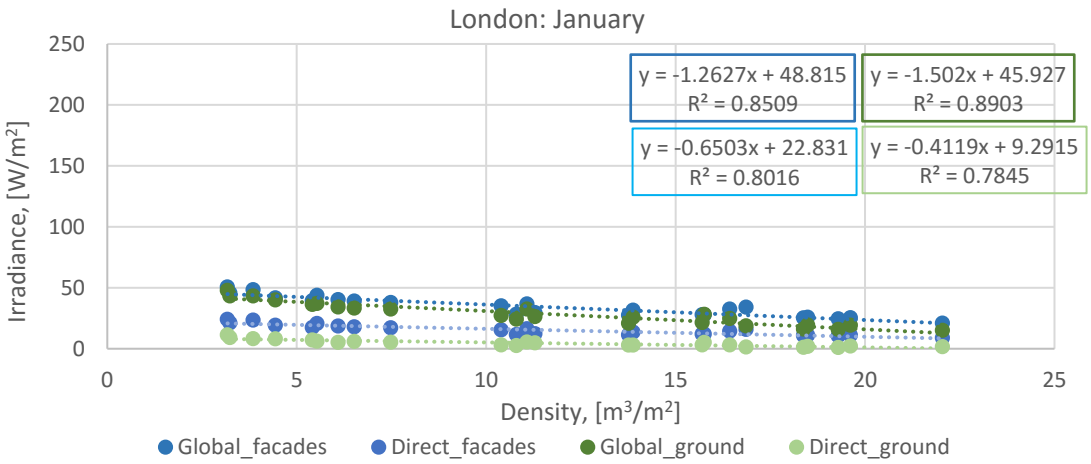

(b)

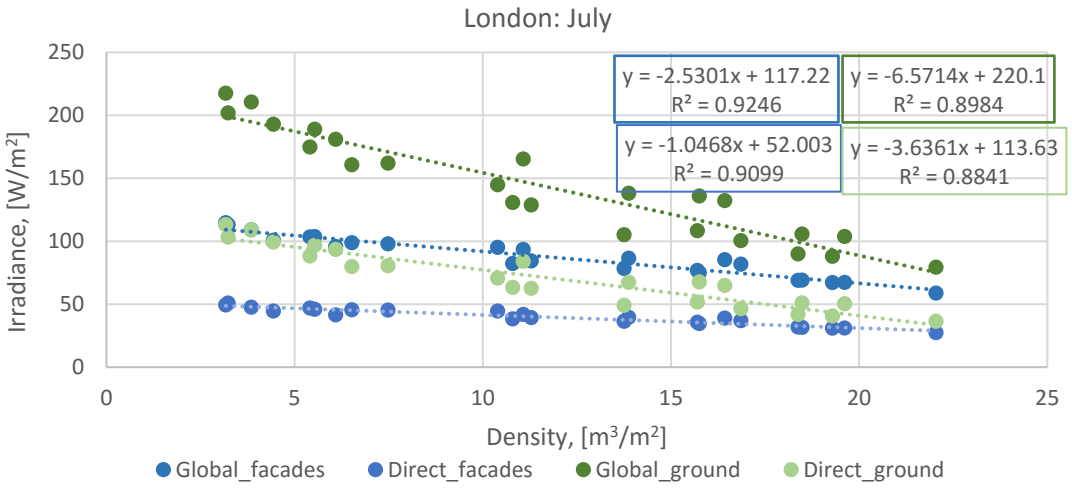

(c)

Figure 5.10: Linear regression models for density variable and mean irradiance values on ground and façades, over the entire year (a), in January (b), and in July (c).

Indicatively, the average value of mean global irradiance for all 24 urban forms in January is 34.1 W/m^2 for façades, and 28.4 W/m^2 for the ground. In July, the respective values increase to 87.7 W/m^2 and 143.5 W/m^2. Therefore, the open spaces receive on average about 5 times more solar radiation in July compared to January, while the solar irradiation of the façades increases by 2.6 times. As concerns the direct solar component, which is highly related to solar angles, the effect of the season on the façades is similar but much more pronounced on the ground. More specifically, mean direct irradiance on the ground is on average 15 times higher in July than in January, i.e. increasing from 4.4 to 71.2 W/m^2, whereas, on building façades by 2.6 times, i.e. from 15.2 to 39.8 W/m^2. Combining the above findings, it can be argued that the seasonal solar effect is much more significant on open spaces compared to building façades, with open spaces suffering from excessive overshadowing in the winter and prolonged solar exposure in the summer.

5.4.2.2.3 Urban layout descriptors and mean irradiance values

The relationships of nine urban layout descriptors with mean solar irradiances were explored by performing partial correlation analysis with control for density. The results are presented analytically for mean global, direct, diffused and reflected irradiances in Tables 5.6 - 5.9, respectively. Focusing on direct and diffused irradiances which constitute the greatest part of the global, the descriptors which affect their annual values were found to be to a large degree common; however, with respect to January and July there were significant differences. Mean diffused irradiances, in all time periods, are affected the most by the same descriptors which were found to affect mSVF. For façades, these are *standard deviation of building height* (StH), *directionality* (Dir) and *complexity* (Cex), and for ground, *site coverage* (SCo), *directionality*, *complexity* and *mean outdoor distance* (MeD). Standard deviation of building footprint (StF) was found to be influential for ground diffused irradiance only for the year and in July; whereas MeD was found to affect façades diffused only in July. Overall, the impact urban layout on diffuse radiation availability does not change significantly in different periods.

Interestingly, urban layout descriptors affecting mean direct irradiances vary remarkably among the three periods. With respect to ground, the availability of direct radiation is affected by all urban layout descriptors but StH. The influence of SCo and Dir is constantly significant, independent to period; whereas, MeD, StF, Cex, Com and NoB are of significance in different time periods. Compared to ground, façades were found to be less affected by urban layout descriptors, i.e. fewer number of them presenting significant correlation with mean direct irradiance by time period. Furthermore, there has not been identified any descriptor being of significance for all three time periods, which may be interpreted in that the relationship between mean façades direct irradiance and urban layout descriptors is more sensitive to different seasons. The effect of StH is statistically significant over the year period, and in January when the sun's position is relatively lower in the sky vault. In the winter

month, NoB is also found to be affecting the insolation of the façades as well as of the ground; the distribution of a given density into a greater number of building volumes allows more solar rays of lower angles to penetrate the urban fabric and reach the ground and building façades. On the other hand, in July, the direct irradiation of façades is influenced by Cex and MeD variables, which are also among the strongest for ground over the same period.

With respect to reflected irradiance, which as seen in Section 5.4.1 does not constitute but a small percentage of global irradiance (always considerably lower than the sum of the other two solar components), its amount on façades is influenced by the same descriptors as mean diffused irradiance in all time periods. On the other hand, mean ground reflected irradiance presents a totally different pattern of correlations. It is not influenced by any of the descriptors which were found to affect direct or diffused, but by *compactness* and *number of building volumes* in the year and July -by both negatively-, and by *standard deviation of building height* and *standard deviation of building footprint* in January, - by the former positively and the latter negatively-. It is worth mentioning that Com and NoB have been found before to correlate positively with ground direct irradiances in January; and they so constitute the only descriptors whose impact change direction depending on solar component considered.

The r values obtained for global irradiance are the average of the respective values for the other three solar components, weighted by their percentage within it. Therefore, it is not a surprise that the descriptors which are the most influential for direct and diffused irradiances affect also global irradiance. Focusing on those affecting it in all three periods, it can be argued that solar availability in open spaces is enhanced by decreasing site coverage, and increasing mean street width and directionality of horizontal layout. Moreover, the solar irradiation of building façades is enhanced all over the year by differentiating buildings' heights and decreasing the surface area of building façades, i.e. less undulated façades.

*Table 5.6. Partial correlation analysis for urban layout descriptors and mean **global** irradiance, controlling for density variable.*

	SCo	MeH	StH	StF	Dir	Cex	Com	NoB	MeD
Ground									
Year	**-0.679****	0.521*	0.174	**-0.451***	**0.487***	**-0.446***	0.197	0.313	**0.703****
January	**-0.699****	0.475*	-0.117	-0.386	**0.529***	-0.331	0.343	0.377	**0.636****
July	**-0.655****	0.529**	0.166	**-0.460***	**0.487***	**-0.449***	0.143	0.286	**0.708****
Façades									
Year	-0.315	0.147	**0.560****	-0.202	**0.485***	**-0.562****	0.096	0.095	0.406
January	-0.391	0.096	**0.596****	-0.338	0.365	**-0.430***	0.264	0.353	0.248
July	-0.227	0.162	**0.510***	-0.078	**0.457***	**-0.590****	-0.013	-0.106	**0.460***

** Correlation is significant at the 0.01 level * Correlation is significant at the 0.05 level

*Table 5.7. Partial correlation analysis for urban layout descriptors and mean **direct** irradiance, controlling for density variable.*

	SCo	MeH	StH	StF	Dir	Cex	Com	NoB	MeD
Ground									
Year	**-0.695****	0.496*	0.154	**-0.465***	**0.477***	-0.407	0.258	0.378	**0.656****
January	**-0.593****	0.301	-0.017	-0.229	**0.503***	-0.091	**0.500***	**0.427***	0.403
July	**-0.657****	0.511*	0.142	**-0.478***	**0.479***	**-0.417***	-0.170	0.329	**0.673****
Façades									
Year	-0.303	0.173	**0.530****	-0.206	**0.485***	**-0.544****	0.062	0.039	**0.425***
January	-0.409	0.081	**0.576****	-0.388	0.298	-0.364	0.312	**0.431***	0.187
July	-0.069	0.169	0.345	-0.074	0.337	**-0.509***	-0.168	-0.375	**0.451***

** Correlation is significant at the 0.01 level * Correlation is significant at the 0.05 level

*Table 5.8. Partial correlation analysis for urban layout descriptors and mean **sky diffused** irradiance, controlling for density variable.*

	SCo	MeH	StH	StF	Dir	Cex	Com	NoB	MeD
Ground									
Year	**-0.666****	0.520*	0.168	**-0.423***	**0.484***	**-0.468***	0.177	0.284	**0.723****
January	**-0.680****	0.509*	0.152	-0.410	**0.496***	**-0.442***	0.227	0.312	**0.708****
July	**-0.657****	0.524*	0.175	**-0.424***	**0.487***	**-0.476***	0.153	0.268	**0.729****
Façades									
Year	-0.290	0.124	**0.576****	-0.184	**0.481***	**-0.592****	0.072	0.082	0.402
January	-0.332	0.110	**0.608****	-0.255	**0.447***	**-0.535****	0.149	0.197	0.342
July	-0.275	0.132	**0.562****	-0.150	**0.490***	**-0.612****	0.046	0.033	**0.426***

** Correlation is significant at the 0.01 level……* Correlation is significant at the 0.05 level

*Table 5.9. Partial correlation analysis for urban layout descriptors and mean **reflected** irradiance, controlling for density variable.*

	SCo	MeH	StH	StF	Dir	Cex	Com	NoB	MeD
Ground									
Year	0.163	0.231	0.325	-0.101	0.082	-0.122	**-0.546****	**-0.503***	0.188
January	-0.382	0.485*	**0.510***	**-0.548****	0.111	-0.197	-0.142	0.047	0.322
July	0.266	0.161	0.238	0.039	-0.033	-0.075	**-0.581****	**-0.580****	0.110
Façades									
Year	-0.386	0.129	**0.555****	-0.225	**0.464***	**-0.487***	0.237	0.269	0.339
January	-0.405	0.129	**0.574****	-0.217	**0.458***	**-0.418***	0.301	0.309	0.286
July	-0.386	0.142	**0.558****	-0.238	**0.467***	**-0.485***	0.216	0.249	0.362

** Correlation is significant at the 0.01 level……* Correlation is significant at the 0.05 level

5.4.2.2.4 Exemplifying the effect of urban layout

To highlight the relevance of the findings of the previous section to real urban forms' solar performance, two pairs of urban forms, which are of similar density but different layouts, were identified and compared (Fig. 5.11). The values of urban geometry variables and solar availability indicators for all 24 urban forms -including the compared ones- are provided analytically in Appendix F. Their comparison exemplifies how urban layout can offset the negative impact of density on urban solar availability.

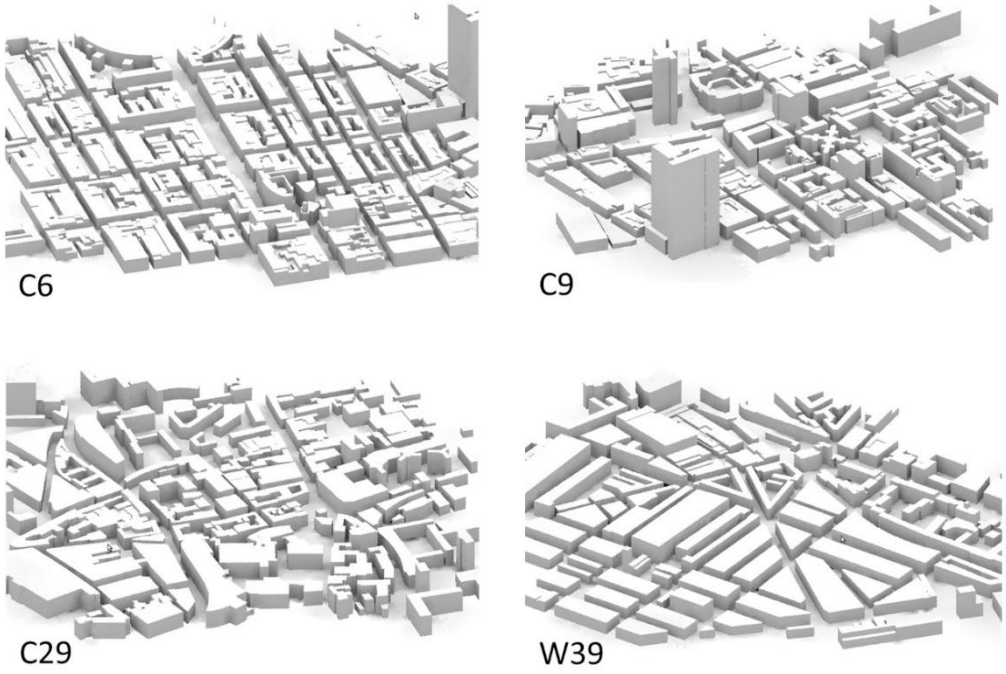

Figure 5.11: South perspectives of PPF models of the pairs of urban forms compared, C6 and C9 above, and C29 and W39 below.

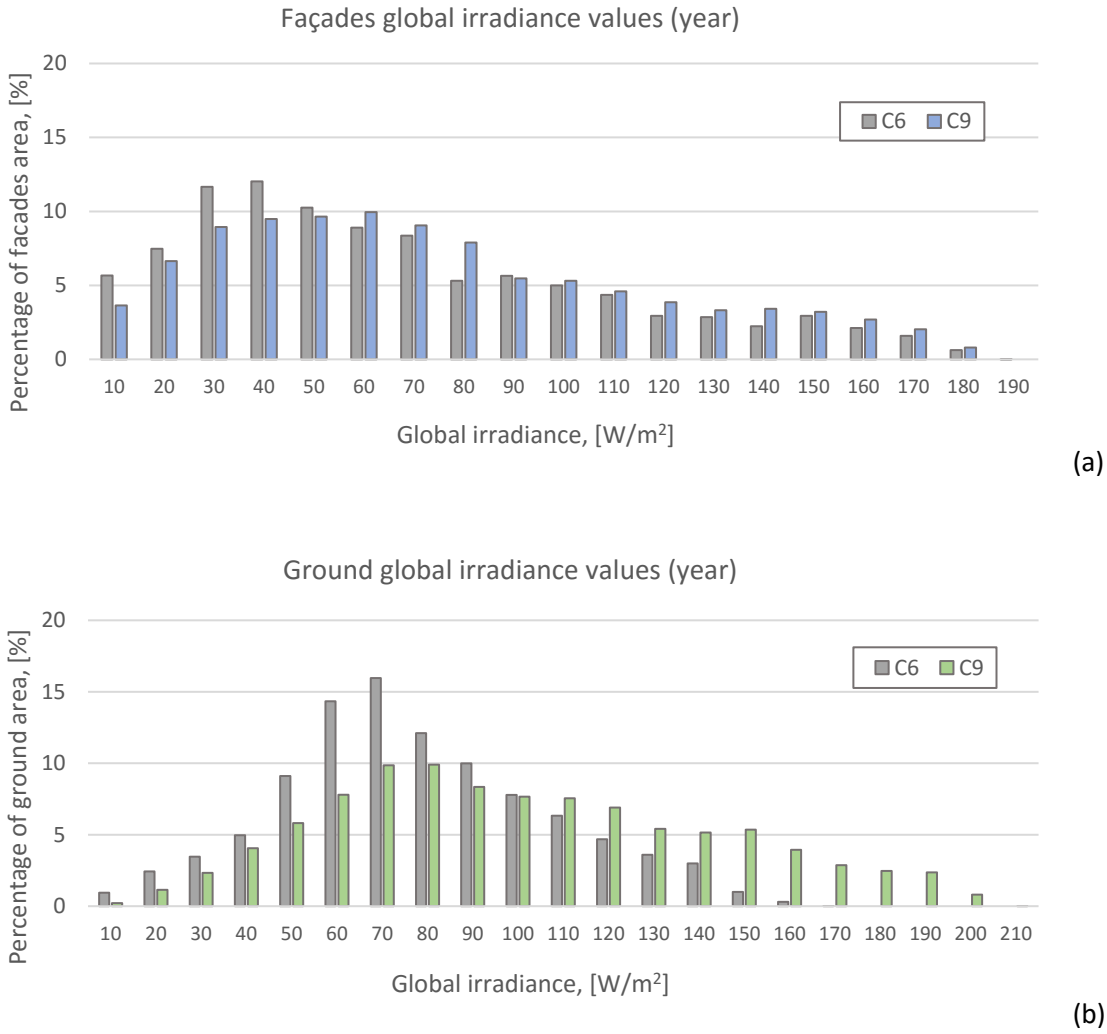

Figure 5.12: Comparison of distribution of irradiance values computed in C9 and C6, as percentage of total surface area: for façades (a), and ground (b).

The first pair consists of two urban forms of central London, i.e. C6 and C9. C6 lies between Regent Park and Oxford Circus; while C9 is situated north-east to the previous, near Euston station. Although they are both of approximately 14m^3/m^2 density, C9 admits more solar radiation incident on its ground and façades, in all different time periods. C9 has lower *site coverage* by 17% and almost double *mean outdoor distance* compared to C6, which explains higher mean global irradiance values on its ground: by 32% over the entire year, 24% in January, and 31% in July. The effect of *directionality* in which C6 performs slightly better seems to be outbalanced by the tightness characterizing its layout. The only case in which the ground of the two urban forms present similar values is January's mean direct irradiance, for which *compactness* and *number of building volumes* have been found earlier to be influential. Regarding the façades, the better performance of C9 is mostly associated to its less uniform vertically form, as expressed by StH, and its higher *mean outdoor distance*; the mean façades global irradiance in C9 is higher by 11%, 15% and 10%, in the year, January and July, respectively. Besides

higher mean values, C9 also presents a more even distribution of irradiance values with greater percentages of its façades and ground receiving more global radiation, compared to C6 (Fig. 5.12).

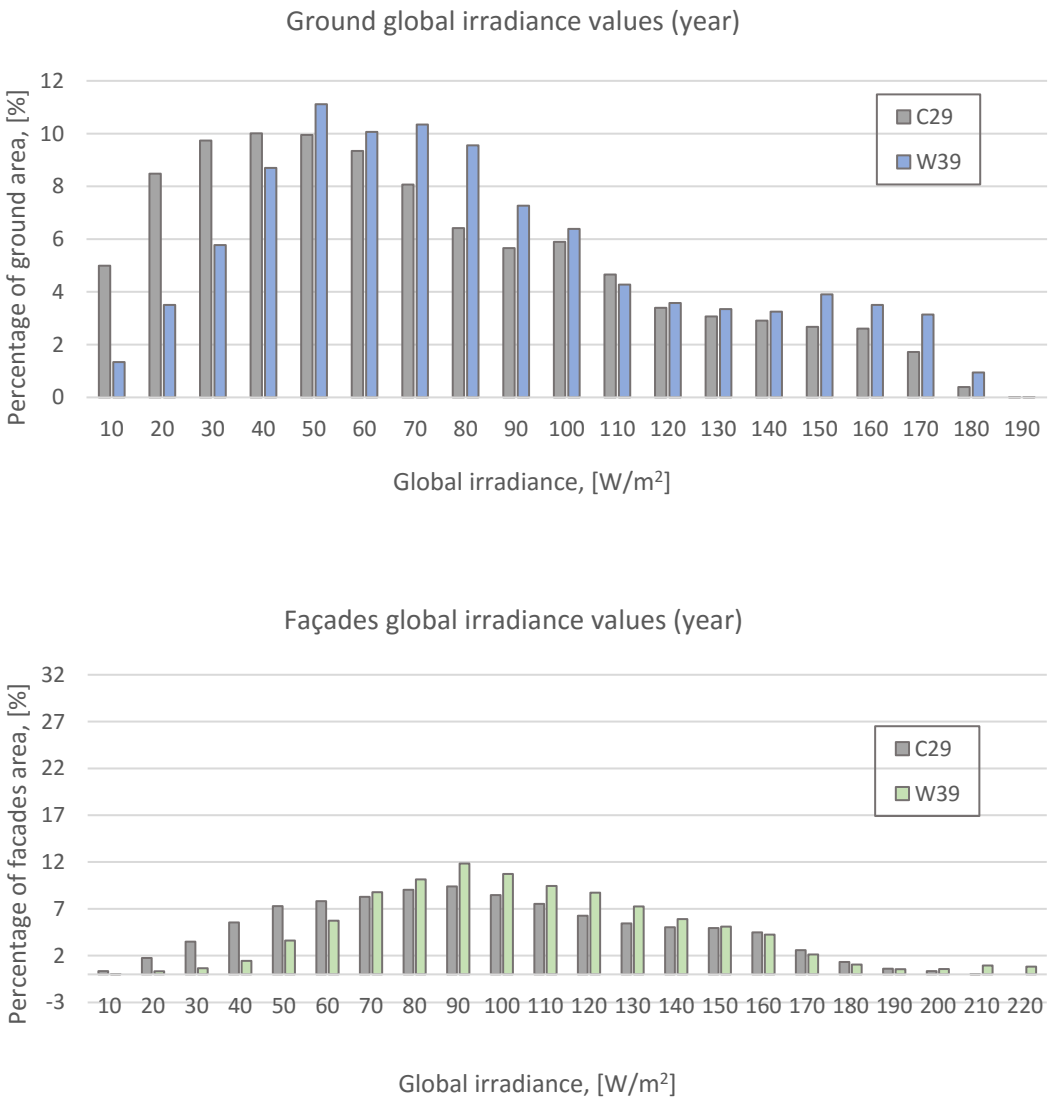

Figure 5.13: Comparison of distribution of irradiance values computed in C29 and W39, as percentage of total surface area: for façades (a), and ground (b).

Another pair of urban forms that exemplifies the effect of urban layout on urban solar availability is that of C29 and W39. Both are of medium density, 10.8 and 10.4 m^3/m^2 respectively, and their values regarding most of the urban layout descriptors are similar. Their difference lies in that W39, located in Westminster, features a geometrical order with the greatest part of it following an orthogonal street layout; while C29 located in the City of London has retained to a great degree the organic street layout of the old city. This is reflected to directionality which is higher by 86% in W39, as well as to complexity which is higher by 28% in C29 depicting a more undulating built form. As shown in the previous section, Dir and Cex are two of the most influential urban descriptors affecting solar availability both on ground

and façades, the former positively and the latter negatively. Hence, their influence justifies why W39 presents higher mean irradiance values in all three periods. Specifically, mean façades global irradiance in W39 is increased by 17%, 24% and 15%, and mean ground one by 12%, 12% and 11% in the year, January and July, respectively. The better performance of W39 is not limited to mean values, but it also appears in the histograms which denote that the percentages of its façades and ground (per surface area) presenting very low global irradiances are limited (Fig. 5.13).

5.4.3 Synergies and conflicts in urban solar design

Urban solar design usually purses multiple objectives which may significantly vary in time and space depending on climate and the intended use of solar radiation. The fulfillment of one objective may act synergistically for the fulfillment of another, facilitating the design decisions, or may conflict with others, creating difficult dilemmas. In temperate climate, such as this of London, a major conflict to be dealt with is related to different seasonal thermal needs: in general, opting for maximising thermal gains in winter and minimising them in summer. Additionally, at the urban scale, conflicts may also stem from the simultaneous consideration of objectives concerning open spaces and buildings. Such a case may arise, for instance, in summer, if photovoltaic systems are employed on building fabrics for generating energy -which requires the maximisation of solar availability all over the year-, while open spaces should be shaded to prevent heat stress.

This section explores to what extent urban layout could promote a more sensitive urban solar design by addressing mutually conflicting objectives. Specifically, it examines comparatively the solar performance of London's 24 urban forms in two ways: (i) comparing ground to façades irradiances, in three time periods, and (ii) comparing January (winter month) to July (summer month) irradiances, separately for ground and façades.

5.4.3.1 Ground irradiance versus façades irradiance

Does an urban form with higher mean façade irradiance have also higher mean ground irradiance compared to others? To answer this question, the investigation focuses on mean global and direct irradiances computed for London's urban forms, for which a statistical analysis was first performed. The relationship between 24 mean façade and ground global irradiance values was found to be almost perfectly linear. Despite that the differences among the three periods are small, it is worth noting that the relationship gets stronger in July and less strong in January (Fig. 5.14). Regarding direct irradiances on façades and ground, their linear relationship remains strong but with significantly lower R^2 values for the two months. Interestingly, the relationship appears stronger in the entire year, rather in July as found before for global irradiance.

Nonetheless, this strong linearity between ground's and façades' mean irradiance is dictated by their strong, negative linear relationship with density. Indeed, performing partial correlation analysis controlling the effect of density, the r coefficients obtained for mean ground and façade global irradiances demonstrate that their correlation is statistically significant but not as strong as the regression results showed before, 0.652 ($p<0.01$) in the entire year, 0.628 ($p<0.01$) in January and 0.498 ($p<0.05$) in July. Whereas, the correlations for mean direct irradiances are considerably lower and especially, this in January ($r=0.404$, $p=0.056$) and July (0.151, $p=0.492$).

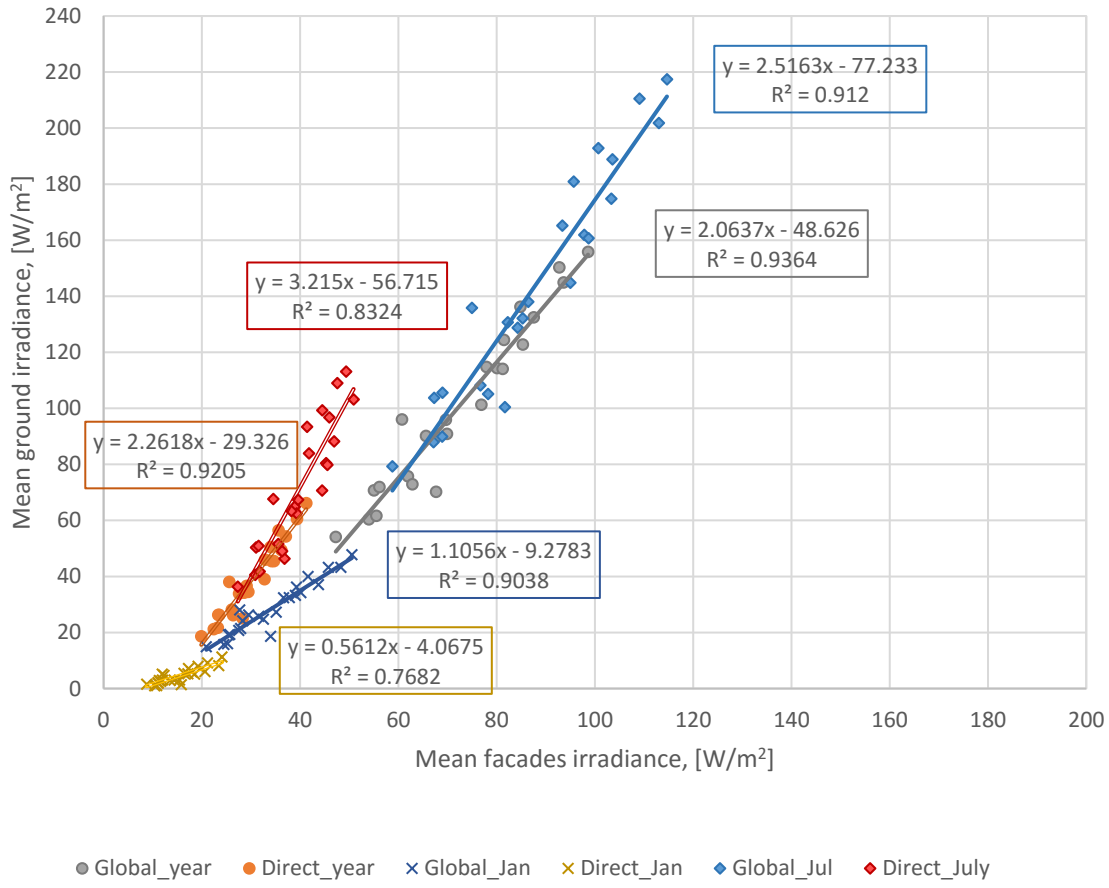

Figure 5.14: Mean facades irradiance against mean ground irradiance, global and direct, for three time periods, and their results of their linear regression analysis.

Next, urban forms which stand out of the general tendency, i.e. that higher ground irradiance means higher façade irradiance, were identified using a simple but effective method. The 24 urban forms were ranked twice, based on their mean façade and ground global irradiances in increasing order (i.e. first ranked the urban form with the lowest value and last that with the highest one). In this way, each urban form was assigned two values, one for their façades and another for their ground, which were next subtracted. If the relationship was perfectly linear, their scores -after the subtraction- would be equal to zero because all the urban forms would have achieved the same ranking both for their façades and ground.

Table 5.10. Ranking of 24 urban forms based on their mean global irradiance for façades and ground in an increasing order, i.e. 1 denoting lowest irradiance value, and their final score, highlighted in blue if ranked higher for facades, green if ranked higher for ground, and grey if neutral, for three time periods.

	Year			January			July		
	Facades	Ground	Score	Facades	Ground	Score	Facades	Ground	Score
C27	1	1	0	1	1	0	1	1	0
C35	3	5	-2	4	5	-1	3	5	-2
C19	2	2	0	2	2	0	2	2	0
C31	5	6	-1	5	6	-1	5	7	-2
C12	4	3	1	3	3	0	4	3	1
C10	10	4	6	13	4	9	9	4	5
C7	13	11	2	12	10	2	12	11	1
C22	6	13	-7	7	14	-7	6	12	-6
C16	7	8	-1	8	8	0	7	8	-1
C9	12	12	0	11	11	0	13	13	0
C6	8	7	1	6	7	-1	8	6	2
C2	11	9	2	10	12	-2	11	9	2
W20	15	17	-2	15	15	0	14	17	-3
C29	9	10	-1	9	9	0	10	10	0
W39	14	14	0	14	13	1	15	14	1
W27	16	16	0	16	16	0	17	16	1
W33	17	15	2	17	17	0	18	15	3
N37	18	19	-1	19	18	1	16	19	-3
W14	21	20	1	21	20	1	21	20	1
N20	20	18	2	18	19	-1	20	18	2
N55	19	21	-2	20	21	-1	19	21	-2
N1	22	23	-1	23	22	1	22	23	-1
N24	23	22	1	22	23	-1	23	22	1
N44	24	24	0	24	24	0	24	24	0

The procedure was repeated for all three time periods and ranking values and scores obtained are provided in Table 5.10. For a more effective presentation, the scores are highlighted in three colours: in grey if the value is zero, in blue if positive (meaning that the urban form was ranked higher regarding façades irradiance) and in green if negative (meaning that the urban form was ranked higher regarding ground irradiance). As seen, in all three time periods, the majority of the scores are different to zero. In most of the cases, the difference in their ranking order is no more than two units; however, there are two urban forms, C10 and C22, the scores of which stand out significantly. The positive score of C10 indicates that its façades receive on average more solar radiation than a greater number of urban forms compared to its ground, or otherwise, there are several urban forms, compared to which, C10 presents higher mean façades irradiance and lower ground irradiance. Reversely, the negative score of C22 indicates that there are urban forms, compared to which, it presents higher mean ground irradiance and lower façades irradiance. It is interesting that both urban forms score far from zero in all time periods.

Considering the urban layout descriptors' values for the two urban forms (see Appendix F), it becomes apparent that the outperformance of C10's façades and C22' s ground is related to specific aspects of their layout. As demonstrated in Table 5.6, the urban layout descriptors affecting mean ground global irradiance in all time periods -but not this of façades- are *site coverage* and *mean outdoor distance*, the former negatively and the latter positively. C22's MeD is equal to 9.4m -which the highest among all urban forms-, and its SCo is equal 49.8% - which is relatively low for its density-. On the other hand, the increased solar availability on the façades of C10 is related to its standard deviation of building height values which is the highest among all the urban forms, 26.3m. *Standard deviation of building height* and *complexity* are the two urban layout descriptors which affects façades global irradiance in all time periods. Unlike Cex though, StH is associated with façades' solar performance but not this of the ground.

5.4.3.2 January irradiance versus July irradiance

Does an urban form with higher mean January irradiance have also higher mean irradiance in July compared to others? This second question was examined separately for ground and façades, following a similar process as for the first question. First, the the relationship between mean global irradiances in January and July was found to be almost perfectly linear with R^2 being particularly high, 0.945 for façades and 0.983 for ground (Fig. 5.15). Regarding January and July direct irradiances, the R^2 values are reduced but still very high, 0.825 for façades and 0.878 for ground. It is thus observed that the relationship is weaker when considering the solar performance of façades; however, there is a great tendency for urban forms with higher irradiance values in January to present higher values in July too, and the reverse.

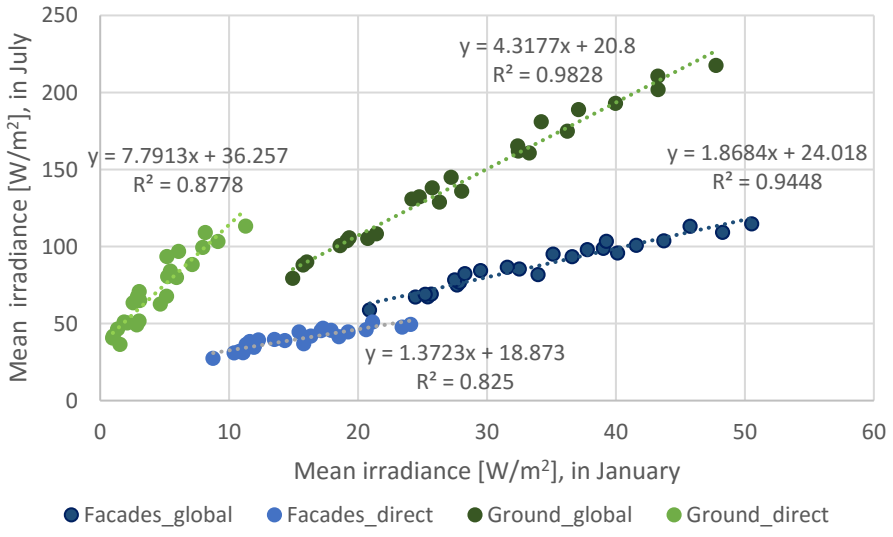

Figure 5.15: Linear regression models of mean global (a) and direct (b) irradiance values in January (x axis) and July (y axis) for façades and ground.

To identify exceptions of this general rule, which is forced by the density parameter, the relative seasonal performance of the 24 urban forms was examined based on the absolute ranking of their mean façade and ground global irradiance, in January and July. In January, their mean irradiance values were ranked positively, i.e. 1 was assigned to the urban form with the lowest mean irradiance value and 24 to the urban form with the highest value, reflecting the desirability of solar radiation in the winter. In contrast, in July, the urban forms' global irradiances were ranked negatively, i.e. 1 was assigned to the urban form with the highest mean irradiance and 24 to the urban form with the lowest one. Next, their seasonal scores were derived by adding their ranking values for January and July. If the relationship was perfectly linear, namely if urban forms with higher mean global irradiance in January presented also higher mean irradiance in July compared to others, then their seasonal score would be equal to 25, indicating a neutral seasonal performance. Rather, it is observed in Table 5.11 that this is the case only for few of them, both in relation to façades and ground. When the seasonal score is above 25, the seasonal performance is positive -highlighted in blue-; whereas, when it is below 25, the urban form presents a negative seasonal performance –highlighted in red-. Finally, their overall seasonal performance was derived by adding their façades' and ground' seasonal scores.

Table 5.11. Ranking of 24 urban forms based on their mean global irradiance in January positively, i.e. 24 denoting the urban forms with the highest irradiance, and in July negatively, i.e. 24 denoting the urban forms with the lowest irradiance, separately for façades and ground, and their seasonal score -the sum of ranking values- highlighted in blue if considered positive (>25), grey if neutral (=25), and red if negative (<25).

	Façades				Ground				Combined	
	January ranking	July ranking	Seasonal score	Seasonal ranking	January ranking	July ranking	Seasonal score	Seasonal ranking	Overall score	Overall ranking
C27	1	24	25	9	1	24	25	7	50	9
C35	4	22	26	3	5	20	25	7	51	5
C19	2	23	25	9	2	23	25	7	50	9
C31	5	20	25	9	6	18	24	17	49	15
C12	3	21	24	15	3	22	25	7	49	15
C10	13	16	29	1	4	21	25	7	54	1
C7	12	13	25	9	10	14	24	17	49	15
C22	7	19	26	3	14	13	27	2	53	2
C16	8	18	26	3	8	17	25	7	51	5
C9	11	12	23	22	11	12	23	23	46	24
C6	6	17	23	22	7	19	26	4	49	15
C2	10	14	24	15	12	16	28	1	52	3
W20	15	11	26	3	15	8	23	23	49	15
C29	9	15	24	15	9	15	24	17	48	22
W39	14	10	24	15	13	11	24	17	48	22
W27	16	8	24	15	16	9	25	7	49	15
W33	17	7	24	15	17	10	27	2	51	5
N37	19	9	28	2	18	6	24	17	52	3
W14	21	4	25	9	20	5	25	7	50	9
N20	18	5	23	22	19	7	26	4	49	15
N55	20	6	26	3	21	4	25	7	51	5
N1	23	3	26	3	22	2	24	17	50	9
N24	22	2	24	15	23	3	26	4	50	9
N44	24	1	25	9	24	1	25	7	50	9

By using this rather simple logic, it was possible to identify urban forms performing relatively better to others, namely urban forms which receive more solar radiation in the winter and less in the summer. With respect to façades' performance, the urban form which ranks first is C10. It achieves higher mean irradiance value in January and lower in July, compared to C7, C9, C2 and C29. Indicatively, comparing C10 to C29, the former is more densely built up by 50%; its façades receive on average more solar radiation in January by 15% and less in July by 3%. Its lower irradiance in the summer month is related to its greater density value as well as its lower *mean outdoor distance*, which was found to affect façades irradiance only in July. However, 3% difference is deemed small considering their density values, and it demonstrates that C10's urban layout counteracts the negative effect of density. Considering the research findings in Section 5.4.2.2.3, it can be argued that the increased solar availability on the façades of C10 is mostly related to its standard deviation of building height value, i.e. 26.3m, which is the highest one among all the urban forms. StH is found to affect

positively all mean façades irradiance values -direct, diffused and reflected-; but its effect in July is rather limited. In particular, its positive correlation with mean direct irradiance in this time period drops to 0.345 and thus it is no more significant. With respect to ground, C10 scores 25 presenting a 'neutral' seasonal performance. Its outstanding seasonal performance regarding the façades and it neutral one regarding the ground have as a result C10 to be ranked first when both parameters considered.

An example of an urban form whose ground seasonal performance stands out is C2. However, its better seasonal performance is related mostly to its July score which is higher (i.e. lower irradiance) than that of other forms of higher density. For instance, compared to C7, it has lower density by 31% and it is therefore reasonable that the mean global irradiance of its ground in January is higher by 6%. However, in July, its mean ground global irradiance is lower by 3% and its mean direct irradiance by 4%. Although the percentages are rather small, it is worth examining what makes C2 urban form's ground to be relatively more protected from solar radiation compared to C7, an urban form of much higher density. It is reminded that July is the only time period -among those considered- in which direct irradiance comprises the largest part of ground global irradiance. C2, even though its *site coverage* is slightly lower, presents 27% lower *mean outdoor distance* than C7, i.e. 6.2m compared to 8.5m. As shown in Table 5.7, MeD is the most significant variable for mean ground direct irradiance in July ($r=0.673$, $p<0.01$). On the other hand, the seasonal performance of C2's façades is negative which is related to their underperformance in January, mostly due to its rather uniform building height (i.e. its StH value is among the lowest ones).

Two more cases of urban forms can be highlighted regarding their seasonal performance: C22, as a positive example, and C9, as a negative example. C22 is the only urban form that presents a positive seasonal performance regarding both façades and ground, ranked as third and second, respectively. C9 scores the lowest value both for façades and ground, and it is ranked in the last place regarding the urban forms' overall seasonal performance. In both cases, its bad seasonal performance is the result of their extremely high mean irradiances in July. As discussed in Section 5.4.2.2.4, C9 exemplifies how urban layout can offset the negative effect of density. In particular, its increased vertical randomness, as appeared in its StH value, and its enhanced openness at the ground level, as expressed by its SCo and MeD values, allow more solar radiation to reach their façades and ground, compared to other forms of similar, or even lower, density. However, these three urban layout descriptors affect global irradiance both in January and July, and it seems that in the case of C9, their positive contribution in January is outbalanced by their negative effect in July.

5.4.4 Discussion

In previous parametric investigations on the topic, the importance of built density, usually expressed by plot ratio (total built floor area to site area), is equated methodologically to that of other urban geometry variables such as site coverage, building height, compactness, etc. (e.g. Martins et al., 2014; Nault et al., 2015). The present study distinguishes the density variable from those quantifying geometric characteristics of urban layout, and argues that this distinction is necessary when relationships between urban geometry and resulting solar performance are explored. The causal relationship between density and solar availability in the urban environment is straightforward: the more the built volume in a given site, the more the sun and sky obstruction, and thus the less solar radiation reaching ground and vertical surfaces. (Roofs may be unaffected under special circumstances, i.e. flat roofs and constant building height.) Nonetheless, as demonstrated by the research findings, the way in which this built volume is being configured in an area might amplify or conversely, offset density's effect.

Reflecting on the findings, there are several issues which have not been mentioned in previous sections and are worth being highlighted. Firstly, the correlation of *density* and solar availability, as concerns direct and diffused irradiance, was found to be higher in July compared to January. This provides further evidence for the finding emerged in Chapter Four, namely that solar angles affect the strength of the relationship, i.e. the relationship becomes weaker at lower solar altitude angles. Furthermore, the relationship between *density* and solar availability was found to be slightly weaker for ground compared to façades, which may be linked to the fact that the level of solar availability on ground is more dependent upon variations of urban layout (more urban layout descriptors affecting it, presenting stronger correlations). Secondly, mean irradiance values of ground and façades are generally affected by different urban layout descriptors; however, for those affecting them both, the sign of the effect is the same independently of the time period (positive or negative on both ground and façades irradiance values). Therefore, the particular descriptors act synergistically in maximising or minimising solar availability on ground and façades. The only exception is the effect of *compactness* and *number of building volumes* which was found to be positive on direct irradiance and negative on reflected irradiance. Thirdly, given that the relationship between urban geometry and solar availability varies depending on solar altitude angles, the location (i.e. latitude) of case studies used for exploring such relationships becomes significant and the comparison across different cities critical.

Based on irradiance findings for London's urban forms, it can be argued that *site coverage* is a key urban layout parameter for ground solar availability as it affects negatively both its diffuse and direct irradiation in all time periods. This is in partial agreement with a study for São Paulo, Brazil, in which variations of site coverage were found to affect both ground and façades solar performance (Cheng

et al., 2006a; 2006b). A potential association of site coverage with façades solar performance may be explained by the fact that lower site coverage can lead to higher mean distance between buildings, especially in generic urban models when open space is usually evenly distributed across the site. Indeed, *mean outdoor distance* was found to significantly affect the direct solar radiation incident on building façades over the year time and in July, which seems to confirm the results of another study for London (Sarralde et al., 2015).

Furthermore, the analysis provides evidence for the positive relationship of vertical randomness and façades' solar performance which has been studied before for cities in the tropics (Cheng et al., 2006b; Ng and Wong, 2004). Unlike vertical randomness, horizontal randomness was found to have a detrimental effect on solar availability. Increasing *directionality*, which is negatively associated to horizontal randomness, is found to be beneficial both for ground and façades solar availability; while increasing *standard deviation of building footprint*, positively related to horizontal randomness, affects negatively ground's exposure to direct radiation in two out of three time periods studied. It is pointed out that this is a first attempt to quantify the particular attribute of urban layout in existing urban areas; and therefore, the variables used need to be further tested, as well as others to be considered.

Complexity is found to affect negatively both façades and ground solar availability, with its influence being more significant for the former. In contrast, in the study of Martins et al. (2014) for a Brazilian city the relationship between solar irradiation and surface area of façades was positive which was linked to an increase in inter-reflections. At this point, it is also worth saying that the nature of the effect of complexity may totally change depending on which criterion is used for assessment i.e. whether it is the solar availability on façades (mean irradiance or irradiation) or solar potential per unit floor area (irradiation divided by total floor area). Increasing façades' surface area, while retaining total floor area constant, results in higher total irradiation of façades and, therefore, higher solar potential per unit floor area (e.g. Hii et al., 2011). Nonetheless, the consideration of potential usefulness of solar availability for buildings and in outdoor spaces is beyond the scope of this study.

Unlike *complexity*, *compactness* does not present any significant correlation with the availability of the major solar components, except with mean ground direct irradiance in January. In general, there is no sufficient evidence in the literature that the particular variable affects urban solar availability. On the other hand, as it is a measure that associates building surface area (i.e. building solar radiation receptor) to building volume (i.e. internal living space), compactness turns into a key geometric factor when solar availability is examined in relation to building energy needs (e.g. Nault et al., 2015; Ratti et al., 2005). Finally, distributing built density into more volumes was found to affect positively ground

and façades insolation in January. The number of built volumes variable is first introduced by the present study and thus, its relevance to solar availability needs to be further tested.

Overall, the study reveals the key role that urban layout plays in counteracting the negative effect of density and modifying the solar environment both in open spaces and on building façades, and in different seasons. The possibility of modifying solar availability in the built environment in space and time was exemplified by examining the layout of urban forms which did not to follow the general rule (i.e. higher solar availability means higher solar availability everywhere and always); and, it is of great importance that these urban forms are of medium-high density. With respect to seasonal performance, this implies that an adequate amount of built volume (i.e. density) is necessary for ensuring overshadowing in summer and, simultaneously, its carefully planned configuration within the site may limit direct radiation losses in winter. Nonetheless, the above argument is valid if assuming that cold and warm periods have the same weighting in terms of duration and harshness. Otherwise, the range of optimum density values may be adjusted to prioritise the major objective, either of maximizing or minimizing ground's and/or façades' solar exposure.

5.4.5 Statistical analysis and limitations

Moving on to issues arising from the statistical analysis, it is worth discussing the extremely high r-values obtained testing the correlation of density with mean solar irradiances (Table 5.5). These are attributed to the combined influence of factors related to the methodology. Firstly, it is important to underline that the negative impact of density on solar availability is certain. Undoubtfully, there are many other urban parameters affecting urban solar availability in real contexts such as vegetation, and reflectance of building materials. However, as discussed in Section 2.4.3, such parameters were deliberately not considered in the models used in the solar analysis, which focuses exclusively on the interaction of solar radiation with urban geometry. In this regard, given that the density value varies considerably in the studied sample, a statistically significant correlation of density with mean solar irradiance was anticipated.

More importantly though, the statistical results are highly related to the specific sample of 24 urban forms, which features a wide, continuous range of densities, with similar values being represented by no more than two forms. This is regarded to amplify the influence of the density variable, causing an almost perfect linearity with solar irradiances. The significance of the profile of density values in the sample was ascertained in the previous chapter comparing London and Paris. In Paris, where different densities are represented by more urban forms compared to London, the correlation between density and SVF, as well as density and insolation of open spaces, was weaker, highlighting the effect of layout. Nevertheless, the layout effect concerns mostly instantaneous insolation of open spaces, rather

average daytime one, leading to the conclusion that the length of time in which a solar indicator is considered matters. In this study, solar irradiances were computed for even longer time periods, i.e. entire year and months, meaning that the influence of the urban layout and orientation on average values is limited. In any case, it is explicitly acknowledged that the extremely high r-values are forced by the particularities of the sample of 24 urban forms used in Chapter Five, and do not represent reality. (The same applies for the r-values obtained by testing the specific urban forms for the sky models of Athens and Helsinki, in Section 5.6.1, presented in Tables 5.13 and 5.14).

Furthermore, the relationships between urban layout descriptors and indicators of solar availability have been investigated by performing partial correlation tests, controlling the density variable. This test was identified as a simple and effective way to cope with the strong interrelation of the urban layout descriptors with density. However, it is acknowledged that more research is required in order for the interdependence of the effects of urban geometry variables to be examined in depth. For instance, in the parametric study of Li et al. (2015) the effect of site coverage was found to decrease in increased site densities. The investigation of such speculations in real urban forms would require a greater sample and/or different methodological approach.

Finally, studying solar availability in real urban forms allows the investigation of aspects of urban solar availability associated to the complexity of actual built environments; however, it may entail some methodological restrictions. For instance, the fact that within London's urban forms building height is not constant does not allow the impact of increasing site coverage and increasing building height -i.e. the two ways of increasing density- to be investigated comparatively. As explained in Section 5.4.2, by averaging buildings' heights in an urban form, a crucial part of the height information is suppressed and, thus, the statistical results for the mean building height (MeH) variable was found to be governed by those of site coverage (SCo).

5.4.6 Introduction to the following sub-studies

As discussed previously, solar access in the built environment, directly related to solar availability, is the result of the urban geometry and its orientation in relation to the sun. The relationship between urban geometry and solar availability was found to be very strong which might indicate the effect of orientation is not that significant. However, acknowledging that the results may be forced by the wide range of density values in the 24 urban forms, the effect of orientation needs to be examined further. In Section 5.5, the amplitude of the orientation effect will be investigated in all three time periods, using the same urban forms, as this to be considered along with the impact of urban geometry.

Moreover, as implied by the findings themselves, the numeric results are to some extent sensitive to the location of the case study. Apart from the geographical latitude, London's weather file should also

be considered when referring to them. Since the relationship of urban geometry with global irradiance, expressing overall solar availability, is influenced by the percentage by which this is composed of the three solar components, the relevant results for London are related to the availability of direct and diffuse radiation in different periods (Table 5.3). Diffused radiation constitutes a great part of the total solar radiation available in London, all over the year and especially in the winter period, which influences the global irradiance results. A sunnier weather file would mean that solar availability is more subject to direct solar radiation's altitude and hence, more sensitive to solar altitudes. On the other hand, the effect of the intensity of solar radiation on numeric outcomes, i.e. correlations between urban geometry variables and direct, diffused and reflected irradiances, is regarded being rather limited. This is speculated by considering that solar intensity was found to be of limited significance examining the relationship between urban geometry (expressed by mean SVF) and average MRT in Chapter Four, and needs to be tested. To test the sensitivity of the results to other latitudes and weather files, the analysis was repeated for two new locations, Athens and Helsinki, and the results are presented and discussed in Section 5.6.

Finally, in Chapter Four, it was found that mean ground SVF can accurately estimate not only longwave radiation availability but also insolation of open spaces. Its relationship with daytime average insolation was stronger, compared to instantaneous one which was affected by solar altitudes. In Section 5.4.2.1, mean ground and façades SVF were found to correlate highly with *density,* but each with different urban layout descriptors. Mean ground SVF was found to be affected by *mean outdoor distance*, *site coverage*, *directionality* and *complexity*; which is in agreement with the respective findings for London's and Paris' urban forms in Chapter Four (see Section 4.4.2.1). Mean façades SVF is influenced by *standard deviation of building height*, *directionality* and *complexity*. Considering Table 5.8, it is of great interest that the urban layout descriptors affecting mean SVF are -to a great degree- the same with those found to be the most influential for annual mean direct irradiances. It can be thus argued that, over the longer period among those analysed, i.e. the whole year, solar exposure is affected by the same parameters affecting the openness of the urban form to the sky. This may be regarded as another evidence confirming that the longer the time period considered, the more accurately mean SVF can predict solar access. To investigate to what extent SVF can be used as indicator of solar availability, another study is conducted and presented in Section 5.7, using mean SVF and solar irradiances values computed for London's location in three time periods.

5.5 The effect of orientation on mean irradiances

Since the urban geometry variables considered in the study are all expressed by single numbers -as to be included in the statistical analysis-, they could not express any relevant information by azimuth. Consequently, the influence of the orientation of the urban forms on their solar availability is not reflected into the results. For this reason, it was deemed as necessary the orientation effect on mean irradiance values to be examined separately and quantified, in order for this to be acknowledged along with the effect of urban geometry.

Mean irradiance values were computed for façades and ground in the 24 urban forms rotating their models by 30° of azimuth from 0°, i.e. actual orientation, to 180°. It is noted that targeted analysis has shown that orientations symmetrical to the N-S axis present very similar results, which allows to consider only half the orientations. Thus, beyond the actual orientation of the urban forms, six more have been computed and studied; 30°, 60°, 90°, 120°, 150° and 180° azimuths. The analysis was repeated using all three sky models of London, as for the orientation effect to be examined separately for the entire year, January and July.

5.5.1 Effect of orientation on annual irradiances

Firstly, the orientation effect was tested considering the year sky model. Analysing the outcomes, it was revealed that the impact of orientation on mean irradiance values, both for façades and ground, is rather limited. Nonetheless, as may be expected, the differences due to varying orientations were greater for mean direct irradiances and almost marginal for diffused and reflected ones. The standard deviation of mean global, direct and diffused irradiances by urban form are presented in Figures 5.16, 5.17, and 5.18, respectively. For the sake of comparison, the scale of the y-axis is kept constant in all three. It is also noted that the standard deviation of mean reflected irradiances is of similar -or even lower- level to that of mean diffused irradiance.

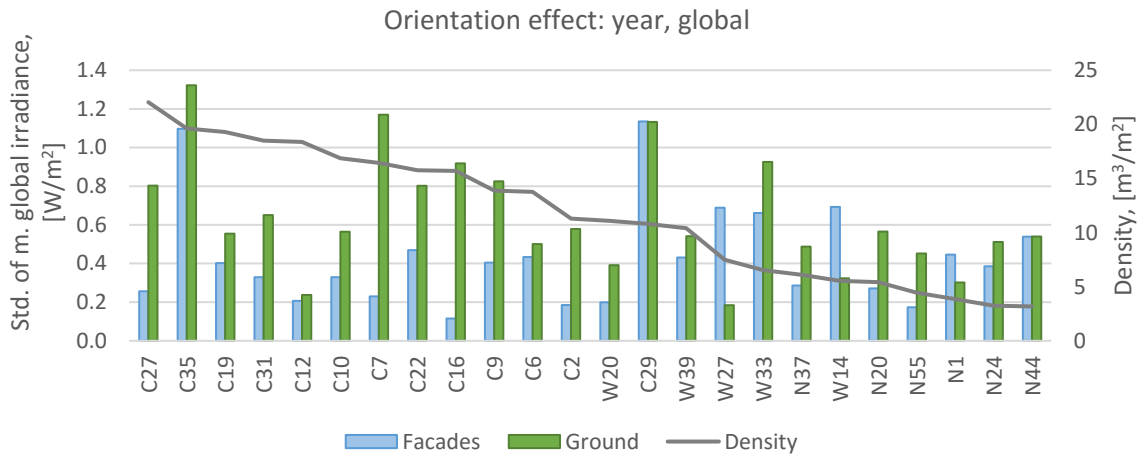

*Figure 5.16: Standard deviation of mean **global** irradiances for seven orientations computed for the year's sky model by urban form.*

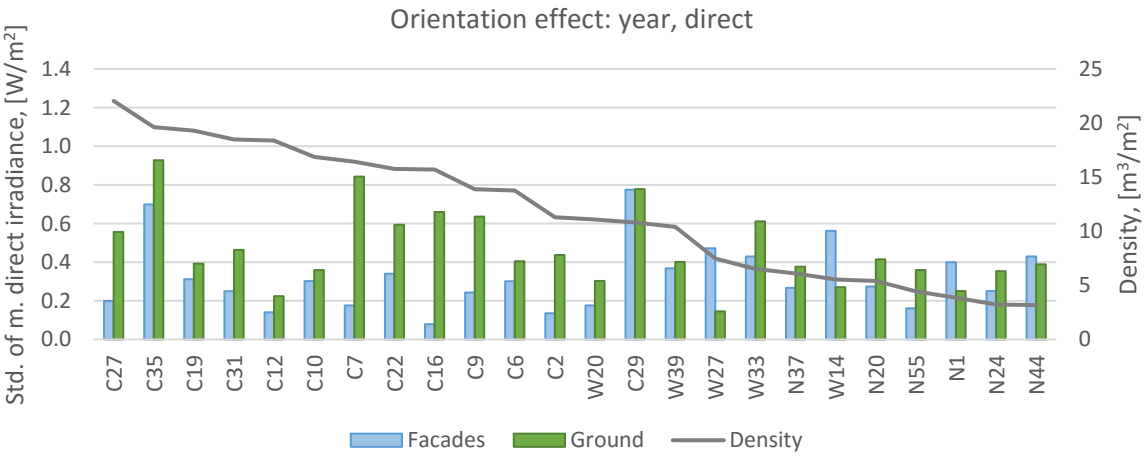

*Figure 5.17: Standard deviation of mean **direct** irradiances for seven orientations computed for the year's sky model by urban form.*

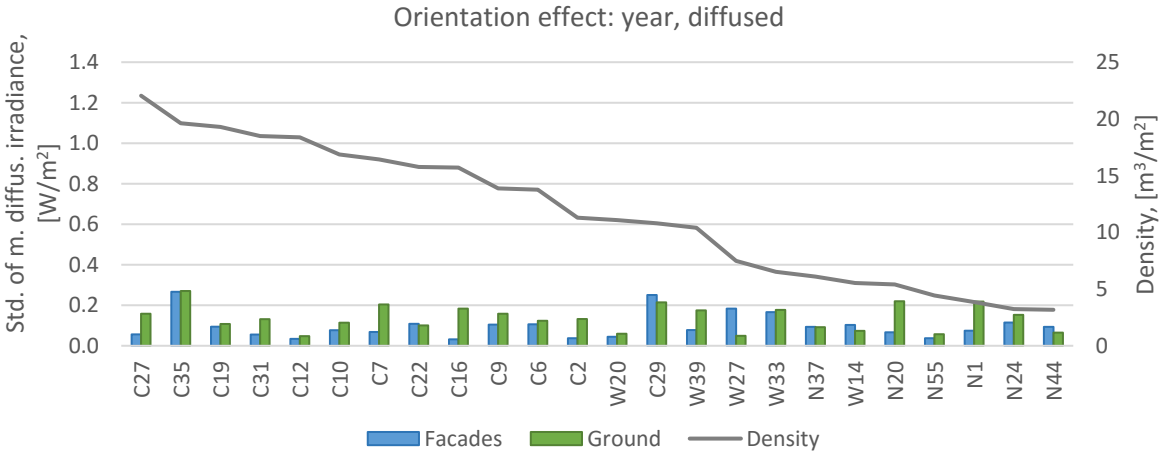

*Figure 5.18: Standard deviation of mean **diffused** irradiances for seven orientations computed for the year's sky model, by urban form.*

As observed, in most of the urban forms, the effect of the orientation is greater on the ground compared to the façades; however, there are several exceptions -all of which identified among the urban forms of lower density- which does not allow any generalization. For the seven orientations examined, the standard deviation of mean ground direct irradiance values is on average 0.5, varying from 0.2 to 0.9 [W/m^2] in different urban forms. The relative maximum difference among the values computed for each urban form is at a level of 1% to 10%. Regarding global irradiance, the standard deviation and relative maximum difference of mean ground values vary from 0.2 to 1.3 [W/m^2] and from 0% to 5%, respectively. With respect to façades, the standard deviation of mean direct irradiances is on average 0.3, varying between 0.1 and 0.8 [W/m^2], and the relative maximum difference is at a level of 1% to 8%. Regarding global irradiance, the respective ranges were 0.1 to 1.1 [W/m^2] and 1 to 5%.

Furthermore, the relationship between the magnitude of orientation effect, expressed by standard deviation of direct irradiances, and density of the urban forms was tested statistically. For façades, the relationship was found of non-significance; while, for ground, the correlation was positive and of medium significance (r=0.432, p=0.035), indicating that the higher the density of an urban form, the greater the orientation effect on annual direct radiation in its open spaces. Lastly, the same test was performed for nine urban layout descriptors and standard deviation of mean direct irradiances. Regarding the orientation effect on façades, none of the descriptors presented any significant correlation; whereas, *mean building height*, *complexity*, *compactness* and *number of building volumes* were found to influence the orientation effect on ground values. However, this was proved to be related to the strong interrelation of the descriptors with density.

5.5.2 Effect of orientation on January irradiances

The effect of orientation on January solar availability was next examined following the same process. With respect to absolute values, the effect of varying the orientation of the urban forms was found to be slightly higher compared to the entire year. The standard deviation of mean direct irradiances in different urban forms is on average 0.7 W/m^2 for ground, and 0.6 W/m^2 for façades, both varying between 0.2 and 1.2. Since the variations of mean diffused and reflected irradiances are significantly lower, the average standard deviation of mean global irradiance in different urban forms does not exceed 0.8 [W/m^2], both for ground and façades.

On the other hand, in terms of relative values, the effect is much more profound as January's mean irradiances are considerably lower than the annual ones. Regarding façades, the relative maximum difference of mean direct irradiances varies between 4% and 26%, and the respective difference for mean global irradiances between 2% and 15%. Regarding mean ground direct irradiances, which as

shown in Section 5.4.1 are extremely low, their relative maximum difference rises up to 150% in some urban forms. However, since the direct solar component comprises a very small percentage of ground global irradiance in January, the relative maximum difference for overall solar availability does not exceed 19%.

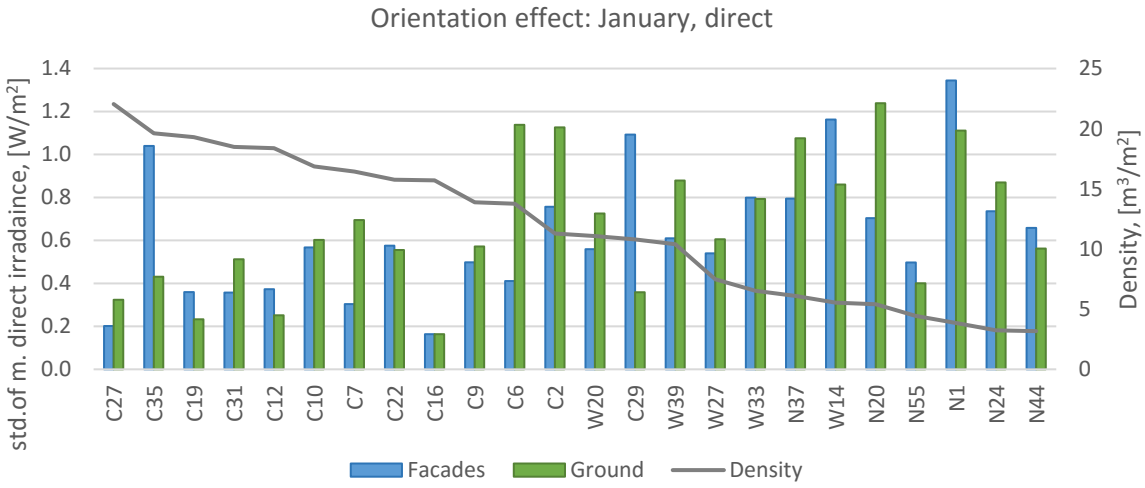

*Figure 5.19: Standard deviation of mean **direct** irradiances for seven orientations computed for January's sky model, and density by urban form.*

Figure 5.19 demonstrates the standard deviation of mean direct irradiance values computed for the 24 urban forms in January, plotted against their density. As seen, in some urban forms, the orientation effect is higher for ground and, in others, for façades. Moreover, higher standard deviations are observed for urban forms of lower density. Indeed, the correlation between density and standard deviation of mean direct irradiance was found statistically significant and negative, both for ground (r=-0.565, p=0.004) and façades (r= -0.551, p=0.005). Hence, the effect of varying urban forms' orientation on direct radiation received by ground and façades in January increases as density decreases. It is noteworthy that, in the previous section, the correlation was found to be significant only for ground's annual mean irradiances, and in that case, it was positive. Lastly, performing partial correlation test with control for density, the effect of orientation on ground direct irradiances was found to be affected positively by *standard deviation of building footprint* (r=0.509, p=0.013), and negatively by *number of building volumes* (r=-0.444, p=0.034). On the other hand, none of the descriptors presented significant correlation with the standard deviation of mean façades irradiance values.

5.5.3 Effect of orientation on July irradiances

Regarding the effect of orientation on solar availability in July, it appears that even though the absolute effect of orientation is slightly increased compared to the year and January, especially on

mean ground irradiances, it remains overall rather limited. The standard deviation of mean direct irradiances is on average 1.6 [W/m^2] - varying between 0.5 and 2.8 - for ground, and 0.8 [W/m^2] - varying between 0.2 and 2 - for façades. Considering mean global irradiances, the average standard deviation is of similar amplitude, i.e. 1.8 for ground and 0.9 for façades [W/m^2]. In terms of relative values, the effect of orientation is found to be reduced for ground -which is related to its increased solar irradiation in July compared to the other time periods- and, approximately of the same level as for annual mean irradiances, for façades. Indicatively, the relative maximum difference of mean direct irradiances computed for different urban forms varies between 1-6% for ground, and 2-11% for façades. Regarding mean global irradiances, the above percentages are reduced to half, i.e. 1-3% and 1-5%, respectively.

The bar graph in Figure 5.20 demonstrates the standard deviation of mean direct irradiances in July for the 24 urban forms, with the dark line indicating their density. Testing the relationship between density and the orientation effect in July, this was found to be negative and significantly strong for façades. Interestingly, the correlation was statistically significant both for standard deviation of mean direct and diffused irradiances, with the r values being -0.825 ($p<0.001$) and -0.491 ($p=0.015$) respectively. On the other hand, the correlation between density and ground solar availability is also negative, but not statistically significant. Finally, regarding the impact of urban layout descriptors, the only significant correlations were those between standard deviation of mean ground direct irradiance and *complexity* (r=-0.494, p=0.024), and *number of building volumes* (r=-0.454, p=0.042). It is reminded that NoB was also found to affect negatively the orientation effect on ground direct irradiance in January (see Section 5.5.2).

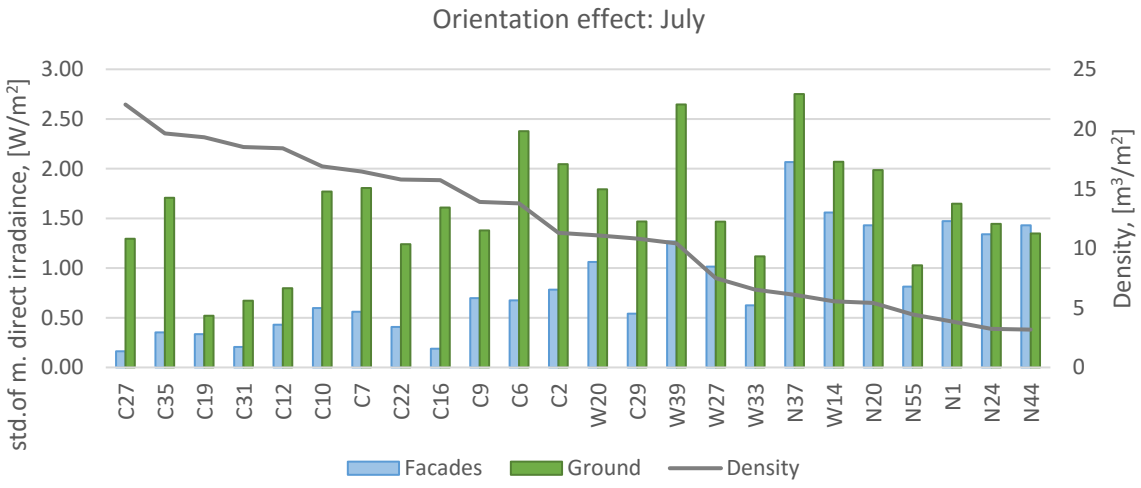

*Figure 5.20: Standard deviation of mean **direct** irradiances for seven orientations computed for July's sky model, and density by urban form.*

5.5.4 Discussion

The effect of orientation on solar availability has been studied extensively for more than half a century now, starting from the pioneering work of Knowles (1974; 1981) who studied the effect of orientation on building and urban forms' solar performance. On the urban scale, the significance of the orientation parameter for ground and façades solar availability has been ascertained by numerous researchers, either focusing on urban street canyons (e.g. Ali-Toudert and Mayer, 2006; Arnfield, 1990; van Esch et al., 2012), or strictly orthogonal layouts (e.g. Kristl and Krainer, 2001; Li et al., 2015). However, there are no studies examining the orientation effect considering real urban forms.

The findings of this study revealed that the orientation effect on 24 urban forms' solar irradiation is fairly limited. This does not mean to dispute that orientation is a parameter of major significance for the solar performance of built forms and open spaces; but it indicates that, zooming out to entire urban areas, its effect on the total solar irradiation of ground and the sum of façades may be reduced due to counterbalanced gains and losses. However, this counterbalance of gains and losses may be linked to the sample of urban forms studied, i.e. of non-orthogonal street layout. In most European cities, it is rather rare that entire urban areas are built by the repetition of a built unit, i.e. block, over a strict grid pattern with fixed orientation; which is the case though for many modern cities, such as American cities.

In an attempt to examine this parameter further, orientation roses were computed for each urban form as presented in Figure 5.21. Surprisingly, for most urban forms, even for some seemingly of irregular street layout, the graphs appear to be cross-shaped. It is noted that, in an urban form produced by the repetition of the same block aligned on a fixed orientation, the graph would be a net cross, symmetrical to two axes. One of the urban forms which seems to present a rather clear cross-shaped graph is N44. Looking at its ground map, it appears that the majority of the building volumes have regular footprints aligned to N-S/E-W axes. In contrast, in N24 - next to it-, there cannot be identified any major orientation, which is also confirmed by its rose graph. The two urban forms are of about the same density, i.e. 3.2 W/m^2, which makes them comparable regarding the amplitude of the orientation effect. Examining Figures 5.16 – 5.20, it is observed that the only case that N44 presents significantly higher standard deviation is in relation to annual mean façades irradiance, namely 0.43 versus 0.25 [W/m^2]. In all other cases, the standard variation values are either similar or higher for N24. Apparently, the comparison of two urban forms is very limited in scope to allow any conclusion about whether the compensation of direct radiation gains and loses occurs due to the irregularity of the 24 urban forms studied. However, if this was the only reason for the limited effect of orientation, the difference between N24 and N44 would be more profound than ascertained. In any

case, further research is required, including case studies of strictly orthogonal street layouts and of different densities, in order for the above argument to be tested and developed.

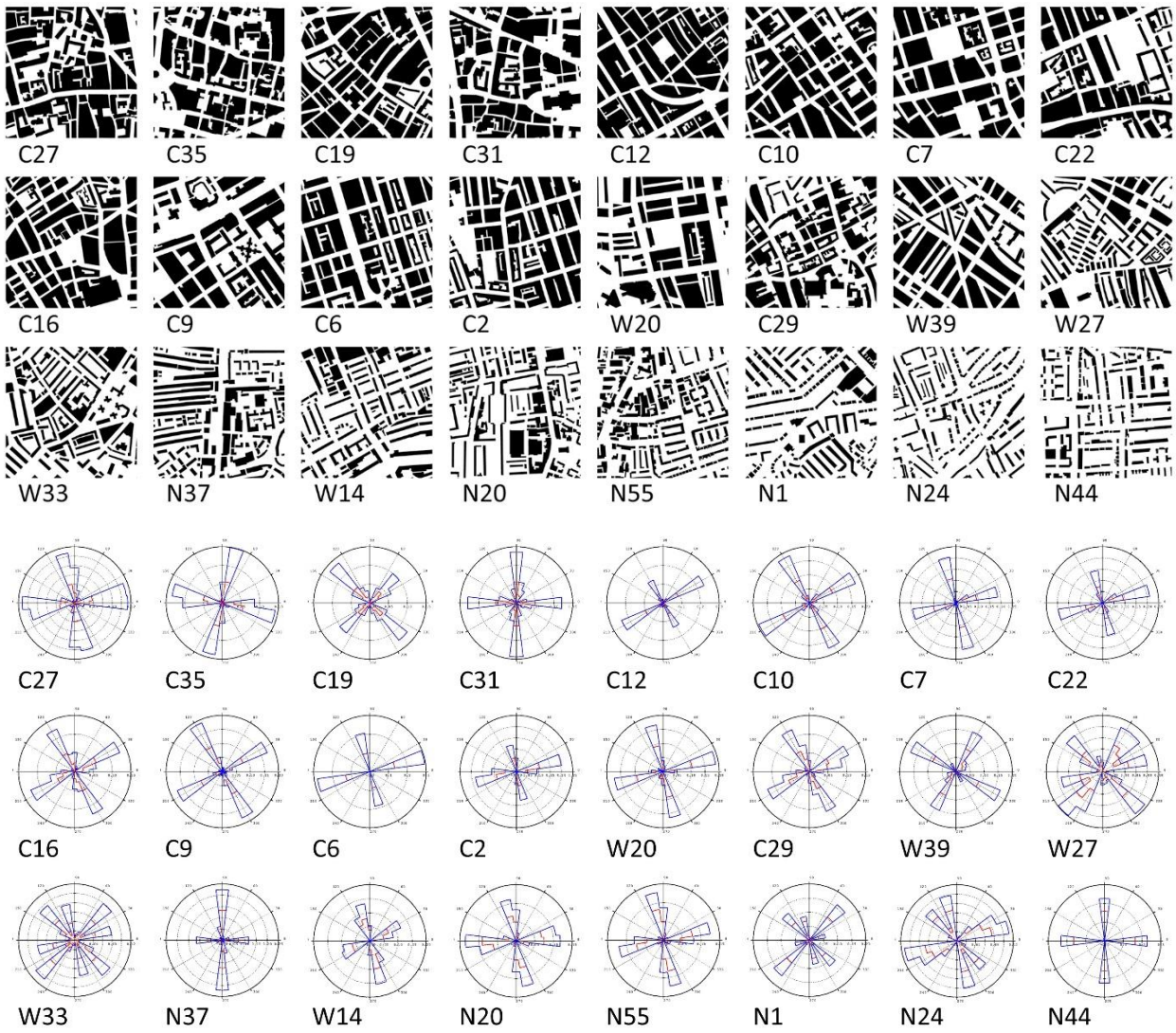

Figure 5.21: Below: Orientation roses depicting façades surface area by 30 orientations for 24 urban forms of London. Above: For comparison, their ground maps.

On the other hand, what appears to be relevant to the counterbalancing of gains and losses in direct radiation received by open spaces and building façades is the time period considered. Comparing the three time periods, the variance of mean direct irradiances due to varying orientations is smaller for the year, compared to the other two periods. This is related to the fact that the annual sky model presents a more even, average radiance distribution. In other words, in the year, the sun passes through much more positions in the sky vault, aggregating a wider range of solar altitudes and azimuths (see Figure 5.3). Consequently, the counterbalance of gains and losses is more effective compared to January and July when the sun path outlines a smaller area in the sky. This is linked to the discussion in Chapter Four, where the orientation effect was examined on instantaneous and

daytime average insolation of open spaces, suggesting that it is of much less significance for the latter. Combining the findings, it can be thus argued that the time period over which the orientation effect is examined affects its significance with it reducing over longer periods.

Another interesting finding is that the impact of the orientation parameter varies with density, in different ways, in different time periods. Over the year, the relationship was found to be significant only for ground and positive, i.e. the higher the density, the greater the impact of the orientation. In contrast, in January and July, the correlation shifts to negative. Specifically, in January, the correlation is of medium degree both for ground and façades; while, in July, the correlation is statistically significant, and particularly high, only for façades. The above imply an association between orientation effect, density and solar altitudes, as discussed in Chapter Four. For instance, an increased effect of orientation on urban forms of lower density is pointed out in Section 4.4.1.1, considering MRT variations in 72 urban forms of London on a sunny winter day.

Finally, regarding the relative effect of varying urban forms' orientation, i.e. difference as percentage of actual mean irradiance, this was found much higher in January because actual mean irradiances in the winter are significantly lower. Indicatively, altering the orientation of an urban form may increase its mean direct irradiance on the ground level by up to 150% and this of façades by 26%, which are interpreted into an increase in the overall solar availability by 19% and 15%, respectively. Considering that during the winter months, increasing solar availability is highly desirable, these percentages may be regarded as potential solar gains which could make a difference in urban forms' solar performance. On the other hand, the potential increase in July's mean global irradiance -related to unwelcome solar gains- does not exceed 3% for ground, and 5% for façades.

5.6 The effect of latitude and sky conditions

The relationship between urban geometry variables and mean irradiances was found to change with months. This is attributed to different sun paths, and especially different solar altitudes characterising them. Therefore, the so far findings may also be affected by geographical latitude of the location, and relevant only to London and locations of similar latitude. In order to examine their sensitivity to the latitude parameter, another study was conducted repeating the solar analysis of 24 urban forms in London using sky models of two other European cities, Athens and Helsinki. Athens (37°58'N 23°43'E) and Helsinki (60°10'N 24°56'E) are located south and north of London, respectively, with them covering a range of latitudes from about 38° to 60°.

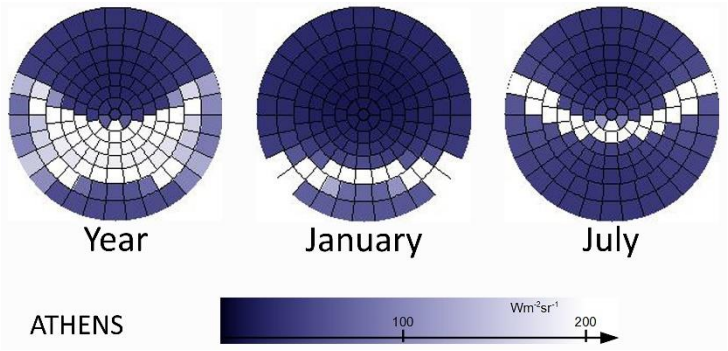

Figure 5.22: Stereographic views of the sky vault representing sky models generated for the year, January and July, and used in PPF simulations, for Athens' location.

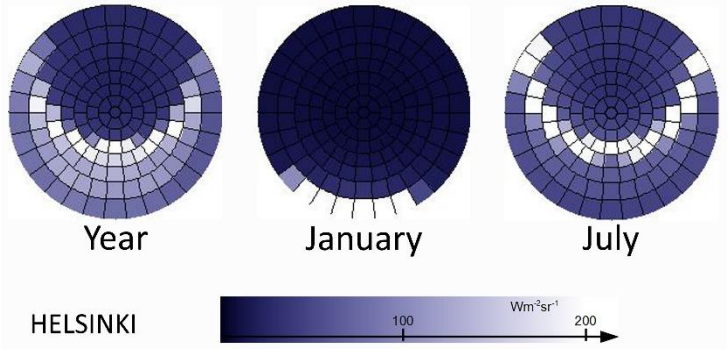

Figure 5.23: Stereographic views of the sky vault representing sky models generated for the year, January and July, and used in PPF simulations, for Helsinki's location.

For each of the new locations, three sky models were produced, as before for London, aggregating the weather data of the entire year, January and July (Fig. 5.22 and Fig. 5.23). As demonstrated in Table 5.12, beyond their latitude, Helsinki and especially Athens present also significant differences compared to London, in terms of solar availability and sky conditions (see Table 5.3). In Athens, direct radiation comprises the largest part of the available solar radiation in all three time periods, with mean direct horizontal values being particularly high. On the other hand, Helsinki's sky conditions are similar to those of London, especially the annual ones; however, mean January irradiances are even lower and the diffuse component is constantly greater than the direct one, even in the summer month.

Table 5.12. Daylight hours, mean direct and diffuse irradiance values in the three sky models for Athens and Helsinki.

	Year	January	July
Athens			
daylight hours, [h]	4397	288	464
mean direct horizontal irradiance, [W/m^2]	265	170	372
mean diffuse horizontal irradiance, [W/m^2]	139	90	139
Helsinki			
daylight hours, [h]	4215	182	534
mean direct horizontal irradiance, [W/m^2]	101	9	137
mean diffuse horizontal irradiance, [W/m^2]	120	32	167

Mean global, direct, diffused and reflected irradiances on ground and façades of the 24 urban forms were computed using Athens' and Helsinki's sky models. The computed values by urban form are provided graphically in Appendix G (Fig. G.1 -G.4), allowing the comparison of the percentages of direct, diffused and reflected irradiances in mean global irradiance by urban form, in different time periods. Regarding Athens, mean direct irradiance is noticeably higher than mean diffused one in all time periods, both for ground and façades. The only exception is the case of mean ground irradiances in the winter month, where the two components are in a fair balance. Because of the increased direct radiation availability in Athens, the reflected component is also found to be more important compared to London, i.e. 10-20% of global irradiance for façades, and 5-15% for ground. Not surprisingly, solar availability in Helsinki is rather limited compared to Athens, with diffuse radiation comprising its greatest percentage. Still, the direct solar component comprises a considerable part, except for January, and especially in the case of ground, that direct radiation constitutes only 10% of the total solar irradiance, in all urban forms.

The relationship of urban geometry variables, i.e. density and nine urban layout descriptors, with mean irradiances in Athens and Helsinki was examined statistically and the results are discussed comparatively to the respective results for London. It is noted that in the presentation and discussion, special emphasis is put on the relationship between urban geometry and mean direct irradiances, as this is the one which is mostly affected by different latitudes and solar altitudes.

5.6.1 Relationship of density and mean irradiances

The relationships between density and mean irradiance values computed for Athens and Helsinki are found to be significantly strong. Tables 5.13 and 5.14 present analytically the correlation coefficient (r) results, which are compared to Table 5.5 for London. As observed, the r values for mean diffused irradiance present marginal differences, with them being constantly about -0.950, independently to location and time period. This indicates that the relationship between density and sky diffuse radiation

received by surface area is not affected -at least remarkably- either by latitude (i.e. solar angles), or sky conditions (i.e. availability of diffuse radiation). With respect to mean direct irradiance, the correlation is significantly strong in all cases, but its strength varies considerably, especially between different time periods, rather between locations.

Firstly, regarding annual direct irradiances, even though the r values are significantly high, they appear to decrease with locations' latitude. Specifically, for Athens, London and Helsinki, the r for mean façades direct irradiance are -0.960, -0.958 and -0.945, while for mean ground direct irradiance they are -0.944, -0.941 and -0.926, respectively. Thus, the outcomes can be read in two ways: first, the relationship between density and mean annual irradiances becomes stronger for locations of lower latitude, but nevertheless its sensitivity to the latitude parameter is rather limited. Moreover, it is worth highlighting that the correlation is always stronger for façades compared to ground, which was first ascertained for London and is now confirmed for other locations.

With respect to the other time periods, in the case of London, it has been found that the strength of the correlation increased from January to July, both for ground and façades. The same pattern is also observed in the results of Athens and Helsinki and, moreover, the difference between January and July r values is found to increase with latitude, i.e. the higher the latitude, the greater the difference. Indicatively, the $|\Delta r|$ value between mean ground direct irradiance in January and July is 0.004 for Athens, 0.054 for London, and 0.18 for Helsinki.

The only case where the correlation with density appears stronger in July than in January is that of mean façades direct irradiance in Athens, with the r values being -0.892 and -0.928, respectively. Considering that, among the sky models used, Athens' one in July presents the highest solar altitudes, this exception seems to support the argument made in Chapter Four (see Section 4.5), that the correlation between density (as so mean SVF) and solar access increases with increasing solar altitude up to a degree, beyond which the strength of the relationship starts to drop. A similar finding is also reported later, in Section 5.7, where the issue will be discussed more thoroughly. Overall, it is pointed out that the sensitivity of the relationship between density and direct solar radiation availability to different latitudes is increased when considering specific months -especially in January- and relatively reduced as concerns the entire year.

Regarding the particularly high r values obtained, as discussed excessively in Section 5.4.5, they are related to the methodology followed and especially, the profile of density values in the sample of urban forms analysed.

Table 5.13. Athens: correlation coefficient values for density and mean irradiance values, for façades and ground, in three time periods.

Athens	Façades				Ground			
	Ig	**Id**	**Ib**	**Is**	**Ig**	**Id**	**Ib**	**Is**
Year	-0.960	-0.960	-0.956	-0.947	-0.948	-0.944	-0.947	-0.722
January	-0.935	-0.928	-0.947	-0.935	-0.943	-0.929	-0.946	-0.926
July	-0.950	-0.892	-0.958	-0.951	-0.941	-0.933	-0.946	-0.893

All significant at 0.001 level

Table 5.14. Helsinki: correlation coefficient values for density and mean irradiance values, for façades and ground, in three time periods.

Helsinki	Façades				Ground			
	Ig	**Id**	**Ib**	**Is**	**Ig**	**Id**	**Ib**	**Is**
Year	-0.945	-0.946	-0.947	-0.932	-0.935	-0.926	-0.935	-0.869
January	-0.894	-0.782	-0.946	-0.924	-0.951	-0.762	-0.949	-0.928
July	-0.961	-0.964	-0.958	-0.945	-0.948	-0.942	-0.947	-0.907

All significant at 0.001 level

5.6.2 Relationship of urban layout descriptors and mean irradiances

The relationships between nine urban layout descriptors and mean irradiances were next tested as to examine to what extent they alter in Athens and Helsinki. For this purpose, partial correlation tests were performed controlling the effect of density; the results are presented in the following sections, grouped by type of irradiance. The results for mean diffused irradiance are presented first, as the more predictable ones, and those for mean global irradiance last, as they constitute the combined results of the three solar components.

5.6.2.1 Diffused irradiance

Regarding the urban layout descriptors affecting mean diffuse irradiances the most, these are in general the same that correlate significantly with mean SVF, independently to location and time period. Comparing Table 5.15 and Table 5.16 for Athens and Helsinki, with Table 5.8 for London, it is seen that mean ground diffused irradiance is constantly affected by *site coverage*, *directionality*, *complexity* and *mean outdoor distance*, whereas, mean façades diffused irradiance by *standard deviation of building height*, *directionality* and *complexity*. There are also two variables which do not correlate -significantly- with mean SVF and are found to influence diffused irradiances; however, their effect changes with location or time period. *Mean outdoor distance* presents a significant correlation with mean façades diffused at all locations, in July. *Standard deviation of building footprint* affects

mean ground diffused in Athens in all time periods, in London in the year and July, and in Helsinki only in July.

*Table 5.15. Partial correlation analysis for urban layout descriptors and mean **sky diffused** irradiance, controlling for density variable, for Athens location.*

Athens	SCo	MeH	StH	StF	Dir	Cex	Com	NOB	MOD
Ground									
Year	**-0.671****	0.517*	0.175	**-0.434***	**0.478***	**-0.464***	0.180	0.298	**0.707****
January	**-0.690****	0.499*	0.158	**-0.416***	**0.485***	**-0.434***	0.249	0.337	**0.688****
July	**-0.637****	0.524*	0.176	**-0.430***	**0.484***	**-0.488***	0.109	0.247	**0.726****
Façades									
Year	-0.316	0.139	**0.574****	-0.198	**0.492***	**-0.581****	0.096	0.102	0.408
January	-0.355	0.129	**0.602****	-0.264	**0.460***	**-0.528****	0.158	0.209	0.355
July	-0.308	0.155	**0.572****	-0.150	**0.489***	**-0.590****	0.084	0.043	**0.431***

** Correlation is significant at the 0.01 level…….* Correlation is significant at the 0.05 level

*Table 5.16. Partial correlation analysis for urban layout descriptors and mean **sky diffused** irradiance, controlling for density variable, for Helsinki location.*

Helsinki	SCo	MeH	StH	StF	Dir	Cex	Com	NOB	MOD
Ground									
Year	**-0.543****	0.407*	0.103	-0.337	**0.458***	**-0.595****	0.087	0.231	**0.651****
January	**-0.678****	0.512*	0.150	-0.409	**0.498***	**-0.444***	0.219	0.305	**0.714****
July	**-0.668****	0.516*	0.169	**-0.433***	**0.477***	**-0.461***	0.183	0.298	**0.711****
Façades									
Year	-0.229	0.069	**0.495***	-0.140	**0.462***	**-0.671****	0.019	0.063	0.366
January	-0.328	0.105	**0.613****	-0.253	**0.438***	**-0.534****	0.148	0.195	0.336
July	-0.296	0.135	**0.567****	-0.166	**0.494***	**-0.590****	0.077	0.063	**0.414***

** Correlation is significant at the 0.01 level…….* Correlation is significant at the 0.05 level

Regarding the strengths of the correlations, they vary considerably among different locations but there is not any general pattern identified to describe them. In this way, the influence of some descriptors was found to be more significant in Athens, and the influence of others in London or Helsinki. Focusing on annual mean ground diffused irradiance for the three locations, it is observed that the effect of *site coverage* and *standard deviation of building footprint* decreases with increasing latitude, that of *complexity* increases with increasing latitude; whereas, *mean outdoor distance* and *directionality* present the highest r values with mean ground diffused irradiance in London. With respect to annual façades diffused irradiance, the effect of *directionality* was found to decrease with

increasing latitude, that of *complexity* to increase, and that of *standard deviation of building height* to be greater in London.

Similarly, other descriptors present higher correlations with mean diffused irradiance in January, and others in July. The results from the three locations agree regarding the impact of solar altitude which is much clearer when comparing the summer and winter months for the same city. As concerns diffuse solar availability on ground, the impact of *site coverage* (negative) and that of *directionality* (positive) is greater in January, thus for lower solar altitude angles; whereas, the impacts of *standard deviation of building footprint* and *complexity* (both negative) is greater in July, thus for higher solar altitude angles. Regarding the urban layout descriptors affecting mean façades diffused irradiance, only the impact of *standard deviation of building height* (positive) is found to be increased for lower solar altitudes, and all the others (i.e. *directionality* -positive-, *complexity* -negative-, and *mean outdoor distance* -positive-) are more influential for high altitudes. Interestingly, directionality which affects both ground and facades diffused, its impact on the former is more significant in January, whereas on the latter it is more significant in July.

Nonetheless, considering the overall results, it becomes apparent that the relationship between urban layout and availability of diffused radiation in open spaces and on building facades is fairly constant at the three locations. This is reasonable since their mean SVF, strongly related to received diffuse radiation, is constant independent of location.

5.6.2.2 Direct irradiance

With respect to the relationship of the urban layout descriptors with mean direct irradiances, the r values obtained for Athens and Helsinki are presented in Table 5.17 and Table 5.18, respectively, and compared to the respective table for London (see Table 5.7). As seen, the differences are more profound compared to diffused irradiance demonstrating that the availability of direct solar radiation is much more sensitive to solar altitudes. Nonetheless, this mostly refers to the results for specific months, rather than annual direct irradiances which are found to be affected -to a large degree- by the same descriptors as diffused irradiance, independently to location. This is attributed to the fact that the annual sky models feature a more even distribution of direct radiance, i.e. direct radiation comes from a wide section of the sky vault. In contrast, in January and July, direct radiation comes from a smaller section of the sky. Consequently, the impact of the solar altitude angle on the relationship between urban layout descriptors and mean direct irradiances is more prominent when comparing January and July results.

*Table 5.17. Partial correlation analysis for urban layout descriptors and mean **direct** irradiance, controlling for density variable, for Athens location.*

Athens	SCo	MeH	StH	StF	Dir	Cex	Com	NoB	MeD
Ground									
Year	**-0.681****	0.538**	0.146	**-0.467***	**0.485***	**-0.414***	0.186	0.316	**0.702****
January	**-0.694****	0.436*	0.066	-0.331	**0.455***	-0.273	**0.419***	0.390	**0.579****
July	**-0.618****	0.540**	0.104	**-0.463***	**0.465***	-0.370	0.089	0.259	**0.682****
Façades									
Year	-0.187	0.153	**0.464***	-0.085	**0.448***	**-0.576****	-0.055	-0.144	**0.444***
January	-0.386	0.115	**0.528****	-0.371	**0.420***	**-0.450***	0.204	0.350	0.279
July	0.099	0.058	0.158	0.247	0.111	-0.359	-0.194	**-0.465***	0.276

** Correlation is significant at the 0.01 level * Correlation is significant at the 0.05 level

*Table 5.18. Partial correlation analysis for urban layout descriptors and mean **direct** irradiance, controlling for density variable, for Helsinki location.*

Helsinki	SCo	MeH	StH	StF	Dir	Cex	Com	NoB	MeD
Ground									
Year	**-0.559****	0.371	0.082	-0.352	**0.457***	**-0.554****	0.161	0.312	**0.587****
January	**-0.433***	0.198	-0.017	-0.252	0.117	0.045	**0.442***	0.349	0.148
July	**-0.684****	0.506*	0.163	**-0.471***	**0.473***	**-0.424***	0.220	0.359	**0.664****
Façades									
Year	-0.243	0.104	**0.463***	-0.179	**0.457***	**-0.640****	0.007	0.052	0.370
January	-0.323	0.030	**0.774****	-0.389	0.257	-0.216	0.320	0.392	0.057
July	-0.193	0.191	**0.473***	-0.073	**0.478***	**-0.572****	-0.089	-0.195	**0.486***

** Correlation is significant at the 0.01 level * Correlation is significant at the 0.05 level

The effect of solar altitude on the relationship between urban layout descriptors and mean direct irradiance was next examined by plotting absolute values of correlation coefficients (|r|) -seen in Table 5.7, Table 5.17 and Table 5.18- for January and July, against average maximum solar altitude for the respective month, by location. The average maximum solar altitude was calculated by adding and averaging the maximum solar altitudes on the first and last day of the month, i.e. 1st and 31st of January and July. These are 9.68° and 50.42° in Helsinki, 18.31° and 59.07° in London and, 31.81° and 72.61° in Athens, in January and July, respectively. It is noted that these angles are used indicatively, representing the different ranges of solar altitudes occurring in each of the six cases, i.e. January-Helsinki, January-London, January-Athens, July-Helsinki, July-London and July-Athens (given in increasing order of average maximum solar altitude).

The lines in Figure 5.24 describe the strength of the correlation between each urban layout descriptors (all except mean building height) and mean ground direct irradiance varying with increasing average

maximum solar altitude. It is noticeable that they are all relative smooth and very different to each other. Examining the most influential descriptors, the negative effect of *site coverage* (SCo) on mean ground direct irradiance appears first to increase with solar altitude and then, to decrease gradually taking its maximum r value in January-Athens case. On the other hand, the line of *mean outdoor distance* (MeD) resembles with a logarithm curve, with its effect to increase significantly in the beginning -starting from very low r values- and then, start to stabilise higher than SCo. Regarding *directionality* (Dir), it presents a totally different line; except for January-Helsinki case in which the r value is very low, the effect of directionality seems to be almost unaffected. Last, the line of *complexity* (Cex) denotes that its significance increases until it takes its maximum value in the case July-Helsinki, after which begins to reduce gradually.

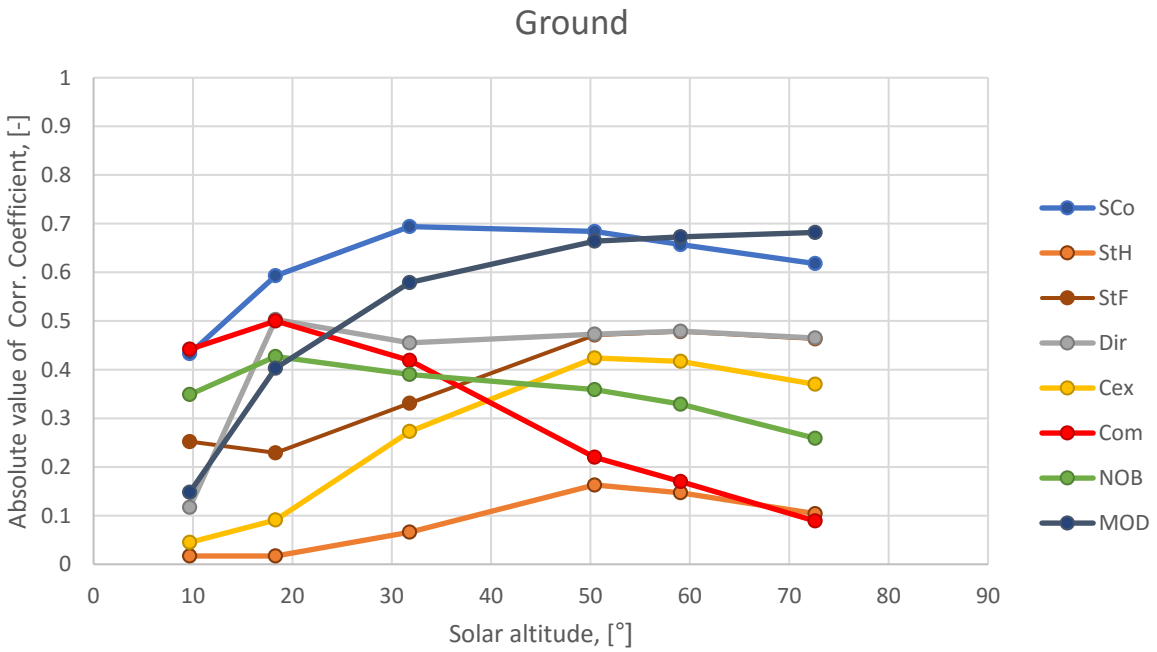

Figure 5.24: Strength of correlation (|r|) between urban layout descriptors and mean ground direct irradiances plotted against average maximum solar altitude angle for month and location they occur.

Plotting the r values for mean façades direct irradiance, the pattern of the lines describing the amplitude of the effect of urban layout descriptors for different ranges of solar altitude is very different (Fig. 5.25). This implies that the principles underlying the relationship between urban layout and solar availability on façades and ground are diverse. Focusing on the most influential descriptors, the effect of *standard deviation of building height* (StH) decreases with solar altitude: it is maximised for the lowest average maximum solar altitude, i.e. January-Helsinki, and minimised for the highest one, i.e. July-Athens. *Complexity* (Cex) and *mean outdoor distance* (MeD) present very similar lines -almost parallel- with a peak recorded in July-Helsinki case. Regarding *directionality* (Dir), its effect on

mean façades direct irradiance is found to be more sensitive to different ranges of solar altitude angle, compared to its effect on direct radiation availability on ground. Like MeD and Cex, the value of r coefficient for Dir first increases to get its maximum in July-Helsinki case and, then starts to reduce. Finally, it is pointed that there are also descriptors, the effect of which first decreases and then increases, presenting prominent lowest r values. Among them, only num*ber of building volumes* (NOB) presents statistically significant correlations with mean façades direct irradiance, which occur in January-London and July-Athens cases.

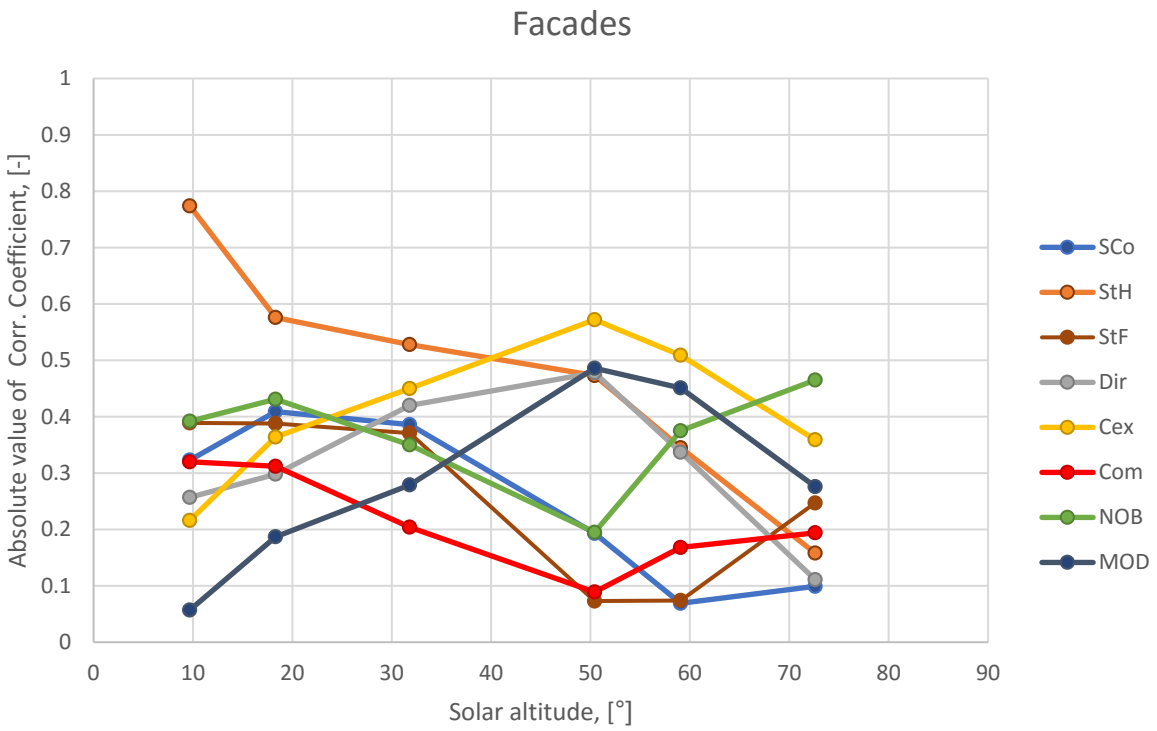

Figure 5.25: Strength of correlation (|r|) between urban layout descriptors and mean façades direct irradiances plotted against average maximum solar altitude angle for month and location they occur.

5.6.2.3 Reflected irradiance

Examining the correlations between nine urban layout descriptors and mean reflected irradiances for Athens and Helsinki, their sensitivity to different locations can be characterised as rather limited. (The results for the two locations are given in tables in Appendix G (Tables G.3 - G.4), while those for London are presented in Table 5.9). Especially, regarding mean ground reflected irradiance, the descriptors which affect it are the same for all the locations and time period. With respect to façades, there are some differences as, in January, mean reflected irradiances in Athens and Helsinki correlate with fewer descriptors compared to London. Among the three most influential descriptors, i.e. StH, Dir and Cex, only *standard deviation of building height* presents a statistically significant correlation for all the

locations and time periods considered. Interestingly, *site coverage* is found to correlate significantly with annual mean reflected in Athens, in a negative way.

5.6.2.4 Global irradiance

The r coefficients for urban layout descriptors and mean global irradiances are presented last, as they are the result of the combination of the respective values for mean direct, diffused and reflected irradiances and the percentage by which they comprise mean global irradiance. Comparing the tables for Athens and Helsinki (Appendix G, see Tables G.1 - G.2) with that for London (Table 5.6), it is observed that they present considerable similarities, especially with respect to the descriptors affecting annual global irradiances. This is related to that the annual direct irradiances were found to correlate to a large degree with the same descriptors, independently of location. Given that the sum of direct and diffused irradiances constitutes the greatest part of global irradiance, it can be argued that for locations within the range of latitudes of the case study locations, i.e. 38° to 60°, annual solar availability in open spaces is affected by *mean outdoor distance* and *directionality*, positively, and *site coverage* and *complexity*, negatively; whereas, annual solar availability on building façades is affected by *standard deviation of building height* and *directionality*, positively, and *complexity*, negatively.

The results regarding mean global irradiances in specific months are much more diverse, as the relationship between urban layout descriptors and mean direct irradiances were found to be less consistent among the different locations, in the respective periods. However, the differences are mostly related to the number of significant descriptors, rather that the significant descriptors differ among different locations. For instance, mean façades global irradiance in July, in Athens, is affected by only one descriptor, i.e. *complexity*, which is though among the four affecting it in London and Helsinki. Finally, it is noted that there are three urban layout descriptors which present strong correlation with global solar availability in open spaces, independently to location and time period, and these are *site coverage*, *directionality* and *mean outdoor distance*. Such a descriptor has not been found regarding solar availability on building façades. Hence, it can be argued that façades' solar performance is more sensitive to different ranges of solar altitudes, as expressed by the different locations examined.

5.6.3 Discussion

The sensitivity of London's results to the location parameter was examined testing the relationship of urban geometry and solar availability for two more European cities, Athens and Helsinki. Using the same urban forms allowed the study to focus on the impact of their sky models, as decided by their different geographical latitudes and climatic data. Not surprisingly, the location parameter was found to influence mostly the relationship between urban geometry and direct radiation received by ground

and building façades. So, the evaluation of the findings centred on the effect of latitude, namely different solar altitude ranges for the time periods considered, which is deemed as the major one differentiating the results for the three locations. The solar intensity in the three locations may affect -slightly thought- the strength of the relationships but its impact is not decisive. This is proven by particular findings which have not mentioned so far, and are worth being discussed.

Firstly, the numeric results, i.e. r-values, regarding annual mean irradiances differ more between London and Helsinki than between London and Athens, even though London and Helsinki present almost identical values of mean direct and diffuse horizontal irradiances over the year. Indicatively, annual direct solar availability in Athens, London and Helsinki is characterised by 265, 102 and 101 W/m^2 irradiances, and the r coefficients for density and mean façades direct irradiance were found to be -0.956, -0.958 and -0.947, and for mean ground direct irradiance -0.944, -0.941, and -0.926. Considering the absolute differences of the above values and the differences of three locations in latitude degrees, it becomes apparent that the effect of solar altitude on the relationship between density and direct solar availability is not constant. In contrast, it appears to increase from Helsinki to London, and reduce from London to Athens. This pattern resembles to that ascertained examining the relationship between mean ground SVF and insolation of open spaces in Chapter Four (see Section 4.5).

Secondly, the correlation between density and mean façades direct irradiance in Athens is weaker, in the year and in July, despite the increased direct solar availability compared to the other locations. This finding is of significance providing evidence for the argument discussed in Section 4.5 that the increasing correlation between density (and mean SVF) and urban solar availability as function of solar altitude presents a maximum point. In other words, it increases up to a “critical” solar altitude angle beyond which it starts to decrease. As discussed previously, the existence of a critical solar altitude angle is a reasonable inference considering that, for 90° solar altitude, the correlation between density and direct irradiance is null, and this applies both to ground and façades. Nevertheless, this critical angle is assumed to be unique for each urban form, affected by particular geometric characteristics, and different for ground and façades. It is intuitively assumed that its value is higher for ground compared to façades -which justifies why the relevant findings concern Athens’ façades and not ground-. In any case, the existence of such an angle, critical for the relationship of density with solar availability, needs to be explored further. A possible way could be testing the full range of possible solar altitude angles in the context of a more theoretical research approach.

Regarding the effect of solar altitude on the significance of urban layout descriptors for direct solar availability, this was found to be greatly diverse. As shown in Figure 5.24 and 5.25, there are identified

descriptors the significance of which increases with increasing solar altitude, others' decreases, or remains almost unaffected. Moreover, the significance of some seems to maximise or minimise for intermediate solar altitude ranges, resuming the discussion about critical angles. Although the findings refer to entire months -rather specific solar altitudes-, plus the cases used are only six (two months by three locations), they underline two major arguments developed in this chapter. First, the relationship between urban layout and solar availability is ruled by different principles than that between density and solar availability. Second, the solar performance of open spaces and building façades is affected by different urban layout parameters, in different months.

Finally, before moving to the next study on the relationship of mean SVF with mean irradiances, it is important to point out that annual direct irradiances were found to be influenced by the same descriptors, independently to location. Given that these descriptors are the same affecting mean SVF, as well as mean diffused irradiance, it is emerged that the relationship between urban layout and annual solar availability is independent of locations/latitudes. Furthermore, considering that the relevant findings for density are similar, it can be overall argued that the relationship between urban geometry and annual solar availability is not subject to important changes altering the case study location. The differences are noticeable when examining the correlations in specific months, and especially the correlations referring to direct solar availability.

5.7 Mean SVF and solar availability

In this chapter, mean SVF has been found to correlate strongly with density, and be affected by specific urban layout descriptors. These descriptors are also the most influential ones for mean diffused irradiances and mean direct irradiances, particularly the annual ones. Following on from Chapter Four, where mean ground SVF was tested as indicator of solar access in open spaces, a statistical study was carried out examining to what extent mean SVF (mSVF) can predict mean irradiances on ground and façades, in different time periods. For this purpose, mean irradiances computed for London's sky models were used and their relationships with mSVF were tested performing correlation and linear regression analysis. Based on linear models obtained, formulas and graphical tools are provided for estimating annual global irradiance in London, as a function of SVF.

5.7.1 Correlation of mean SVF and mean irradiances

The statistical analysis revealed a strong linearity between mSVF and all mean irradiances, in all time periods considered, both for façades and ground. The Pearson Correlation results are given analytically in Table 5.19 and, as shown, all r values are higher than 0.9, with only exception those for mean ground reflected irradiance in the year and July. Hence, it is not only mean diffused irradiances that correlate strongly with mSVF but also mean direct irradiances, which justifies the strong

correlation of mSVF with mean global irradiances. Furthermore, regarding global, direct and diffused irradiances, the relationship appears to be stronger for annual values and less strong in January.

As discussed previously in Section 5.4.5, although the strong effect of SVF (and density) on solar availability is certain, the particularly high r values are related the methodology and methods used, and especially caused by the profile of density values in the sample of 24 urban forms analysed.

Table 5.19. Correlation coefficients from Pearson Correlation testing mean SVF and mean irradiance values, for façades and ground, in three time periods.

	Façades				Ground			
	Ig	**Id**	**Ib**	**Is**	**Ig**	**Id**	**Ib**	**Is**
Year	0.999	0.997	1.000	0.995	1.000	0.998	1.000	0.834
January	0.985	0.966	0.997	0.988	0.994	0.941	0.999	0.938
July	0.996	0.977	1.000	0.995	0.999	0.997	1.000	0.803

All significant at 0.001 level

Comparing Table 5.19 with Table 5.5 which demonstrates the respective r values testing density and mean irradiance values, it appears that mSVF achieves stronger correlations in all cases. Even though the difference is very small, as the r coefficients for density are already very high, the above finding indicates that mSVF integrate more urban geometry information and thus, can predict better solar availability. The superiority of mSVF over density as predictor of solar quantities has been also ascertained in Chapter Four, investigating the radiant environment in open spaces.

5.7.2 Mean façades SVF and irradiance values by orientation

The correlation between mSVF and mean irradiances was found particularly high, independently to type of irradiance and time period. Nonetheless, solar availability on building façades and, especially, the direct solar component is strongly affected by their orientation to the sun path. Thus, the averaging of solar availability indicators' values for the whole urban form may suppress significant variations occurring at different orientations. For this reason, the relationship between mean façades SVF and irradiances was next examined considering 30 orientations at 12-degree intervals, which coincide with the patches into which the round perimeter of PPF sky models is divided. The numbering of the orientations starts from North (Orientation 1: -6 ≤ azimuth < 6) and counts clockwise.

Mean SVF and irradiances were computed for all 30 orientations in each urban form; the pairs of mean SVF and irradiance values by orientation were next grouped together. The process was repeated separately for each time period. In total, 120 regression analysis tests, i.e. 30 orientations by four irradiance components, were carried out for each time period considered, thus, 360 in total. It is noted that some urban forms were found not featuring façades facing specific orientations, which means

that, in some cases, the sample on which the regression analysis was based included less than 24 cases, i.e. urban forms. However, for each orientation, the sample used included at least 21 urban forms.

5.7.2.1 Year

The R^2 values obtained for façades mSVF and mean annual irradiances are presented graphically in a polar chart in Figure 5.26a. Not surprisingly, the relationship between SVF and sky diffuse irradiance is found to be perfectly linear for all orientations. Regarding direct irradiance though, the relationship is clearly affected by orientation and related to the azimuth range of the annual sun path in London. It is considerably strong (R^2>0.8) for orientations corresponding to azimuths between 60° and 300° (from East to West); while for the rest nearing North, the R^2 values are reduced and vary significantly. In contrast, the relationship between SVF and reflected by buildings irradiance appears to be independent to orientation as the R^2 fluctuates unevenly around different orientations. Finally, regarding global irradiance, it is of great interest that the R^2 value is constantly above 0.8. Given that global irradiance is calculated as the sum of three solar components, this is explained by that: (i) the reflected part consists a very small percentage of the total irradiance received by building façades, and (ii) the global irradiance of façades of azimuth out of the range of annual solar azimuths is dominated by the diffused one.

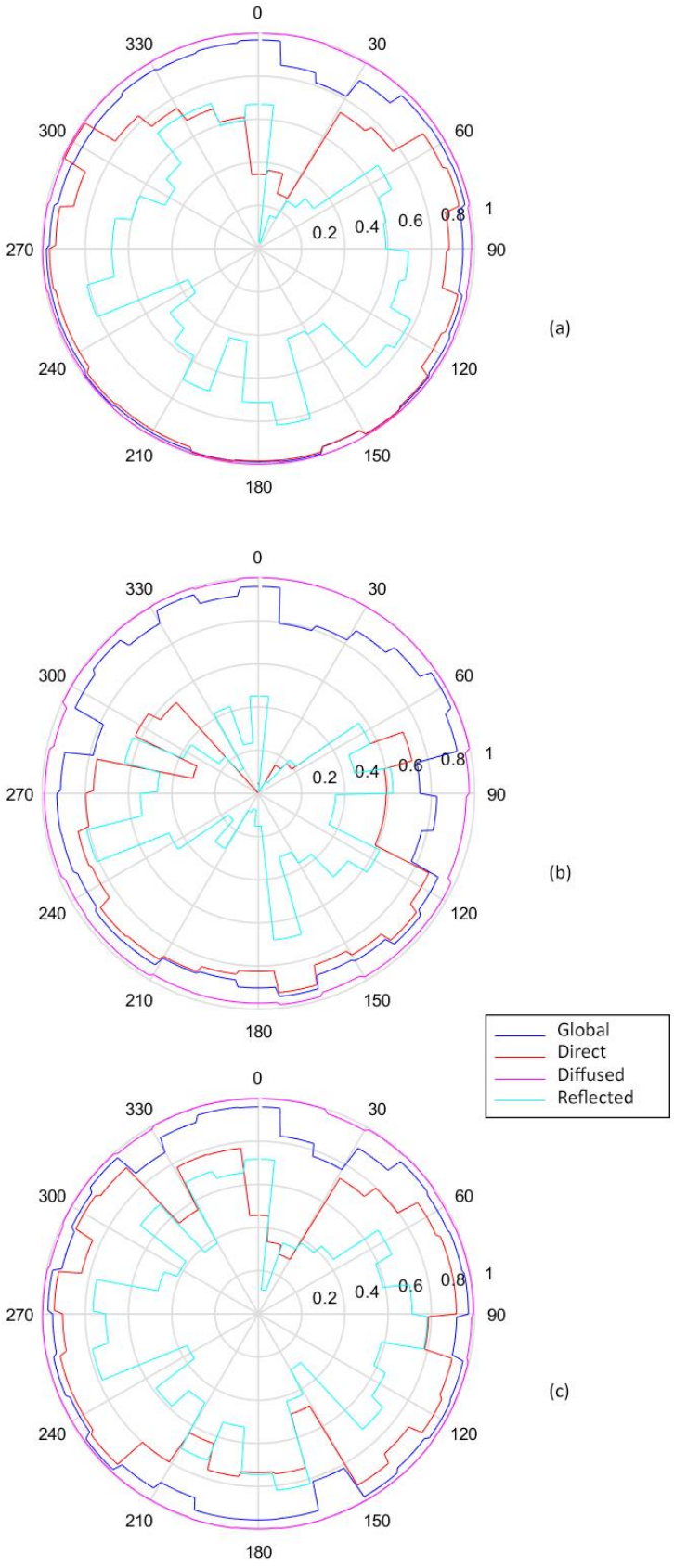

Figure 5.26: R^2 values describing the linear relationship of SVF and mean irradiance values, for 30 orientations, in the year (a), January (b) and July (c): global (blue); direct (red); diffuse (magenta); reflected (cyan).

5.7.2.2 January

Figure 5.26b demonstrates the R^2 values obtained for mean façades SVF and January mean irradiances for 30 orientations. Comparing it with Figure 5.26a, it is observed that the variations of R^2 with orientation for different type of irradiance present the same logic. The relationship of mean SVF with mean diffused is perfectly linear for all orientations, while the strength of the relationship between mean SVF and mean reflected fluctuates significantly and independently to orientation. On the other hand, the correlation of mean SVF and mean direct irradiance is found to strong for half of the orientations, those representing the southern part of the sky vault. Specifically, the relationship is significantly strong for azimuths approximately from 120° to 270°, with R^2 being close or above 0.8. In general, the non-absolute symmetry of R^2 to the N-S axis may be random, caused by the sample, or related to the availability of direct radiation coming from different directions. Nonetheless, the range of azimuths for which the relationship between mSVF and mean direct irradiance is statistically significant is related to the range of solar azimuths in January; for this reason, it is smaller compared to that for the entire year. Finally, regarding mean global irradiance, the R^2 values are above or close to 0.8, indicating a strong linear relationship, with only exception azimuths near 90°.

5.7.2.3 July

Regarding July, as shown Figure 5.26c, the patterns of relationships of mSVF with diffused and reflected irradiances remain the same as in the entire year and January. Regarding mean direct irradiance, the orientations for which the relationship is characterised by high R^2 are associated with July's sun path. Surprisingly though, the relationship is found to be stronger and more consistent for east and west orientations, rather than for south ones. Regarding south orientations, it is observed that R^2 values are reduced -below 0.8- which is attributed to that these solar azimuths in July correspond to significantly high solar altitudes. Specifically, when the sun exceeds a relative height in the sky vault, its beams -coming from above- can reach a great part of façades facing to it and thus, their obstruction by the surrounding buildings becomes less influential. This explains why mean SVF become less capable to predict their insolation. Furthermore, due to lower incident angles of direct radiation on façades facing south, their direct irradiance is reduced compared to east and west orientations. In this way, although the R^2 values for mean direct irradiance reduce below 0.8 for azimuths between 150° and 210°, the R^2 values for mean global irradiance remain significantly high. Overall, regarding mean global irradiance, it is observed that its relationship with mean SVF remains significantly strong independently to orientation, for the same reasons discussed before.

5.7.3 Predicting mean global irradiance for London

Predicting solar availability in urban environments using SVF values would be of relevance to researchers and professionals in the field of urban environmental design. As mSVF was found to perform extremely well as indicator of solar availability on building façades and in opens spaces, presenting an almost perfectly linear relationship with mean global irradiance, this section presents some graphical tools for the estimation of global irradiance as a function of SVF. They were all produced elaborating the annual global irradiance results and hence, refer to a typical year in London. For all linear models reproduced below the intercept is set to zero. This was found to affect slightly the coefficients of determination which remain significantly high. Figure 5.27 illustrates linear models estimating annual mean global irradiance in open spaces and building façades, for the entire range of possible SVF values, i.e. 0 to 1 for ground, and 0 to 0.5 for façades. In both cases, the R^2 value is above 0.990. Referring to mean façades and ground SVF of entire urban areas, these could be quickly estimated based on density values using the formulas provided in Figure 5.7 and Figure 5.8, respectively.

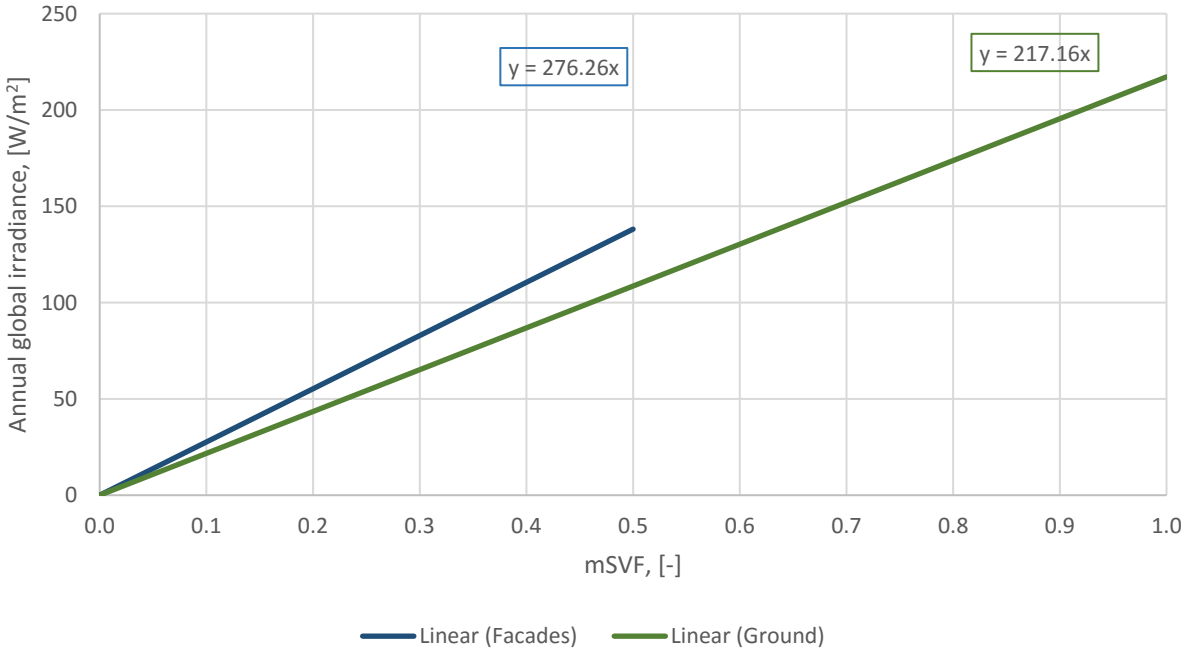

Figure 5.27: Graph describing the relationship between mSVF and annual mean global irradiance on façades and ground, for a typical year in London.

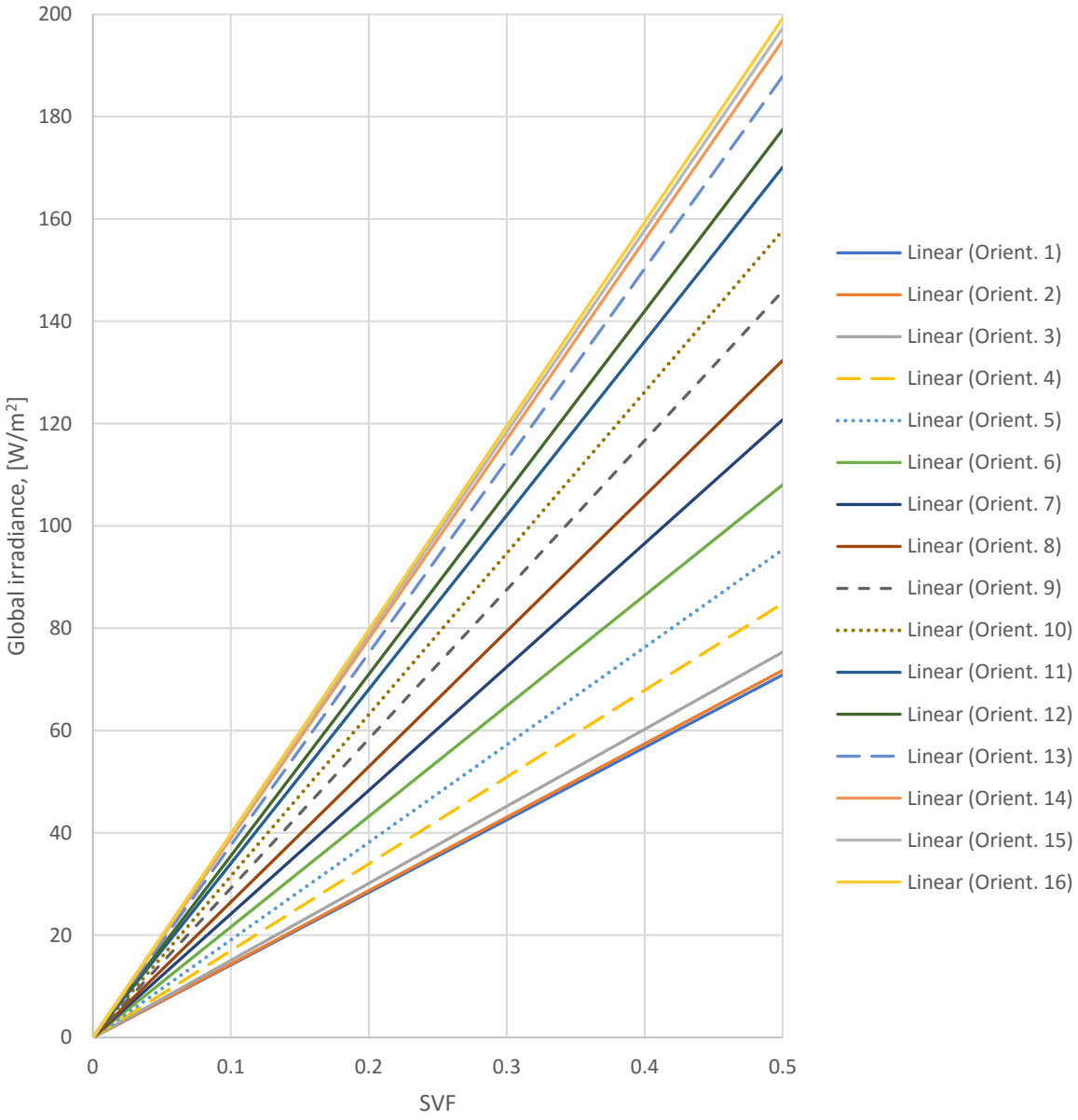

Figure 5.28: Lines predicting annual global irradiance in London based on SVF, for façade orientations from North (Orientation 1) to South (Orientation 16), clockwise, when intercept set to zero.

Similarly, Figure 5.28 demonstrates linear models predicting annual façades global irradiance by façade orientation. It is pointed out that the effect of mSVF on mean global irradiance, i.e. inclination of the lines, is almost identical for orientations symmetrical to the North-South axis. For this reason, the graph is limited to half orientations: North to South, clockwise. The numeric expressions of the linear models as well as the azimuth ranges to which each orientation corresponds are given analytically in a table in Appendix H. Lastly, Figure 5.29 demonstrates annual façades global irradiance as a function of façade azimuth, for five representative SVF values, i.e. 0.1, 0.2, 0.3, 0.4 and 0.5.

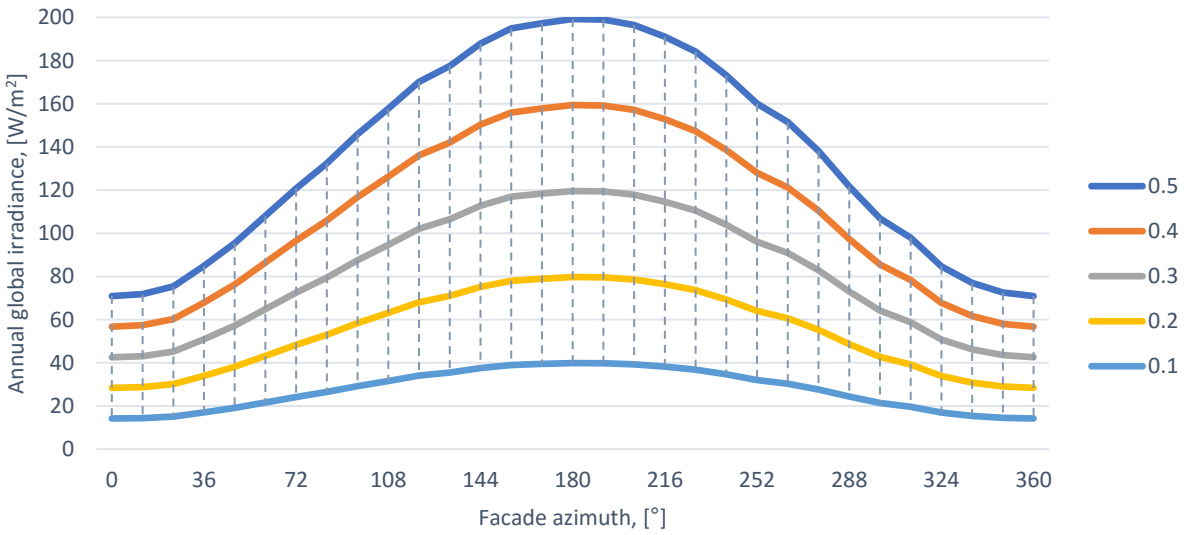

Figure 5.29: Lines representing annual global irradiance admitted by façades of SVF equal to 0.1, 0.2, 0.3, 0.4, and 0.5, as function of façade azimuth, for a typical year in London.

5.7.4 Discussion

Testing the relationship between mean SVF and mean irradiances, this was found to be linear and significantly strong, not only for diffused irradiance but for all solar components, and in all time periods examined. The above justifies the findings in Section 5.5 referring to the limited effect of orientation on urban forms' solar availability. Since mean façades and ground SVF are constant values - independent to orientation- and correlate so strong with mean irradiances, it is understandable why altering urban forms' orientation do not affect them significantly. Moreover, among the three periods considered, the orientation effect was found to be relatively reduced in the year and slightly increased in January, which is related to that the correlation of mSVF appears to be stronger considering annual irradiances, and less strong in January.

Furthermore, acknowledging the significance of façade orientation for their potential solar performance, the relationship between mean façades SVF and irradiances was tested for different orientations. The R^2 values obtained from the linear regression analysis revealed the different patterns describing the relationship of mSVF with each of three solar components (Fig. 5.26). The relationship of mSVF with mean diffused irradiance is almost perfectly linear, independently to orientation; whereas that with reflected one is rather random with the R^2 fluctuating unevenly around different orientations. On the other hand, the R^2 values for mean direct irradiance, even varying greatly, appear to be generally high for façade orientations coinciding within the ranges of solar azimuth in the respective period, i.e. façade orientations which admit an adequate amount of direct radiation. Overall, what is important is that mSVF was found to correlate strongly (R^2 above or close to 0.8) and thus, it can predict with a relative accuracy façades global irradiance for all facade azimuths, and in all

time periods. This is fully explained by the proportions in which façades global irradiance consists of the three solar radiation components in different cases, i.e. time period/orientation.

Regarding mean facades direct irradiance, its correlation with mSVF is also found to be affected by solar altitudes. In particular, it is noteworthy that, in July, mSVF can predict more accurately direct solar radiation received by east- and west-facing façades rather south-facing ones. Considering that in July, solar azimuths close to 180° coincide with the highest solar altitudes examined, indicatively 56-61° at noon, this confirms the existence of a critical solar altitude angle, above which the capability of built obstruction measurements, such as SVF and density, to estimate insolation of and direct radiation availability on building façades reduces. Previously, in Section 5.6.1, a similar finding was emerged examining the correlation of density with mean façades direct irradiance in July, in Athens. As suggested in Sections 4.5 and Section 5.6.3, reflecting on the geometric explanation of the existence of the critical angle, this must also occur for ground direct irradiance but, presumably, is higher than for façades.

Overall, building on the conclusions of Chapter Four (see Section 4.6), this study showed that mean SVF can be used for estimating levels of solar availability in open spaces and on building façades, on an annual basis as well as in specific months. Considering the findings of Section 5.6 -regarding the limited effect of location on the relationship between urban geometry and solar availability-, it is deemed that the correlation between mean SVF and solar availability is not supposed to be greatly affected by considering different locations. Nonetheless, this remains for the time being a speculation which needs to be studied.

5.8 Limitations

The studies comprising this chapter are all based on a sample of 24 urban forms, selected from the 72 urban forms in London initially analysed. A major selection criterion was to cover a wide, continuous range of density values found in the city, with similar values being represented by no more than two urban forms. This served the purposes of the studies allowing significant -qualitative- findings about the effect of density on urban solar availability to be revealed, e.g. its temporal and spatial characteristics, which may be otherwise suppressed.

At the same time though, this deliberate methodological decision cannot but affect the statistical results and more precisely, the strength of the correlations between density, SVF, and mean solar irradiances. The causal relations linking these parameters are known and intuitively perceived. Given that the solar analysis focused exclusively on the interaction of urban geometry with solar radiation, neglecting parameters such as vegetation and building materials, their correlation was expected to be

significant. However, it is acknowledged that their almost perfect linearity is strongly related to the analysed sample.

As ascertained in Chapter Four comparing London's and Paris' results, the profile of density values in the analysed sample of urban forms has a profound influence on the strength of the specific correlations. A wider range of densities tends to stress the density effect, and reversely. The sample of London's urban forms analysed in this chapter reflects the density values found in the city, excluding only some very high ones which were considered as extreme cases. However, it is not representative of the frequency in which different densities are found in London. As discussed in Section 2.3 and 2.3.2, high densities are found only in the central area of London, out of which they reduce gradually. Therefore, a representative sample should consist of a pyramid profile of density values, i.e. lower values being represented by more urban forms, which was not the case in the analysed sample. This could potentially affect the statistical results, if the density variable did not correlate so strongly with most of the urban layout descriptors in London, especially site coverage and building height. In Chapter Four, for instance, where the analysed sample of London's urban forms, 72 in total, features a more representative profile of density values, the correlations were found significantly high too. In other words, the effect of urban layout on solar availability when examining the impact of geometry in London is compensated by the fact that density increases equally in vertical and horizontal means, which is a very special characteristic of London. This was the reason that the effect of urban layout descriptors on solar irradiances was examined performing partial correlation with control for density.

To summarise, the particularly high r and R^2 characterising the relationships of density, SVF, and solar irradiances do not represent reality in the urban forms studied as crucial parameters affecting solar availability are neglected in the solar modelling. However, they are indicative of the increased significance of the density variable in London. In any case, due to the sensitivity of the statistical analysis to the sample analysed, it is important to acknowledge the influence of the wide range of density values included in it when referring to the statistical results of the research.

5.9 Conclusions

Chapter Five presents a thorough investigation on the causal relationships between urban geometry and solar availability on building façades and at the ground level, analyzing 24 urban forms in London and three time periods: the entire year, January and July. Beyond the main study, three smaller, targeted ones were conducted to explore the sensitivity of the results on specific parameters and to broaden the understanding about the subject matter. The conclusions of the main study are summarized in the followings:

- The strong negative effect of density on the solar irradiation of ground and façades can be modified to an important degree by urban layout, namely the way in which the given built density is distributed, horizontally and vertically, within an area. For instance, comparing a pair of urban forms of similar density but fairly different layout, ground and façades of the one was found to be receiving more global irradiation by 32% and 11%, respectively.
- Mean ground SVF and diffuse irradiance are significantly affected by *mean outdoor distance*, *site coverage*, *directionality*, and *complexity*; whilst for façades the strongest urban layout variables were *complexity*, *standard deviation of building height* and *directionality* (given in effect's decreasing order). Most of the above variables are also the most influential for annual mean direct irradiances on ground and building façades, respectively.
- However, urban layout descriptors affecting mean direct irradiance the most are found to be different in time periods considered, especially in January and July. This differentiation is attributed to the occurrence of different ranges of solar altitude angles which are, in general, lower in January and higher in July.
- Considering a temperate climate, such as London, the fact that the level of solar availability on urban surfaces is influenced by different urban layout descriptors in winter and summer presents the possibility of enhancing urban forms' seasonal solar performance.
- Finally, the seasonal effect on solar availability appears to be much more pronounced for ground rather than for building façades, with open spaces suffering from excessive overshadowing in the winter and prolonged solar exposure in the summer.

With respect to the following sub-studies, these contribute to the evaluation and utilization of the above conclusions by adding the following:

- The effect of urban forms' orientation on the solar availability in their open spaces and building façades is found to be limited, in terms of absolute values, in all time periods. Furthermore, among the three periods, its effect is further reduced on the annual mean irradiances.
- The location parameter affects basically the urban layout descriptors influencing direct solar irradiance in specific months, rather than in the entire year, which is attributed to distinct ranges of solar altitudes characterizing January and July in different latitudes. Thus, for locations within the range of the studied latitudes, i.e. 38° to 60°, annual solar availability in open spaces and on building façades is found to be affected by the same descriptors affecting mean ground and façades SVF, respectively (mentioned above).

- Mean ground and façades SVF can be used for evaluating mean direct and diffused irradiances and so, mean global irradiances, in London, in all time periods. Furthermore, mean façades SVF can predict at a significant level the overall solar availability on façades, as a function of façade azimuth.

5.9.1 Guidelines for London

The environmental, and thus solar design of our cities should apply to multiple principles formulated at a global, national and local level. In London Plan Chapter 5, *London's response to climate change*, these principles are hierarchised as follows: 1. Be lean: use less energy; 2. Be clean: supply energy efficiently; 3. Be green: use renewable energy. Furthermore, in Chapter 7, it is highlighted that "[…] *public and private open spaces, and the building that frame those spaces, should contribute to the highest standards of comfort* […]". Table 5.20 associates the findings of this chapter to different solar design goals for ground and façades by demonstrating which solar indicator and which sky model is relevant to each goal, when designing a masterplan in temperate climates, including London.

Table 5.20. Solar indicators and sky models relevant to different design goals applied to façades and ground.

Optimisation goals	Year sky model	January sky model (i.e. winter)	July sky model (i.e. summer)
Thermal comfort in open spaces		Mean ground global irradiance	Mean ground global irradiance
Passive solar gains through buildings' façades		Mean façades global irradiance	
Buildings' overheating limitation			Mean façades global irradiance
Active solar energy collection on buildings' façades	Mean façades global irradiance		

Red colour for indicators to be maximised

Blue colour for indicators to be minimised

The study adopts a particular perspective focusing on the thermal implications of solar radiation, i.e. thermal gains on building façades and heat in open spaces, the desirability of which differs from winter to summer. In this context, interpreting the research findings in design and planning guidelines for London would first suggest opting for developments of medium density as they present a greater potential for promoting mutually the different seasonal objectives. Since in such developments shading in summer would be partially ensured by overshadowing due to building volumes, designers should prioritise to enhance solar availability in winter. This could be achieved by breaking the given built volume into smaller blocks, which is beneficial both for façades and ground. The winter solar

performance of façades could be also enhanced by differentiating considerably the height of the buildings; while this of ground by increasing compactness parameter, i.e. surface-to-volume ratio. Site coverage and directionality of the development should be considered carefully, as they affect ground's solar availability both in winter and summer. Regarding summer solar protection, increasing the undulations of built forms and decreasing the distance between buildings could be an option; however, these may affect significantly the overall (annual) insolation of the development and thus, an optimum value should be sought. Finally, emphasis should be put on the solar design of open spaces as their insolation in winter and solar protection in summer are more difficult to be achieved.

In the case that the recommendations aim at increasing façades' solar potential for generating electricity or heating water, then they should focus on the urban layout descriptors found to be influential for mean façades irradiance values over the entire year. More specifically, the findings suggest that the differentiation of buildings' heights, avoidance of unnecessary undulations of façades and aligned buildings in site plan enhance the annual solar irradiation of facades. Moreover, the design should ensure long enough distances between buildings, for instance, by distributing evenly the open space across the site, as the specific parameter is related to annual direct solar availability on facades. Along with the above design recommendations, Section 5.7.3 provides formulas and graphical tools, based on linear regression models, which can be used by urban designers practising in London for the estimation of annual solar availability in open spaces and building façades.

Finally, urban design recommendations could be made also for Athens and Helsinki interpreting the results presented in Tables 5.15 - 5.18, as well as in Appendix G (Tables G.1 - G.4). With respect to annual -façade and ground- global irradiance, the urban layout descriptors affecting it are similar for all three cities; hence, what is recommended for London applies also to Athens and Helsinki. On the other hand, the January and July results are affected by the latitude of the city, and should be examined separately. Moreover, the climate in three cities changes considerably and may pose different priorities as concerns the solar thermal design, with the winter being the most uncomfortable thermally season in Helsinki and the summer in Athens.

Before moving on to Chapter Six, it is worth highlighting that conflicts caused by multiple objectives in urban solar design can be handled thanks to the fact that the aspects of urban layout affecting solar availability in open spaces and building façades, and at different solar altitudes, differ considerably. Looking for urban forms which differentiate from the broad tendency yielded by the density parameter, i.e. higher density leads to reduced solar availability both on the ground level and façades all over the year, and conversely, it was ascertained that these are of medium-high densities.

Weighting the different uses of solar radiation in terms of necessity and utility, and prioritising the relevant solar objectives, preferable densities may need to be adjusted higher or lower. However, it becomes evident that an adequate quantity of built volume is necessary since the resolution of any sun-related conflict is reached through a modification/moderation process, i.e. the density effect is deliberately modified/moderated by urban layout. Such arguments may fuel the discussion about the consideration of optimum built densities in urban settlements and provide environmental grounds for opting for a “moderate” densification. The next chapter explores the relevance of optimum densities for enhancing thermal diversity in open spaces, associated with their responsiveness, inclusiveness, attractiveness and thus, their increased and meaningful use.

Chapter Six

Thermal diversity in open spaces

Chapter Six presents a study which focuses again on the open spaces of the urban forms exploring the occurrence of spatial thermal diversity. The provision of thermal diversity in open spaces, namely a variety of microclimatic conditions over time and space, is deemed highly desirable as it can enhance humans' outdoor thermal experience and thus, the use of the urban space. Spatial thermal diversity is mapped in the open spaces of the urban forms based on combined availability of sun and wind, and using average shadow patterns on an equinox day and annual prevailing winds' data. Spatial thermal diversity is next quantified using a proposed formula, and its relationship with degree of urban built obstruction, expressed by *density* and *site coverage,* is examined.

6.1 Introduction

Open spaces are a vital part of the urban environment and it is widely acknowledged that they can contribute to the quality of urban life. In the Urban Task Force Report (1999, pp. 57), Lord Rogers highlights, "*public space* [be it a street, park or a square] *should be conceived of as an outdoor room with a neighbourhood, somewhere to relax, and enjoy the urban experience, a venue for a range of different activities, from outdoor eating to street entertainment; from sport and play venues to a venue for civic or political functions; and most importantly of all a place for walking and sitting-out*". In this context, a successful public space can be considered as that network of open spaces which accommodates or even encourages the full range of outdoor activities. Such activities may significantly promote individual and collective well-being of inhabitants contributing to more liveable and sustainable cities (Gehl, 1971; Nikolopoulou et al., 2001; Thompson, 2002).

An urban attribute that is identified as highly contributing to cities' livability and people's engagement with urban life is diversity – or variety – (Bentley et al., 1985; Jabareen, 2006; Jacobs, 1993) which can refer to all different aspects that constitute the city, such as land use, activities, architecture, etc. Bringing into the environmental perception as an essential dimension of the experience of urban space, urban diversity can also be perceived through our senses, i.e. vision, hearing, smell, etc., as well as thermal

sensation (Carmona et al., 2010). In this context, a diverse urban space is a more responsive, inclusive and more attractive space to be, to walk and interact in.

The occurrence of thermal diversity in open spaces, i.e. a variety of microclimatic conditions over space and time, is deemed especially desirable as it may enhance people's outdoor experience in multiple ways. Indeed, the microclimatic conditions in open spaces -by governing people's thermal experience- affect the duration and quality of their outdoor activities (Nikolopoulou and Lykoudis, 2007) as well as their intention to walk or cycle to their destination (de Montigny et al., 2012). However, research has shown that humans' thermal experience and preference, both indoors and outdoors, are to a great extent subjective as they are also influenced by psychological and cultural parameters (Nikolopoulou and Steemers, 2003). The acknowledgement of the human parameter in defining thermal comfort has yielded a significant shift to the design objectives. As Hawkes (1996, pp. 103) points out referring to the *new environment,* "*No longer is control within narrow, quantitatively defined limits seen as the goal, nor is absolute environmental uniformity throughout a space* […] *regarded as desirable*". Therefore, it is not a matter of providing an optimum and constant thermal environment but of allowing people to articulate their own environmental preferences by ensuring a wider range of microclimatic conditions through design (Steane and Steemers, 2004). This becomes even more imperative when designing open spaces as outdoor activities like sitting, walking, running, etc., involve diverse metabolic rates.

Additionally, 'perceived control' has been identified as one of the most significant psychological parameters determining outdoor thermal comfort (Nikolopoulou and Steemers, 2003). With respect to spatial thermal diversity, it can be interpreted as having options for adaptation, i.e. by choosing a different space to sit or a different route to one's destination it may increase people's thermal satisfaction, even if these options are not exploited. Finally, the experience of diverse microclimatic conditions by the users of open spaces may enrich their overall experience by raising their thermal consciousness. Referring to the three principles of Vitruvius for architectural design, i.e. commodity, firmness and delight, Steane and Steemers (2004) argue that the absence of discomfort in our living environment is a 'commodity' that might be recommended but yet eliminates any potential 'delight' that can be experienced by some degree of contrast and stimulus. Following up on this point, the experience of thermal stimuli may be integral to the accomplishment of a state of comfort, and to the outdoor experience itself which aspires to the delight of "naturalness", i.e. the experience of a naturally varying physical environment (Nikolopoulou, 2012).

For all the above reasons, the occurrence of thermal diversity within open spaces is regarded as a desirable feature of the urban environment and hence, an objective for urban designers. It is important however to

underline that this argument mostly applies to temperate climates and mild climatic conditions. In extreme conditions, the goals of environmental design are very specific and dictated by the necessity that such conditions stress. In other words, in very hot and cold climates, the significance of thermal diversity is undermined by the absolute need for mitigating the already severe thermal conditions.

The thermal environment that a body senses is the result of the combination of four environmental parameters, i.e. air temperature, relative humidity, mean radiant temperature and wind speed. Unlike air temperature and humidity, mean radiant temperature and wind speed may significantly vary within the open spaces of an urban form, even in very close proximity. This is because of the directional nature of solar radiation – related to mean radiant temperature – and wind, and so their interaction with the building geometry. The two parameters can be effectively controlled through design, namely by designing physical obstructions, that explains why environmental design is centered on solar and wind strategies for achieving desirable thermal environments.

6.2 Previous work and objectives

The combined availability of sun and wind results in four possible microclimatic conditions: sunny-windy, shaded-lee, sunny-lee, and shaded-windy. The sunny-windy condition refers to the availability of direct solar radiation and simultaneous exposure to the wind, shaded-lee to the protection from both direct solar radiation and wind, and so forth. The layout of these four combinations over a site plan has first been suggested by Brown and DeKay (2001) as a microclimate analysis tool for informing design decisions. In their methodology, such a microclimatic site analysis map is generated by overlaying a *sun layer* (indicating sunny and shaded areas for representative hours/days) and a *wind layer* (indicating windy and lee areas for prevailing wind directions). This is demonstrated by the authors using plans for a simple site; however, if it is to be applied in real, complex settlements, the process requires the extensive use of computer-based tools. For instance, Potvin et al. (2009) applying Brown and Dekay's methodology for assessing the microclimatic impact of a proposed development, needed to use several different programmes, one for solar analysis, one for wind analysis and one for combining the sun and wind conditions, following a rather complicated process.

Similarly, the mapping of thermal diversity in open spaces of urban forms, introduced by Steemers et al. (2004a; 2004b), has been based on the overlapping of different layers for sun and wind conditions. Their idea was facilitated by the introduction of digital elevation models (DEMs) of cities and image processing techniques for the environmental analysis of urban forms, which it fully incorporates. Their proposed

technique - described in the following section - presents significant advantages as it allows for the entire analysis as well as the visualization of the maps to be done using one single software, MATLAB software. However, despite the significance of the topic and the increasing availability of DEMs, the idea has remained up to now fairly unexplored.

The present study, following on from the work that has been previously done on the mapping of microclimatic combinations in open spaces, explores the occurrence of thermal diversity in 72 urban forms of London and 60 urban forms of Paris. As discussed in Chapter Three, and reflected in the outcomes of Chapter Four, the two cities present significant differences regarding their urban geometry which affect the correlations of urban geometry variables with indicators of environmental performance. Thus, the comparative analysis of Paris -as a second case study- was deemed necessary for testing the quantitative and qualitative findings for London. The research objectives are two: first, to examine the relationships between spatial thermal diversity and urban geometry and, more precisely degree of built obstruction in real urban forms, and second, by doing so, to contribute to establishing a methodology for the assessment of spatial thermal diversity in open spaces.

6.3. Methodology

6.3.1 Mapping the thermal diversity

The study is based on the method of Steemers et al. (2004a; 2004b) for mapping the thermal diversity in outdoor spaces of urban forms which is described below in brief for outlining emerging methodological issues. As mentioned before, the method is entirely based on the use of DEMs and image processing techniques; therefore, when referring to maps, these are digital images of urban forms' ground plans.

For a thermal diversity map to be produced, a sun map and a wind map are required as the environmental parameters considered. Each of these should demonstrate availability or not of the respective parameter for every pixel. Consequently, the maps ought to be binary images, i.e. black and white: the pixels' value can be either 1 (indicating sunny/windy pixels) or 0 (indicating shaded/lee pixels). Sun and wind maps are both generated by applying a *shadow casting* algorithm (Ratti, 2001) which casts buildings' shadow on open spaces using two inputs, azimuth and altitude angles. In casting sun shadow, the input angles define the precise position of the sun in the sky for which the shadow pattern is produced. In wind shadow casting, the azimuth angle defines the direction of the wind, and the altitude controls the length of the shadow -i.e. distance of influence downwind- in relation to the building height. Unlike sun shadow patterns, which are very accurate, the use of the shadow casting algorithm for wind analysis represents a

rather simplified solution for identifying “windy” and “lee” areas for a given wind direction. It is based on that a solid obstruction, such as a building, facing the wind interrupts its free passage through the site creating lee conditions on the opposite side to the wind direction.

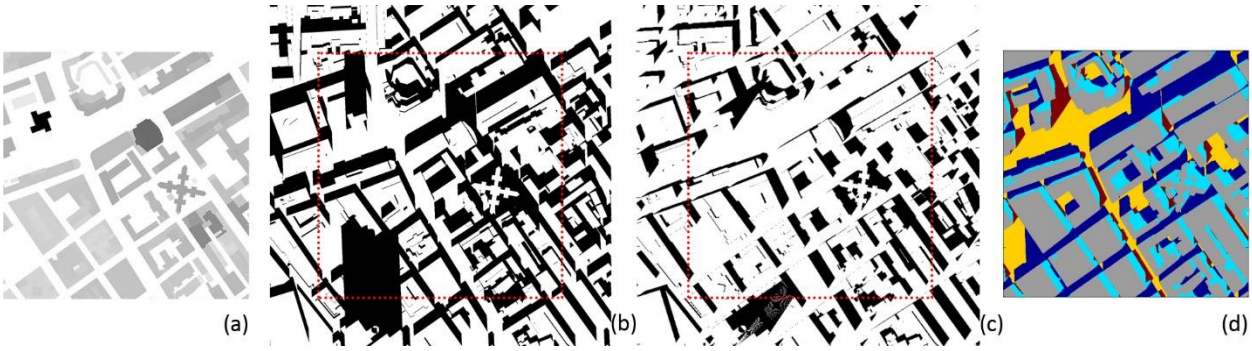

Figure 6.1: Urban form in central London (i.e. C9): DEM (a), sun map, sun shadow pattern at midday on an equinox day (b), wind map, wind shadow pattern for SW wind direction (c), - instantaneous - thermal diversity map produced by overlapping the sun and wind maps (colour index: blue for shaded-windy, cyan for shaded-lee, yellow for sunny-windy, and red for sunny-lee).

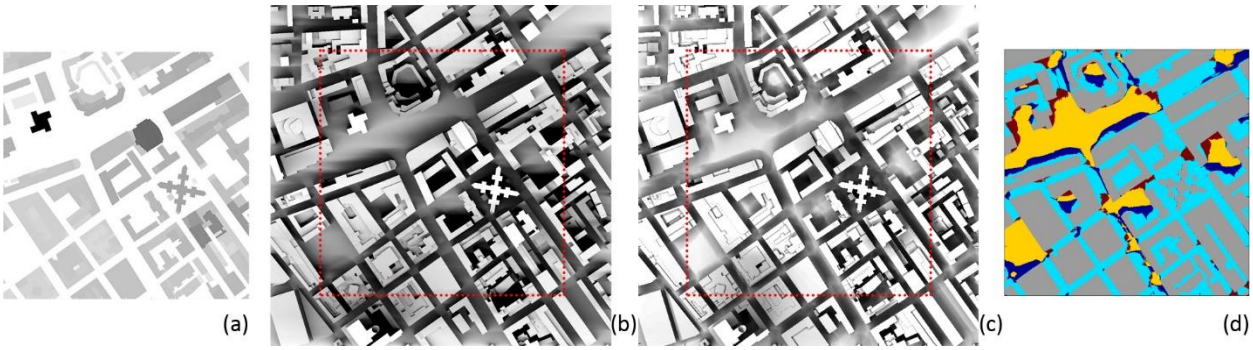

Figure 6.2: Same urban form as in Figure 6.1: DEM (a), average sun shadow pattern on an equinox day (b), average annual wind shadow pattern weighted by frequency (c), - average - thermal diversity map produced by overlapping the average sun and wind shadow patterns aside after applying to them threshold values (colour index as in Figure 6.1).

For particular pairs of input angles, i.e. considering a specific sun’s position and specific wind direction, the shadow patterns produced by the buildings over the outdoor space are defined and thus, the maps produced are binary images. Once such sun and wind maps are obtained and combined in an appropriate programme, a diversity map for that case (i.e. day/hour and wind direction) is generated (Fig. 6.1). If the diversity map is meant to be representative of a longer time period taking into account average shadow patterns and prevailing winds over a certain time period, the respective sun and wind maps represent averaged and cumulative information, respectively. The values of the pixels in such maps indicate availability of sun and wind as a percentage over the time or wind directions considered, meaning they

are no longer binary but greyscale images. To convert them into binary a threshold value is required, above which a pixel is assigned as sunny/windy, and below which shaded/lee (Fig. 6.2).

Two methodological issues thus arise and need to be considered when mapping thermal diversity. The first one is related to what the sun and wind maps will be representative of, and the second -in the case that those represent average/cumulative information – what threshold values will be set for defining sunny/shaded, windy/lee conditions. As the purpose of the so-far publications on the mapping of thermal diversity was essentially the demonstration of the proposed method, the information provided regarding methodological issues is sparse. Indicatively, the sun map used for mapping thermal diversity in a site in Cambridge, UK, was the average daytime shadow pattern on 22 June, and the respective threshold value was 6 hours of sunshine which corresponds to approximately 40% of the daytime hours on that day. Whereas, regarding the production of wind map, it is only mentioned that it was generated based on the prevailing wind directions for Cambridge.

6.3.2 Case studies and urban geometry variables used

Initially, the study concerned the relationship of density with spatial thermal diversity in 72 urban forms of London. Acknowledging though that London constitutes a special example of urban geometry, it was regarded as necessary the case of Paris, represented by 60 urban forms, to be also included in the analysis for comparison reasons. In addition, because the range of density values in Paris is significantly limited compared to London, site coverage was also selected to be examined as a second urban geometry variable, strongly related to density and degree of built obstruction in the urban environment. Density is measured as the total built volume over an area and thus expresses the 3D urban built obstruction; whereas, site coverage, expressing the percentage of the built-up area over the total site area [%], quantifies the 2D obstruction at the ground level. While the range of density values in London is about 5 times greater than in Paris (i.e. 3 to 33 m^3/m^2 and 5 to 11 m^3/m^2, respectively), the ranges of coverage values in the two cities are relatively close (i.e. 20-69% for London, 32-67% for Paris) allowing a more direct comparison of the respective results. Testing the linearity of the density-coverage relationship, the coefficient of determination (R^2) obtained for London's urban forms was 0.812 ($p<0.001$) (see Fig. 3.10b) and for those of Paris, 0.683 ($p<0.001$) (see Fig. 3.11b). More information about their variance in the two cities as well as their interrelation with the rest of the urban geometry variables is provided in Section 3.4.

6.3.3 Thermal diversity analysis

6.3.3.1 Method and tools used

The occurrence of spatial thermal diversity in the open spaces of the urban forms was examined on an average annual basis as for the results to be representative of the entire year. The shadow patterns used for generating sun maps were the average daytime ones on 21 March (equinox day) -computed before in SOLWEIG-, and the wind maps were produced considering annual daytime prevailing winds for London and Paris. Wind data was respectively obtained from the weather files for Heathrow Airport and Orlay Airport (EnergyPlus Weather Data).

With respect to wind shadow maps, they were computed entirely in MATLAB considering the frequency of annual daytime prevailing winds by direction; for each urban form, wind shadows were casted for every 6 degrees of azimuth and weighted by the respective frequency value. The final wind maps were next generated by averaging wind shadows for all 60 directions. The altitude angle in the algorithm was set to 45° which determines that the distance of influence of a building, i.e. wind shadow length on the leeward side of the building, is equal to its building height. According to Oke's graph (1987, pp. 244), for obstacles of high density such as a building, on their leeward side and within a distance equal to their height, the wind speed is reduced by 80% compared to the unobstructed wind speed. Hence, with such a reduction in wind speed, a lee wind zone can be considered.

Apart from the thermal diversity maps which were meant to be representative of average annual diversity -to be referred to as *average*-, another series of diversity maps were produced using the shadow patterns at noon on the same day, i.e. 21 March, and an -identified as major- wind direction which for both cities was south-west. The main purpose of these maps -to be referred to as *instantaneous*- is to explore whether the average diversity findings are related to / representative of instantaneous aspects of thermal diversity.

6.3.3.2 Insolation and wind exposure analysis for threshold values

In the absence of an established methodology for assessing thermal diversity, the present study first carried out an investigation on average insolation and wind exposure of the open spaces of the studied urban forms. The purpose was to select the threshold values to be used in defining average diversity. Average insolation values in the urban forms were computed based on their average daytime shadow patterns on 21 March (12 hours day duration) and express the average percentage of daytime hours during which the open space of the urban forms is sunlit. Among London's urban forms, the maximum, minimum and mean average insolation values were 44%, 4% and 26% respectively (i.e. 5.3, 0.5 and 3.1

hours); while in Paris the respective values were 37%, 10% and 27% (i.e. 4.4, 1.2 and 3.2 hours). Considering the mean average values in the two cities as well as the middle points of their ranges, the threshold value for generating sun maps was rounded to 25%, meaning that a pixel in the average sun shadow maps is assigned as “sunny” when it is exposed to the sun for more than the one fourth of the daytime hours.

The same analysis was performed for investigating the average wind exposure of the urban forms. Wind shadow maps were generated considering 60 wind directions (without being weighted by frequency) and next, average values of wind exposure of the outdoor spaces were computed. In this case, the value expresses the average percentage of wind directions to which the outdoor space of an urban form is exposed. Among London’s urban forms the maximum, minimum and mean average wind exposures were 74%, 14% and 51%; while for Paris the respective values were 62%, 22% and 43%. Following the same logic as before, the threshold value for identifying “windy” pixels would be close 45%; instead the slightly higher but more meaningful value of 50% was opted for. This means that a pixel in the average wind shadow maps is assigned as “windy” when it is exposed to more than the half of the annual daytime prevailing wind directions.

The relationships of average insolation and wind exposure with density and coverage were investigated by performing regression analysis. All the relationships were found linear and strong; however, they were stronger for coverage, average wind exposure, and London compared to density, average insolation and Paris, correspondingly (Fig. 6.3a-d).

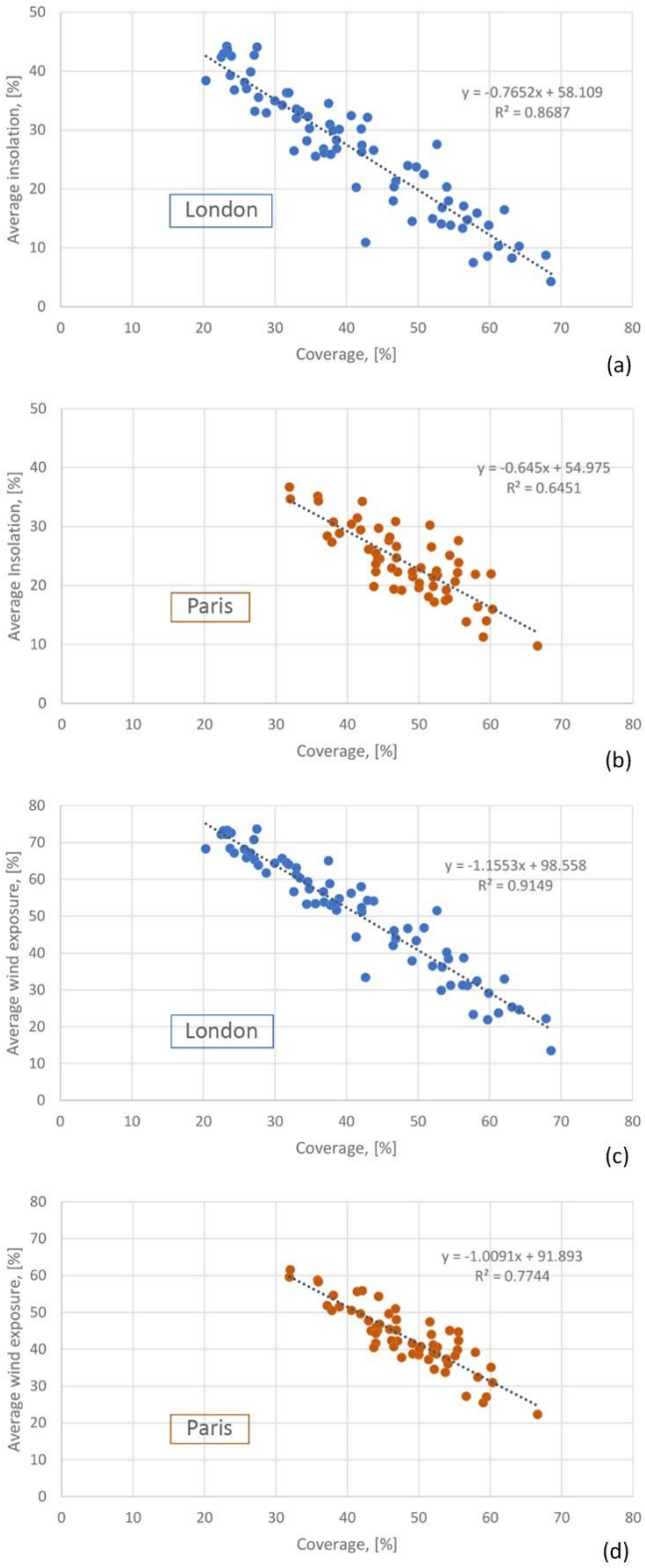

Figure 6.3: Linear models for coverage, and average insolation on 21 March (a-b) and wind exposure (c-d), for London and Paris.

6.3.3.3 Measuring thermal diversity

Thermal diversity maps are images, i.e. matrices which can be fully processed and analysed in MATLAB. For instance, information that can be easily computed for a thermal diversity map is the number of pixels and, so the total surface area, of the open space which corresponds to each of the four microclimatic combinations. The distribution of the open space's pixels into the four conditions can be next visualised as a histogram (Fig. 6.4). The histograms express graphically the thermal diversity occurring in an urban form, but they do not quantify it. For the sake of comparison of the urban forms, an absolute measurement of thermal diversity is required. In response, the present study developed and proposes the following formula:

$$d = 1 - \frac{\sqrt{(x_1 - x_m)^2 + (x_2 - x_m)^2 + (x_3 - x_m)^2 + (x_4 - x_m)^2}}{x_s \times f}$$

Where x_1, x_2, x_3 and x_4, the number of pixels that are identified as sunny-windy, sunny-lee, shaded-windy, and shaded-lee, respectively; x_s, the total number of the pixels of outdoor spaces i.e. $x_s=x_1+x_2+x_3+x_4$; x_m the mean value of x_1, x_2, x_3, and x_4, i.e. $x_m= x_s \div 4$; and *f,* a constant which scales the values between 0 and 1 and is equal to:

$$f = \frac{\sqrt{12}}{4}$$

According to this formula, the diversity takes its highest value, 1 when the numbers of pixels representing each of the microclimatic combinations are equal to each other, i.e. $x_1 = x_2 = x_3 = x_4$. In contrast, it takes the lowest value, 0 when the number of pixels of any microclimatic combination is equal to the total number of pixels of the outdoor space.

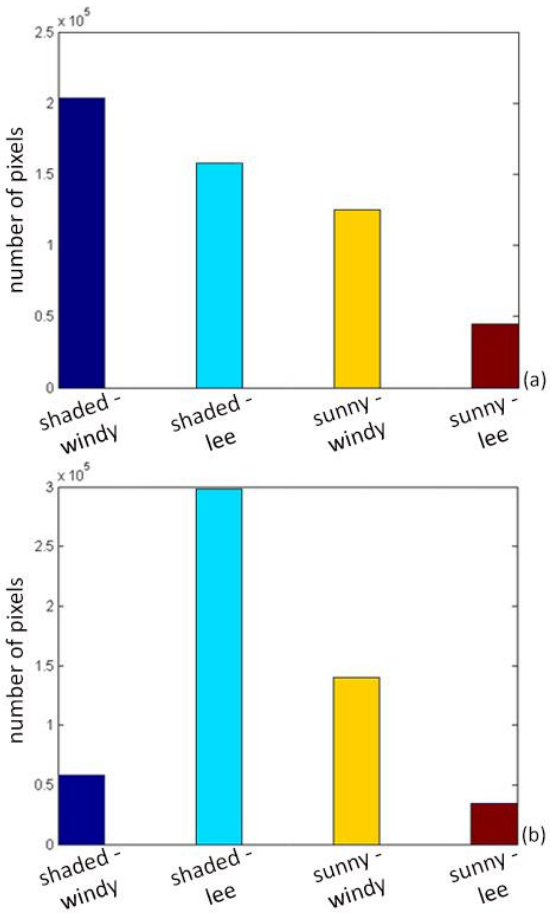

Figure 6.4: Distribution of the open space's pixels in each of the four microclimatic combinations as identified in thermal diversity maps in Figure 6.1d (a) and Figure 6.2d (b).

6.4 Results

6.4.1 Thermal diversity in London

The values of average and instantaneous thermal diversity for the open spaces of London's urban forms were computed based on the formula described in Section 6.3.3.3, and their relationships with density and coverage were next statistically tested. A major finding is that, in all the cases, the relationship is best described by polynomial models rather than linear ones. Plotting average and instantaneous thermal diversity values against the two urban geometry variables, the points appear to follow curves which present a maximum point and open downward (Fig. 6.5 - 6.6). The shape of the curves implies that there are density and coverage values, within the respective ranges of values, for which thermal diversity is maximised. Considering the maximisation of thermal diversity as an objective for urban design, it can be argued that the given values represent optimum density and coverage for London.

As seen in Figure 6.5(a-b), the curves describing the relationship of coverage with average and instantaneous thermal diversity are well described by a second-degree polynomial - i.e. quadratic - function with R^2 values being 0.765 and 0.648, respectively. Resolving the quadratic functions, the x-coordinate of the vertex of the parabola is 39.6 [%] for average, and 47.6 [%] for instantaneous thermal diversity. Given that coverage in London's urban forms ranges from 20 to 69%, the optimum values are found near the middle of the existing range.

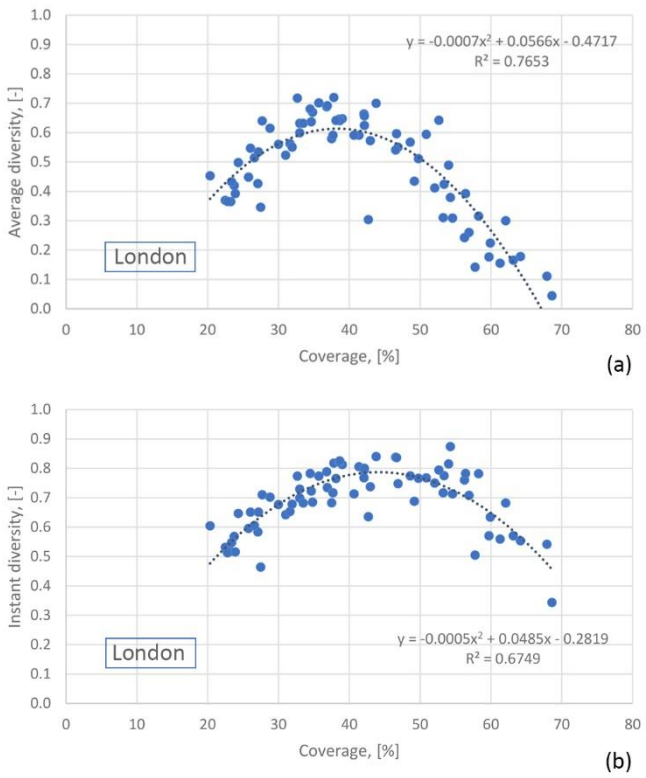

Figure 6.5: Average (a) and instantaneous (b) thermal diversity against coverage in London's urban forms.

Plotting thermal diversity against density, a similar pattern is revealed; the curves created by the given points indicate density values for which maximum average and instantaneous diversities are achieved. However, the curves appear to be less symmetrical compared to those for coverage, with maximum diversity being achieved by density values far lower within the given range. Additionally, quadratic models were found to poorly fit the curves but rather polynomial models of higher degree are needed. Cubic models have been selected and presented in Figure 6.6(a-b) as the simplest function describing them adequately enough; as seen, the R^2 values obtained are 0.715 for average diversity and 0.713 for instantaneous diversity. Resolving the cubic functions, the x-coordinate of the first critical point -local

maximum point- of the curves was found to be 9.1 [m^3/m^2] for average and 11.3 [m^3/m^2] for instantaneous diversity.

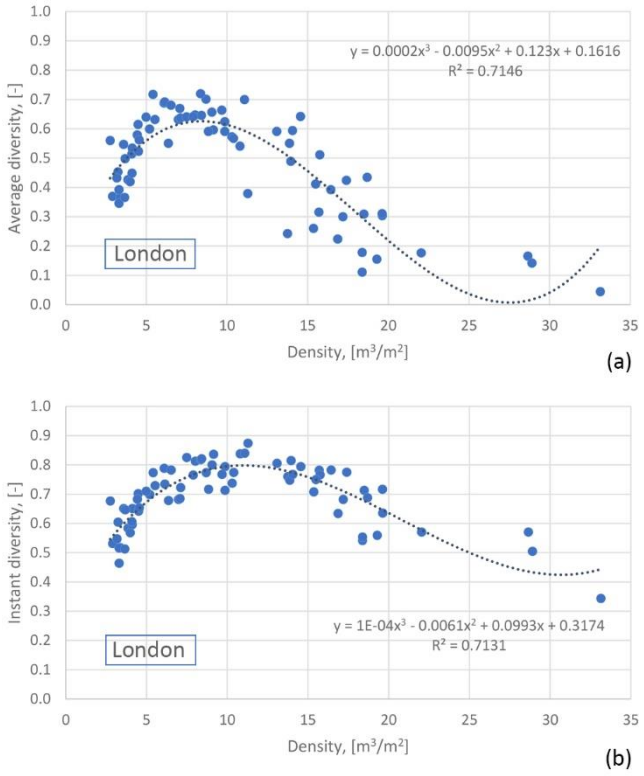

Figure 6.6: Average (a) and instantaneous (b) thermal diversity against density in London's urban forms.

6.4.2 Thermal diversity in Paris

Following the same process as before for London, the relationships between the two urban geometry variables and spatial thermal diversity in Paris' urban forms were examined. In general, the relationships were found to be weaker compared to London which is related to the fact that in London density and coverage variables explain a greater part of the variance of the urban geometry (see Section 3.4). Nonetheless, some significant similarities are revealed between the two cities.

The scatter plots for density-coverage against average-instantaneous diversity demonstrate that in all four cases, the points follow a parabola that presents a maximum point and opens downwards. Therefore, as before, optimum density and coverage values are identified for which the thermal diversity in open spaces is maximised. Regarding coverage, the maximum thermal diversity values are achieved within the given range of coverage values. The quadratic models describing its relationship with average and instantaneous diversity are presented in Figure 6.7(a-b). According to them, the x-coordinate of the vertex of the

parabola, and thus the optimum coverage value for average diversity was found equal to 35.6 [%]; whereas for instantaneous diversity it was 44.9 [%].

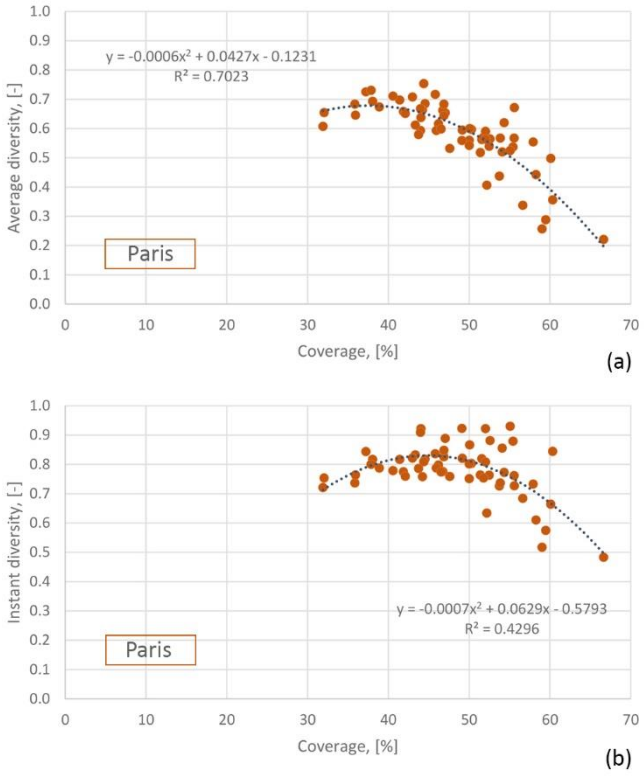

Figure 6.7: Average (a) and instantaneous (b) thermal diversity against coverage in Paris' urban forms.

Moving on to the relationship between density and thermal diversity in Paris' urban forms, this was also found to be better described by quadratic models (Fig. 6.8). With respect to instantaneous diversity, the maximum point of the parabola and thus the highest diversity value is achieved for density value 7.9 [m^3/m^2]. Regarding average thermal diversity, its maximum values seem to be achieved by urban forms of densities close to 7 [m^3/m^2]. However, this notional curve -evident by observation- is not reflected by the obtained quadratic model which specifies the optimum density below the given range of density values, i.e. at 4.3 m^3/m^2. The discrepancy may be related to the fact that, in Paris' urban forms, the range of density values is relatively limited, plus that the urban forms of density lower than 7 [m^3/m^2] are only six -out of 60- and do not allow the maximum point of the parabola to be accurately determined.

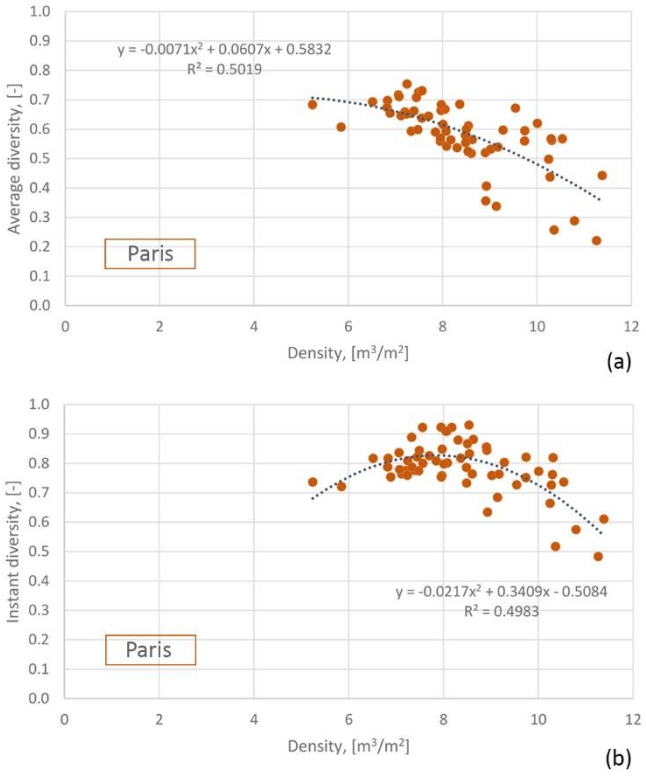

Figure 6.8: Average (a) and instantaneous (b) thermal diversity against density in Paris' urban forms.

6.4.3 Synergetic and conflicting microclimatic combinations

The findings for London and Paris are in general agreement and demonstrate that there is an optimum degree of urban built obstruction for maximising spatial thermal diversity. To gain a deeper insight into the significance of this, the relationship between the degree of obstruction of the urban environment and the spatial occurrence of the four microclimatic combinations (sunny-windy; sunny-lee; shaded-lee; shaded-windy) was next examined. Generally, the more obstructed an urban environment is the less exposed to the sun and wind its outdoor space is, and reversely. Either obstruction is meant in the 3D space -related to density- or at the ground level -related to coverage-, the effect of varying the degree of obstruction is more or less straightforward. As shown in Figure 6.3, the relationship is linear and negative: increasing density and coverage, average insolation and wind exposure of urban forms decrease; while decreasing density and coverage, they increase. Therefore, the microclimatic combinations, sunny-windy and shaded-lee, are referred to below as *synergetic* microclimatic combinations, because varying the degree of built obstruction their sun and wind condition components are affected in the same way. On the other hand, sunny-lee and shaded-windy are referred to as *conflicting* combinations because varying

the degree of built obstruction has an opposite effect on their sun and wind condition components, i.e. increasing the one and decreasing the other.

The relationship between the occurrence of the four microclimatic combinations with density and coverage was examined based on the average and instantaneous thermal diversity maps of the urban forms of London and Paris. Despite any differences among the cases, some general relationship patterns emerge when plotting percentage of outdoor space experiencing each microclimatic combination against the two urban geometry variables. The relationship of density and coverage with the occurrence of synergetic combinations was found to be linear and significantly strong; while their relationship with conflicting combinations is less strong and not linear.

These identified relationship patterns are exemplified below focusing on the occurrence of the four microclimatic combinations in the average thermal diversity maps of London's urban forms, tested against their coverage values. As shown in Figure 6.9(a-b), the relationship between coverage and percentage of open spaces experiencing synergetic combinations is almost perfectly linear, with R^2 values being 0.894 for sunny-windy and 0.921 for shaded-lee. In contrast, plotting the percentage of open spaces experiencing conflicting combinations against coverage (Fig. 6.9c-d), it is observed that the best curve fitting is achieved by quadratic models and the R^2 values obtained are significantly smaller. The same relationship patterns are also found to apply when considering synergetic and conflicting combinations in instantaneous thermal diversity maps, as shown in Figure 6.10(a-d).

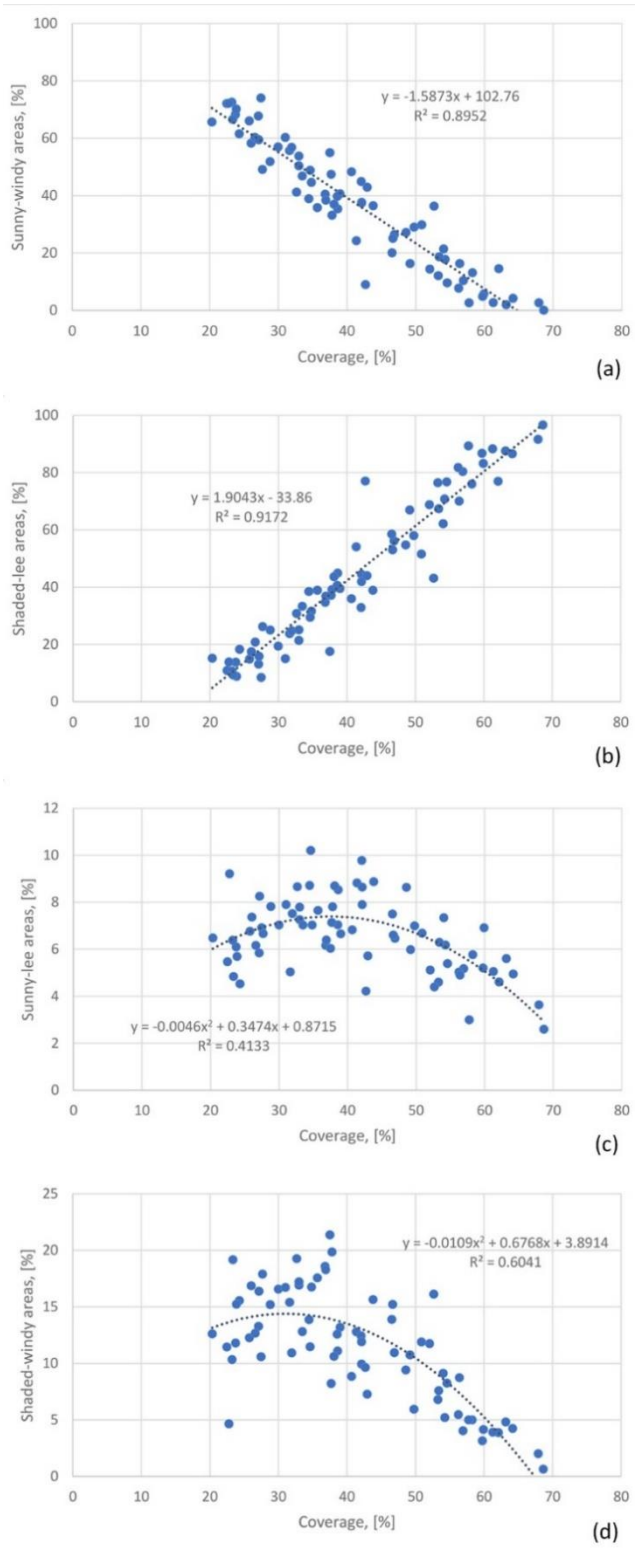

Figure 6.9: Occurrence of synergetic (a-b) and conflicting (c-d) microclimatic combinations -percentage of outdoor space experiencing them over total outdoor space- against coverage, based on average thermal diversity maps for London's urban forms.

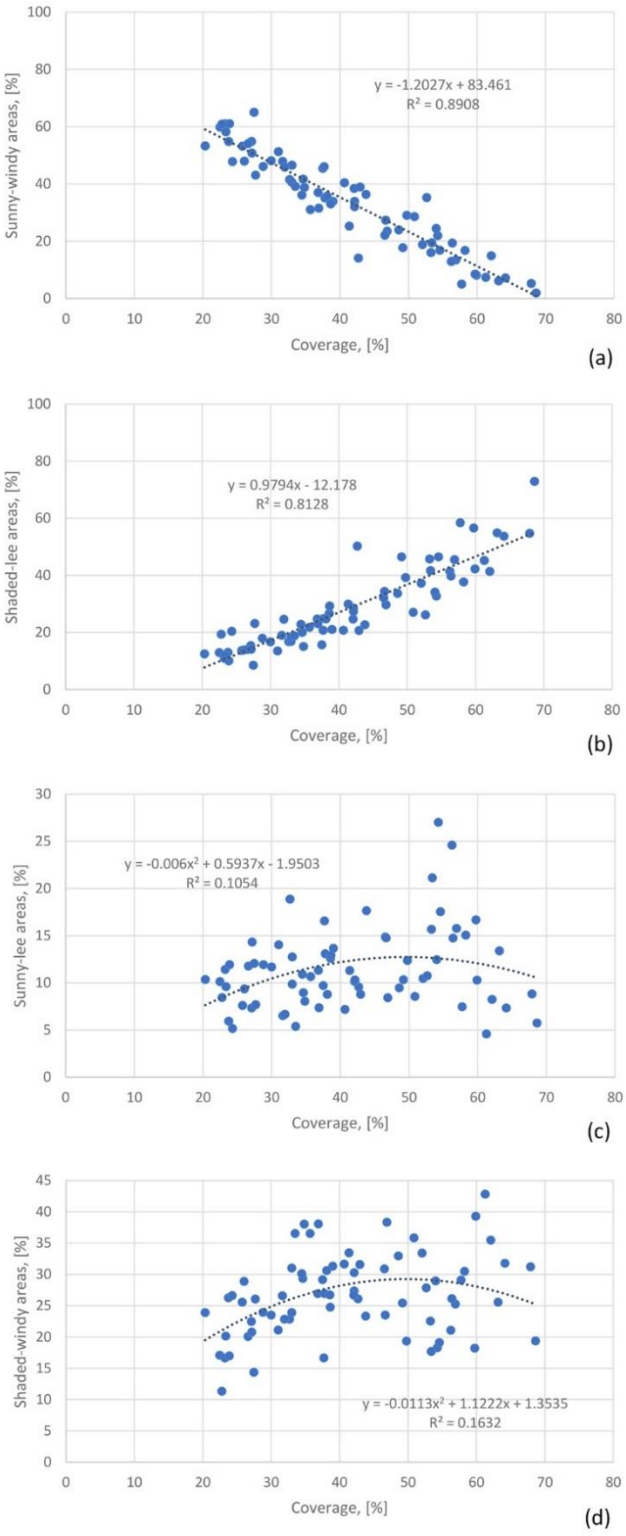

Figure 6.10: Occurrence of synergetic (a-b) and conflicting (c-d) microclimatic combinations -percentage of outdoor space experiencing them over total outdoor space- against coverage, based on instantaneous thermal diversity maps for London's urban forms.

Comparing the range of y-values in the graphs in Figure 6.9, it is observed that the percentage of the open space being sunny-windy and shaded-lee varies considerably among London's urban forms, ranging approximately from 0 to 78% and from 0 to 98% of the open space, respectively. In contrast, the sunny-lee and shaded-windy combinations do not comprise more than about 10% and 20% of the urban forms' open space, respectively. As reflected in the proposed formula, spatial thermal diversity is being increased when all different microclimatic combinations tend to occur over the same area in the open space of an urban form, i.e. 25% of it. In order for this to be accomplished, the percentage of sunny-windy and shaded-lee areas ought to be in a fair balance, while the percentage of sunny-lee and shaded-windy areas should reach their maximum possible values. The interception point of the linear models of Figure 6.9a and 6.9b has x-value 39 [%] which represents the coverage value for which the two synergetic microclimatic combinations occur in open spaces by the same percentage. It is reminded that 39% is the optimum coverage value for maximising average thermal diversity in open spaces of London's urban forms. It becomes thus apparent that the shape of the curve in Figure 6.5b is to a great degree the result of the combination of those in Figure 6.9a and 6.9b.

Regarding the conflicting microclimatic combinations, resolving the quadratic models shown in Figure 6.9c and 6.9d, the coverage values for which the percentage of sunny-lee and shaded-windy areas is maximised are 37.3 [%] and 30.3 [%] respectively, and thus lower but still close to the optimum 39%. In any case, and in contrast to the synergetic combinations, the relationship between the occurrence of conflicting ones and coverage -as well as density- is not causal, rather conditional. Varying the coverage or density parameter in the urban planning process will not yield a direct effect on the occurrence of conflicting combinations in the open spaces; rather there is a coverage and density value close to which the possibility for them to occur is increased, possibly due to associated favourable urban geometry circumstances.

6.5 Discussion

The exploration of spatial thermal diversity in London and Paris, two cities of similar latitude, allows the effect of the specific parameter on the research findings to be controlled. This was necessary because, as shown in previous chapters, solar altitude angle affects the strength of the relationship between urban geometry and solar availability. Therefore, the differences in the numerical results of the two cities can be directly related to their considerably different urban geometries as exemplified by the urban forms studied. In particular, the lower optimum density and coverage values obtained for Paris' urban forms compared to those for London is attributed to the relatively greater degree of compactness and uniformity characterising their geometry as well as the increased coverage values for a given density. In any case, the

interrelation of urban built obstruction with other aspects of urban geometry, i.e. other urban layout descriptors, in defining the occurrence of thermal diversity in open spaces is worth being examined further.

Furthermore, optimum density and coverage values were found to be higher when examining instantaneous thermal diversity. The above is mostly related to the sun shadow patterns used for the two types of spatial thermal diversity. At noon, the sun's altitude is the highest occurring in the day and thus, the insolation of the urban forms is generally increased compared to the average daytime. Additionally, performing Pearson Correlation test for the average and instantaneous diversity values of the urban forms of the two cities, the correlation was found to be significant at the level of 0.01, with r being in both cases close to 0.6. However, the R^2 values obtained performing linear regression test, 0.427 for London and 0.368 for Paris, indicate that the instantaneous diversity values can be hardly explained by the average ones, and inversely. Nonetheless, what is of great importance is that the relationships of average and instantaneous diversity with the two urban geometry variables considered are of the same nature, highlighting the presence of optimum values. In addition, the optimum density and coverage values for which the two types of diversity take their maximum values are close enough to be comparable.

Regarding the method used for the mapping of spatial thermal diversity, as mentioned in Section 6.3.3.1, the application of the shadow casting algorithm for wind analysis purposes do not produce results of the same accuracy and sophistication as when applied for solar analysis. Apparently, this is a wider issue to be addressed when simulating the urban wind environment and related to the complexity of wind phenomena compared to the highly predictable solar rays' attitude. The wind analysis performed identifies exposed to and sheltered from the wind areas acknowledging the horizontal wind flow. In other words, it is based on that on the opposite to the wind direction side and in a certain distance from the building, the wind speed reduction is such that lee conditions can be considered. However, it does not take into account vertical air flows that may be induced into the urban canopy due to large variations in building heights (Britter and Hanna, 2003). Nevertheless, such variations are only found in few urban forms of the two cities, i.e. in the City of London and some urban forms on the outskirts of Paris.

Considering the number and scale of the urban forms analysed, the use of a CFD (Computational Fluid Dynamics) software for the generation of the required wind maps was not an option. That would require extensive computer resources, and be extremely time consuming. Beyond that, the present method for mapping thermal diversity relies on the compatibility of the produced files at all different stages of the analysis which is achieved by the use of DEMs -instead of modelling the geometry of the city- and their

analysis in MATLAB. As the results of Ratti et al. (2006, pp. 77) suggest, "*the DEM format is an extremely versatile tool to investigate the urban intermediate scale, allowing analyses that would be very difficult or impossible to be carry out using traditional vectorial models".* Very recently, Johansson et al. (2015) introduced a model for assessing the spatial distribution of wind speed at street level, and at scales from neighbourhood to city, using the known shadow-casting algorithm operating on raster data. Their research work is deemed very relevant, and promising as it breaks new ground towards sophisticated wind simulation avoiding intensive CFD modelling. It could thus be employed in the future for the wind analysis of urban forms as part of their thermal diversity mapping; however, it is still at a preliminary stage and more work is needed for its calibration and validation.

Finally, with respect to future work, temporal thermal diversity, i.e. variations of microclimatic conditions in open spaces of urban forms in time, is another aspect of thermal diversity which is worth being studied. Temporal thermal diversity is particularly relevant to temperate climates as it might assess to what extent the seasonal variations of microclimatic conditions respond to seasonal outdoor thermal objectives. For this purpose, a new methodology should be developed as well as a formula which quantifies it based on representative days in the year.

6.6 Conclusions

The study proposes a mathematical formula for measuring spatial thermal diversity in open spaces of urban forms, identifying four microclimatic combinations as the result of the combined availability of sun and wind (i.e. sunny-windy, sunny-lee, shaded-lee, shaded-windy). Average and instantaneous spatial thermal diversity values are computed for -in total- 132 urban forms in London and Paris based on shadow patterns on an equinox day and annual prevailing winds' data. The obtained values are then tested statistically against two urban geometry variables, density and coverage, which express the degree of 3D and 2D urban built obstruction, respectively. The relationships were found to be statistically significant and better described by quadratic or cubic models presenting maximum and local maximum values. In other words, it is revealed that there are optimum density and coverage values for which spatial thermal diversity is maximised.

Regarding average thermal diversity, which is meant to be representative of annual spatial diversity, the optimum coverage value for London was identified at 39.6%, and for Paris at 35.6%. Moreover, the optimum density value for London was found to be 9.1 [m^3/m^2]; whereas, for Paris there is a discrepancy between the observed and derived from the statistical model values, close to 7 and 4.3 [m^3/m^2]

respectively. This is attributed to the limited range of densities in Paris' sample of urban forms. Further differences among the numerical results for the two cities are related to their vastly different urban geometries, highlighting potential interrelations between spatial thermal diversity, urban built obstruction and other parameters of urban geometry.

The existence of an optimum degree of urban built obstruction for enhancing spatial thermal diversity in open spaces is also confirmed by the investigation of the relationships between the two urban geometry variables with the four microclimatic combinations considered. The results of the analysis indicate that, for spatial thermal diversity to be increased, areas experiencing sunny-windy and shaded-lee conditions -referred to as *synergetic*- ought to be in a fair balance. On the other hand, the occurrence of sunny-lee and shaded-windy conditions -referred to as *conflicting*-, which is less dependent on the urban built obstruction, should be maximised. Both are achieved by medium density and coverage values, close to the optimum ones for increasing thermal diversity.

Overall, the findings of the present study aspire to inform urban designers' and planners' decisions by contributing to the discourse on optimum levels of densification of the urban built environment. Increased built density is an objective of urban planning as it is associated positively with urban sustainability, especially at the city scale; whereas, at the neighbourhood scale, increasing built density may restrict significantly solar availability and ventilation in the urban fabric. The existence of optimum values of density and coverage for enhancing spatial thermal diversity in open spaces provides evidence towards the acknowledgement of a golden mean regarding desirable levels of urban densification.

Chapter Seven

Conclusions

The last chapter of the thesis summarises the major findings of the research, and discusses its contribution to the field of urban environmental research and practice. It consists of four parts. In the first one, the research outcomes of the three studies are combined and presented in relation to the overall research aim and questions as those were defined in Section 1.2. The second part discusses the contribution of the findings to the ongoing research and discourse on the subject matter emphasising their significance for the theory of urban environmental design. Next, major findings and recommendations for London are outlined providing useful information to architects and urban designers working in the city. In the fourth part, different directions for future research work are identified which would foster the developments signified by this research work.

7.1 Introduction

The motivation for the present research has been the key role of urban geometry in pursuing multiple solar design objectives and thus, promoting urban environmental sustainability. This can be specified otherwise in the following statement: enhancing our understanding about how urban geometry affects sun-related phenomena taking place in the urban environment contributes towards a more sophisticated and informed solar design, namely solar design which responds to conflicting environmental interests in a positive and effective way. The good timing and purposefulness of the research are also related to relatively recently available methods and resources which allow nowadays the relevant topic to be explored in real urban forms.

Acknowledging the wide scope of the topic, the research was carried out in three parts, focusing on different aspects of urban environmental performance, namely solar exposure of and spatial thermal diversity in open spaces, and solar availability in open spaces and on building façades. In this way, the overall research questions are approached from diverse perspectives and each study revisits or complements the findings of the others in a different context. This furthers the overall aim of the research which is to establish a conceptual framework for the subject matter; whereas, at the same time, each study individually provides a considerable insight into particular aspects of the effect of urban geometry.

Moreover, some of the findings present immediate relevance for the professionals working in the field of urban design and planning, especially regarding London, which has been the main case study. The dependence of the findings on the case of London has been examined by analysing comparatively a second city, Paris, in the first and the third studies, and considering two more locations, Athens and Helsinki, in the second study.

Furthermore, the research addresses methodological issues regarding the analysis of real urban forms and their geometry. In particular, the research demonstrates that built density needs to be distinguished methodologically from all other urban geometry variables referring to urban layout when the effect of urban geometry on solar potential is explored. This approach has been applied in the second study, on solar availability in open spaces and building façades, the findings of which exemplify the purposefulness of such a distinction. Additionally, since outdoor thermal diversity is a relatively newly introduced urban environmental quality and the relevant literature is very limited, an important part of the third study deals with developing a methodology for its definition and quantification.

Overall, the contribution of the thesis is deemed to be multilevel casting light on some theoretical but fundamental aspects of the topic, developing specific and practical knowledge for promoting urban environmental sustainability, and applying new methodological approaches for the study of urban geometry and resulting environmental phenomena. At the same time, the research exemplifies the vast possibilities offered by the use of urban DEMs and image processing techniques for the analysis of real urban forms.

7.2 Overall conclusions

In this section, the key findings of the three studies of the thesis are combined and discussed with respect to the three research questions posed in the introductory chapter (see Section 1.2). For the sake of the discussion, it is reminded that the solar analysis performed for the simulation of solar access and availability in the studied urban forms focuses exclusively on the interaction of solar radiation with urban geometry -neglecting any other parameter that may be affecting them-. Therefore, the interpretation of the results into findings is based on the theoretical scheme depicted in Figure 4.1, assuming that at any given time the solar exposure of an urban form is determined by two factors, a constant one which is the geometry (i.e. density and layout) of the form and a varying one, which is the orientation of the form in relation to the Sun.

- To what extent does built density decide environmental phenomena related to the availability of solar radiation and which is the role of urban layout?

This question reflects the subject matter of the thesis and constitutes the thematic umbrella under which the three distinct studies become relevant to each other. Through a comparative analysis approach, the research demonstrates that the answer is not straightforward as the effect of urban geometry may vary with time, location, phenomenon examined, and type of urban surfaces considered.

The negative impact of built density on urban solar availability is reasonable and intuitively perceived, meaning that increasing the built volume contained within a site will decrease to some degree the solar irradiation of urban surfaces. However, the strength of this causal relationship is statistically sensitive to the case study city and the sample of urban forms studied, as shown when comparing the results of London and Paris in the first study. The dominant role of density in defining solar access and availability in London is attributed to the wide range of density values found in the city, as well as the strong correlation of density with most of the urban layout parameters, including site coverage and building height. For the opposite reasons, the relationship of density with solar access in Paris is relatively less significant implying that the influence of urban layout is considerably increased. Nevertheless, the difference between the two cities is reflected to the statistical relationship of density, and SVF, with instantaneous insolation. In contrast, when examining the relationship of SVF with daytime average insolation, this appears equally strong for London and Paris. Therefore, replying to what extent built density affects solar availability in the urban environment, this is also related to the time over which the effect is considered. Furthermore, examining sun-related phenomena, time entails different sun's positions / sun paths, the impact of which was found to be crucial for the relationship between urban geometry and solar availability; the relevant findings are discussed extensively in the next section.

Despite of the strong effect of density in London, urban forms of similar densities but diverse layouts were found to perform considerably differently in the second study. As shown by the comparison of pairs of urban forms, this is related to specific urban layout parameters, some of which are found to have a positive effect, increasing solar availability, and others, a detrimental one. The possibility of compensating the negative effect of increased density through a deliberate manipulation of urban layout has been ascertained by several studies in the past (e.g. Cheng et al., 2006a; 2006b; Lee et al., 2016; Li et al., 2015; Lu and Du, 2013). However, most of them are based on parametric analysis and examine basic urban geometry variables, such as site coverage and building height, or are restricted to descriptive classification of layouts, for instance, random versus uniform layouts. The present research expands and enriches the

existing literature by investigating the effect of layout in real contexts, namely using real urban forms for its statistical exploration. Studying real urban forms also allowed the consideration of more, and more sophisticated layout parameters, all expressed by numeric variables. For instance, the effect of vertical randomness was quantified by considering the *standard deviation of building height* variable, and that of horizontal randomness by considering *directionality* and *standard deviation of building footprint*. Especially, the quantification of the horizontal randomness parameter using specific geometric measures was first proposed and tested in this research.

Furthermore, the research examined the impact of urban geometry comparatively for open spaces and building façades, with each of the two types of urban surfaces being related with different solar design objectives. Very few studies have examined so far urban solar availability with respect to outdoor microclimate and solar potential of buildings, either focusing on urban canyon geometry (van Esch et al., 2012) or evaluating specific urban typologies (e.g. Zhang et al., 2006). Importantly, the comparative analysis reveals that the influence of urban geometry is not quantitatively and qualitatively constant when considering solar availability on ground and façades. As concerns built density, the strength of the relationship -causality- as well as the amplitude of the effect were found to change. Regarding the effect of urban layout, different parameters were found to be the most influential for open spaces and building façades. Some layout parameters affect only ground's solar irradiation, some only façades' solar irradiation, and others both. It is worth underlining though that the effect of urban layout parameters affecting ground and façades was found to be positive or negative for both.

Solar availability in open spaces is primarily affected by the quantity of the open space within an urban form, expressed negatively by site coverage and positively by mean distance between buildings. This was first ascertained examining average SVF in open spaces in London and Paris, and then confirmed by the second study considering ground SVF and global irradiances in 24 urban forms of London. Other parameters correlating significantly with solar availability in open spaces are horizontal randomness and complexity of building façades, with both affecting it negatively. Horizontal randomness and complexity deteriorate also the solar potential on building façades whereas, vertical randomness was found to enhance it. The fact that there are urban layout parameters affecting only open spaces' or building façades' solar performance justifies why some urban forms admit more solar radiation on their ground and less on their vertical surfaces, or the reverse, compared to others. In other words, the findings indicate that it is feasible to promote conflicting solar design objectives associated with open spaces and building façades through the appropriate handling of the urban layout.

Finally, the last study examined the effect of urban geometry on the occurrence of spatial thermal diversity in open spaces, identifying four microclimatic combinations as the result of the combined availability of sun and wind (i.e. sunny-windy, sunny-lee, shaded-lee, shaded-windy). The results revealed the key role of built obstruction, expressed by density and site coverage, in enhancing the microclimatic variations and hence the responsiveness and use of the open space. Unlike the relationship between built obstruction and solar availability which is to a great degree linear, the relationship between built obstruction and thermal diversity is best described by quadratic or cubic curves presenting maximum and local maximum values. This significant finding emerged from the analysis of London and Paris, and implies the existence of optimum density and site coverage values for which spatial thermal diversity is maximised.

- Whether, and how does the varying solar geometry affect the relationship between urban geometry and sun-related phenomena?

Solar geometry is a key parameter when referring to sun-related phenomena in the built environment since the solar exposure of an urban form is determined by its geometry and the position of it in relation to the sun. The position of the sun changes continually in time, daily and seasonally, and with geographical latitude, and so its interaction with urban geometry. The present research explored the impact of solar geometry on the relationship between urban geometry and solar availability, both in time and examining locations of different latitudes.

In the first study, the relationship of urban geometry and average insolation of open spaces in urban forms of London and Paris, two cities of similar latitude, was examined in time, on representative days of the year. The results demonstrated that the effect of density and SVF, as well as their correlation with average insolation of open spaces vary in the day. Specifically, both increase with increasing solar altitudes, namely the higher the sun's altitude the greater their effect and the stronger their correlation with average insolation. However, the impact of solar altitude is not constant, but significant during the early morning and late afternoon hours and reduced close to midday. Plotting the R^2 results against solar altitude, it revealed that the relationship between built obstruction and solar access gets stronger as solar altitude increases up to a point, beyond which their correlation is already strong enough and no more sensitive to a further increase of solar altitude. In fact, it is assumed that there is a critical angle for which the correlation is maximised. The argument is reasonable considering that for maximum solar altitude, i.e. 90°, the correlation of density with solar exposure becomes null both for ground and façades. Evidence for the existence of such a critical solar altitude angle is provided in the second study. Specifically, the

correlation between density and SVF with solar availability on façades was found to reduce noticeably when tested for combinations of time period, location and façade orientation meaning high solar altitudes. The fact that this was only ascertained in the case of façades and not for the ground implies that the critical angle is different for the two types of urban surfaces, and higher for the ground.

The finding that the correlation between density and solar availability is much more sensitive to lower solar altitudes compared to higher ones is also confirmed by the analysis of daytime average insolation of open spaces on the studied days. Their relationship with SVF was found to be equally strong (R^2>0.9) on 21 June and 21 March, for both cities, and remarkably weaker on 21 December. The comparison of the results regarding instantaneous and daytime average insolation provides also evidence about the effect of open spaces' layout and orientation. It appears that they may play a key role for instantaneous solar access; however, their impact on daytime average insolation was found to be limited. This is directly associated with the range of diverse solar azimuths occurring during a day, and less with solar altitudes. Specifically, since the orientation of open spaces of urban forms may be favourable for their insolation at different times in the day, by averaging their insolation over the day, the orientation effect is offset and what primarily affects it is the degree of built obstruction.

The second study investigated the impact of density and urban layout parameters on solar availability focusing on 24 urban forms in London, and examining three time periods: the entire year, January and July. Taking into account that the relationship between urban geometry and solar access was found to vary as a function of solar altitude, the consideration of winter and summer months aimed to explore to what extent urban geometry can contribute to enhancing seasonal solar performance of urban forms. As may be expected, the solar component which was found to be mostly affected by different ranges of solar altitudes -as those are defined by the sun paths in the two months- is the direct solar radiation. Both for open spaces and façades, the correlation between density and direct irradiances was found to be stronger in July, i.e. higher average solar altitudes, compared to January, i.e. lower average solar altitudes, agreeing with the findings of the first study. Furthermore, the seasonal effect of density on solar availability appears much more pronounced for ground rather than for building façades, with open spaces suffering from excessive overshadowing in the winter and prolonged solar exposure in the summer.

Interestingly, the analysis also showed that the impact of urban layout changes considering different sun paths. Precisely, the availability of direct radiation was found to be influenced by different urban layout parameters in January and July. For instance, regarding direct solar irradiation of façades, the most influential parameters in January were standard deviation of building height and number of buildings

within the site; whereas, in July, they were complexity of building façades and distance between buildings. Respectively, the parameters affecting solar availability in open spaces in January but not in July are compactness of building volumes and number of buildings contained within a site; whereas, standard deviation of building footprint, complexity of building façades and distance between buildings are influential in July but not in January. The significance of the specific finding lies in that it demonstrates the possibility of promoting the seasonal solar performance of urban forms in temperate climates, such as in London, by controlling specific urban layout parameters during the design process.

In the same study, the sensitivity of the above results to different locations was also examined by testing London's urban forms for two other European cities, Athens and Helsinki. A first finding was that the relationship between urban geometry and solar availability is sensitive to the latitude parameter rather the weather conditions in different locations. Comparing the results obtained for the three locations, it was shown that different latitudes affect the relationship between urban geometry and direct solar radiation received by ground and façades in January and July, and less in the year. This is mainly referred to the urban layout parameters influencing solar availability in particular months, which are different in the three cities. In spite of any differences from one location to another, the results prove that the promotion of seasonal solar design objectives is possible for a wide range of latitudes across Europe, i.e. from Athens (37°58'N) to Helsinki (60°10'N).

On the other hand, annual direct solar availability was found to be less dependent on latitude which is attributed to the fact that the annual sun paths cover a wide, similar section of the sky vault and hence, the differences among the three locations are eliminated. The strength of the relationship between density and annual direct irradiances was found to decrease with location's latitude; however, the urban layout parameters affecting them are to a large degree common, and the same with those affecting SVF and diffuse solar radiation. It can thus be argued that the annual solar availability at locations within the respective range of latitudes, i.e. approximately from 38° - 60°, is influenced by the same urban layout parameters. These are *site coverage*, *complexity*, *directionality* and *mean outdoor distance*, for ground, and *standard deviation of building height*, *directionality* and *complexity*, for facades. The effect of *site coverage* and *complexity* on solar availability is negative, and all the others' positive.

- Are there environmentally preferable density values?

This question has been approached by examining two different environmental issues, first the role of urban geometry in promoting conflicting seasonal solar design objectives and second, in enhancing thermal diversity in open spaces.

Due to the powerful, negative effect of the density parameter, urban forms of higher density tend to receive less solar radiation both in winter and summer months, in their open spaces and on building façades, and the reverse. In this context, medium densities may be considered preferable in temperate climates as they balance the different seasonal needs, i.e. maximising solar radiation in winter and controlling it in summer. In support of that, the research showed that the effectiveness of urban layout in modifying solar availability increases in medium, medium-high densities. ("Medium" and "medium-high" refer to the range of density values in the sample of 24 urban forms in London used in the second study.)

Specifically, having ascertained that urban layout parameters affecting solar availability change depending on the month, it was possible to identify some urban forms in London which constitute exceptions to the general tendency, namely presenting higher average irradiances in January and lower in July compared to others. These urban forms with a relative better seasonal solar performance are of medium and medium-high density, which highlights that an adequate amount of built volume (i.e. density) is necessary for the effect of urban layout to be noticeably profound. In particular, medium densities provide sufficient overshadowing in summer, whereas, the carefully planned configuration of buildings within the site may limit direct radiation losses in winter. Similarly, examining to what extent urban forms with higher façades solar irradiance present also higher ground solar irradiance, compared to others, it was ascertained that those deviating from the general rule are also of medium/high densities.

It is acknowledged that the above cases are identified based on a simplified comparison of the urban forms' performance, and the highlighted densities may be also related to the sample examined. In addition, solar design objectives linked with solar irradiation of open spaces and façades, in different seasons, may not have the same weighting in the decision-making process and hence, density values may be adjusted to prioritise the major ones. For instance, if considering that London belongs to the heating-dominated climatic zone of Europe (Littlefair et al., 2000, pp. 21) the optimum range of densities may be quite lower to prioritise the insolation of the urban forms. Therefore, the examples used are not meant to recommend optimal built densities for London, rather to highlight that in medium and medium-high densities, the potential of urban layout to modify selectively the solar urban environment is optimised.

The desirability of medium built densities was also revealed in the third study, examining the impact of built obstruction on the occurrence of thermal diversity in open spaces. It became apparent that medium densities ensure a relative balance between *synergetic* microclimatic combinations, sunny-windy and shade-lee, and increase the possibility of *conflicting* ones, sunny-lee and shade-windy, to occur; thus, they provide a greater variety of outdoor microclimatic conditions. In other words, thermal diversity exemplifies sun-related environmental phenomena on which the effect of density is neither positive or negative, rather optimum density values should be sought for their enhancement.

7.3 Contribution to urban environmental research and design

The research addressing multiple questions regarding the role of urban geometry in promoting urban environmental sustainability, especially with respect to sun-related phenomena, emerges a series of findings of significant research interest. Its major contribution to the ongoing research and discourse in the field of urban environmental design is that it reveals the great potential offered by considering urban geometry as a dynamic and multifaceted factor. This may be specified in the following:

- An urban form is characterised by the total built volume that it contains -expressed by density- and the way that this built volume is expressed spatially within its boundaries -referred to as layout-. The findings demonstrate that urban layout may amplify or offset the negative impact of density on urban solar availability and thus, its effect should be fully considered both in urban environmental studies and urban design practice.
- To what degree and in which way, density and layout affect the occurrence of solar and sky-related quantities in the urban environment differ when considering open spaces or building façades. With the two types of urban surfaces to be related with different environmental phenomena and objectives, urban geometry may be adjusted appropriately to act for the optimisation of outdoor and indoor environmental quality.
- Not least, the relationship between urban geometry and solar access varies constantly in time, daily and seasonally, due to its sensitivity to the sun's position, and especially its altitude. This rather theoretical at first sight finding is proven to have practical implications and applications in urban solar design. Focusing on a temperate climate, such as this of London, the research exemplifies its usefulness in promoting conflicting, seasonal solar needs.

Another key issue that is of high relevance for researchers and professionals in the field of urban environmental design and urban climatology, is whether geometric measures can be used as indicators of

urban solar availability, and more widely, urban radiant environment. Employing geometric measures for estimating the environmental performance of urban forms enables the quick evaluation and comparison of entire urban areas, the environmental analysis of which would require extensive computer resources and time. In relation to that, the research focuses on SVF, an integrated geometric measure, and its relationship with average insolation of open spaces and mean radiant temperature, and average solar irradiances in open spaces and on building façades. As expected, its relationship with outdoor mean radiant temperature in absence of direct solar radiation, and diffuse solar irradiance, is almost perfectly linear denoting its high relevance to long-wave radiation availability. More importantly, the research showed that average SVF can be also used as indicator of solar exposure of ground and façades.

The capability of SVF to estimate solar exposure and thus, direct solar radiation received by urban surfaces was found to be affected by two parameters, both associated with time. The first parameter is solar altitude, which varies constantly in time. In general, the higher the solar altitude, the stronger the relationship between SVF and solar exposure is. Specifically, the findings indicate that SVF can predict better instantaneous insolation of open spaces close to midday compared to morning and afternoon hours, and average direct irradiance in July compared to January. Nonetheless, as discussed in Section 7.2, the effect of increasing solar altitude is not constant and may inverse for solar altitudes above a critical value. The second parameter is the length of the time period over which solar exposure/availability is examined. According to the results, SVF is more reliable in predicting average daytime insolation than instantaneous insolation, and annual solar irradiances rather monthly ones. In other words, the longer the period over which a solar performance indicator is considered, the stronger its relationship with SVF is.

Since SVF defines sky diffuse irradiation and can also estimate average direct irradiances on an annual and monthly basis, it can be used as indicator of global solar availability over the respective time period. In addition, with respect to façades, the research demonstrates that the capability of SVF to predict total solar irradiation is not limited to average values in an urban form, but it can equally well predict average values by façade orientation. The applicability of the relevant findings is exemplified through a series of graphical tools to be used for the estimation of annual global irradiance on ground and façades in London (see Section 5.7.3). The strong relationship between average SVF and annual direct irradiance in London is related to that both are found to be affected by the same urban layout parameters. Since annual ground and façades direct irradiances in Athens and Helsinki are influenced by the same urban layout parameters

as in London, there is a strong indication that SVF can be used as indicator of annual solar availability for locations of latitude 38° - 60°, independently of climate (i.e. sky conditions).

Furthermore, the strong relationship between average SVF values and solar irradiances explains why the effect of orientation of urban forms on solar irradiances was found to be limited. As SVF is a geometric measure, independent of orientation, rotating an urban form the total solar radiation received by its ground and façades hardly varies. Apparently, relative differences in mean solar irradiances are increased in winter months when solar availability is significantly reduced. Nonetheless, regarding absolute differences, these are found to be very small, with the highest to be reported for ground in July not exceeding 3 W/m^2. Interestingly, the amplitude of the orientation effect was found to be affected by urban forms' density in opposite way in different time periods. Specifically, increasing density was found to increase the effect of orientation on annual ground direct irradiance, and decrease it in January both for façades and ground, and in July only for façades. Overall, the study on the orientation effect provides firm evidence that orientation is a major factor affecting the instantaneous insolation of an urban form, but regarding total solar irradiation of urban forms over longer periods, its effect is limited. The sensitivity of this finding needs to be tested using different case studies and at different scales, because, if it can be generalised, as assumed, it will cause a fundamental shift in the significance ascribed to the orientation of urban areas and its implication for their solar potential.

Moreover, the research contributes to the timely discussion about optimum built densities for sustainable urban settlements. Increased built densities present a series of advantages which are deemed crucial for promoting urban sustainability; however, they also create environmental problems, such as reduced levels of solar and illuminance availability, which affect the energy efficiency of buildings and well-being of cities' inhabitants. Examining two different aspects of environmental performance of urban forms, at the neighbourhood scale, the outcomes provide environmental grounds for opting for a "moderate" urban densification. Specifically, it was demonstrated that medium densities facilitate the attainment of conflicting solar design objectives and increase thermal diversity in open spaces.

Since conflicts result from the need to enhance or control solar availability at different instances or with respect to different type of urban surfaces (ground/façades), an adequate amount of built volume ensures first a balance between the two needs. In addition to that, the capability of urban layout to modify selectively solar availability in the urban environment was found to increase in higher medium densities. Specifically, urban forms of relatively better seasonal performance were found to belong to the half urban forms of higher density among 24 analysed in the second study. Nonetheless, the definition of a range of

built densities for optimising urban solar performance requires a more thorough consideration of different energy and environmental targets as well as the efficacy of different solar strategies to be employed for their fulfilment. Thus, the argument for the desirability of medium densities, especially in temperate climates, should be considered as a general recommendation which needs to be specified into numeric values through further research work.

Finally, the research deals also with a less-known and less-studied environmental quality of the open space, particularly relevant to temperate climates, namely outdoor thermal diversity. Except for the significance of the results themselves, the relevant study contributes to the establishment of a methodology for the exploration of the topic. The major contribution is considered the introduction of a mathematical formula for the quantification of spatial thermal diversity, based on the percentage of the open space experiencing the four sun and wind microclimatic combinations: sunny-windy, shaded-lee, sunny-lee, and shaded-windy. With the quality of open spaces to become a focal issue on the agenda for urban environmental sustainability, it is anticipated that outdoor thermal diversity will receive more research attention in the future, and the proposed methodology might be tested and developed further.

7.4 Findings and recommendations for London

London constitutes the main case study of this research. Its selection was based on various criteria among which, the diversity of its urban geometry -mostly related to the wide range of density values- and its temperate climate. As the scope and aim of the research expanded beyond the study of London, dealing with wider issues concerning the role of urban geometry in urban environmental design, the methodology was adjusted accordingly following a rather theoretical approach. Nonetheless, some of the outcomes present a practical value and can be interpreted into useful information for architects and urban designers working in the city.

First of all, the geometric analysis of urban forms of London and their comparison with Paris was very informative revealing some particularities of the city and the way in which major geometric parameters are interrelated in producing the existing urban fabric. Except for the wide range of density values which are geographically defined -reducing from the city centre outwards-, the statistical analysis showed a significantly strong correlation of built density with most of the urban layout descriptors. Among them, site coverage and mean building height are of the first importance as they control the way in which density increases. With site coverage denoting horizontality and building height verticality of a built form, their positive linear relationship with density, and with each other, indicates that the built form in London

increases equally in both directions. This should be acknowledged as a special characteristic of London, which, for instance does not represent Paris, and has a direct impact on the statistical outcomes.

Research has shown that the way in which density increases -horizontally or vertically- matters when examining solar and daylight quantities in the urban environment. Reversely, it may be put as that increasing density in a constant way, the relationship between density and solar and daylight availability is expected to be stronger. In this regard, the significantly strong correlations of density with solar performance indicators found out in the case of London -compared to Paris- are justified by the strong interrelation of density, site coverage and building height characterising in the city. Following on that, a general conclusion that can be drawn is that the performance of density and, by extension, SVF as indicators of solar and daylight availability may vary with city, with them being much more reliable in London than Paris.

Having ascertained and explained the strong statistical relationships of density, SVF and solar performance indicators in London, the equations obtained from regression analysis could be used for assessing solar and daylight availability in urban forms of the city. In this context, SVF can play a key role linking density with resulting solar performance. Considering that average SVF values are not readily available but require computer simulation tools, their calculation based on simple urban geometric metrics, such as density, would facilitate its use as an environmental performance indicator. In the case of London, average SVF values can be estimated based on built density, using the equations provided in the first study for ground (see Figure 4.10), and the second one for façades (see Figure 5.8). Next, average daytime insolation of open spaces (mSOL) on the summer solstice, equinox day and winter solstice can be estimated as a function of average ground SVF (mSVF) using the following exponential equations: $mSOL_{21Jun}=0.095e^{2.665mSVF}$ ($R^2=0.963$), $mSOL_{21Mar}=0.035e^{3.802mSVF}$ ($R^2=0.959$), $mSOL_{21Dec}=0.006e^{4.986mSVF}$ ($R^2=0.773$). (The respective scatter plots are presented in Figure 4.13). Similarly, mean annual global irradiance in open spaces and on building facades of an urban form can be roughly predicted using the linear models appeared in Figure 5.27.

As the above equations referring to average values in urban areas, it is admitted that their relevance to architects and architectural practice may be limited. Especially, the solar potential of facades, which is crucial for active and passive solar strategies to be employed, needs to be calculated locally, for specific façades of new or existing buildings, or sections of them. In response, the relationship of SVF and annual façade solar irradiance was examined for different orientation sections, and found significantly strong independently of façade azimuth. The linear models obtained from regression analysis, provided in

Appendix H, have been integrated into a graphical tool (Figure 5.29) which can be used by architects for a quick estimation of the annual solar irradiation of façades in London as a function of their average SVF and azimuth.

Another part of the research findings concerns the role of urban layout in promoting solar design objectives and can be interpreted into urban design recommendations for London. As solar design objectives are multiple, associated with different uses of solar radiation outdoors and indoors, the recommendations should reflect environmental priorities. For instance, to improve the seasonal performance of urban areas in London, *urban layout descriptors* which correlate with the availability of direct solar radiation only in January or July should be considered. Interpreting the relevant findings would first suggest opting for more, and smaller buildings instead of large building blocks. This was found to promote solar availability in the winter, both on the ground and building façades. The winter solar irradiation of façades could be also enhanced by differentiating considerably the height of the buildings; while that of ground by increasing their compactness. Regarding the provision of shading in the summer, increasing the undulations of built forms and decreasing the distance between buildings could be an option; however, they may affect significantly the annual solar irradiation of the development and hence, an optimum value should be sought. Furthermore, emphasis should be put on the solar design of open spaces as their insolation in winter and solar protection in summer are more difficult to be achieved. In this regard, site coverage and directionality of the development should be carefully considered, as they affect ground's solar availability both in winter and summer, the former negatively and the latter positively.

Similar recommendations can be also made for Athens and Helsinki based on the results of their analysis. Apparently, the winter and summer conditions experienced in the three cities differ enormously in harshness and, in turn, their energy and comfort implications. For instance, providing solar shading is an objective of limited relevance to Helsinki but crucial in Athens during the summer period. Therefore, urban designers should prioritise thermal needs which are dominant in each climate, namely those exerting the greatest impact on buildings' heating/cooling energy demands and outdoor thermal comfort. It is also acknowledged that thermal needs indoors and outdoors are not always identical -in time- as indoor thermal environment is modified by the building fabric as well as internal gains which are related to the building use and occupancy. As a result, the period during which solar radiation is welcome in open spaces is usually longer compared to the heating period for buildings.

If the main environmental strategy for a new urban development is to harness solar energy on building façades through photovoltaic systems and solar collectors, then emphasis should be put on the *urban layout descriptors* affecting annual solar irradiation of façades, namely *standard deviation of building height*, *complexity* and *directionality*. Interestingly, annual solar irradiation is influenced by the same urban layout descriptors, in all three locations examined; hence, the recommendations are common. Specifically, for increasing annual solar irradiation of façades, urban designers should avoid uniform building heights and complex building shapes which increase self-shading and overshadowing effect. Furthermore, they should carefully consider the positioning and configuration of the building volumes as to enhance the directionality of the development. However, since enhanced directionality is also associated with higher solar irradiances in open spaces in July, the degree and direction of the alignment of buildings should be selected wisely as to provide some shading during the summer months.

In general, among the three significant parameters for façades' annual solar performance, special emphasis should be put on the differentiation of building heights, both for its effectiveness in increasing façades' solar potential as well as for its non-interference with ground solar objectives. The specific parameter can significantly contribute to the enhancement of solar availability in densely built-up areas, such as Central London. In addition, if the random skyline is combined with relatively low site coverage, namely increasing mean building height for achieving the desirable density value, the solar access can substantially increase both on façades and ground. A characteristic example is the area near Euston Station which, combining the above features, outperforms areas of similar density but more compact layout (see Section 5.4.2.2.4). Summarising, one way to increase density in London controlling though its negative effect on solar and daylight availability is by increasing and varying the building height.

Finally, regarding desirable and environmentally preferable built densities, the third study approaches the topic from another perspective, that of outdoor thermal diversity. Specifically, the outcomes illustrate the existence of optimum density and coverage for enhancing the microclimatic variations in open spaces, providing specific values for London and Paris. In London, thermal diversity was found to maximise for density 9.1 [m^3/m^2] and coverage 39.6 [%]. If excluding some extremely densely built-up areas in the City of London, the above values represent medium values in the city. Among the three areas studied in London, density values close to 9-10 [m^3/m^2] are found mostly in the west area, and more widely, peripherally to the city center. It is acknowledged that the specific values are to some degree sensitive to the methodology followed; hence, they are indicative and as such should be referred to. Nonetheless, the environmental advantages of opting for medium densities have already discussed with respect to the

conflicting, seasonal solar objectives in temperate climates, and the consideration of thermal diversity as another urban environmental quality fully supports the argument.

7.5 Future research suggested

The research revealed the vast possibilities offered by conscious manipulation of urban geometry for promoting more efficient and environmentally friendly cities, and points the way towards new, unexplored grounds for study. Suggestions for future studies are made separately in the discussion section of each of the studies, while some major directions are outlined below.

The research can be used as a precedent in two main ways, either extending it testing its findings into different contexts, or going into more depth integrating its findings into more holistic research approaches. The former is related to the fact that both in terms of methodology and topics explored, the existing literature is rather limited. Thus, the applicability of the methodology and the validity of the research findings to different contexts, namely urban geometries and climates, could and should be investigated. For instance, one of the distinctive characteristics of the methodology is that it is based from the beginning until the end on the analysis of real urban forms and the statistical exploration of the results. This was proven to be a particularly suitable approach for the investigation of various environmental phenomena and their association with urban geometry parameters. Provided that the availability of 3D digital models of cities is gradually increasing, the study of real urban forms is anticipated to create a new body of literature on causal relationships governing the environmental performance of cities.

One of the advantages of using real urban forms as case studies is that it enabled to distinguish methodologically the effect of density and urban layout. The effect of layout was examined considering nine urban layout descriptors, some of which had not been used before in similar studies. Taking into account that urban layout was found to play a key role in the modification of urban solar availability, its impact should be examined in different cities as well as testing more urban layout descriptors. Furthermore, another finding which is definitely worth being explored is the varying relationship between urban geometry and solar availability in time, due to the varying solar geometry. For the high expectations that this discovery creates to be fulfilled, more research work is necessary to investigate possible implementations of it in the context of a more sophisticated and responsive urban solar design. Other findings, such as the limited effect of orientation on the total solar radiation received by façades and open spaces, should be tested considering various urban geometries, at different urban scales.

Regarding the second research direction suggested, it should aim to link the findings with actual implications for outdoor thermal comfort and building energy performance in London. The present study examined simultaneously the impact of urban geometry on solar availability in open spaces and building façades, using solar indicators meaningful in both cases, namely SVF and irradiance values. The particular indicators facilitated the comparison of different urban forms in terms of solar availability but cannot be interpreted directly into thermal conditions experienced in open spaces, or potential energy offsets for buildings, respectively. The interpretation of façade solar irradiation into energy or heat implications for buildings is relatively straightforward, and could be easily done based on some assumptions regarding building materials and use, efficacy of active systems, etc. On the other hand, the evaluation of outdoor thermal conditions in extensive urban areas presents considerable difficulties, with a major one being the estimation of spatial variations of wind speed. As discussed in Section 6.5, new tools are being developed for this purpose using urban DEMs and image processing techniques. Once these are available to researchers, they will foster the study of outdoor thermal environment at the neighbourhood scale and allow issues, such as outdoor thermal diversity, to be explored more thoroughly and systematically.

References

A

Adolphe, L., 2001. A simplified model of urban morphology: Application to an analysis of the environmental performance of cities. *Environment and Planning B: Planning and Design,* 28(2), pp. 183-200.

Adolphe, L., 2009. Morphometric integrators of a sustainable city. *PLEA2009 - 26th International Conference on Passive and Low Energy Architecture.* Quebec City, Canada, 22-24 June 2009.

Ahmed, S., 2016. *London can't wait for solar*. [pdf] London: Energy for London, Greenpeace UK. Available at: http://www.greenpeace.org.uk/sites/files/gpuk/Solar-London-Election-2016-Report.pdf [Accessed 6 December 2016].

Aida, M., 1982. Urban albedo as a function of the urban structure - A model experiment - Part I. *Boundary-Layer Meteorology,* 23(4), pp. 405-413.

Ali-Toudert, F. and Mayer, H., 2006. Numerical study on the effects of aspect ratio and orientation of an urban street canyon on outdoor thermal comfort in hot and dry climate. *Building and Environment,* 41(2), pp. 94-108.

Ali-Toudert, F. and Mayer, H., 2007a. Thermal comfort in east-west oriented street canyon in Freiburg (Germany) under hot summer conditions. *Theoretical and Applied Climatology*, 87, pp. 223-237.

Ali-Toudert, F. and Mayer, H., 2007b. Effects of asymmetry, galleries, overhanging façades and vegetation on thermal comfort in urban street canyons. *Solar Energy,* 81(6), pp. 742-754.

Andreou, E. and Axarli, K., 2012. Investigation of urban canyon microclimate in traditional and contemporary environment: experimental investigation and parametric analysis. *Renewable Energy,* 43, pp. 354-363.

Arboit, M., Diblasi, A., Fernández Llano, J.C. and de Rosa, C., 2008. Assessing the solar potential of low-density urban environments in Andean cities with desert climates: The case of the city of Mendoza, in Argentina. *Renewable Energy,* 33(8), pp. 1733-1748.

Arboit, M., Mesa, A., Diblasi, A., Fernández Llano, J.C. and de Rosa, C., 2010. Assessing the solar potential of low-density urban environments in Andean cities with desert climates: The case of the city of Mendoza, in Argentina. 2nd. Part. *Renewable Energy,*35(7), pp. 1551-1558.

Arnfield, A.J., 1990. Street design and urban canyons solar access. *Energy and Buildings*, 14, pp. 117-131.

B

Baker, N. and Steemers, K., 1996. LT Method 3.0 - A strategic energy-design tool for Southern Europe. *Energy and Buildings,* 23(3), pp. 251-256.

Baker, N. and Steemers, K. 2000. *Energy and Environment in Architecture: a Technical Design Guide*. London: E & FN Spon.

Banzhaf, E. and Netzband, M., 2012. Monitoring urban land use changes with remote sensing techniques. In: Richter, M. and Weiland, U., (eds.) *Applied Urban Ecology*. Chichester: Wiley-Blackwell, pp.18-32.

Batty, M., 2008. The size, scale, and shape of cities. *Science,* 319(5864), pp. 769-771.

Batty, M. and Longley, P., 1994. *Fractal Cities: A Geometry of Form and Function*. London: Academic Press.

Batty, M. and Sik Kim, K., 1992. Form Follows Function: Reformulating Urban Population Density Functions. *Urban Studies,* 29(7), pp. 1043-1069.

Benevolo, L., 1993. *The European city*. Oxford: Blackwell Publishers.

Bentley, I., (ed.) 1985. *Responsive environments: A manual for designers*. London: The Architectural Press.

Berghauser Pont, M.Y. and Haupt, P.A., 2010. *Spacematrix: Space, Density and Urban Form*. Rotterdam: NAi Publishers.

Biljecki, F., Stoter, J., Ledoux, H., Zlatanova, S. and Çöltekin, A., 2015. Applications of 3D City Models: State of the Art Review. *ISPRS International Journal of Geo-Information*, 4(4), pp. 2842-2889.

Bohnenstengel, S.I., Evans, S., Clark, P.A. and Belcher, S.E., 2011. Simulations of the London urban heat island. *Quarterly Journal of the Royal Meteorological Society,* 137(659), pp. 1625-1640.

Bourbia, F. and Awbi, H.B., 2004a. Building cluster and shading in urban canyon for hot dry climate: Part 1: Air and surface temperature measurements. *Renewable Energy,* 29(2), pp. 249-262.

Bourbia, F. and Awbi, H.B., 2004b. Building cluster and shading in urban canyon for hot dry climate Part 2: Shading simulations. *Renewable Energy,* 29(2), pp. 291-301.

Bourbia, F. and Boucheriba, F., 2010. Impact of street design on urban microclimate for semi arid climate (Constantine). *Renewable Energy,* 35(2), pp. 343-347.

Bourdic, L., Salat, S. and Nowacki, C., 2012. Assessing cities: a new system of cross-scale spatial indicators. *Building Research & Information*, 40(5), pp. 592-605.

Braulio-Gonzalo, M., Bovea, M.D., Ruá, M.J. and Juan, P., 2016. A methodology for predicting the energy performance and indoor thermal comfort of residential stocks on the neighbourhood and city scales. A case study in Spain. *Journal of Cleaner Production,* 139, pp. 646-665.

Brito, M.C., Gomes, N., Santos, T. and Tenedório, J.A., 2012. Photovoltaic potential in a Lisbon suburb using LiDAR data. *Solar Energy*, 86(1), pp. 283-288.

Britter, R.E. and Hanna, S.R., 2003. Flow and dispersion in urban areas. *Annual Review of Fluid Mechanics,* 35, pp. 469-496.

Brown, G.Z. and DeKay, M., 2001. *Sun, Wind and Light: Architectural design strategies*. New York: Wiley.

Bruse, M. and Fleer, H., 1998. Simulating surface-plant-air interactions inside urban environments with a three dimensional numerical model. *Environmental Modelling and Software,* 13(3-4), pp. 373-384.

Buonanno, G., Fuoco, F.C. and Stabile, L., 2011. Influential parameters on particle exposure of pedestrians in urban microenvironments. *Atmospheric Environment,* 45(7), pp. 1434-1443.

Burian, S.J., Han, W.S. and Brown, M.J., 2005. *Morphological Analyses using 3D Building Databases: Seattle, Washington*. LA-UR-05-1822, Los Alamos National Laboratory, NM.

C

Capeluto, I. and Shaviv, E., 2001. On the use of 'solar volume' for determining the urban fabric. *Solar Energy*, 70(3), pp. 275-280.

Capeluto, I. Yezioro, A., Bleiberg T. and Shaviv E., 2006. Solar rights in the design of urban spaces. *PLEA2006* - 23rd International *Conference on Passive and Low Energy Architecture*. Geneva, Switzerland, 6-8 September 2006.

Carmona, M., Tiesdell, S., Heath, T. and Oc, T., 2010. *Public spaces - Urban spaces: The dimensions of urban design*. 2nd ed. Oxford: Architectural Press.

Carneiro, C., Morello, E. and Desthieux, G., 2009. Assessment of solar irradiance on the urban fabric for the production of renewable energy using lidar data and image processing techniques. *Lecture Notes in Geoinformation and Cartography*, pp. 83.

Centre for Environmental Data Archive. Online database: http://www.ceda.ac.uk/ [Shapefile downloaded June 2012].

Chan, A.T., So, E.S.P. and Samad, S.C., 2001. Strategic guidelines for street canyon geometry to achieve sustainable street air quality. *Atmospheric Environment,* 35(24), pp. 4089-4098.

Chan, A.T., Au, W.T.W. and So, E.S.P., 2003. Strategic guidelines for street canyon geometry to achieve sustainable street air quality - Part II: Multiple canopies and canyons. *Atmospheric Environment,* 37(20), pp. 2761-2772.

Chen, L. and Ng, E., 2012. Outdoor thermal comfort and outdoor activities: A review of research in the past decade. *Cities,* 29(2), pp. 118-125.

Chen, Y., Lin, T. and Matzarakis, A., 2014. Comparison of mean radiant temperature from field experiment and modelling: a case study in Freiburg, Germany. *Theoretical and Applied Climatology,* 118(3), pp. 535-551

Cheng, V., Steemers, K., Montavon, M. and Compagnon, R., 2006a. Compact cities in a sustainable manner. *2nd International Solar Cities Congress*. Oxford, U.K., 3-6 April 2006.

Cheng, V., Steemers, K., Montavon, M. and Compagnon, R., 2006b. Urban form, density and solar potential. *PLEA2006 - 23rd International Conference on Passive and Low Energy Architecture.* Geneva, Switzerland, 6-8 September 2006.

Cheung, H.K.W., Coles D. and Levermore, G.L., 2016. Urban heat island analysis of Greater Manchester, UK using sky view factors. *Building Services Engineering Research and Technology*, 37(1), pp. 5-17.

Choudhary, R., 2012. Energy analysis of the non-domestic building stock of Greater London. *Building and Environment,* 51, pp. 243-254.

Choudhary, R. and Tian, W., 2014. Influence of district features on energy consumption in non-domestic buildings. *Building Research and Information,* 42(1), pp. 32-46.

Coles, A., Piterou, A. and Genus, A., 2016. Sustainable energy projects and the community: Mapping single-building use of microgeneration technologies in London. *Urban Studies,* 53(9), pp. 1869-1884.

Compagnon, R., 2000. PRECis: Assessing the Potential for Renewable Energy in Cities. Annexe 3: Solar and Daylight availability in urban areas. Cambridge, UK.

Compagnon, R., 2004. Solar and daylight availability in the urban fabric. *Energy and Buildings*, 36(4), pp. 321–328.

D

Day, A.R., Jones, P.G. and Maidment, G.G., 2009. Forecasting future cooling demand in London. *Energy and Buildings,* 41(9), pp. 942-948.

De Montigny, L., Ling, R. and Zacharias, J., 2012. The effects of weather on walking rates in nine cities. *Environment and Behavior,* 44(6), pp. 821-840.

Di Sabatino, S., Buccolieri, R. and Salizzoni, P., 2013. Recent advancements in numerical modelling of flow and dispersion in urban areas: A short review. *International Journal of Environment and Pollution,* 52(3-4), pp. 172-191.

Drew, D.R., Barlow, J.F. and Lane, S.E., 2013. Observations of wind speed profiles over Greater London, UK, using a Doppler lidar. *Journal of Wind Engineering and Industrial Aerodynamics,* 121, pp. 98-105.

E

Echevarria Sanchez, G.M., Van Renterghem, T., Thomas, P. and Botteldooren, D., 2016. The effect of street canyon design on traffic noise exposure along roads. *Building and Environment,* 97, pp. 96-110.

Edussuriya, P., Chan, A. and Ye, A., 2011. Urban morphology and air quality in dense residential environments in Hong Kong. Part I: District-level analysis. *Atmospheric Environment,* 45(27), pp. 4789-4803.

Eliasson, I., 1996. Urban nocturnal temperatures, street geometry and land use. *Atmospheric Environment*, 30(3), pp. 179-192.

Emmanuel, R., Rosenlund, H. and Johansson, E., 2007. Urban shading - A design option for the tropics? A study in Colombo, Sri Lanka. *International Journal of Climatology*, 27(14), pp. 1995–2004.

EnergyPlus Weather Data. Online source: https://energyplus.net/weather

EPBD, 2010. Directive 2010/31/EU of the European Parliament and of the Council of 19 May 2010 on the energy performance of buildings. *Official Journal of the European Union*, pp. 13-35.

ESRI ArcGIS. [Computer software]. Website: http://www.esri.com/arcgis/about-arcgis

Evenson, N., 1979. *Paris: A century of change, 1878-1978.* New Haven and London: Yale University Press.

F

Falkner, R., 2014. Global environmental politics and energy: Mapping the research agenda. *Energy Research & Social Science,* 1, pp. 188-197.

Frankhausser, P., 1994. *La fractalité des structures urbaines*. Paris: *Anthropos.*

Freitas, S., Catita, C., Redweik, P. and Brito, M.C., 2015. Modelling solar potential in the urban environment: State-of-the-art review. *Renewable and Sustainable Energy Reviews,* 41, pp. 915-931.

Fu, P. and Rich P.M., 2000. *The Solar Analyst 1.0 User Manual*. Helios Environmental Modeling Institute, Lawrence, KS.

G

Gal, T. and Unger, J., 2009. Detection of ventilation paths using high-resolution roughness parameter mapping in a large urban area. *Building and Environment*, 44(1), pp. 198-206.

Gal, T., Lindberg, F. and Unger, J., 2009. Computing continuous sky view factors using 3D urban raster and vector databases: comparison and application to urban climate. *Theoretical and Applied Climatology*, 95(1), pp. 111-113.

Gehl, J., 1971. *Life between buildings: using public space*. Washington: Island Press.

Geiß, C., Taubenböck, H., Wurm, M., Esch, T., Nast, M., Schillings, C. and Blaschke, T., 2011. Remote sensing-based characterization of settlement structures for assessing local potential of district heat. *Remote Sensing,* 3(7), pp. 1447-1471.

Ghosh, S. and Vale, R., 2009. Typologies and basic descriptors of New Zealand residential urban forms. *Journal of Urban Design,* 14(4), pp. 507-536.

Gil, J., Beirão, J.N., Montenegro, N. and Duarte, J.P., 2012. On the discovery of urban typologies: Data mining the many dimensions of urban form. *Urban Morphology,* 16(1), pp. 27-40.

Giridharan, R. and Kolokotroni, M., 2009. Urban heat island characteristics in London during winter. *Solar Energy,* 83(9), pp. 1668-1682.

Giridharan, R., Lau, S.S.Y., Ganesan, S. and Givoni, B., 2007. Urban design factors influencing heat island intensity in high-rise high-density environments of Hong Kong. *Building and Environment*, 42(10), pp. 3669-3684.

Givoni, B., 1998. *Climate considerations in building and urban design*. New York: John Wiley & Sons.

Grawe, D., Thompson, H.L., Salmond, J.A., Cai, X. and Schlünzen, K.H., 2013. Modelling the impact of urbanisation on regional climate in the Greater London Area. *International Journal of Climatology,* 33(10), pp. 2388-2401.

Grimmond, C.S.B. and Oke, T.R., 1999. Aerodynamic properties of urban areas derived from analysis of surface form. *Journal of Applied Meteorology,* 38(9), pp. 1262-1292.

Guedes, I.C.M., Bertoli, S.R. and Zannin, P.H.T., 2011. Influence of urban shapes on environmental noise: A case study in Aracaju – Brazil. *Science of the Total Environment,* 412-413, pp. 66-76.

Gupta, V.K., 1984. Solar radiation and urban design for hot climates. *Environment and Planning B: Planning and Design*, 11(4), pp. 435-454.

H

Hall, P., 1989. *London 2001*. London: Unwin Hyman.

Hamaina, R., Leduc, T. and Moreau, G., 2012. Towards urban fabrics characterization based on buildings footprints. *Lecture Notes in Geoinformation and Cartography*, pp. 327.

Hawkes, D., 1996. *The environmental tradition*. London: E & FN Spon.

Hawkes, D., Owens, J., Rickaby, P. and Steadman, P., (eds.) 1987. *Energy and Urban Built Form*. London: Butterworths.

He, X., Miao, S., Shen, S., Li, J., Zhang, B. Zhang, Z. and Chen, X., 2015. Influence of sky view factor on outdoor thermal environmental and physiological equivalent temperature. *International Journal of Biometeorology,* 59(3), pp. 285-297.

Hermosilla, T., Gil-Yepes, J.L., Recio, J.A. and Ruiz, L.A., 2012a. Change detection in Peri-urban areas based on contextual classification. *Photogrammetrie, Fernerkundung, Geoinformation,* 2012(4), pp. 359-370.

Hermosilla, T., Ruiz, L.A., Recio, J.A. and Cambra-López, M., 2012b. Assessing contextual descriptive features for plot-based classification of urban areas. *Landscape and Urban Planning,* 106(1), pp. 124-137.

Hermosilla, T., Palomar-Vázquez, J., Balaguer-Beser, T., Balsa-Barreiro, J. and Ruiz, L.A., 2014. Using street based metrics to characterize urban typologies. *Computers, Environment and Urban Systems,* 44, pp. 68-79.

Heutschi, K., 1995. A simple method to evaluate the increase of traffic noise emission level due to buildings, for a long straight street. *Applied Acoustics,* 44(3), pp. 259-274.

Hii, D.J.C., Heng, C.K., Malone-Lee, L.C., Zhang, J., Ibrahim, N., Huang, Y.C. and Janssen, P., 2011. Solar radiation performance evaluation for high density urban forms in the tropical context. *Proceedings of Building Simulation 2011: 12th Conference of International Building Performance Simulation Association*, pp. 2595.

Hillier, B., 1996. *Space is the machine*. Cambridge: Cambridge University Press.

Hillier, B. and Hanson, J., 1984. *The Social Logic of Space*. Cambridge: Cambridge University Press.

Hofierka, J. and Zlocha, M., 2012. A new 3D solar radiation model 3D city models. *Transactions in GIS*, 16(5), pp. 681-690.

Höppe, P., 1999. The physiological equivalent temperature - A universal index for the biometeorological assessment of the thermal environment. *International journal of biometeorology,* 43(2), pp. 71-75.

Horvat, M. and Dubois, M.-C., 2012. Tools and methods for solar design – an overview of IEA SHC Task 41, Subtask B. *Energy Procedia*, 30, pp. 1120-1130.

Huang, J., Lu, X.X. and Sellers, J.M., 2007. A global comparative analysis of urban form: Applying spatial metrics and remote sensing. *Landscape and Urban Planning,* 82(4), pp. 184-197.

I

IEA SHC Task 51 Solar Energy in Urban Planning (2013-2017). International Energy Agency: Solar Heating Cooling programme (http://task51.iea-shc.org/).

Inostroza, L., Baur, R. and Csaplovics, E., 2013. Urban sprawl and fragmentation in Latin America: A dynamic quantification and characterization of spatial patterns. *Journal of environmental management,* 115, pp. 87-97.

International Energy Agency, 2014. *World Energy Outlook*. Paris: OECD Publishing.

J

Jabareen, Y.R., 2006. Sustainable Urban Forms: Their Typologies, Models, and Concepts. *Journal of Planning Education and Research,* 26(1), pp. 38-52.

Jacobs, J., 1993. *The death and life of great American cities*. New York: The Modern Library.

Jakubiec, J.A. and Reinhart, C.F., 2011. DIVA 2.0: Integrating daylight and thermal simulations using Rhinoceros 3D, Daysim and EnergyPlus. *BS2011 - 12th International Conference of International Building Performance Simulation Association*. Sydney, Australia, 14-16 November 2011.

Jakubiec, J.A. and Reinhart, C.F., 2013. A method for predicting city-wide electricity gains from photovoltaic panels based on LiDAR and GIS data combined with hourly Daysim simulations. *Solar Energy,* 93, pp. 127-143.

Jenks, M., Burton, E. and Williams, K., (eds.) 1996. *The Compact City: A sustainable Urban Form?* London: E & FN Spon.

Johansson, E., 2006. Influence of urban geometry on outdoor thermal comfort in a hot dry climate: A study in Fez, Morocco. *Building and Environment,* 41(10), pp. 1326-1338.

Johansson, E. and Emmanuel, R., 2006. The influence of urban design on outdoor thermal comfort in the hot, humid city of Colombo, Sri Lanka. *International journal of biometeorology,* 51(2), pp. 119-133.

Johansson, L., Onomura, S., Lindberg, F. and Seaquist, J., 2015. Towards the modelling of pedestrian wind speed using high-resolution digital surface models and statistical methods. *Theoretical and Applied Climatology*, 124(1), pp. 189-203.

K

Kakon, A.N., Mishima, N. and Kojima, S., 2009. Simulation of the urban thermal comfort in a high density tropical city: Analysis of the proposed urban construction rules for Dhaka, Bangladesh. *Building Simulation,* 2(4), pp. 291-305.

Knowles, R.L., 1974. *Energy and Form*. Cambridge, Massachussetts: The MIT Press.

Knowles, R.L., 1981. *Sun Rhythm Form*. Cambridge, Massachussetts: The MIT Press.

Kolokotroni, M., Giannitsaris, I. and Watkins, R., 2006. The effect of the London urban heat island on building summer cooling demand and night ventilation strategies. *Solar Energy,* 80(4), pp. 383-392.

Kolokotroni, M., Ren, X., Davies, M. and Mavrogianni, A., 2012. London's urban heat island: Impact on current and future energy consumption in office buildings. *Energy and Buildings,* 47, pp. 302-311.

Kristl, Ž. and Krainer, A., 2001. Energy evaluation of urban structure and dimensioning of building site using iso-shadow method. *Solar Energy,* 70(1), pp. 23-34.

Krüger, E.L., Minella, F.O. and Rasia, F., 2011. Impact of urban geometry on outdoor thermal comfort and air quality from field measurements in Curitiba, Brazil. *Building and Environment,* 46(3), pp. 621-634.

Krüger, E., Drach, P., and Broede, P., 2016. Outdoor comfort study in Rio de Janeiro: site-related context on reported thermal sensation. *International Journal of Biometeorology*, [Article in press].

L

Lau, K.K.-L., Lindberg, F., Rayner, D. and Thorsson, S., 2015. The effect of urban geometry on mean radiant temperature under future climate change: a study of three European cities. *International journal of biometeorology,* 59(7), pp. 799-814.

Lee, K.S., Lee, J.W. and Lee, J.S., 2016. Feasibility study on the relation between housing density and solar accessibility and potential uses. *Renewable Energy,* 85, pp. 749-758.

Leung, K. S., 2009. Rediscovering urban vernacular for high-density housing in the tropics. *International Conference on Planning for Low Carbon Cities*, Hong Kong, 22-23 May 2009.

Li, D., Liu, G. and Liao, S., 2015. Solar potential in urban residential buildings. *Solar Energy*, 111, pp. 225–235.

Lin, T.-P., Matzarakis, A. and Hwang, R.-L., 2010. Shading effect on long-term outdoor thermal comfort. *Building and Environment,* 45(1), pp. 213-221.

Lindberg, F. and Grimmond, G.S.B., 2010. Continuous sky view factor maps from high resolution urban digital elevation models. *Climate Research*, 42, pp. 177-183.

Lindberg, F. and Grimmond, G.S.B., 2011a. Nature of vegetation and building morphology characteristics across a city: Influence on shadow patterns and mean radiant temperatures in London. *Urban Ecosystems*, 14(4), pp. 617–634.

Lindberg, F. and Grimmond, C.S.B., 2011b. The influence of vegetation and building morphology on shadow patterns and mean radiant temperatures in urban areas: Model development and evaluation. *Theoretical and Applied Climatology,* 105(3), pp. 311-323.

Lindberg, F., Holmer, B. and Thorsson, S., 2008. SOLWEIG 1.0 - Modelling spatial variations of 3D radiant fluxes and mean radiant temperature in complex urban settings. *International journal of biometeorology,* 52(7), pp. 697-713.

Lindberg, F., Holmer, B., Thorsson, S. and Rayner, D., 2014. Characteristics of the mean radiant temperature in high latitude cities-implications for sensitive climate planning applications. *International journal of biometeorology,* 58(5), pp. 613-627.

Lindberg, F., Jonsson, P., Honjo, T. and Wästberg, D., 2015. Solar energy on building envelopes - 3D modelling in a 2D environment. *Solar Energy,* 115, pp. 369-378.

Lindberg, F., Onomura, S. and Grimmond, G.S.B., 2016. Influence of ground surface characteristics on the mean radiant temperature in urban areas. *International Journal of Biometeorology*, 60(9), pp. 1439-1452.

Littlefair, P., 1998. Passive solar urban design: ensuring the penetration of solar energy into the city. *Renewable and Sustainable Energy Reviews*, 2(3), pp. 303-326.

Littlefair, P., 2001. Daylight, sunlight and solar gain in the urban environment. *Solar Energy*, 70(3), pp. 177-185.

Littlefair, P., 2011. *Site layout planning for daylight and sunlight: A Guide to good practice, BRE209*. 2nd ed. Garston: BRE.

Littlefair, P.J., Santamouris, M., Alvarez, S., Dupagne, A., Hall, D., Teller, J., Coronel, J.F. and Papanikolaou, N., 2000. *Environmental site layout planning: solar access, microclimate in urban areas, BRE308*. Garston: BRE.

London Plan. London of Mayor, London Assembly. Available at: https://www.london.gov.uk/what-we-do/planning/london-plan/current-london-plan [Accessed 9 January 2017].

LSE cities, 2014. *Cities and Energy. Urban Morphology and Heat Energy Demand.* Final Report [pdf]. London: The London School of Economics and Political Science. Available at: https://files.lsecities.net/files/2014/03/LSE-Cities-EIFER-2011-Morphology-and-Energy-Report1.pdf [Accessed on 9 January 2017].

Lu, M. and Du, J., 2013. Assessing the daylight and sunlight availability in high-density residential areas: a case in North-east China. *Architectural Science Review*, 56(2), pp. 168-182.

M

Malinverni, E.S., 2011. Change detection applying landscape metrics on high remote sensing images. *Photogrammetric Engineering and Remote Sensing,* 77(10), pp. 1045-1056.

March, L. and Steadman, L., 1971. *The geometry of the environment*. London: RIBA Publications.

Mardaljevic, J., 2010. Multi-Scale Climate-Based Daylight Modelling. *SEUS - Solar Energy at Urban Scale*, Compiègne, France, 25-26 May 2010, pp. 46-51. Available at: https://www.utc.fr/fileadmin/user_upload/SITE-UTC/documents/Presse/Evenements/abstract_seus.pdf [Accessed 9 January 2017].

Mardaljevic, J. and Rylatt, M., 2003. Irradiation mapping of complex urban environments: an image-based approach. *Energy and Buildings*, 35(1), pp. 27-35.

Marshall, S., 2009. *Cities, design and evolution*. Abingdon: Routledge.

Martin, L. and March, L., (eds.) 1972. *Urban spaces and structures.* Cambridge: Cambridge University Press.

Martinelli, L., Lin, T.-P. and Matzarakis, A., 2015. Assessment of the influence of daily shadings pattern on human thermal comfort and attendance in Rome during summer period. *Building and Environment,* 92, pp. 30-38.

Martins, T.A.I., Adolphe, L., and Bastos, L.E.G., 2014. From solar constraints to urban design opportunities: Optimization of built form typologies in a Brazilian tropical city. *Energy and Buildings*, 76, pp. 43–56.

Matzarakis, A., Mayer, H. and Iziomon, M.G., 1999. Applications of a universal thermal index: physiological equivalent temperature. *International Journal of Biometeorology*, 43, pp. 76–84.

Matzarakis, A., Rutz, F. and Mayer, H., 2007. Modelling radiation fluxes in simple and complex environments - Application of the RayMan model. *International journal of biometeorology,* 51(4), pp. 323-334.

Matzarakis, A., Rutz, F. and Mayer, H., 2010. Modelling radiation fluxes in simple and complex environments: Basics of the RayMan model. *International journal of biometeorology,* 54(2), pp. 131-139.

Mavrogianni, A., Davies, M., Batty, M., Belcher, S.E., Bohnenstengel, S.I., Carruthers, D., Chalabi, Z., Croxford, B., Demanuele, C., Evans, S., Giridharan, R., Hacker, J.N., Hamilton, I., Hogg, C., Hunt, J., Kolokotroni, M., Martin, C., Milner, J., Rajapaksha, I., Ridley, I., Steadman, J.P., Stocker, J., Wilkinson, P. and Ye, Z., 2011. The comfort, energy and health implications of London's urban heat island. *Building Services Engineering Research and Technology,* 32(1), pp. 35-52.

Mees, P., 2009. *Transport for Suburbia: Beyond the automobile age*. London: Earthscan.

Mennis, J., 2006. Socioeconomic-vegetation relationships in urban, residential land: The case of Denver, Colorado. *Photogrammetric Engineering and Remote Sensing,* 72(8), pp. 911-921.

Mohajeri, N., Upadhyay, G., Gudmundsson, A., Assouline, D., Kämpf, J. and Scartezzini, J.-L., 2016. Effects of urban compactness on solar energy potential. *Renewable Energy*, 93, pp. 469–482.

Montavon, M., Scartezzini, J.-L. and Compagnon, R., 2004. Comparison of the solar energy utilisation potential of different urban environments. *PLEA2004 – 21st International Conference on Passive and Low Energy Architecture*. Eindhoven, The Netherlands, 19-22 September 2004.

Morello, E. and Ratti, C., 2009. Sunscapes: 'Solar envelopes' and the analysis of urban DEMs. *Computers, Environment and Urban Systems,* 33(1), pp. 26-34.

N

Nault, E., Peronato, G., Rey, E. and Andersen, M., 2015. Review and critical analysis of early-design phase evaluation metrics for the solar potential of neighborhood designs. *Building and Environment*, 92, pp. 679–691.

Newman, P. and Kenworthy, J., 2000. Sustainability and Cities: Overcoming Automobile Dependence. Washington: Island Press.

Ng, E. and Wong, N.H., 2004. Better daylight and natural ventilation by design. *PLEA2004 – 21st International Conference on Passive and Low Energy Architecture*. Eindhoven, The Netherlands, 19-22 September 2004.

Ng, E. and Wong, H.-H., 2005. Building heights and better ventilated design for high density cities. *PLEA2005 - 22nd International Conference on Passive and Low Energy Architecture.* Lebanon, 13-16 November 2005, pp. 607.

Ng, E., Yuan, C., Chen, L., Ren, C. and Fung, J.C.H., 2011. Improving the wind environment in high-density cities by understanding urban morphology and surface roughness: A study in Hong Kong. *Landscape and Urban Planning,* 101(1), pp. 59-74.

Nikolopoulou, M., 2012. Urban open spaces and adaptation to climate change. In: Richter, M. and Weiland, U., (eds.) *Applied Urban Ecology*. Chichester: Wiley-Blackwell, pp.106-122.

Nikolopoulou, M. and Lykoudis, S., 2007. Use of outdoor spaces and microclimate in a Mediterranean urban area. *Building and Environment,* 42(10), pp. 3691-3707.

Nikolopoulou, M. and Steemers, K., 2003. Thermal comfort and psychological adaptation as a guide for designing urban spaces. *Energy and Buildings,* 35(1), pp. 95-101.

Nikolopoulou, M., Baker, N. and Steemers, K., 2001. Thermal comfort in outdoor urban spaces: understanding of the human parameter. *Solar Energy,* 70(3), pp. 227-235.

NOAA Solar Position Calculator. US Department of Commerce, National Oceanic Atmospheric Administration, Earth System Research Lab. Online tool: http://www.esrl.noaa.gov/gmd/grad/solcalc/azel.html

O

Oke, T.R., 1981. Canyon geometry and the nocturnal urban heat island: Comparison of scale model and field observations. *Journal of Climatology,* 1(3), pp. 237-254.

Oke, T.R., 1987. *Boundary Layer climates*. 2nd ed. London: Routledge.

Oke, T.R., 1988. Street design and urban canopy layer climate. *Energy and Buildings*, 11(1-3), pp. 103-113.

Oke, T.R., 2006. Towards better scientific communication in urban climate. *Theoretical and Applied Climatology,* 84, pp. 179-190.

Oliveira, V. and Monteiro, C., 2015. A comparative study of urban form. *Urban Morphology*, 19(1), pp. 73-92.

Oliveira Panão, M.J.N., Gonçalves, H.J.P. and Ferrão, P.M.C., 2008. Optimization of the urban building efficiency potential for mid-latitude climates using a genetic algorithm approach. *Renewable Energy,* 33(5), pp. 887-896.

Owens, S., 1987. The urban future: Does energy really matters? In: Hawkes, D., Owers, J., Rickaby, P. and Steadman, P., (eds.) *Energy and Urban Built Form,* Butterworths: London.

P

Patino, J.E. and Duque, J.C., 2013. A review of regional science applications of satellite remote sensing in urban settings. *Computers, Environment and Urban Systems,* 37(1), pp. 1-17.

Pearlmutter, D., Bitan, A. and Berliner, P., 1999. Microclimatic analysis of “compact” urban canyons in an arid zone. *Atmospheric Environment,* 33(24-25), pp. 4143-4150.

Pearlmutter, D., Berliner, P. and Shaviv, E., 2007. Urban climatology in arid regions: Current research in the Negev desert. *International Journal of Climatology,* 27(14), pp. 1875-1885.

Peeters, A. and Etzion, Y., 2012. Automated recognition of urban objects for morphological urban analysis. *Computers, Environment and Urban Systems,* 36(6), pp. 573-582.

Peng, S., Piao, S., Ciais, P., Friedlingstein, P., Ottle, C., Bréon, F.-M., Nan, H., Zhou, L. and Myneni, R.B., 2011. Surface urban heat island across 419 global big cities. *Environmental Science and Technology*, 46(2), pp. 696-703.

Population Reference Bureau, 2015. World Population Data Sheet. Available at: http://www.prb.org/Publications/Datasheets/2015/2015-world-population-data-sheet.aspx [Accessed 9 January 2017].

Potvin, A., Demers, C. and Paré, M.P., 2009. Microclimatic performance of urban developments: a simplified analysis and representation technique. *PLEA2009 - 26th International Conference on Passive and Low Energy Architecture.* Quebec City, Canada, 22-24 June 2009.

Project PREcis, 2000. *PREcis: Assessing the Potential for Renewable Energy in Cities*. Final report, Project no. JOR3-CT97-0192, 2000.

Project RUROS, 2004. *RUROS: Rediscovering the urban realm and open spaces*. Final Report. Athens: Centre for renewable resources.

Project ZED, 1997. *Project ZED: Towards Zero Emission Urban Development*. Final report, Project no. APAS-RENA CT94-00016, 1997.

Przybylak, R., Uscka-Kowalkowska J., Araźny, A., Kejna M., Kunz, M. and Maszewski, R., 2017. Spatial distribution of air temperature in Toruń (Central Poland) and its causes. *Theoretical and Applied Climatology*, 127(1), pp. 441-463.

R

Ratti, C., 2001. *Urban analysis for environmental prediction*. Ph.D. Thesis, University of Cambridge, UK.

Ratti, C., 2004. *Space syntax: Some inconsistencies*. *Environment and Planning B: Planning and Design,* 31(4), pp. 487-499.

Ratti, C., 2005. The lineage of the line: Space syntax parameters from the analysis of urban DEMs. *Environment and Planning B: Planning and Design,* 32(4), pp. 547-566.

Ratti, C. and Richens, P., 1999. Urban texture analysis with image processing techniques. In: Augenbroe, G. and Eastman, C., (eds). *Computers in Building: Proceedings of CAAD Futures 99*. Boston: Kluwer Academic, pp. 49-64.

Ratti, C. and Richens, P., 2004. Raster analysis of urban form. *Environment and Planning B: Planning and Design,* 31(2), pp. 297–309.

Ratti, C., Raydan, D. and Steemers, K., 2003. Building form and environmental performance: Archetypes, analysis and an arid climate. *Energy and Buildings,* 35(1), pp. 49-59.

Ratti, C., Baker, N. and Steemers, K., 2005. Energy consumption and urban texture. *Energy and Buildings,* 37(7), pp. 762-776.

Ratti, C., Di Sabatino, S. and Britter, R., 2006. Urban texture analysis with image processing techniques: Winds and dispersion. *Theoretical and Applied Climatology,* 84(1), pp. 77-90.

Redweik, P., Catita, C. and Brito, M., 2013. Solar energy potential on roofs and facades in an urban landscape. *Solar Energy*, 97, pp. 332-341.

Remund, J., Müller, S., Kunz, S., Huguenin-Landl, B., Studer, C., Klauser, D., Schilter, C. and Lehnherr, R., 2015. *METEONORM – Global Meteorological Database, Handbook Part I & II, Version 7*. Bern: Meteotest & Swiss Federal Office for Energy. Available at: http://www.meteonorm.com/en/downloads/documents [Accessed 25 March 2016].

Richens, P., 1997. Image processing for urban scale environmental modelling. *In: Proc 5th International IBPSA Conference: Building Simulation 97*. Prague, Czech Republic, 8-10 September 1997.

Robinson, D., 2006. Urban morphology and indicators of radiation availability. *Solar Energy*, 80, pp. 1643–1648.

Robinson, D. and Stone, A., 2005. A simplified radiosity algorithm for general urban radiation exchange. *Building Services Engineering Research and Technology*, 26(4), pp. 271–284.

Robinson D., Campbell, N., Gaiser, W., Kabel, K., Le-Mouel A., Morel, N., Page, J., Stankovic, S. and Stone, A., 2007. SUNtool – A new modelling paradigm for simulating and optimising urban sustainability. *Solar Energy*, 81(9), pp. 1196-1211

Robinson, D., Haldi, F., Kämpf, J., Leroux, P., Perez, D., Rasheed, A. and Wilke, U., 2009. CitySim: Comprehensive micro-simulation of resource flows for sustainable urban planning. *In: Proc 11th International IBPSA Conference, Building Simulation 2009*. Glasgow, Scotland, 27-30 July 2009.

Rode, P., Keim, C., Robazza, G., Viejo, P. and Schofield, J., 2014. Cities and energy: Urban morphology and residential heat-energy demand. *Environment and Planning B: Planning and Design,* 41(1), pp. 138-162.

Rylatt, R.M., Gadsden, S. and Lomas, K., 2003a. Using GIS to estimate the replacement potential of solar energy for urban dwellings. *Environment and Planning B: Planning and Design,* 30(1), pp. 51-68.

Rylatt, R.M., Gadsden, S.J. and Lomas, K.J. 2003b. Methods of predicting urban domestic energy demand with reduced datasets: A review and a new GIS-based approach. *Building Services Engineering Research and Technology,* 24(2), pp. 93-102.

Ryu, H., Park, I.K., Chun, B.S. and Chang, S.I., 2017. Spatial statistical analysis of the effects of urban form indicators on road-traffic noise exposure of a city in South Korea. *Applied Acoustics*, 115, pp. 93-100.

S

Salat, S., 2009. Energy loads, CO2 emissions and building stocks: morphologies, typologies, energy systems, and behaviour. *Building Research and Information*, 35(7), pp. 589-609.

Salat, S. and Bourdic, L., 2011. Power Laws for Energy Efficient and Resilient Cities. *Procedia Engineering,* 21, pp. 1193-1198.

Salat, S. and Nowacki, C., 2010. De l'importance de la morphologie dans l'efficience énergétique des villes. *Liaison énergie-francophonie*, 86, pp. 141-146.

Salat, S., Bourdic, L. and Nowacki, C., 2010. Assessing urban complexity. Technical Report. *SUSB Journal* 2(1), pp. 160-167. Available at: http://www.urbanmorphologyinstitute.org/resources/assessing-urban-complexity/ [Accessed 6 December 2016].

Sanaieian, H., Tenpierik, M., Linden, K. Van Den, Mehdizadeh Seraj, F. and Mofidi Shemrani, S.M., 2014. Review of the impact of urban block form on thermal performance, solar access and ventilation. *Renewable and Sustainable Energy Reviews*, 38, pp. 551–560.

Santamouris, M., 2001. The canyon effect. In: Santamouris, M., (ed.) *Energy and climate in the urban built environment*. London: James & James Publisher, pp. 69-96.

Santamouris, M., 2015. Analyzing the heat island magnitude and characteristics in one hundred Asian and Australian cities and regions. *Science of the Total Environment,* 512-513, pp. 582-598.

Santamouris, M., Papanikolaou, N., Livada, I., Koronakis, I., Georgakis, C., Argiriou A. and Assimakopoulos, D.N., 2001. On the impact of urban climate on the energy consumption of buildings. *Solar Energy*, 70(3), pp. 201-216.

Sarralde, J.J., Quinn, D.J., Wiesmann, D. and Steemers, K., 2015. Solar energy and urban morphology: Scenarios for increasing the renewable energy potential of neighbourhoods in London. *Renewable Energy*, 73, pp. 10–17.

Schirmer, P.M. and Axhausen, K.W., 2016. A multiscale classification of urban morphology. *Journal of Transport and Land Use,* 9(1), pp. 101-130.

Service de la Topographie et de la Documentation Foncière, Mairie de Paris. Online database: https://www.data.gouv.fr [Shapefile downloaded March 2014].

Shahrestani, M., Yao, R., Luo, Z., Turkbeyler, E. and Davies H., 2015. A field study in urban microclimates in London. *Renewable Energy*, 73, pp. 3-9.

Sharmin, T., Steemers, K. and Matzarakis, A., 2015. Analysis of microclimatic diversity and outdoor thermal comfort perceptions in the tropical megacity Dhaka, Bangladesh. *Building and Environment,* 94, pp. 734-750.

Simms, R.W., Djokic, S.Z. and Murray, A.F., 2008. Renewable generation in the London built environment. *Journal of Energy Engineering,* 134(2), pp. 71-79.

Space Syntax. Website: http://www.spacesyntax.com

Steadman, P., 2014. Density and built form: Integrating 'Spacemate' with the work of Martin and March. *Environment and Planning B: Planning and Design,* 41(2), pp. 341-358.

Steadman, P., Evans, S. and Batty, M., 2009. Wall area, volume and plan depth in the building stock. *Building Research and Information,* 37(5-6), pp. 455-467.

Steadman, P., Hamilton, I. and Evans, S., 2014. Energy and urban built form: An empirical and statistical approach. *Building Research and Information,* 42(1), pp. 17-31.

Steemers, K., 2003. Energy and the city: Density, buildings and transport. *Energy and Buildings*, 35, pp. 3–14.

Steane, M.A. and Steemers, K. 2004. Environmental diversity in architecture. In: Steemers, K. and Steane M.A., (eds.) *Environmental Diversity in Architecture*. London: Spon Press, pp.3-16.

Steemers, K., Baker, N., Crowther, J., Dubiel, J., Nikolopoulou, M. and Ratti, C., 1997. City texture and microclimate. *Urban Design Studies*, 3, pp. 25-50.

Steemers, K., Baker, N., Crowther, D., Dubiel, J. and Nikolopoulou, M., 1998. Radiation absorption and urban texture. *Building Research and Information,* 26(2), pp. 103-112.

Steemers, K., Ramos, M. and Sinou, M., 2004a. Urban diversity. In: Steemers, K. and Steane, M.A., (eds.) *Environmental Diversity in Architecture*. London: Spon Press, pp.85-100.

Steemers, K., Ramos, M. and Sinou, M., 2004b. Urban Morphology. In: Marialena, N., (ed.) *Designing open spaces in the urban environment*. Report. Project RUROS. Athens: CRES, pp.17-21. Available at: http://www.cres.gr/kape/education/1.design_guidelines_en.pdf [Accessed 9 January 2017].

Steyn, D.G., 1980. The calculation of view-factors from fisheye-lens photographs: Research note. *Atmosphere-Ocean*, 18(3), pp. 254-258.

Strano, E., Viana, M., Costa, L.F., Cardillo, A., Porta, S. and Latora, V., 2013. Urban street networks, a comparative analysis of ten European cities. *Environment and Planning B: Planning and Design,* 40(6), pp. 1071-1086.

Strømann-Andersen, J. and Sattrup, P.A., 2011. The urban canyon and building energy use: Urban density versus daylight and passive solar gains. *Energy and Buildings,* 43(8), pp. 2011-2020.

Šúri, M. and Hofierka, J., 2004. A new GIS-based solar radiation model and its application to photovoltaic systems. *Transactions in GIS*, 8, pp. 175-190.

T

Taubenböck, H., Wegmann, M., Roth, A., Mehl, H. and Dech, S., 2009. Urbanization in India - Spatiotemporal analysis using remote sensing data. *Computers, Environment and Urban Systems,* 33(3), pp. 179-188.

Teller, J. and Azar, S., 2001. TOWNSCOPE II – A computer system to support solar access decision-making. *Solar Energy*, 70(3), pp. 187-200.

Thomas, I. and Frankhauser, P., 2013. Fractal dimensions of the built-up footprint: Buildings versus roads. Fractal evidence from Antwerp (Belgium). *Environment and Planning B: Planning and Design,* 40(2), pp. 310-329.

Thomas, I., Frankhauser, P. and Biernacki, C., 2008. The morphology of built-up landscapes in Wallonia (Belgium): A classification using fractal indices. *Landscape and Urban Planning,* 84(2), pp. 99-115.

Thompson, C.W., 2002. Urban open space in the 21st century. *Landscape and Urban Planning*, 60(2), pp. 59-72.

Thorsson, S., Lindberg, F., Björklund, J., Holmer, B. and Rayner, D., 2011. Potential changes in outdoor thermal comfort conditions in Gothenburg, Sweden due to climate change: The influence of urban geometry. *International Journal of Climatology,* 31(2), pp. 324-335.

Tian, W., Song, J. and Li, Z., 2014. Spatial regression analysis of domestic energy in urban areas. *Energy,* 76, pp. 629-640.

Tian, W., Liu, Y., Heo, Y., Yan, D., Li, Z., An, J. and Yang, S., 2016. Relative importance of factors influencing building energy in urban environment. *Energy,* 111, pp. 237-250.

Tompalski, P. and Woyk, P., 2012. Lidar and VHRS data for assessing living quality in cities - An approach based on 3D spatial indices. *International Archives of the Photogrammetry, Remote Sensing and Spatial Information Sciences - ISPRS Archives*, pp. 173.

Tooke, T.R., Coops, N.C. and Webster, J., 2014a. Predicting building ages from LiDAR data with random forests for building energy modelling. *Energy and Buildings,* 68 (Part A), pp. 603-610.

Tooke, T.R., van der Laan, M. and Coops, N.C., 2014b. Mapping demand for residential building thermal energy services using airborne LiDAR. *Applied Energy,* 127, pp. 125-134.

Tzavali, A., Paravantis, J.P., Mihalakakou, G., Fotiadi, A. and Stigka, E., 2015. Urban heat island intensity: A literature review. *Fresenius Environmental Bulletin,* 24(12B), pp. 4537-4554.

U

UN-Habitat, 2008. State of the world's cities 2008/2009: harmonious cities. London: United Nations Human Settlements Programme. Available at: http://mirror.unhabitat.org/pmss/listItemDetails.aspx?publicationID=2562&AspxAutoDetectCookieSupport=1 [Accessed 9 January 2017].

Unger, J., 2006. Modelling of the annual mean maximum urban heat island using 2D and 3D surface parameters. *Climate Research,* 30(3), pp. 215-226.

Urban Task Force, 1999. *Towards an urban renaissance*. Report for Department of the Environment, Transport and The regions, London, UK.

V

Van Esch, M.M.E., Looman, R.H.J. and De Bruin-Hordijk, G.J., 2012. The effects of urban and building design parameters on solar access to the urban canyon and the potential for direct passive solar heating strategies. *Energy and Buildings,* 47, pp. 189-200.

Vermeulen, T., Knopf-Lenoir, C., Villon, P. and Beckers, B., 2015. Urban layout optimization framework to maximize direct solar irradiation. *Computers, Environment and Urban Systems,* 51, pp. 1-12.

W

Wall, M., Probst, M.C.M., Roecker, C., Dubois, M.-C., Horvat, M., Jørgensen, O.B. and Kappel, K., 2012. Achieving solar energy in architecture – IEA SHC Task 41. *Energy Procedia*, 30, 1250–1260.

Walton, D., Dravitzki, V. and Donn, M., 2007. The relative influence of wind, sunlight and temperature on user comfort in urban outdoor spaces. *Building and Environment,* 42(9), pp. 3166-3175.

Wang, Y. and Akbari, H., 2014. Effect of sky view factor on outdoor temperature and comfort in Montreal. *Environmental Engineering Science*, 31(6), pp.272-287.

Ward Larson, G. and Shakespeare, R., 1998. *Rendering with Radiance: The Art and Science of Lighting Visualisation*. San Francisco: Morgan Haufmann.

Watkins, R., Palmer, J., Kolokotroni, M. and Littlefair, P., 2002. The London heat island: Results from summertime monitoring. *Building Services Engineering Research and Technology,* 23(2), pp. 97-106.

Watkins, R., Palmer, J. and Kolokotroni, M., 2007. Increased temperature and intensification of the urban heat island: Implications for human comfort and urban design. *Built Environment,* 33(1), pp. 85-96.

Watson, I.D. and Johnson, G.T., 1987. Graphical estimation of sky view-factors in urban environments. *Journal of Climatology,* 7(2), pp. 193-197.

WBCSD, 2009. *Energy efficiency in buildings: transforming the market*. World Business Council for Sustainable Development. Available at: http://www.wbcsd.org/Projects/Energy-Efficiency-in-Buildings/Resources/Transforming-the-Market-Energy-Efficiency-in-Buildings [Accessed 9 January 2017].

Wheeler, S.M., 2015. Built Landscapes of Metropolitan Regions: An International Typology. *Journal of the American Planning Association,* 81(3), pp. 167-190.

Williams, K., Burton, E. and Jenks, M., (eds.) 2000. *Achieving Sustainable Urban Form*. London: Spon Press.

X

Y

Yamashita, S., Sekine K., Shoda M., Yamashita, K., and Hara, Y., 1986. On relationships between heat island and sky view factor in the cities of Tama River basin, Japan. *Atmospheric Environment*, 20(4), pp. 681-686.

Yang, F. and Chen, L., 2016. Developing a thermal atlas fir climate-responsive urban design based on empirical modelling and urban morphological analysis. *Energy and Buildings*, 111, p. 120-130.

Yoshida, H. and Omae, M., 2005. An approach for analysis of urban morphology: Methods to derive morphological properties of city blocks by using an urban landscape model and their interpretations. *Computers, Environment and Urban Systems,* 29(2), pp. 223-247.

Yu, B., Liu, H., Wu, J. and Lin, W., 2009. Investigating impacts of urban morphology on spatio-temporal variations of solar radiation with airborne LIDAR data and a solar flux model: A case study of downtown Houston. *International Journal of Remote Sensing,* 30(17), pp. 4359-4385.

Yuan, C. and Ng, E., 2012. Building porosity for better urban ventilation in high-density cities – A computational parametric study. *Building and Environment,* 50, pp. 176-189.

Z

Zhang, J., Heng, C.K., Malone-Lee, L.C., Hii, D.J.C., Janssen, P., Leung, K.S. and Tan, B.K., 2012. Evaluating environmental implications of density: A comparative case study on the relationship between density, urban block typology and sky exposure. *Automation in Construction,* 22, pp. 90-101.

Appendices

Appendix A: Monthly weather data for London and Paris.

Climate data for London, 1981-2010													
Month	**Jan**	**Feb**	**Mar**	**Apr**	**May**	**Jun**	**Jul**	**Aug**	**Sep**	**Oct**	**Nov**	**Dec**	**Year**
Average high, [°C] [1]	8.5	8.9	11.7	15.7	18.6	22.4	23.6	23.2	20.8	16.1	11.9	8.6	15.8
Daily mean, [°C] [1]	6.8	6.8	8.8	12	14.8	18.3	19.6	19.4	17.3	13.5	10	7	12.8
Average low, [°C] [1]	5	4.7	5.8	8.2	10.9	14.1	15.5	15.5	13.7	10.9	8	5.4	9.8
Average precipitation, [mm] [2]	55.2	40.9	41.6	43.7	49.4	45.1	44.5	49.5	49.1	68.5	59	55.2	601.7
Average precipitation, [days] [2]	11.1	8.5	9.3	9.1	8.8	8.2	7.7	7.5	8.1	10.8	10.3	10.2	109.5
Mean monthly sunshine hours [2]	61.5	77.9	114.6	168.7	198.5	204.3	212	204.7	149.3	116.5	72.6	52	1,632.60

[1] Source: London Weather Center analysis. Retrieved 17 November 2014

[2] Source: London Heathrow Airport Met Office. Retrieved 17 November 2014

Climate data for Paris (Parc Montsouris), 1981-2010													
Month	**Jan**	**Feb**	**Mar**	**Apr**	**May**	**Jun**	**Jul**	**Aug**	**Sep**	**Oct**	**Nov**	**Dec**	**Year**
Average high, [°C]	7.2	8.3	12.2	15.6	19.6	22.7	25.2	25	21.1	16.3	10.8	7.5	16
Daily mean, [°C]	5	5.6	8.8	11.5	15.3	18.3	20.6	20.4	16.9	13	8.3	5.5	12.5
Average low, [°C]	2.7	2.8	5.3	7.3	10.9	13.8	15.8	15.7	12.7	9.6	5.8	3.4	8.5
Average precipitation mm	53.7	43.7	48.5	53	65	54.6	63.1	43	54.7	59.7	51.9	58.7	649.6
Average precipitation days	10.2	9.3	10.4	9.4	10.3	8.6	8	6.9	8.5	9.5	9.7	10.7	111.5
Mean monthly sunshine hours	62.5	79.2	128.9	166	193.8	202.1	212.2	212.2	167.9	117.8	67.7	51.4	1,661.70

Source: Meteo France

(Data obtained online from https://en.wikipedia.org/)

Appendix B: DEMs of 24 urban forms in London studied in Chapter Five.

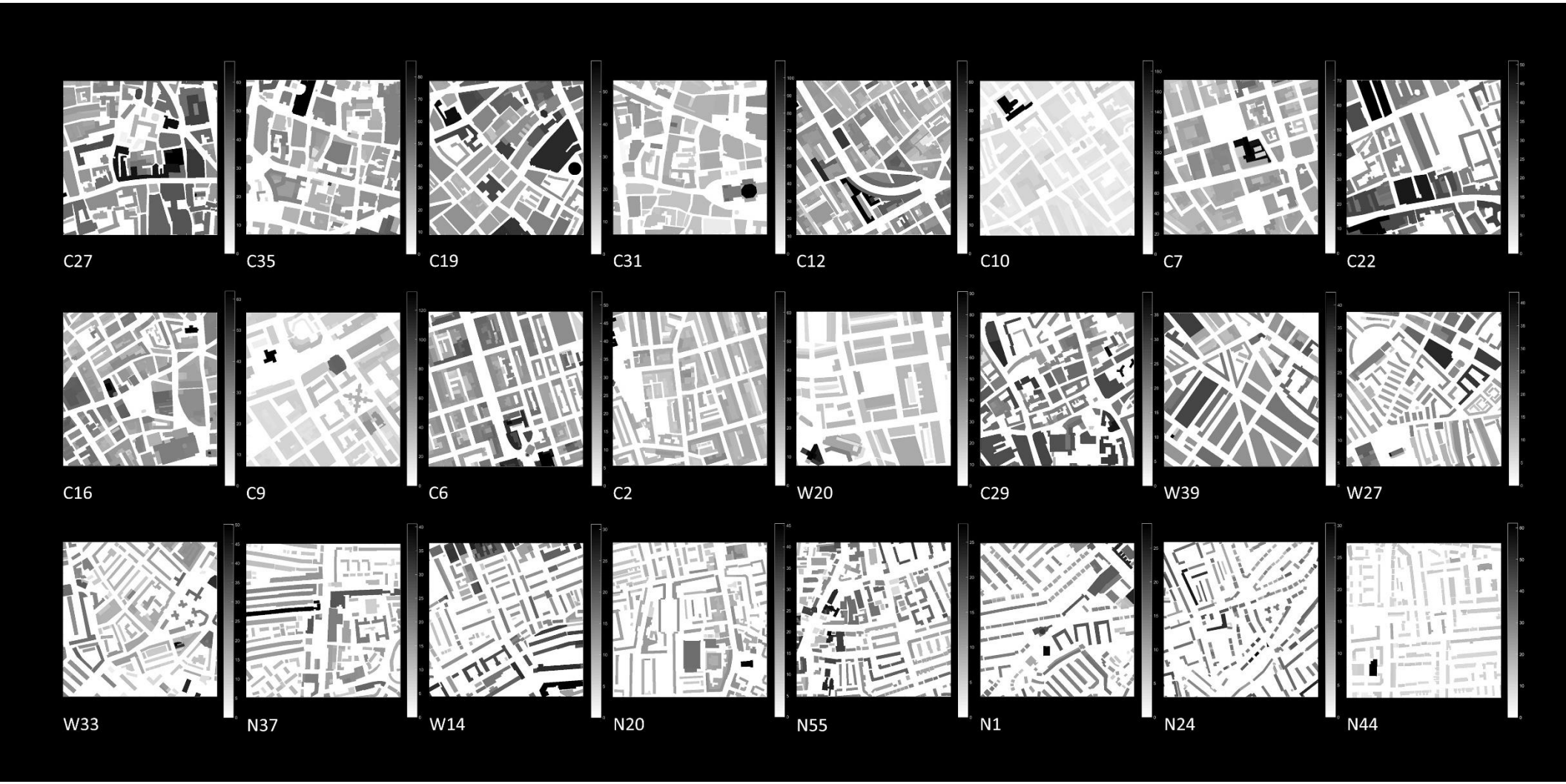

Appendix C: Algorithm for the calculation of the *directionality* variable in MATLAB.

```
% Define no. of directions considered
n=36;

% open DEM saved as .mat file
a=load('urbanDEM.mat');
a=double(a);

% convert the image into binary
a=~(~a);

[s1,s2]=size(a);

s=min(size(a));

% main core
final1=[];

x1=round((s1/2)-(s/(2*sqrt(2))));
x2=round((s2/2)-(s/(2*sqrt(2))));
x3=round((s1/2)+(s/(2*sqrt(2))));
x4=round((s2/2)+(s/(2*sqrt(2))));

for index=0:(n/2)-1
    b1=imrotate(a, (360/n)*index, 'bicubic', 'crop');
    b2=b1(x1:x3, x2:x4);
    final1=[final1 std(mean(b2)/mean(mean(b2)))];
end


dir=std(final1); % directionality value
```

Appendix D: Statistic data from the geometric analysis of London and Paris.

Table D.2. Descriptive statistics for 18 urban geometry variables computed for 72 urban forms of London.

Descriptive Statistics

LONDON	N	Range	Minimum	Maximum	Mean	Std. Deviation	Variance
Density	72	30.4	2.8	33.1	10.5	6.8	46.0
Sco	72	48.3	20.3	68.6	41.4	13.0	167.9
MeH	72	38.3	11.8	50.1	23.3	8.8	77.2
StH	72	25.3	3.2	28.5	8.7	5.5	30.8
StS	72	27.6	5.3	32.9	12.8	6.1	37.2
MaH	72	166.5	23.7	190.2	61.6	36.1	1303.2
MeD	72	9.3	4.1	13.4	7.5	1.8	3.2
StD	72	11.5	3.3	14.8	6.7	2.2	4.8
MaD	72	58.9	21.5	80.4	43.6	12.0	144.6
Com	72	0.289	0.086	0.375	0.205	0.075	0.006
Cex	72	2.181	0.742	2.922	1.314	0.427	0.183
FSt	72	7.43	0.95	8.38	2.35	1.35	1.83
NOB	72	178	37	215	94.3	43.4	1882.6
MeF	72	3292	271	3562	1248	885	782708
StF	72	4966	235	5201	1588	1167	1362958
MeV	72	184358	3352	187710	47344	46839	2193874092
StV	72	569778	3352	573131	66988	91239	8324562047
Dir	72	0.123	0.020	0.144	0.063	0.024	0.001
Valid N (listwise)	72						

Table D.3. Descriptive statistics for 18 urban geometry variables computed for 60 urban forms of Paris.

Descriptive Statistics

PARIS	N	Range	Minimum	Maximum	Mean	Std. Deviation	Variance
Density	60	6.1	5.2	11.4	8.4	1.3	1.7
Sco	60	34.7	31.9	66.6	48.3	7.4	54.9
MeH	60	6.9	14.6	21.5	17.4	1.6	2.6
StH	60	13.7	5.5	19.2	8.5	2.3	5.4
StS	60	6.1	8.7	14.8	10.4	1.0	1.1
MaH	60	72.0	28.5	100.5	42.7	14.3	203.2
MeD	60	6.3	3.1	9.4	5.8	1.5	2.1
StD	60	7.9	2.6	10.5	5.7	1.7	2.9
MaD	60	53.2	20.4	73.6	41.6	12.4	153.6
Com	60	0.099	0.224	0.323	0.280	0.024	0.00058
Cex	60	1.207	1.259	2.466	1.853	0.275	0.076
FaS	60	5.09	1.85	6.94	3.73	1.06	1.113
NoB	60	88	31	119	61.2	18.6	347.4
MeF	60	3102	674	3776	1509	727	528480
StF	60	3715	1111	4827	2435	838	702038
MeV	60	95768	10879	106647	38135	19910	396401186
StV	60	88764	24740	113504	54795	19104	364962385
Dir	60	0.060	0.020	0.080	0.046	0.014	0.00021
Valid N (listwise)	60						

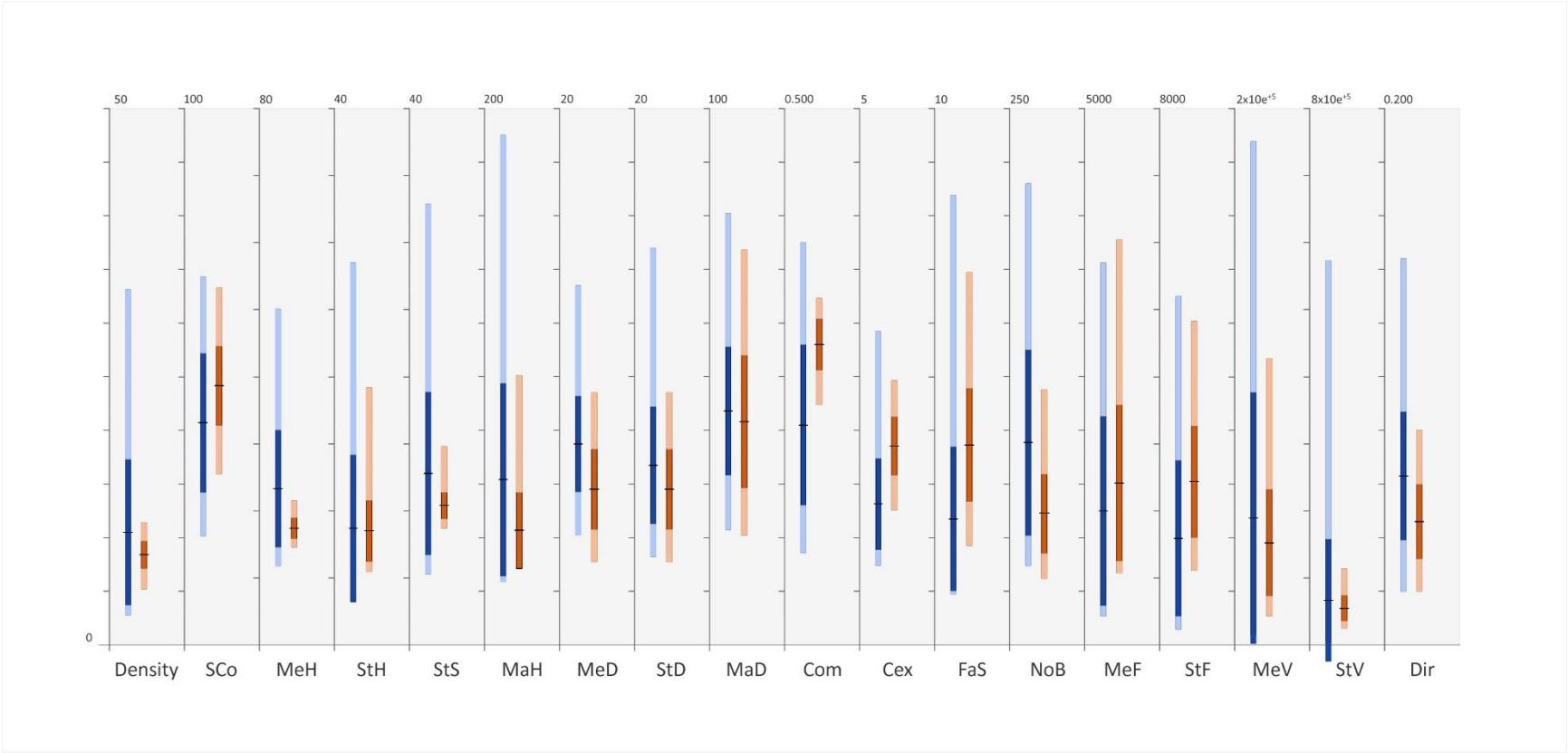

Figure D.9: Graphical visualisation of descriptive statistics for 18 urban geometry variables computed for London's (blue bars) and Paris' (orange bars) urban forms: range of values (light colour), mean values, standard deviation of values (dark colour).

*Table D.4. Pearson Correlation (two-tailed) results for 18 urban geometry variables computed for 72 urban forms of **London**.*

Correlations

		Density	Sco	MeH	StH	StS	MaH	MeD	StD	MaD	Com	Cex	FaS	NoB	MeF	StF	MeV	StV	Dir
Density	Pearson Corr.	1	.901**	.960**	.805**	.949**	.734**	-.306**	-0.070	-0.095	-.854**	.944**	.959**	-.757**	.735**	.790**	.925**	.715**	-.620**
	Sig. (2-tailed)		0.000	0.000	0.000	0.000	0.000	0.009	0.559	0.426	0.000	0.000	0.000	0.000	0.000	0.000	0.000	0.000	0.000
Sco	Pearson Corr.	.901**	1	.785**	.582**	.778**	.589**	-.389**	-0.063	-0.055	-.902**	.830**	.877**	-.829**	.892**	.839**	.849**	.633**	-.635**
	Sig. (2-tailed)	0.000		0.000	0.000	0.000	0.000	0.001	0.600	0.645	0.000	0.000	0.000	0.000	0.000	0.000	0.000	0.000	0.000
MeH	Pearson Corr.	.960**	.785**	1	.854**	.978**	.753**	-0.143	0.035	0.000	-.836**	.930**	.883**	-.746**	.613**	.721**	.884**	.689**	-.575**
	Sig. (2-tailed)	0.000	0.000		0.000	0.000	0.000	0.231	0.769	1.000	0.000	0.000	0.000	0.000	0.000	0.000	0.000	0.000	0.000
StH	Pearson Corr.	.805**	.582**	.854**	1	.932**	.904**	-0.208	-0.135	-0.162	-.614**	.794**	.743**	-.531**	.393**	.504**	.722**	.584**	-.495**
	Sig. (2-tailed)	0.000	0.000	0.000		0.000	0.000	0.079	0.257	0.174	0.000	0.000	0.000	0.000	0.001	0.000	0.000	0.000	0.000
StS	Pearson Corr.	.949**	.778**	.978**	.932**	1	.842**	-0.195	-0.028	-0.061	-.812**	.920**	.878**	-.722**	.592**	.689**	.868**	.683**	-.580**
	Sig. (2-tailed)	0.000	0.000	0.000	0.000		0.000	0.100	0.814	0.612	0.000	0.000	0.000	0.000	0.000	0.000	0.000	0.000	0.000
MaH	Pearson Corr.	.734**	.589**	.753**	.904**	.842**	1	-0.194	-0.086	-0.113	-.584**	.755**	.705**	-.540**	.462**	.444**	.643**	.393**	-.451**
	Sig. (2-tailed)	0.000	0.000	0.000	0.000	0.000		0.103	0.474	0.346	0.000	0.000	0.000	0.000	0.000	0.000	0.000	0.001	0.000
MeD	Pearson Corr.	-.306**	-.389**	-0.143	-0.208	-0.195	-0.194	1	.905**	.721**	0.077	-.364**	-.453**	-0.019	-.308**	-0.155	-0.165	-0.087	.578**
	Sig. (2-tailed)	0.009	0.001	0.231	0.079	0.100	0.103		0.000	0.000	0.519	0.002	0.000	0.876	0.009	0.193	0.167	0.466	0.000
StD	Pearson Corr.	-0.070	-0.063	0.035	-0.135	-0.028	-0.086	.905**	1	.842**	-0.198	-0.144	-0.216	-.283*	0.010	0.079	0.059	0.038	.382**
	Sig. (2-tailed)	0.559	0.600	0.769	0.257	0.814	0.474	0.000		0.000	0.096	0.227	0.068	0.016	0.933	0.507	0.623	0.752	0.001
MaD	Pearson Corr.	-0.095	-0.055	0.000	-0.162	-0.061	-0.113	.721**	.842**	1	-0.188	-0.166	-.242*	-.277*	-0.009	0.088	0.034	0.042	.239*
	Sig. (2-tailed)	0.426	0.645	1.000	0.174	0.612	0.346	0.000	0.000		0.113	0.164	0.040	0.019	0.943	0.462	0.779	0.724	0.043
Com	Pearson Corr.	-.854**	-.902**	-.836**	-.614**	-.812**	-.584**	0.077	-0.198	-0.188	1	-.769**	-.751**	.941**	-.763**	-.817**	-.808**	-.645**	.555**
	Sig. (2-tailed)	0.000	0.000	0.000	0.000	0.000	0.000	0.519	0.096	0.113		0.000	0.000	0.000	0.000	0.000	0.000	0.000	0.000
Cex	Pearson Corr.	.944**	.830**	.930**	.794**	.920**	.755**	-.364**	-0.144	-0.166	-.769**	1	.962**	-.691**	.684**	.639**	.822**	.524**	-.659**
	Sig. (2-tailed)	0.000	0.000	0.000	0.000	0.000	0.000	0.002	0.227	0.164	0.000		0.000	0.000	0.000	0.000	0.000	0.000	0.000
FaS	Pearson Corr.	.959**	.877**	.883**	.743**	.878**	.705**	-.453**	-0.216	-.242*	-.751**	.962**	1	-.661**	.724**	.684**	.845**	.573**	-.637**
	Sig. (2-tailed)	0.000	0.000	0.000	0.000	0.000	0.000	0.000	0.068	0.040	0.000	0.000		0.000	0.000	0.000	0.000	0.000	0.000
NoB	Pearson Corr.	-.757**	-.829**	-.746**	-.531**	-.722**	-.540**	-0.019	-.283*	-.277*	.941**	-.691**	-.661**	1	-.747**	-.762**	-.757**	-.569**	.452**
	Sig. (2-tailed)	0.000	0.000	0.000	0.000	0.000	0.000	0.876	0.016	0.019	0.000	0.000	0.000		0.000	0.000	0.000	0.000	0.000
MeF	Pearson Corr.	.735**	.892**	.613**	.393**	.592**	.462**	-.308**	0.010	-0.009	-.763**	.684**	.724**	-.747**	1	.788**	.763**	.481**	-.497**
	Sig. (2-tailed)	0.000	0.000	0.000	0.001	0.000	0.000	0.009	0.933	0.943	0.000	0.000	0.000	0.000		0.000	0.000	0.000	0.000
StF	Pearson Corr.	.790**	.839**	.721**	.504**	.689**	.444**	-0.155	0.079	0.088	-.817**	.639**	.684**	-.762**	.788**	1	.894**	.865**	-.495**
	Sig. (2-tailed)	0.000	0.000	0.000	0.000	0.000	0.000	0.193	0.507	0.462	0.000	0.000	0.000	0.000	0.000		0.000	0.000	0.000
MeV	Pearson Corr.	.925**	.849**	.884**	.722**	.868**	.643**	-0.165	0.059	0.034	-.808**	.822**	.845**	-.757**	.763**	.894**	1	.830**	-.530**
	Sig. (2-tailed)	0.000	0.000	0.000	0.000	0.000	0.000	0.167	0.623	0.779	0.000	0.000	0.000	0.000	0.000	0.000		0.000	0.000
StV	Pearson Corr.	.715**	.633**	.689**	.584**	.683**	.393**	-0.087	0.038	0.042	-.645**	.524**	.573**	-.569**	.481**	.865**	.830**	1	-.388**
	Sig. (2-tailed)	0.000	0.000	0.000	0.000	0.000	0.001	0.466	0.752	0.724	0.000	0.000	0.000	0.000	0.000	0.000	0.000		0.001
Dir	Pearson Corr.	-.620**	-.635**	-.575**	-.495**	-.580**	-.451**	.578**	.382**	.239*	.555**	-.659**	-.637**	.452**	-.497**	-.495**	-.530**	-.388**	1
	Sig. (2-tailed)	0.000	0.000	0.000	0.000	0.000	0.000	0.000	0.001	0.043	0.000	0.000	0.000	0.000	0.000	0.000	0.000	0.001	

**. Correlation is significant at the 0.01 level (2-tailed).

*. Correlation is significant at the 0.05 level (2-tailed).

*Table D.5: Partial correlation results for 17 urban layout descriptors computed for 72 urban forms of **London**, with control for the density variable.*

Correlations

Control Variables			Sco	MeH	StH	StS	MaH	MeD	StD	MaD	Com	Cex	FaS	NoB	MeF	StF	MeV	StV	Dir
Density	Sco	Correlation	1	-0.660	-0.557	-0.569	-0.247	-0.273	0.000	0.071	-0.589	-0.147	0.104	-0.519	0.782	0.479	0.094	-0.038	-0.223
		Sig. (2-tailed)		0.000	0.000	0.000	0.038	0.021	0.998	0.555	0.000	0.222	0.386	0.000	0.000	0.000	0.437	0.752	0.062
	MeH	Correlation	-0.660	1	0.492	0.763	0.253	0.566	0.366	0.327	-0.113	0.258	-0.477	-0.105	-0.490	-0.216	-0.034	0.015	0.091
		Sig. (2-tailed)	0.000		0.000	0.000	0.033	0.000	0.002	0.005	0.346	0.030	0.000	0.385	0.000	0.070	0.778	0.902	0.450
	StH	Correlation	-0.557	0.492	1	0.901	0.778	0.068	-0.134	-0.144	0.235	0.176	-0.171	0.204	-0.494	-0.362	-0.099	0.021	0.009
		Sig. (2-tailed)	0.000	0.000		0.000	0.000	0.574	0.267	0.230	0.048	0.142	0.155	0.089	0.000	0.002	0.410	0.861	0.938
	StS	Correlation	-0.569	0.763	0.901	1	0.680	0.320	0.122	0.095	-0.010	0.229	-0.375	-0.016	-0.500	-0.317	-0.089	0.018	0.039
		Sig. (2-tailed)	0.000	0.000	0.000		0.000	0.006	0.310	0.431	0.934	0.054	0.001	0.897	0.000	0.007	0.462	0.880	0.749
	MaH	Correlation	-0.247	0.253	0.778	0.680	1	0.048	-0.051	-0.063	0.121	0.275	0.003	0.036	-0.169	-0.326	-0.138	-0.277	0.008
		Sig. (2-tailed)	0.038	0.033	0.000	0.000		0.691	0.674	0.600	0.314	0.020	0.983	0.764	0.160	0.006	0.252	0.019	0.950
	MeD	Correlation	-0.273	0.566	0.068	0.320	0.048	1	0.931	0.730	-0.372	-0.239	-0.593	-0.404	-0.128	0.148	0.328	0.198	0.520
		Sig. (2-tailed)	0.021	0.000	0.574	0.006	0.691		0.000	0.000	0.001	0.045	0.000	0.000	0.289	0.217	0.005	0.098	0.000
	StD	Correlation	0.000	0.366	-0.134	0.122	-0.051	0.931	1	0.841	-0.496	-0.237	-0.531	-0.516	0.091	0.220	0.326	0.126	0.433
		Sig. (2-tailed)	0.998	0.002	0.267	0.310	0.674	0.000		0.000	0.000	0.047	0.000	0.000	0.450	0.065	0.006	0.295	0.000
	MaD	Correlation	0.071	0.327	-0.144	0.095	-0.063	0.730	0.841	1	-0.520	-0.230	-0.537	-0.536	0.091	0.267	0.322	0.159	0.230
		Sig. (2-tailed)	0.555	0.005	0.230	0.431	0.600	0.000	0.000		0.000	0.053	0.000	0.000	0.450	0.024	0.006	0.186	0.053
	Com	Correlation	-0.589	-0.113	0.235	-0.010	0.121	-0.372	-0.496	-0.520	1	0.215	0.460	0.866	-0.384	-0.447	-0.093	-0.095	0.061
		Sig. (2-tailed)	0.000	0.346	0.048	0.934	0.314	0.001	0.000	0.000		0.071	0.000	0.000	0.001	0.000	0.439	0.433	0.611
	Cex	Correlation	-0.147	0.258	0.176	0.229	0.275	-0.239	-0.237	-0.230	0.215	1	0.601	0.112	-0.045	-0.525	-0.403	-0.652	-0.284
		Sig. (2-tailed)	0.222	0.030	0.142	0.054	0.020	0.045	0.047	0.053	0.071		0.000	0.353	0.710	0.000	0.000	0.000	0.016
	FaS	Correlation	0.104	-0.477	-0.171	-0.375	0.003	-0.593	-0.531	-0.537	0.460	0.601	1	0.355	0.095	-0.426	-0.395	-0.574	-0.187
		Sig. (2-tailed)	0.386	0.000	0.155	0.001	0.983	0.000	0.000	0.000	0.000	0.000		0.002	0.428	0.000	0.001	0.000	0.118
	NoB	Correlation	-0.519	-0.105	0.204	-0.016	0.036	-0.404	-0.516	-0.536	0.866	0.112	0.355	1	-0.431	-0.409	-0.226	-0.059	-0.034
		Sig. (2-tailed)	0.000	0.385	0.089	0.897	0.764	0.000	0.000	0.000	0.000	0.353	0.002		0.000	0.000	0.058	0.623	0.776
	MeF	Correlation	0.782	-0.490	-0.494	-0.500	-0.169	-0.128	0.091	0.091	-0.384	-0.045	0.095	-0.431	1	0.499	0.323	-0.094	-0.077
		Sig. (2-tailed)	0.000	0.000	0.000	0.000	0.160	0.289	0.450	0.450	0.001	0.710	0.428	0.000		0.000	0.006	0.433	0.523
	StF	Correlation	0.479	-0.216	-0.362	-0.317	-0.326	0.148	0.220	0.267	-0.447	-0.525	-0.426	-0.409	0.499	1	0.700	0.699	-0.011
		Sig. (2-tailed)	0.000	0.070	0.002	0.007	0.006	0.217	0.065	0.024	0.000	0.000	0.000	0.000	0.000		0.000	0.000	0.928
	MeV	Correlation	0.094	-0.034	-0.099	-0.089	-0.138	0.328	0.326	0.322	-0.093	-0.403	-0.395	-0.226	0.323	0.700	1	0.636	0.147
		Sig. (2-tailed)	0.437	0.778	0.410	0.462	0.252	0.005	0.006	0.006	0.439	0.000	0.001	0.058	0.006	0.000		0.000	0.220
	StV	Correlation	-0.038	0.015	0.021	0.018	-0.277	0.198	0.126	0.159	-0.095	-0.652	-0.574	-0.059	-0.094	0.699	0.636	1	0.100
		Sig. (2-tailed)	0.752	0.902	0.861	0.880	0.019	0.098	0.295	0.186	0.433	0.000	0.000	0.623	0.433	0.000	0.000		0.405
	Dir	Correlation	-0.223	0.091	0.009	0.039	0.008	0.520	0.433	0.230	0.061	-0.284	-0.187	-0.034	-0.077	-0.011	0.147	0.100	1
		Sig. (2-tailed)	0.062	0.450	0.938	0.749	0.950	0.000	0.000	0.053	0.611	0.016	0.118	0.776	0.523	0.928	0.220	0.405	

*Table D.6. Pearson Correlation (two-tailed) results for 18 urban geometry variables computed for 60 urban forms of **Paris**.*

Correlations

		Density	Sco	MeH	StH	StS	MaH	MeD	StD	MaD	Com	Cex	FaS	NoB	MeF	StF	MeV	StV	Dir
Density	Pearson Corr.	1	.826**	.288*	-.612**	-0.092	-.514**	-.497**	-.401**	-.397**	-.371**	.795**	.840**	-.653**	.772**	.573**	.730**	.520**	-0.185
	Sig. (2-tailed)		0.000	0.026	0.000	0.484	0.000	0.000	0.001	0.002	0.004	0.000	0.000	0.000	0.000	0.000	0.000	0.000	0.158
Sco	Pearson Corr.	.826**	1	-.292*	-.779**	-.551**	-.601**	-.724**	-.508**	-.473**	0.061	.846**	.948**	-.624**	.692**	.606**	.620**	.392**	-.266*
	Sig. (2-tailed)	0.000		0.023	0.000	0.000	0.000	0.000	0.000	0.000	0.641	0.000	0.000	0.000	0.000	0.000	0.000	0.002	0.040
MeH	Pearson Corr.	.288*	-.292*	1	.340**	.820**	0.193	.400**	0.188	0.140	-.746**	-0.090	-0.172	-0.085	0.132	-0.042	0.195	0.236	0.127
	Sig. (2-tailed)	0.026	0.023		0.008	0.000	0.140	0.002	0.151	0.285	0.000	0.492	0.189	0.519	0.315	0.748	0.135	0.070	0.335
StH	Pearson Corr.	-.612**	-.779**	.340**	1	.784**	.862**	.591**	.319*	.271*	-0.202	-.701**	-.708**	.457**	-.509**	-.425**	-.472**	-0.209	.304*
	Sig. (2-tailed)	0.000	0.000	0.008		0.000	0.000	0.000	0.013	0.036	0.122	0.000	0.000	0.000	0.000	0.001	0.000	0.108	0.018
StS	Pearson Corr.	-0.092	-.551**	.820**	.784**	1	.646**	.516**	0.230	0.172	-.600**	-.388**	-.453**	0.150	-0.172	-0.222	-0.103	0.087	0.232
	Sig. (2-tailed)	0.484	0.000	0.000	0.000		0.000	0.000	0.077	0.190	0.000	0.002	0.000	0.252	0.190	0.088	0.433	0.509	0.074
MaH	Pearson Corr.	-.514**	-.601**	0.193	.862**	.646**	1	.459**	0.251	0.185	-0.118	-.567**	-.567**	.346**	-.438**	-.341**	-.384**	-0.153	.270*
	Sig. (2-tailed)	0.000	0.000	0.140	0.000	0.000		0.000	0.054	0.158	0.368	0.000	0.000	0.007	0.000	0.008	0.002	0.242	0.037
MeD	Pearson Corr.	-.497**	-.724**	.400**	.591**	.516**	.459**	1	.873**	.634**	-.413**	-.758**	-.746**	0.122	-.296*	-.357**	-0.189	-0.139	.471**
	Sig. (2-tailed)	0.000	0.000	0.002	0.000	0.000	0.000		0.000	0.000	0.001	0.000	0.000	0.353	0.022	0.005	0.149	0.290	0.000
StD	Pearson Corr.	-.401**	-.508**	0.188	.319*	0.230	0.251	.873**	1	.800**	-0.172	-.522**	-.538**	0.033	-0.216	-.299*	-0.097	-0.153	.321*
	Sig. (2-tailed)	0.001	0.000	0.151	0.013	0.077	0.054	0.000		0.000	0.188	0.000	0.000	0.802	0.097	0.020	0.461	0.244	0.012
MaD	Pearson Corr.	-.397**	-.473**	0.140	.271*	0.172	0.185	.634**	.800**	1	-0.068	-.441**	-.472**	0.125	-0.170	-.309*	-0.155	-0.227	0.192
	Sig. (2-tailed)	0.002	0.000	0.285	0.036	0.190	0.158	0.000	0.000		0.607	0.000	0.000	0.340	0.193	0.016	0.238	0.081	0.141
Com	Pearson Corr.	-.371**	0.061	-.746**	-0.202	-.600**	-0.118	-.413**	-0.172	-0.068	1	0.247	0.124	.423**	-.381**	-0.187	-.429**	-.403**	-0.200
	Sig. (2-tailed)	0.004	0.641	0.000	0.122	0.000	0.368	0.001	0.188	0.607		0.057	0.347	0.001	0.003	0.153	0.001	0.001	0.126
Cex	Pearson Corr.	.795**	.846**	-0.090	-.701**	-.388**	-.567**	-.758**	-.522**	-.441**	0.247	1	.937**	-.389**	.499**	.436**	.445**	.287*	-.323*
	Sig. (2-tailed)	0.000	0.000	0.492	0.000	0.002	0.000	0.000	0.000	0.000	0.057		0.000	0.002	0.000	0.000	0.000	0.026	0.012
FaS	Pearson Corr.	.840**	.948**	-0.172	-.708**	-.453**	-.567**	-.746**	-.538**	-.472**	0.124	.937**	1	-.509**	.646**	.560**	.555**	.366**	-.269*
	Sig. (2-tailed)	0.000	0.000	0.189	0.000	0.000	0.000	0.000	0.000	0.000	0.347	0.000		0.000	0.000	0.000	0.000	0.004	0.038
NoB	Pearson Corr.	-.653**	-.624**	-0.085	.457**	0.150	.346**	0.122	0.033	0.125	.423**	-.389**	-.509**	1	-.607**	-.542**	-.724**	-.662**	0.067
	Sig. (2-tailed)	0.000	0.000	0.519	0.000	0.252	0.007	0.353	0.802	0.340	0.001	0.002	0.000		0.000	0.000	0.000	0.000	0.611
MeF	Pearson Corr.	.772**	.692**	0.132	-.509**	-0.172	-.438**	-.296*	-0.216	-0.170	-.381**	.499**	.646**	-.607**	1	.722**	.797**	.454**	0.100
	Sig. (2-tailed)	0.000	0.000	0.315	0.000	0.190	0.000	0.022	0.097	0.193	0.003	0.000	0.000	0.000		0.000	0.000	0.000	0.447
StF	Pearson Corr.	.573**	.606**	-0.042	-.425**	-0.222	-.341**	-.357**	-.299*	-.309*	-0.187	.436**	.560**	-.542**	.722**	1	.674**	.736**	0.029
	Sig. (2-tailed)	0.000	0.000	0.748	0.001	0.088	0.008	0.005	0.020	0.016	0.153	0.000	0.000	0.000	0.000		0.000	0.000	0.827
MeV	Pearson Corr.	.730**	.620**	0.195	-.472**	-0.103	-.384**	-0.189	-0.097	-0.155	-.429**	.445**	.555**	-.724**	.797**	.674**	1	.678**	0.098
	Sig. (2-tailed)	0.000	0.000	0.135	0.000	0.433	0.002	0.149	0.461	0.238	0.001	0.000	0.000	0.000	0.000	0.000		0.000	0.455
StV	Pearson Corr.	.520**	.392**	0.236	-0.209	0.087	-0.153	-0.139	-0.153	-0.227	-.403**	.287*	.366**	-.662**	.454**	.736**	.678**	1	0.017
	Sig. (2-tailed)	0.000	0.002	0.070	0.108	0.509	0.242	0.290	0.244	0.081	0.001	0.026	0.004	0.000	0.000	0.000	0.000		0.895
Dir	Pearson Corr.	-0.185	-.266*	0.127	.304*	0.232	.270*	.471**	.321*	0.192	-0.200	-.323*	-.269*	0.067	0.100	0.029	0.098	0.017	1
	Sig. (2-tailed)	0.158	0.040	0.335	0.018	0.074	0.037	0.000	0.012	0.141	0.126	0.012	0.038	0.611	0.447	0.827	0.455	0.895	

**. Correlation is significant at the 0.01 level (2-tailed).

*. Correlation is significant at the 0.05 level (2-tailed).

Table D.7(a-b). Principal Component Analysis including all 18 urban geometry variables computed for 72 urban forms of London. Left (a): communalities, i.e. influence of each variable from all three factors extracted; right (b): component matrix (no rotation) depicting loading factors, i.e. correlations between specific variables and specific factors. (In support of Figure 3.15).

Communalities

	Initial	Extraction
Density	1.000	0.969
Sco	1.000	0.947
MeH	1.000	0.950
StH	1.000	0.949
StS	1.000	0.989
MaH	1.000	0.836
MeD	1.000	0.945
StD	1.000	0.944
MaD	1.000	0.803
Com	1.000	0.902
Cex	1.000	0.905
FaS	1.000	0.907
NoB	1.000	0.842
MeF	1.000	0.817
StF	1.000	0.872
MeV	1.000	0.900
StV	1.000	0.580
Dir	1.000	0.612

Extraction Method: Principal Component Analysis.

Component Matrix[a]

	Component		
	1	2	3
Density	0.983	-0.021	0.054
Sco	0.927	-0.005	-0.298
MeH	0.944	0.085	0.228
StH	0.810	-0.101	0.531
StS	0.946	0.018	0.306
MaH	0.758	-0.077	0.506
MeD	-0.309	0.883	0.264
StD	-0.064	0.967	0.068
MaD	-0.069	0.893	-0.035
Com	-0.894	-0.279	0.155
Cex	0.930	-0.132	0.148
FaS	0.931	-0.199	0.034
NoB	-0.818	-0.375	0.179
MeF	0.786	0.057	-0.443
StF	0.840	0.200	-0.357
MeV	0.936	0.138	-0.058
StV	0.734	0.167	-0.116
Dir	-0.669	0.372	0.161

Extraction Method: Principal Component Analysis.

a. 3 components extracted.

*Table D.8(a-b). Principal Component Analysis including all 18 urban geometry variables computed for 60 urban forms of **Paris**. Left (a): communalities, i.e. influence of each variable from all three factors extracted; right (b): component matrix (no rotation) depicting loading factors, i.e. correlations between specific variables and specific factors. (In support of Figure 3.16).*

Communalities

	Initial	Extraction
Density	1.000	0.895
Sco	1.000	0.926
MeH	1.000	0.739
StH	1.000	0.866
StS	1.000	0.940
MaH	1.000	0.638
MeD	1.000	0.936
StD	1.000	0.867
MaD	1.000	0.698
Com	1.000	0.807
Cex	1.000	0.782
FaS	1.000	0.878
NoB	1.000	0.700
MeF	1.000	0.764
StF	1.000	0.605
MeV	1.000	0.833
StV	1.000	0.590
Dir	1.000	0.277

Extraction Method: Principal Component Analysis.

Component Matrix[a]

	Component		
	1	2	3
Density	0.860	0.366	-0.147
Sco	0.959	-0.066	0.049
MeH	-0.176	0.763	-0.355
StH	-0.821	0.248	-0.361
StS	-0.517	0.644	-0.508
MaH	-0.688	0.192	-0.358
MeD	-0.748	0.497	0.359
StD	-0.572	0.339	0.652
MaD	-0.521	0.206	0.620
Com	0.011	-0.888	0.137
Cex	0.859	-0.161	-0.134
FaS	0.931	-0.080	-0.071
NoB	-0.632	-0.492	-0.243
MeF	0.733	0.448	0.160
StF	0.700	0.334	0.066
MeV	0.689	0.567	0.195
StV	0.511	0.571	-0.056
Dir	-0.285	0.373	0.237

Extraction Method: Principal Component Analysis.

a. 3 components extracted.

Appendix E: Weather files used in SOLWEIG for mean radiant temperature simulation.

Input information: year, month, day, hour, air temperature [°C], relative humidity [%], global, diffused and incident irradiance [W/m^2]. (For three representative days presented in Section 4.4.1.1.)

19 January. Cloudy winter day.

year	month	day	hour	Ta	RH	radG	radD	radI
2002	1	19	0	5.1	100	0	0	0
2002	1	19	1	3.7	95	0	0	0
2002	1	19	2	3.4	89	0	0	0
2002	1	19	3	3.4	93	0	0	0
2002	1	19	4	2.9	92	0	0	0
2002	1	19	5	2.4	94	0	0	0
2002	1	19	6	2.9	90	0	0	0
2002	1	19	7	2.4	91	0	0	0
2002	1	19	8	1.9	85	0	0	0
2002	1	19	9	1.4	92	18	18	0
2002	1	19	10	2.8	86	31	31	0
2002	1	19	11	4.2	82	49	49	0
2002	1	19	12	6.2	75	60	60	0
2002	1	19	13	7.1	70	61	61	0
2002	1	19	14	7.5	79	54	54	0
2002	1	19	15	7.1	73	38	38	0
2002	1	19	16	7.4	83	33	33	0
2002	1	19	17	7.4	92	2	2	0
2002	1	19	18	6.1	98	0	0	0
2002	1	19	19	4.9	100	0	0	0
2002	1	19	20	4.9	100	0	0	0
2002	1	19	21	4.3	100	0	0	0
2002	1	19	22	4.2	100	0	0	0
2002	1	19	23	3.5	100	0	0	0

26 July. Sunny summer day.

year	month	day	hour	Ta	RH	radG	radD	radI
2002	7	26	0	14.5	99	0	0	0
2002	7	26	1	14.5	92	0	0	0
2002	7	26	2	13.4	99	0	0	0
2002	7	26	3	12.9	99	0	0	0
2002	7	26	4	12.9	99	0	0	0
2002	7	26	5	12.8	99	10	10	0
2002	7	26	6	12.9	99	124	38	508
2002	7	26	7	12.9	99	259	94	514
2002	7	26	8	14.0	88	393	143	532
2002	7	26	9	16.1	74	520	156	602
2002	7	26	10	17.6	65	621	186	608
2002	7	26	11	19.1	56	695	208	611
2002	7	26	12	19.5	56	732	240	586
2002	7	26	13	20.2	59	729	265	550
2002	7	26	14	20.1	55	698	253	549
2002	7	26	15	19.9	63	545	163	604
2002	7	26	16	20.5	59	370	204	331
2002	7	26	17	19.9	60	228	146	229
2002	7	26	18	20.0	60	143	68	371
2002	7	26	19	19.6	68	17	17	0
2002	7	26	20	17.9	78	0	0	0
2002	7	26	21	16.5	92	0	0	0
2002	7	26	22	15.3	91	0	0	0
2002	7	26	23	14.5	92	0	0	0

29 December. Sunny winter day.

year	month	day	hour	Ta	RH	radG	radD	radI
2002	12	29	0	0.5	71	0	0	0
2002	12	29	1	1.5	75	0	0	0
2002	12	29	2	0.8	69	0	0	0
2002	12	29	3	0.8	72	0	0	0
2002	12	29	4	-0.3	79	0	0	0
2002	12	29	5	-0.7	81	0	0	0
2002	12	29	6	-0.6	88	0	0	0
2002	12	29	7	-0.8	85	0	0	0
2002	12	29	8	-0.9	80	0	0	0
2002	12	29	9	-0.4	74	12	12	0
2002	12	29	10	0.1	70	78	50	194
2002	12	29	11	1.0	71	168	55	517
2002	12	29	12	2.1	63	204	67	532
2002	12	29	13	2.5	50	206	67	532
2002	12	29	14	2.7	42	167	69	441
2002	12	29	15	2.2	42	99	47	346
2002	12	29	16	2.2	46	13	13	0
2002	12	29	17	2.0	47	0	0	0
2002	12	29	18	2.2	56	0	0	0
2002	12	29	19	1.6	63	0	0	0
2002	12	29	20	0.7	63	0	0	0
2002	12	29	21	0.3	58	0	0	0
2002	12	29	22	1.1	60	0	0	0
2002	12	29	23	0.3	68	0	0	0

Appendix F: Results for 24 urban forms of London studied in Chapter Five.

Table: Urban geometry variables (density and nine urban layout descriptors), mean SVF and mean global and direct irradiances computed for the entire year, January and July, by urban form, ranked in decreasing order of density.

	Urban Geometry										Façades						Ground					
												Global Irradiance (W/m²)			Direct Irradiance (W/m²)				Global Irradiance (W/m²)			Direct Irradiance (W/m²)		
	Density [m³/m²]	SCo [%]	MeH [m]	StH [m]	StF [m²]	Dir (*10⁻²)	Cex [m²/m²]	Com [m²/m³]	NOB	MeD [m]	SVF	Year	Jan.	Jul.	Year	Jan.	Jul.	SVF	Year	Jan.	Jul.	Year	Jan.	Jul.
C27	22.0	59.7	36.9	12.0	196.7	2.041	2.245	0.126	57	5.0	0.173	47.2	20.9	58.8	19.9	8.8	27.3	0.264	54.1	14.9	79.3	18.6	1.6	36.4
C35	19.6	53.3	36.8	13.0	144.9	5.246	2.032	0.128	66	6.6	0.196	55.0	25.4	67.3	23.3	11.1	31.0	0.333	70.7	19.2	103.7	26.3	2.1	50.3
C19	19.3	61.3	31.5	11.1	183.0	3.581	1.818	0.123	68	4.5	0.199	54.0	24.5	67.1	22.4	10.4	30.9	0.291	60.4	15.7	87.9	21.2	1.0	40.6
C31	18.5	54.6	33.9	12.7	130.5	4.331	1.841	0.126	62	6.7	0.205	56.1	25.7	69.0	23.5	11.1	31.5	0.342	71.9	19.3	105.6	26.3	1.9	50.9
C12	18.4	64.2	28.6	10.3	173.9	4.658	1.888	0.135	53	5.1	0.205	55.5	25.2	68.9	23.2	10.8	31.8	0.300	61.6	16.0	89.9	21.7	1.0	41.8
C10	16.9	59.9	28.1	26.3	143.9	4.216	1.731	0.135	57	4.6	0.248	67.7	34.0	81.7	28.3	15.8	36.8	0.334	70.2	18.6	100.4	25.1	1.4	46.3
C7	16.4	56.4	29.1	10.2	164.8	5.143	1.562	0.127	45	8.5	0.253	69.9	32.5	85.3	29.5	14.3	38.9	0.432	90.9	24.8	132.2	34.5	3.1	64.9
C22	15.8	49.8	31.7	9.6	135.0	6.261	1.600	0.130	48	9.4	0.224	60.7	27.7	75.0	25.6	11.9	34.5	0.445	96.0	28.1	135.8	38.1	5.2	67.6
C16	15.7	58.3	27.0	7.2	123.1	3.236	1.630	0.137	75	5.7	0.227	61.9	27.9	76.7	26.1	12.0	35.5	0.357	75.8	21.4	108.2	28.2	3.0	51.6
C9	13.9	46.9	29.6	16.1	133.7	5.925	1.509	0.139	48	9.0	0.254	69.7	31.6	86.4	29.1	13.5	39.6	0.451	95.9	25.8	138.0	36.6	2.9	67.4
C6	13.8	56.3	24.5	7.6	226.5	6.329	1.593	0.152	55	5.0	0.232	62.8	27.5	78.3	26.4	11.3	36.3	0.352	72.9	20.8	105.1	26.2	2.9	49.0
C2	11.3	54.3	20.8	4.9	132.6	5.794	1.423	0.169	59	6.2	0.246	67.7	29.5	84.3	28.7	12.3	39.3	0.424	89.9	26.3	128.8	34.2	4.7	62.5
W20	11.1	43.8	25.3	10.6	100.6	8.952	1.192	0.147	59	9.7	0.284	77.9	36.6	93.4	32.8	16.3	41.8	0.526	114.7	32.4	165.2	46.0	5.5	84.0
C29	10.8	46.5	23.2	5.5	108.7	2.750	1.436	0.170	71	6.1	0.243	65.6	28.3	82.3	27.6	11.6	38.2	0.429	90.2	24.2	130.7	33.9	2.6	63.4
W39	10.4	48.6	21.4	5.3	120.9	5.110	1.121	0.154	60	6.8	0.279	76.9	35.1	95.0	32.7	15.4	44.5	0.472	101.3	27.2	144.8	39.0	3.0	70.7
W27	7.5	38.6	19.4	6.8	50.4	5.042	1.208	0.213	101	6.9	0.286	80.1	37.8	97.8	34.2	17.1	45.3	0.525	114.3	32.4	161.9	45.5	5.2	80.4
W33	6.5	34.5	18.9	7.1	57.1	5.272	1.243	0.243	105	6.9	0.290	81.2	39.0	98.7	34.7	17.9	45.5	0.521	114.1	33.3	160.7	45.5	5.9	79.8
N37	6.1	36.8	16.6	6.9	34.4	5.580	1.120	0.233	132	5.8	0.297	81.5	40.1	95.7	34.0	18.5	41.4	0.564	124.4	34.2	180.9	50.5	5.2	93.4
W14	5.5	33.0	16.8	5.7	30.5	7.999	1.038	0.247	131	7.0	0.313	87.5	43.7	103.6	37.1	20.6	45.9	0.599	132.5	37.1	188.8	54.3	6.1	96.8
N20	5.4	32.7	16.6	5.0	54.6	8.240	1.135	0.257	121	6.4	0.306	85.3	39.3	103.3	36.2	17.3	46.9	0.558	122.8	36.2	174.8	49.4	7.1	88.2
N55	4.4	33.0	13.5	4.5	28.3	5.860	1.028	0.289	175	6.0	0.304	84.8	41.6	100.7	35.6	19.2	44.5	0.618	136.2	40.0	192.8	56.5	8.0	99.3
N1	3.9	27.1	14.2	3.9	39.5	6.580	0.830	0.271	159	7.6	0.334	92.8	48.3	109.1	38.8	23.4	47.6	0.677	150.3	43.3	210.5	63.4	8.2	109.0
N24	3.2	20.3	15.9	4.2	15.7	8.290	0.950	0.338	162	7.9	0.337	93.6	45.8	113.0	39.4	21.1	50.9	0.658	144.9	43.3	201.8	60.5	9.1	103.2
N44	3.2	23.9	13.3	7.5	22.0	8.890	0.790	0.305	167	7.5	0.353	98.6	50.5	114.7	41.2	24.1	49.4	0.699	155.8	47.8	217.4	66.2	11.3	113.1

Appendix G: Additional results from the sub-study considering Athens and Helsinki locations.

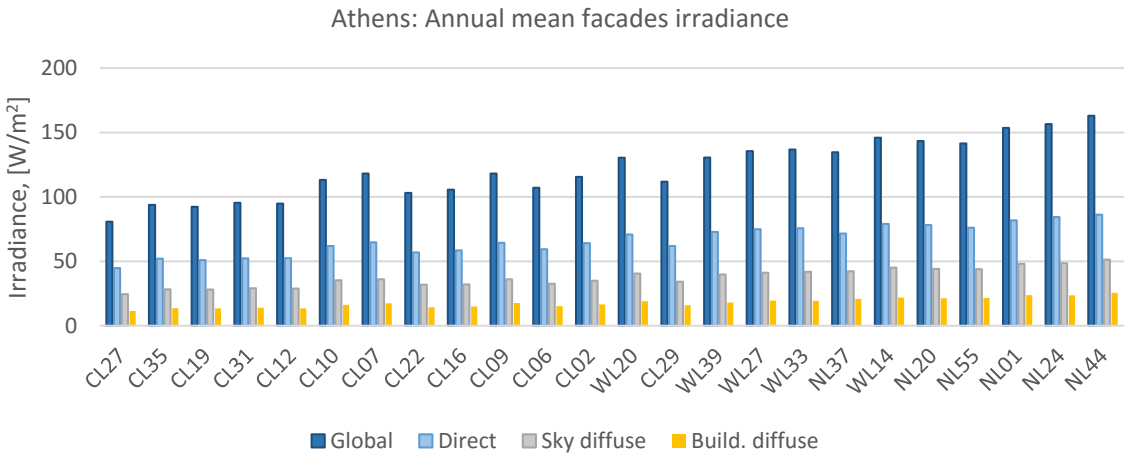

(a)

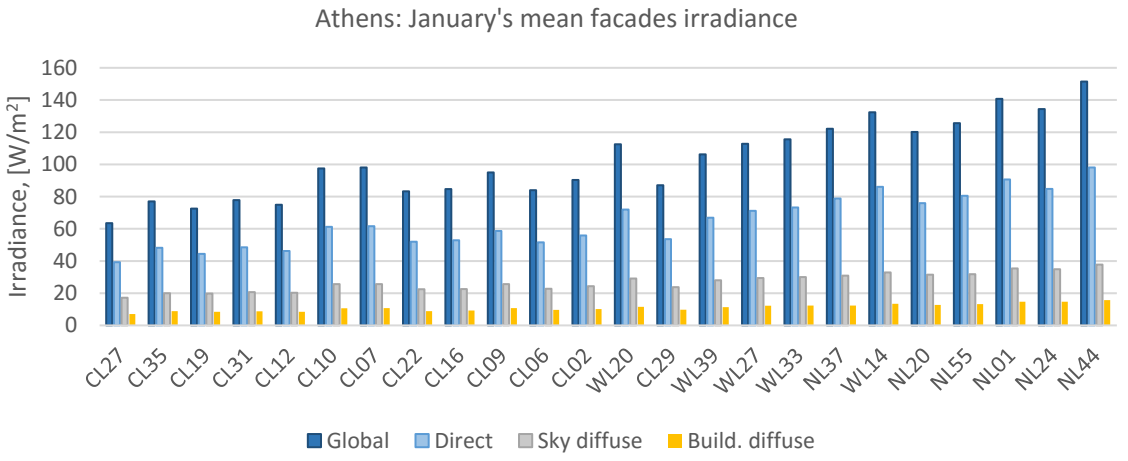

(b)

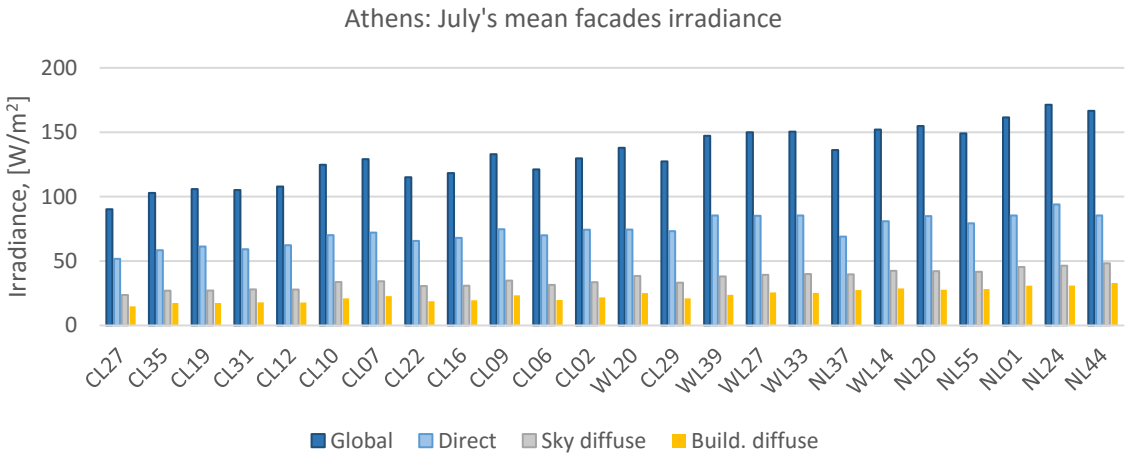

(c)

*Figure G.1: Mean global, direct, diffused and reflected **façade** irradiances computed for **Athens** location by urban form, for the entire year (a), January (b) and July (c).*

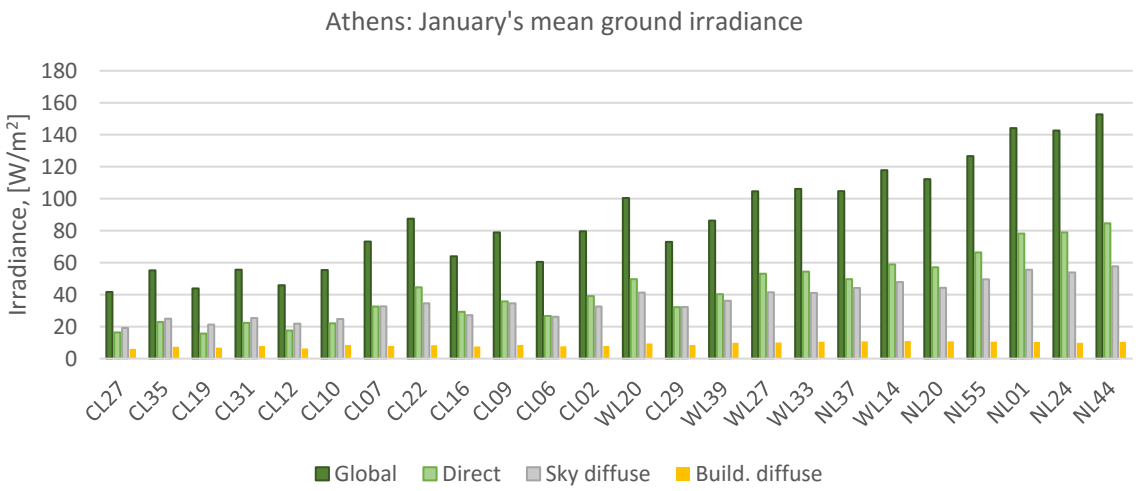

(a)

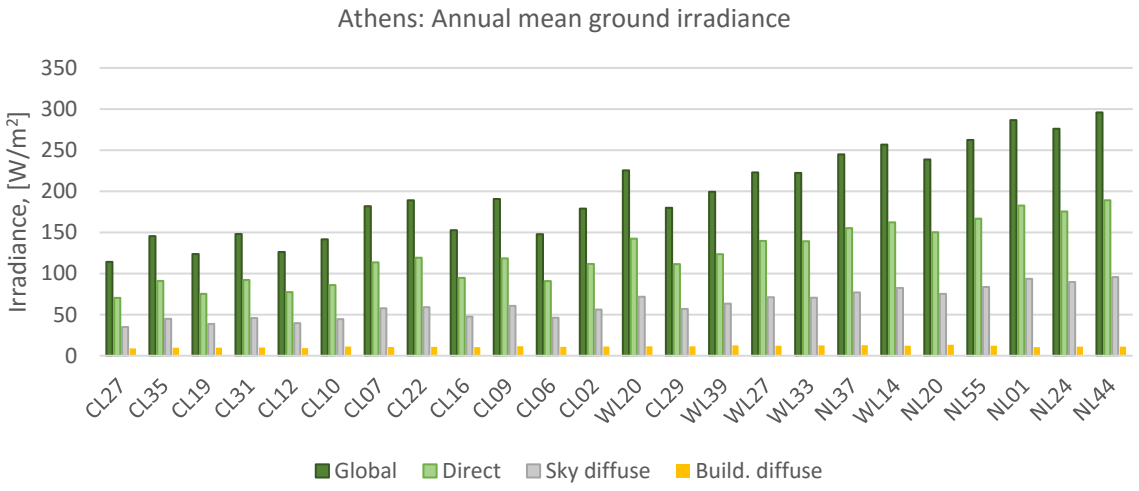

(b)

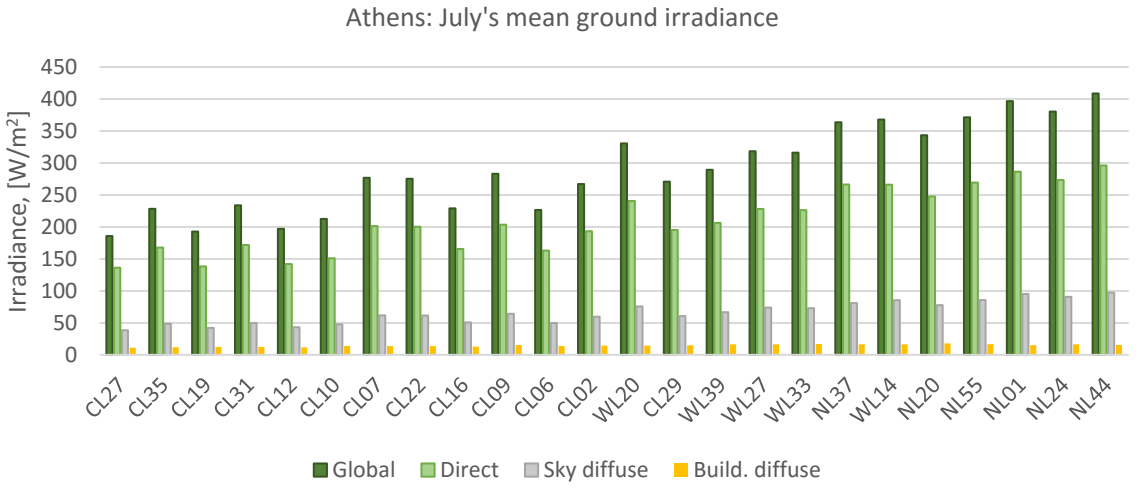

(c)

*Figure G.2: Mean global, direct, diffused and reflected **ground** irradiances computed for **Athens** location, by urban form, for the entire year (a), January (b) and July (c).*

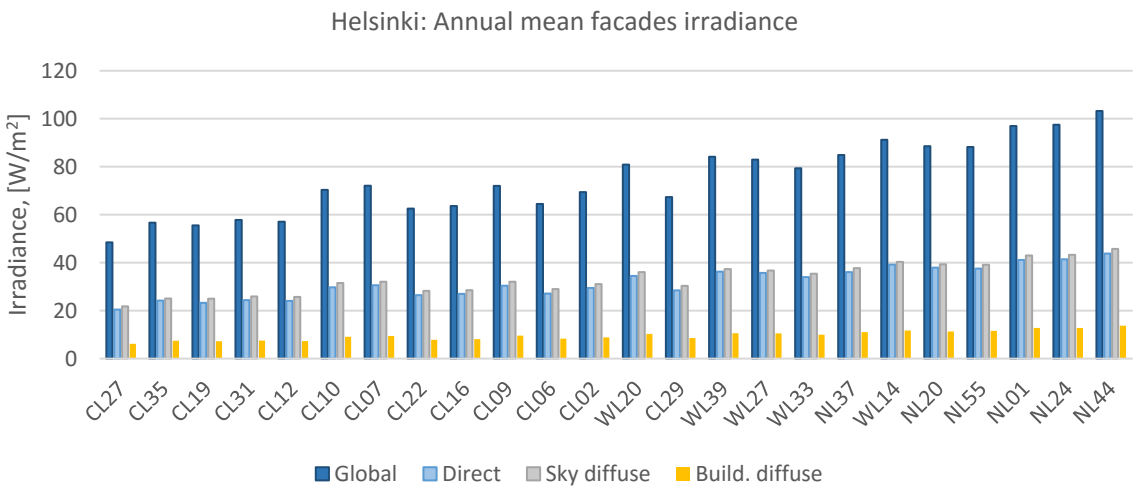

(a)

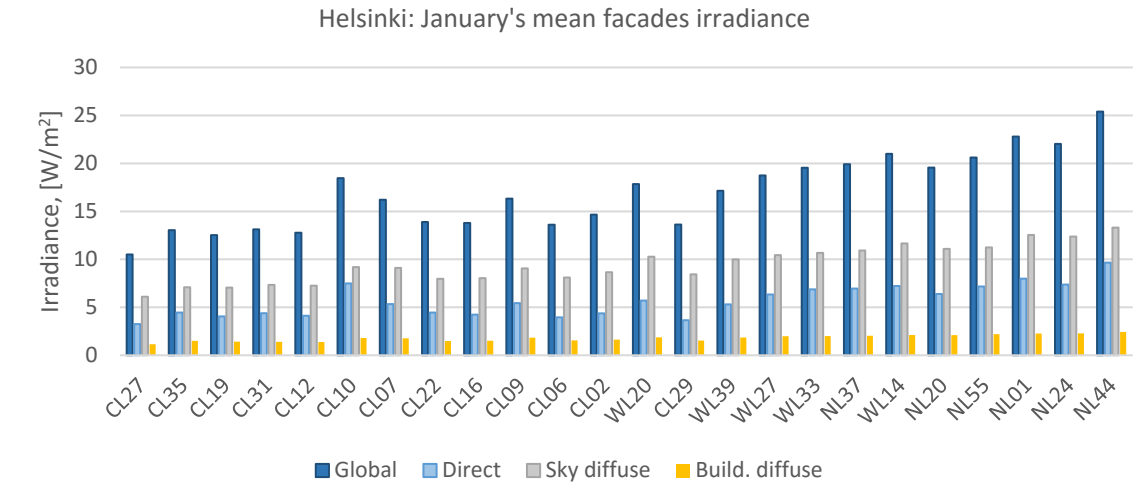

(b)

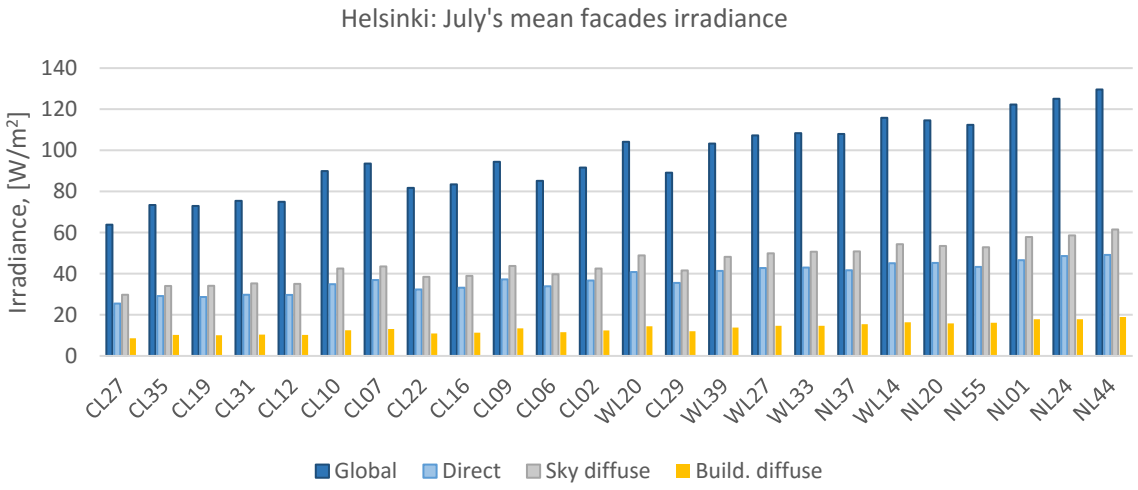

(c)

*Figure G.3: Mean global, direct, diffused and reflected **façade** irradiances computed for **Helsinki** location by urban form, for the entire year (a), January (b) and July (c).*

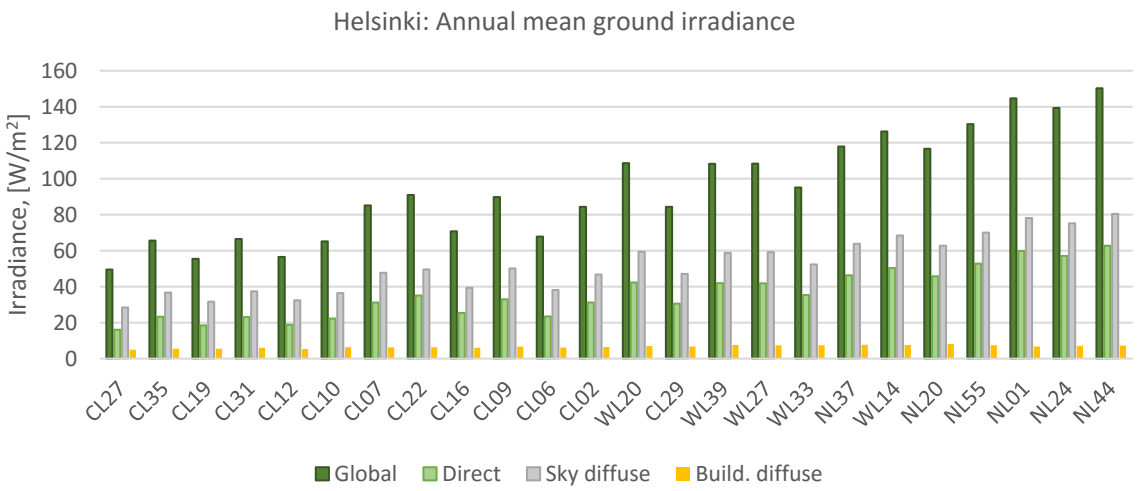

(a)

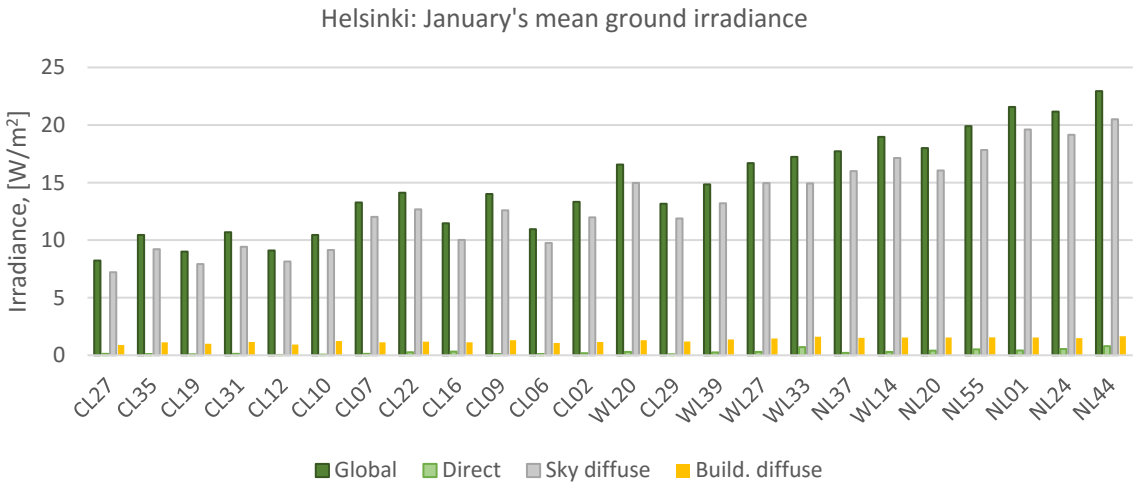

(b)

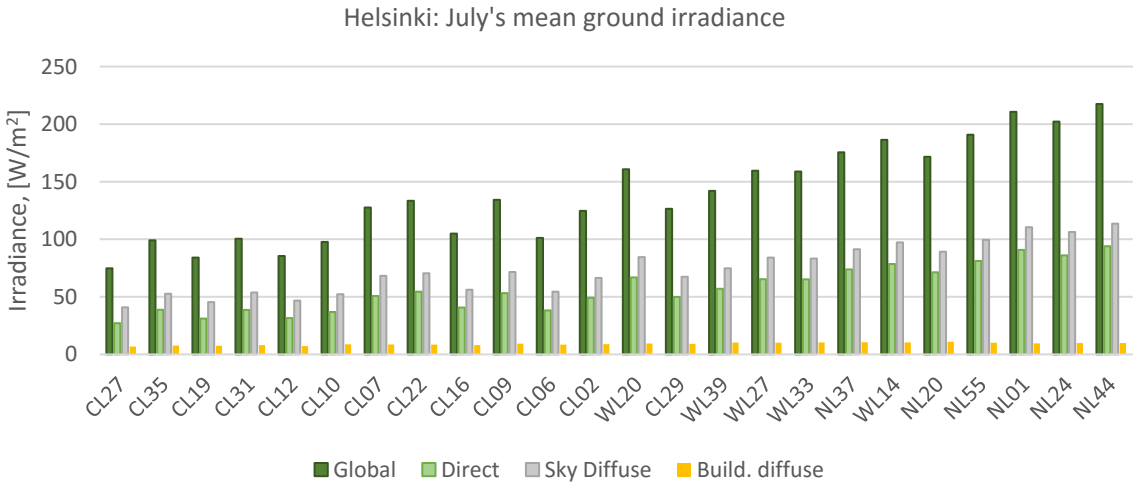

(c)

*Figure G.4: Mean global, direct, diffused and reflected **ground** irradiances computed for **Helsinki** location, by urban form, for the entire year (a), January (b) and July (c).*

*Table G.1. Partial correlation analysis for urban layout descriptors and mean **global** irradiance, controlling for density variable, for **Athens** location.*

Athens	SCo	MeH	StH	StF	Dir	Cex	Com	NOB	MOD
Ground									
Year	**-0.672****	0.543**	0.169	**-0.461***	**0.488***	**-0.439***	0.160	0.289	**0.717****
January	**-0.713****	0.484*	0.122	-0.387	**0.479***	-0.342	0.353	0.373	**0.638****
July	**-0.625****	0.551**	0.133	**-0.460***	**0.473***	-0.405	0.079	0.241	**0.706****
Façades									
Year	-0.281	0.152	**0.526****	-0.159	**0.485***	**-0.580****	0.053	0.020	**0.432***
January	-0.385	0.119	**0.556****	-0.339	**0.433***	**-0.469***	0.206	0.321	0.297
July	-0.101	0.115	0.390	0.077	0.326	**-0.532****	-0.069	-0.262	0.402

** Correlation is significant at the 0.01 level

* Correlation is significant at the 0.05 level

*Table G.2 Partial correlation analysis for urban layout descriptors and mean **global** irradiance, controlling for density variable, for **Helsinki** location.*

Helsinki	SCo	MeH	StH	StF	Dir	Cex	Com	NOB	MOD
Ground									
Year	**-0.545****	0.399	0.103	-0.348	**0.463***	**-0.586****	0.100	0.250	**0.630****
January	**-0.703****	0.528**	0.176	**-0.442***	**0.484***	**-0.416***	0.248	0.327	**0.699****
July	**-0.673****	0.522*	0.179	**-0.456***	**0.480***	**-0.451***	0.181	0.310	**0.699****
Façades									
Year	-0.249	0.087	**0.485***	-0.163	**0.460***	**-0.650****	0.033	0.082	0.364
January	-0.336	0.066	**0.735****	-0.342	0.343	-0.353	0.258	0.322	0.177
July	-0.284	0.160	**0.546****	-0.148	**0.498***	**-0.583****	-0.046	-0.007	**0.442***

** Correlation is significant at the 0.01 level

* Correlation is significant at the 0.05 level

*Table G.3. Partial correlation analysis for urban layout descriptors and mean buildings **reflected** irradiance, controlling for density variable, for **Athens** location.*

Athens	SCo	MeH	StH	StF	Dir	Cex	Com	NOB	MOD
Ground									
Year	0.385	0.053	0.230	0.071	-0.094	-0.017	**-0.592****	**-0.585****	0.004
January	-0.145	0.364	**0.464***	**-0.417****	0.106	-0.202	-0.334	-0.138	0.242
July	0.225	0.154	0.259	0.079	-0.102	0.008	**-0.443***	**-0.527***	0.068
Façades									
Year	**-0.415***	0.139	**0.498***	-0.254	**0.471***	**-0.468***	0.258	0.313	0.349
January	-0.391	0.108	**0.579****	-0.216	0.409	**-0.418***	0.297	0.311	0.259
July	-0.375	0.137	**0.516***	-0.245	**0.484***	**-0.493***	0.200	0.249	0.376

** Correlation is significant at the 0.01 level

* Correlation is significant at the 0.05 level

*Table G.4. Partial correlation analysis for urban layout descriptors and mean buildings **reflected** irradiance, controlling for density variable, for **Helsinki** location.*

Helsinki	SCo	MeH	StH	StF	Dir	Cex	Com	NOB	MOD
Ground									
Year	0.248	0.177	0.248	-0.030	0.048	-0.188	**-0.606****	**-0.560****	0.170
January	-0.400	0.457*	**0.589****	**-0.542****	0.107	-0.085	-0.025	0.111	0.240
July	0.219	0.205	0.314	-0.024	0.047	-0.145	**-0.594****	**-0.573****	0.173
Façades									
Year	-0.314	0.083	**0.498***	-0.174	**0.441***	**-0.589***	0.148	0.215	0.322
January	-0.320	0.129	**0.683****	-0.252	0.405	-0.387	0.199	0.249	0.262
July	-0.388	0.139	**0.552****	-0.225	**0.471***	**-0.500***	0.220	0.255	0.363

** Correlation is significant at the 0.01 level

* Correlation is significant at the 0.05 level

Appendix H: Prediction of annual global façade irradiance in London as a function of SVF.

Table. Linear models for prediction of annual global irradiance (Ig) on façades in London, based on SVF value, for 30 orientations.

Orientation	Azimuths sections	Factor (f) where, Ig= f*SVF	R^2
1	-6 ≤ a< 6	141.79	0.959
2	6 ≤ a < 18	143.54	0.740
3	18 ≤ a < 30	150.66	0.772
4	30 ≤ a < 42	169.72	0.898
5	42 ≤ a < 54	190.73	0.968
6	54 ≤ a < 66	216.07	0.973
7	66 ≤ a < 78	241.5	0.976
8	78 ≤ a < 90	264.72	0.945
9	90 ≤ a < 102	291.8	0.946
10	102 ≤ a < 114	315.55	0.964
11	114 ≤ a < 126	340.25	0.976
12	126 ≤ a < 138	355.01	0.985
13	138 ≤ a < 150	375.76	0.991
14	150 ≤ a < 162	389.8	0.963
15	162 ≤ a < 174	394.56	0.992
16	174 ≤ a < 186	398.49	0.986
17	186 ≤ a < 198	397.94	0.988
18	198 ≤ a < 210	392.86	0.983
19	210 ≤ a < 222	382.1	0.983
20	222 ≤ a < 234	368.31	0.989
21	234 ≤ a < 246	346.4	0.974
22	246 ≤ a < 258	320.07	0.971
23	258 ≤ a < 270	302.98	0.978
24	270 ≤ a < 282	276.18	0.956
25	282 ≤ a < 294	243.38	0.947
26	294 ≤ a < 306	213.78	0.940
27	306 ≤ a < 318	195.86	0.941
28	318 ≤ a < 330	169.24	0.960
29	330 ≤ a < 342	154.06	0.946
30	342 ≤ a < 354	145.06	0.938

Appendix I: Articles and conference papers published.

- Chatzipoulka, C., Compagnon, R. and Nikolopoulou, M., 2016. Urban geometry and solar availability on façades and ground of real urban forms: using the case of London. *Solar Energy*, 138, pp. 53-66.
- Chatzipoulka, C., Compagnon, R. and Nikolopoulou, M., 2015. Comparing the solar performance of urban forms in London. *PLEA2015 - 31th International Conference on Passive and Low Energy Architecture.* Bologna, Italy, 9-11 September 2015.
- Chatzipoulka, C., Nikolopoulou, M. and Watkins, R., 2015. The impact of urban geometry on the radiant environment in outdoor spaces. *ICU9 – 9th International Conference on Urban Climate jointly with 12th Symposium on the Urban Environment*. Toulouse, France, 20-24 July 2015.